

DISSERTATION

The Role of Cdc42, ADF/Cofilin, Myosin II and Waves during the Establishment of Neuronal Polarity

Submitted by

Kevin Carl Flynn

Graduate Degree Program in Cell and Molecular Biology

In partial fulfillment of the requirements
for the degree of Doctor of Philosophy

Colorado State University

Fort Collins, Colorado State University

Summer 2008

UMI Number: 3332700

INFORMATION TO USERS

The quality of this reproduction is dependent upon the quality of the copy submitted. Broken or indistinct print, colored or poor quality illustrations and photographs, print bleed-through, substandard margins, and improper alignment can adversely affect reproduction.

In the unlikely event that the author did not send a complete manuscript and there are missing pages, these will be noted. Also, if unauthorized copyright material had to be removed, a note will indicate the deletion.

UMI®

UMI Microform 3332700

Copyright 2008 by ProQuest LLC.

All rights reserved. This microform edition is protected against unauthorized copying under Title 17, United States Code.


ProQuest LLC
789 E. Eisenhower Parkway
PO Box 1346
Ann Arbor, MI 48106-1346

COLORADO STATE UNIVERSITY

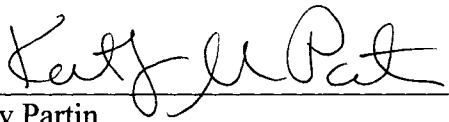
April 22, 2008

WE HEREBY RECOMMEND THAT THE DISSERTATION
PREPARED UNDER OUR SUPERVISION BY KEVIN FLYNN ENTITLED
THE ROLE OF CDC42, ADF/COFILIN, MYOSIN II AND WAVES DURING
THE ESTABLISHMENT OF NEURONAL POLARITY BE ACCEPTED AS
FULFILLING IN PART THE REQUIREMENTS FOR THE DEGREE OF
DOCTOR OF PHILOSOPHY

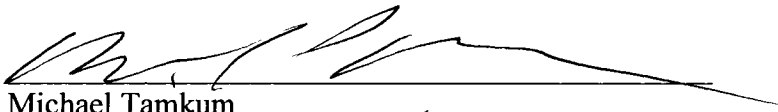
Committee on Graduate Work



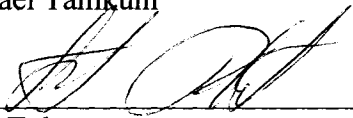
Robert Handa



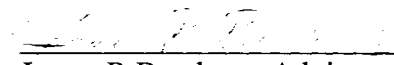
Kathy Partin



Michael Tamkun



Stuart Tobet



James R Bamberg, Advisor



Norman Curthoys, Director

Abstract of Dissertation

The Role of Cdc42, ADF/Cofilin, Myosin II and Growth Cone-Like Waves in the Establishment of Neuronal Polarity

The establishment of neuronal polarity is an essential developmental process, underlying the unidirectional flow of information in neurons and the overall function of the nervous system. In cultured hippocampal neurons, the first signs of polarity occur as one of several undifferentiated processes begins to elongate rapidly to form the axon (axonogenesis). The regulation of the cytoskeleton and intracellular trafficking are crucial to the proper development of neuronal polarity. This dissertation explores both of these polarity-developing mechanisms, identifying actin-regulating components in the signaling pathways as well as characterizing growth-cone like “waves” that correlate with axonogenesis.

This study begins by analyzing the functional consequences of the loss of the Rho GTPase, cdc42, on the polarization of hippocampal neurons. Neurons from the cdc42 knock-out (cdc42KO) mouse have severe deficiencies in their ability to extend axons *in vivo* and in culture which is exerted through the regulation of actin dynamics. The actin regulating protein, cofilin is normally asymmetrically enriched in its active form in axonal growth cones but in cdc42 KO neurons there is an increase in the phosphorylation (inactivation) of cofilin. Cofilin expression promotes axon growth, whereas cofilin knockdown results in polarity defects analogous to those seen upon cdc42 ablation. Taken together,

these data suggest that cdc42 is a key regulator of axon specification and that cofilin is a downstream effector of during this process.

Though these studies suggest the involvement of cofilin downstream of cdc42; active cofilin cannot rescue polarity deficits in cdc42KO neurons. This suggests that other actin regulating proteins may also be required for axon formation. The actin motor protein, myosin-II also shows an increased activation in the cdc42KO brain. Inhibition of myosin II activity promotes axon formation and acts in synergy with cofilin on inducing supernumerary axons. Furthermore, the combined inhibition of myosin and activation of cofilin rescues axon formation in cdc42KO neurons while either treatment individually does not. Thus, the concurrent inhibition of myosin and activation of cofilin can contribute to the regulation of actin dynamics during axon specification.

Axon specification is dependent on the transport of materials to the developing axonal growth cone. “Waves” – growth cone-like structures, propagate down neurites and correlate with neurite extension; thus, waves have been suggested as a mechanism for transporting materials that support this growth. Waves occur in all processes during early neuronal development, but are more frequent in the developing axon. Proteins enriched in axonal growth cones are also localized to waves and proteins such as cofilin and actin appears to be transported via waves to the growth cone, suggesting that waves represent a transport mechanism. Wave arrival at neurite tips was also coincident with an increase in growth cone size and dynamics. In addition, waves can promote neurite branching, either by supporting the growth of existing branches or by

facilitating the growth of nascent branches. Waves are observed in neurons in organotypic hippocampal slices, a 3-dimensional growth environment reflecting the *in vivo* environment. Together, these data indicate that waves contribute to axon differentiation and growth both through the transport of actin and by increasing growth cone dynamics.

Kevin Carl Flynn
Graduate Degree Program in Cell and Molecular Biology
Colorado State University
Fort Collins, CO 80523
Summer 2008

Acknowledgements

Here at the culmination of my PhD, it is amazing to consider every influence that has allowed me to successfully traverse this long, strange journey. The aptitude and attitude that is required for this achievement is something that has been shaped by my life experience, especially the relationships with various people from diverse walks of life. Of all the people who deserve my gratitude, my family was perhaps the most vital in shaping my abilities to succeed and commitment to persevere through the last five years. I offer a thousand, thousand thanks to my mom, Winnie, my father, Peter, and my brother Chris. Your support throughout this endeavor has been astounding.

The hardships encountered the last five years have also been endured through the love and support of one of the most amazing women I have ever known, my wife Lisa. Without you, I have no doubt I would have lost my way long ago. Your love provides me with purpose, your encouragement provides motivation, your sympathy give me solace, and who you are as a person gives me inspiration to attempt. Moreover, you have gracefully dealt with massive amounts of stress, anger, and tumultuous mood swings. Your monumental understanding, especially these last few months, has been wonderful. Thank you for being who you are and, as a consequence, what you are to me.

On a personal level, there are many others to thank. Regrettably, time and space prevent me from personalizing my thanks to all those friends who have inspired me and provided support and encouragement throughout my life and

throughout the pursuit of my PhD. It is also important to enjoy life and my friends have always helped me achieve that end. To all my friends, good friends I have now and good friends I have lost along the way, I offer my humblest and deepest gratitude.

Although deserving gratitude on a personal level, my thesis advisor, James Bamburg also deserves appreciation on a professional and intellectual level. I joined his laboratory as an ignorant, foolish apprentice who had big dreams of succeeding in science. Although subject to debate, I am now not so ignorant, nor so foolish, but I still truly believe that I can succeed in science, and this is directly attributable to the Jim's guidance and support. No one could ask for a better mentor. You have freely offered your wisdom and experience as a means for improving me as a scientists as well as a person. You have taught me the how to advance an existing paradigm as well as the progressive notion of breaking outside of conformity and going beyond convention. The training you have provided has well-equipped me with the knowledge and capabilities necessary to excel in the future and for that I am ever grateful.

The Bamburg laboratory provided an ideal environment for the excellent training and development of a scientist. Particularly, it was the personal that made it such a great place to pursue a PhD. The members of the Bamburg laboratory, both permanent fixtures, as well as transitory students and postdocs have all contributed to the successful completion of my PhD thesis. Again, I regret that I can not single out individually in what specific ways everyone has helped me, but I do want to extend special thanks to Laurie who provided a

professional and personal level of support and encouragement that uplifted my spirits when times were rough. I also extend to all JRBL's my sincere and utmost gratitude: Barb Bernstein, Laurie Minamide, Alisa Shaw, O'Neil Wiggan, Chi Pak, Mike Maloney, Hilary Bowden, Hui Hung, Lubna Tahtmouni, Patrick Sarmiere, Sankar Maiti, Judy Boyle, Jennifer Whitehall, Christy Bill, Rashmi Sampath, Janice Gonsalus, Yu Ueda, Matt Stonebreaker, Janel Funk, Shay Perea-Boettcher and Tucker Palmer. Richard Davis deserves exceptional gratitude for his generous sacrifice of time and energy improving the efficiency of the compilation and the quality of this dissertation. As an extension of the laboratory I also need to express gratitude towards the laboratory of Frank Bradke at the Max Plank Institute in Martinsried, Germany. Particularly, I would like to thank Frank and Boyan Garvalov for being great collaborators. Indeed, much of the work presented in this dissertation has been performed in conjunction with research performed in the Bradke laboratory. You have helped me see that not only is the progress of science accelerated by collaboration, but it is also made more enjoyable by working with others who are also passionate about scientific research.

Penultimately, I would like to thank my committee: Kathy Partin, Robert Honda, Mike Tamkum, and Stuart Tobet. I have learned a great deal from each of you as course instructors as well as mentors. You have helped guide me through the completion of my dissertation without leading me astray. In fact, you probably have kept me focused since my natural tendency is to tangentially pursue any idea, no matter how crazy, that arises. However, you also had to

perception to recognize some ideas that I was passionate about (waves, for example) and encourage me to pursue those ideas in an effective manner. I also need to thank you for dealing with my long committee meetings and the extensive nature of this dissertation.

Finally, I would like to dedicate my dissertation to my sister, Keri, and my brother, Michael, who have both passed from this world. More than anything else in the world, their lives and deaths has shaped who I am, who I want to be and what I want to pursue with my life. Both died of neurological-based disorders, my sister from a transparent development disease, and my brother from a veiled neurological-based malady that nevertheless claimed his life. Keri and Michael were outstanding and loving human beings who excelled in spite of whatever limitations they had. They inspired me to pursue research in neurobiology not only as a means to satisfy the longing for knowledge and understanding disease, but also as a means to advance scientific knowledge in the hope of benefiting others by contributing in any way to improve the treatment of people with neurological disorders. I thank you Keri and Michael for your love and for being in my life, showing me how to live and how not to live my life and instilling in me the desire to be a better scientist and a better person.

Table of Contents

Signature Page	ii
Abstract of the Dissertation	iii
Acknowledgments	vi
Table of Contents	x
List of Figures	xii
List of Movies	xv
Table of Abbreviations	xvi
Chapter One: Introduction	
Introduction to Neuronal Polarity	1
The Cytoskeleton	2
Actin	2
ADF/Cofilin	14
Actin binding proteins	22
Microtubules	32
Microtubule binding proteins	34
Rho GTPases	41
Cytoskeletal Dynamics in the Growth Cone	45
The cytoskeletal features of growth cones	45
Regulation of actin binding proteins during growth cone guidance	49
Actin superstructures in growth cones?	52
The Development of Neuronal Polarity	56
Hippocampal neurons as a model system	57
Intracellular trafficking	59
Trafficking during axonogenesis	59
Evolving functional domains	66
Cellular signaling pathways	68
Signaling to the Rho GTPases	68
Signaling to actin	74
Signaling to microtubules	78
Summary of dissertation	80
Chapter Two: Cdc42 regulates cofilin during the establishment of neuronal polarity	
Preface and Acknowledgement	85
Abstract	85
Introduction	86
Materials and Methods	88
Results	95
Discussion	117

Chapter Three: Evidence for the synergistic regulation of myosin inhibition and cofilin activation during axon formation	
Abstract	135
Introduction	136
Materials and Methods	139
Results	142
Discussion	165
Chapter Four: Growth cone-like waves transport actin, increase growth cone dynamics and contribute to axon formation and branching	
Abstract	180
Introduction	181
Materials and Methods	183
Results	190
Discussion	238
Chapter 5: General Discussion and Future Directions	
General Discussion	246
A unified model for cdc42, myosin II, cofilin and waves during neuronal polarization	247
Future Directions	253
References	272

List of Figures

Figure 1.1	Neuronal Morphology (polarity)
Figure 1.2	Cytoskeletal organization of growth cone
Figure 1.3	G-actin and F-actin structure
Figure 1.4	Actin treadmilling
Figure 1.5	ADF/Cofilin structure
Figure 1.6	ADF/Cofilin regulation of actin dynamics
Figure 1.7	Other actin binding proteins
Figure 1.8	Myosin II and actomyosin contraction
Figure 1.9	Microtubule dynamics
Figure 1.10	Microtubules binding proteins
Figure 1.11	Rho GTPases and signaling to AC in growth cones
Figure 1.12	Growth cone dynamic
Figure 1.13	Model of actin at the leading edge of growth cones
Figure 1.14	The Stages of Neuronal Development
Figure 1.15	Stage 2-3 transition: changes in intracellular trafficking
Figure 1.16	Signaling pathways during the establishment of neuronal polarity
Figure 1.17	Stage 2-3 transition: changes in the cytoskeleton
Figure 1.18	Stage 2-3 transition actin, microtubules and total cofilin
Figure 2.1	Cdc42 depletion <i>in vivo</i>
Figure 2.2	Analysis of the phenotype of Cdc42 knock-out hippocampal neurons
Figure 2.3	The polarization defects are rescued by cdc42 re-expression and actin depolymerization but not affected by inhibition of apoptosis
Figure 2.4	Transient actin depolymerization rescues axon formation in cdc42 knockout neurons
Figure 2.5	Effects of Cdc42 ablation on the actin cytoskeleton
Figure 2.6	Microtubule organization in the enlarged growth cones of Cdc42 null neurons
Figure 2.7	Rho and Rac activity and Par polarity complex in wild type and Cdc42 knockout neurons
Figure 2.8	The level of cofilin phosphorylation in Cdc42 knock-out neurons is increased
Figure 2.9	The phosphorylation of cofilin, but not profilin II is strongly enhanced in Cdc42 mutants
Figure 2.10	Active cofilin is enriched in axonal growth cones
Figure 2.11	Wildtype and unphosphorylatable cofilin enhance axonogenesis
Figure 2.12	Characterization of Cofilin/ADF expression in mouse hippocampal neurons and quantification of adenovirus-mediated cofilin siRNA silencing
Figure 2.13	Cofilin is necessary for axon formation

Figure 2.14	Inhibition of GSK-3 and PAK further suppresses the axon forming capacity of Cdc42 null neurons
Figure 3.1	Expression levels of active myosin and cofilin changes during neuronal development.
Figure 3.2	The levels of pMLC are higher in more mature neurons in the same culture
Figure 3.3	Localization of active myosin and cofilin in during neuronal development.
Figure 3.4	Active myosin and active cofilin have distinct localization in the presumptive axonal growth cone of stage 2+ neurons and in the axonal growth cone of stage 3 neurons
Figure 3.5	Active myosin and active cofilin have distinct localization in the presumptive axonal growth cone of stage 2+ neurons
Figure 3.6	Increasing inhibition of myosin II with blebbistatin is directly correlated to increasing axonogenesis
Figure 3.7	Myosin II inhibition results in increased neurite branching
Figure 3.8	Blebbistatin has rapid effects on neurite elongation and branching
Figure 3.9	Cofilin over-expression and myosin inactivation have a synergistic effect on axonogenesis.
Figure 3.10	IGF-1 alters cofilin and myosin II activity.
Figure 3.11	ROCK inhibition affects cofilin and myosin activity.
Figure 3.12	Myosin II activity is increased in cdc42 KO brain.
Figure 3.13	Myosin inactivation and cofilin activation rescue axon formation in cdc42 KOs.
Figure 4.1	DiI labeling of neurons within an organotypic hippocampal slice.
Figure 4.2	Wave traveling in the anterograde direction
Figure 4.3	Waves are growth cone-like structures that propagate along the lengths of neurites.
Figure 4.4	Waves have a similar composition as growth cones
Figure 4.5	Waves are involved in the formation and growth of neurite branches.
Figure 4.6	Waves support the formation and growth of new neurite arbors
Figure 4.7	Wave frequency and impact on neurite growth are associated with axonogenesis.
Figure 4.8	Proteins associated with axon growth localize to waves.
Figure 4.9	NT-3 has substrate-dependent effects on axonogenesis, neurite branching and wave frequency
Figure 4.10	Inhibition of myosin II influences wave dynamics
Figure 4.11	Active myosin II is enriched in advance of and in the wake of waves
Figure 4.12	Cofilin activity may be involved in wave propagation.
Figure 4.13	Waves increase growth cone size and dynamics

Figure 4.14	Wave-mediated changes in growth cone dynamics depends on the existing dynamics of the growth cone when waves arrive
Figure 4.15	Waves transport actin
Figure 4.16	Waves increase actin levels in the growth cone
Figure 4.17	Cofilin travels in waves
Figure 4.18	Wave-like structures occur <i>in vivo</i>
Figure 4.19	Waves can be visualized in neurons within hippocampal slices by DiI labeling their membrane
Figure 4.20	Waves occur in Thy1-YFP labeled neurons in hippocampal slices
Figure 4.21	Waves occur in neurons expressing GFP-actin in hippocampal slices: waves contribute to branch growth in hippocampal slice cultures
Figure 5.1	A comprehensive model for the role of cdc42, cofilin, myosin II and waves during neuronal polarization
Figure 5.2	Arp2/3 localization in developing neurons
Figure 5.3	siRNA-mediated silencing of Arp3 depresses axon formation in a cell-cell contact dependent manner
Figure 5.4	Growth cone motility is decreased in neurons with depleted cofilin levels.
Figure 5.5	Photoactivation of PA-GFP-actin can be used to follow retrograde actin flow in growth cones
Figure 5.6	EB-1-GFP dynamics in growth cones allows tracking of microtubule tips
Figure 5.7	NT3 affects ADF/Cofilin phosphorylation in neurons

List of Movies (Supplemental CD)

Movie 1.1	Growth cone actin dynamics
Movie 2.1	Phase contrast time-lapse movie of wild-type neuron.
Movie 2.2	Phase contrast time-lapse movie of cdc42 knockout neuron
Movie 3.1	DIC time-lapse movie of hippocampal neuron before blebbistatin treatment
Movie 3.2	DIC time-lapse movie of hippocampal neuron after blebbistatin treatment
Movie 4.1	DIC time-lapse movie of propagating “wave”
Movie 4.2	DIC time-lapse movie of wave induction of neurite branching
Movie 4.3	Waves occur more frequently in the developing axon during the stage 2-3 transition
Movie 4.4	DIC time-lapse movie of waves before myosin inhibition with blebbistatin.
Movie 4.5	DIC time-lapse movie of waves after myosin inhibition with blebbistatin
Movie 4.6	DIC time-lapse movie of growth cone before and after wave arrival
Movie 4.7	DIC time-lapse movie of growth cone before and after wave arrival
Movie 4.8	Time-lapse movie of RFP-actin traveling in a wave
Movie 4.9	Pseudocolor time-lapse movie of fluorescent actin in a wave
Movie 4.10	Reconstructed time-lapse movie of DiI labeled neuron in hippocampal slice; a wave traveling in 3D
Movie 4.11	Time-lapse movie of GFP-actin in a hippocampal slice; evidence for wave induction of neurite branching <i>ex vivo</i>
Movie 5.1	Time-lapse movie of RFP-actin in the growth cone of a neuron expressing control siRNA
Movie 5.2	Time-lapse movie of RFP-actin in the growth cone of a neuron expressing cofilin siRNA
Movie 5.3	Time-lapse movie of photoactivatable-GFP-Actin in a growth cone; retrograde flow of actin

Table of Abbreviations

A	Alanine
aa	Amino Acid
Ab	Antibody
ABPs	Actin Binding Proteins
AC	ADF/Cofilin
APC	Adenomaous Polyposis Coli
Arp2/3	Actin Related Protein 2/3
CA	Constitutively active
CaM kinase-II	Calcium Calmodulin-dependent Kinase II
CBS	Cytoskeletal-buffering solution
CIN	Chronophin Phosphatase
CRMP2	Collapsin Response Mediated Protein
CytoD	Cytochalasin D
div	Days in Vitro (vitro in this case is in culture)
DIC	Differential Contrast Microscopy
DN	Dominant negative
E	glutamic acid
EB-1	End binding protein
Ena	Enabled (drosophila)
GAP	GTPase activating proteins
GAP43	growth associated protein 43
GEF	guanine nucleotide exchange factor
GSK3 β	glycogen synthase kinase 3 beta
HMW	High molecular weight, in reference to tropomyosins
ILK	integrin-linked kinase
KO	knock-out
Jasp	Jasplakinolide
LatA	Latrunculin A
LIM	Lis-11, Isl-1, Mec-3
LIMK	Lim kinase
LMW	low molecular weight, in reference to tropomyosins
MAG	myelin associated glycoprotein
MAP	Microtubule associated protein
Mena	Mammalian Enabled
MLC	Myosin Light Chain
MLCK	Myosin Light Chain Kinase
MLCP	Myosin Light Chain Phosphatase
MHC	Myosin Heavy Chain
MTOC	Microtubule organizing center
PA	Photo-Activation
Par	<i>Partitioning</i> (cell division defects)
PBS	Phosphate Buffered Saline
PDK	phosphoinositide-linked kinase
PIP ₂	Phosphatidylinositol-4,5-bisphosphate

PTEN	phosphatase and tensin homolog
pAC	phosphorylated ADF/Cofilin
pMLC	phosphorylated Myosin Light Chain
S	Serine
siRNA	small interfering RNA
SSH	Slingshot
LimK	Lim kinase
PAK	p21 activated Kinase
ROCK	Rho-activated kinase
TesK	testicular kinase
+Tips	Microtubule plus end tacking proteins
WASP	Wiskott-Aldrich-syndrome protein
WAVE	WASP family Verprolin-homologous protein
wt	wild-type

Chapter 1: Introduction

The role of the cytoskeleton and intracellular trafficking in the establishment of neuronal polarity

Overview of Neuronal Polarity

Neurons are morphologically complex cells, typically extending from their soma multiple thin neurites that can traverse extensive distances and convoluted pathways to connect with other cells. This morphology imparts a single neuron with the unique properties of being able to receive input from one area and transmit a signal to another region which may be a long distance from the initial input. An example of a more complex neuron is an upper motor neuron in the cerebral cortex, which is multipolar with several branching dendrites networking near the soma and one long axon (up to several thousand times the diameter of the cell body) that extends down the spinal cord to synapse on a lower motor neuron in the anterior horn. Other neurons need not be so complex. An example of a neuron with a simpler morphology, very limited extensions and connectivity is a GNRH neuron in the basal forebrain, which can be round with one or two processes extending only micrometers away from the cell body. Despite their obvious differences, both of these neurons, the motor neuron and the simple GNRH neuron, have a very fundamental and basic feature that defines how all neuron functions: they are polarized (Figure 1). The basic structural polarization of a neuron imparts how it receives electro-chemical signals in the soma and dendrites and transmits signals to the post-synaptic target via the axon. Although there are higher levels of polarization and specialization that vary from neuron to neuron, the basic polarization is almost ubiquitous, with one notable exception: dorsal root ganglion neurons have one bifurcating “axon” which extends into the periphery in one direction and into the spinal cord in the other. However, even this neuron has distinct compartmentalization (or polarization) that is necessary for its functionality.

How do neurons become polarized? This simple question in developmental

neuroscience is one that has received tremendous attention in recent years. With all that attention, it is not surprising that significant advances have been achieved in understanding the development of neuronal polarization. As a model system, hippocampal neurons have been the subject of most studies on the subject but the vast findings in this system are certainly applicable to other neuron types. These findings have suggested that the regulation of the cytoskeleton, both actin and microtubules, are essential for proper development of neuronal polarity. The regulation of intracellular transport for the segregated delivery of cellular material is also important. Thus, this introduction will review the cytoskeleton and intracellular transport and how these aspects of cell physiology are managed during the development of a polarized neuron.

The Cytoskeleton

In neurons, like all cells, networks of fibrous elements including actin, microtubules, and intermediate filaments not only provide structural support but also facilitate the intracellular movement of the organelles, chromosomes, proteins and RNAs. Moreover, the movement of the cell itself relies upon the dynamic changes in these cytoskeletal elements. This is exemplified by the growth cone, the highly motile tip of growing neurons. Actin dynamics are vital for determining growth cone motility and its ability to properly navigate, but it is microtubules that are the driving force behind neurite extension. There are various types of actin networks (or superstructures) in the peripheral domain of growth cones while microtubules comprise the central region of the growth cone (Figure 2). Since both of these cytoskeletal elements are crucial for growth cone behavior and axon formation, a conceptual basis of actin and microtubules is necessary for a complete understanding of the regulation of neuronal polarization.

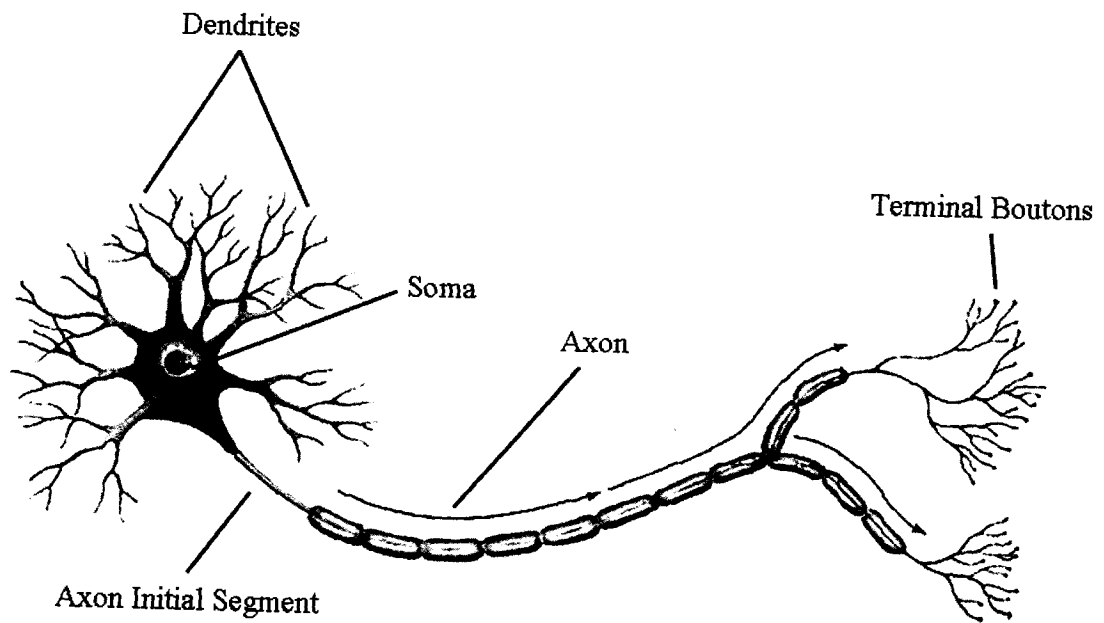
Actin

Actin structure and function

Actin is one of the most abundant proteins in the eukaryotic cell, comprising 1-15 percent of

Figure 1.1. The morphology of a polarized neuron. Shown here is a generic neuron. All neurons, regardless of type, polarize into discrete functional domains. The most fundamental specializations are those of the somatodendritic compartment and the axon. These regions or domains are specialized for either receiving (somatodendritic compartment) or transmitting (axons) signals that underlie all neuronal communication. The regions of a neuron can further be subdivided based on even greater levels of specialization, based on function and the underlying molecular composition. Typically, neurons have one or more dendrites, a soma, an axon and terminal boutons. Although these regions are different in morphology, they also differ in their physiological function. The dendrites are the input component, the soma is the integrative component, the axon is the conductile component, and the terminal boutons are the output component. Different regions contain distinct repertoires of signaling proteins, cytoskeletal elements, and membrane components. For example, dendrites are enriched in neurotransmitter-gated ion channels, allowing for the proper reception of a synaptic input. Axons are enriched in voltage gated sodium and potassium channels which are responsible for the propagation of an action potential.

The Morphology of a Polarized Neuron



total cellular protein. As such, it is not surprising that it is essential to cell viability. This is due to its crucial role in many indispensable cellular processes including the maintenance of structural integrity of the cytoplasmic matrix, cell locomotion, cell division, organelle transport, endo- and exocytosis, and, in differentiated cells it has more specialized functions, for example contraction of smooth, cardiac and skeletal muscle. Through its interaction with a plethora of proteins, actin has pervasive influence in these diverse cellular activities. Given such important functions, actin is a favorite protein among scientists, with books dedicated solely to it. Therefore, this section will only provide a brief review of actin as needed for understanding growth cone motility.

Encoded by a large highly conserved gene family, actin is ubiquitous among eukaryotes (Pollard et al., 2001). Single-celled organisms typically have one actin gene, whereas multicellular organisms may have multiple actin genes; humans, for example, have six actin genes which encode β -actin, γ -actin and four α -actin isoforms. The actin expression profile also varies in different tissues; skeletal muscle expresses the three major isoforms, α -actin being the predominant form, with β -actin and γ -actin expressed in lower levels. Neurons have two isoforms, β -actin and γ -actin, which are expressed at near equal levels. Although they are over 90% identical and have analogous biochemical properties, β -actin and γ -actin seem to have distinct functions *in vivo*. One important difference is N-terminal arginylation that occurs only on β -actin, which may explain why these isoforms form distinct actin structures (Kashina, 2006). These isoforms and the mRNAs giving rise to them are differentially localized in neurons, as well as in other cells, and this may impart specialized and important spatial differences in the regional actin networks in the cell. γ -Actin localizes in the cell body and is enriched in stress fiber-like structures (Otey et al., 1986; Kashina, 2006)), whereas β -actin is localized to the dynamic actin networks in growth cones (Bassell et al., 1998).

Actin exists in two forms, a monomeric, globular form (G-actin) and a polymerized, filamentous form (F-actin). In its monomeric state, G-actin, an average size protein (~42kD), is thought to be “in limbo,” pending conditions that will accelerate its reincorporation into an

actin filament. An actin monomer has four sub-domains with a repeating motif consisting of a multi-strand β -sheet, a β -turn, and a right-handed $\beta\alpha\beta$ -unit (Aguda et al., 2005). In between subdomains II and IV there is deep nucleotide binding cleft that typically is occupied by a Mg^{2+} ion in complex with either ATP, ADP-Pi, or ADP (Figure 3A; Pollard et al., 1992). In a cell, ATP bound G-actin predominates, whereas ADP-Pi and ADP bound actin subunits predominate in actin filaments. Although not necessary for actin polymerization *in vitro*, these nucleotide binding properties of actin have important implications for the behavior of actin filaments in cells as we shall discuss later.

Actin filaments are long polymers of G-actin formed in two parallel strands twisted around each other into a helical formation (Figure 3B). The twist in F-actin confers differences in the thickness along the filament observed in two dimensional flattened images, where it alternates at regular intervals between a thinner diameter (7nm) and a thicker diameter (9nm) depending on how the helical twist is being observed. Although no X-Ray crystal structure of F-actin has been obtained, other imaging methods such as high resolution electron cryomicroscopy contributed to a general consensus for a model of F-actin as a two start, right-handed long-pitch helix. In this model there are 24-28 monomers per helical turn and a twist of -167° between consecutive monomers with an axial rise of 2.75nm (Bamburg et al., 1999; McGough et al., 1997). There is a second, more twisted form of F-actin that occurs as a minor stable form at room temperature (Galkin et al., 2001) in which consecutive monomers have a -162° rotation. The twisted state of an actin filament is influenced and/or maintained by the presence of actin binding proteins such as ADF/Cofilin.

The assembly of F-actin will occur *in vitro* under physiological salt conditions; G-actin will assemble into actin filaments in three phases. *In vitro* this occurs without the presence of any other proteins or catalytic substances. This self-organizing capability of actin is an important feature of actin with implications in the cell. *De novo* actin assembly *in vitro* is rate-limited by nucleation, the first phase of actin polymerization, in which three subunits must come together to provide a stable nucleus. *In vivo*, however, the presence of actin nucleators greatly accelerates *de novo* actin assembly (Zigmond, 1993; see below). Once a nucleus forms, the elongation phase of polymerization begins and a filament is

Figure 1.2. Actin superstructures in neuronal growth cones. **A.** The model growth cone has been classically subdivided into three distinct regions: the peripheral domain (shown in yellow), the central domain (shown in blue), and the transition domain (shown in green). In the peripheral domain at least two actin superstructures exist, underlying the major morphological features of growth cones. Linear actin bundles comprise filopodia, which protrude outward, and mesh-like gels comprise the lamellipodia (called veils when in between filopodia). In the transition domain transverse bundles of actin filaments, called actin arcs are present. The central domain is largely void of actin, but is rich in microtubules and organelles. **B.** An axonal growth cone portrays the major features of a growth cone represented schematically in A. The central domain contains microtubules (red) which splay out from the neurite shaft. The peripheral domain consists of actin-rich (green) filopodia and lamellipodia. Importantly, there are the occasional microtubules that splay out into the peripheral domain along F-actin bundles.

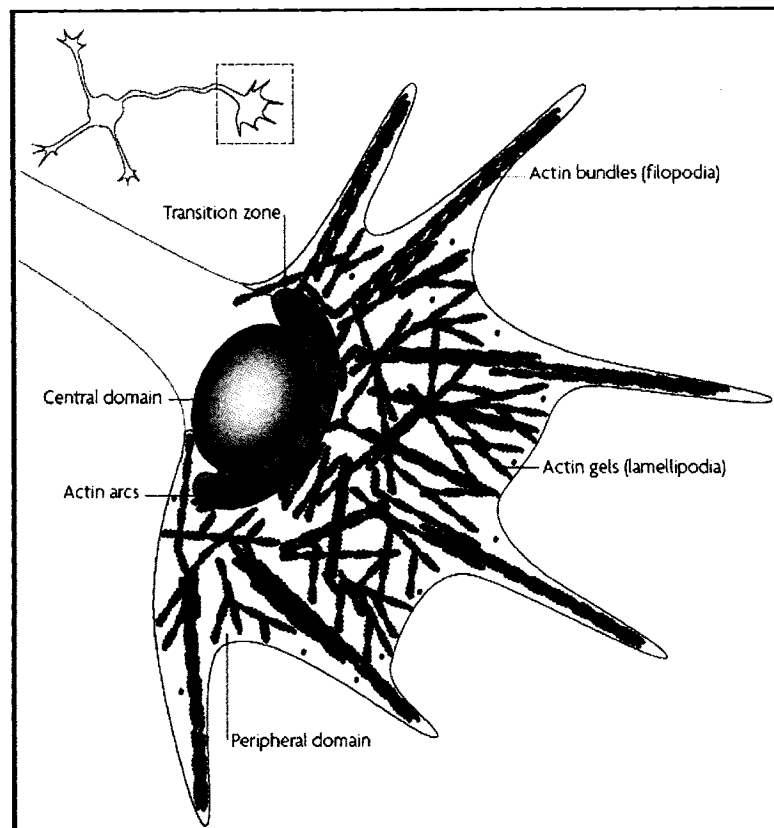
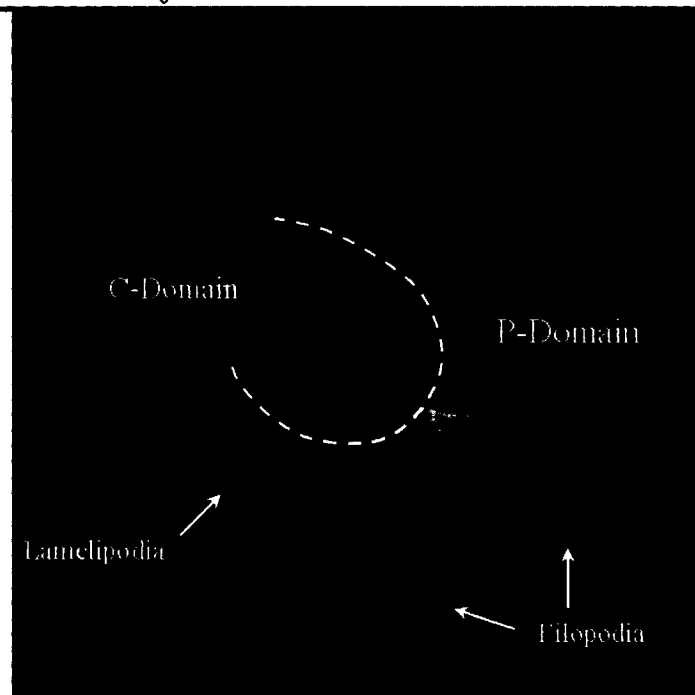
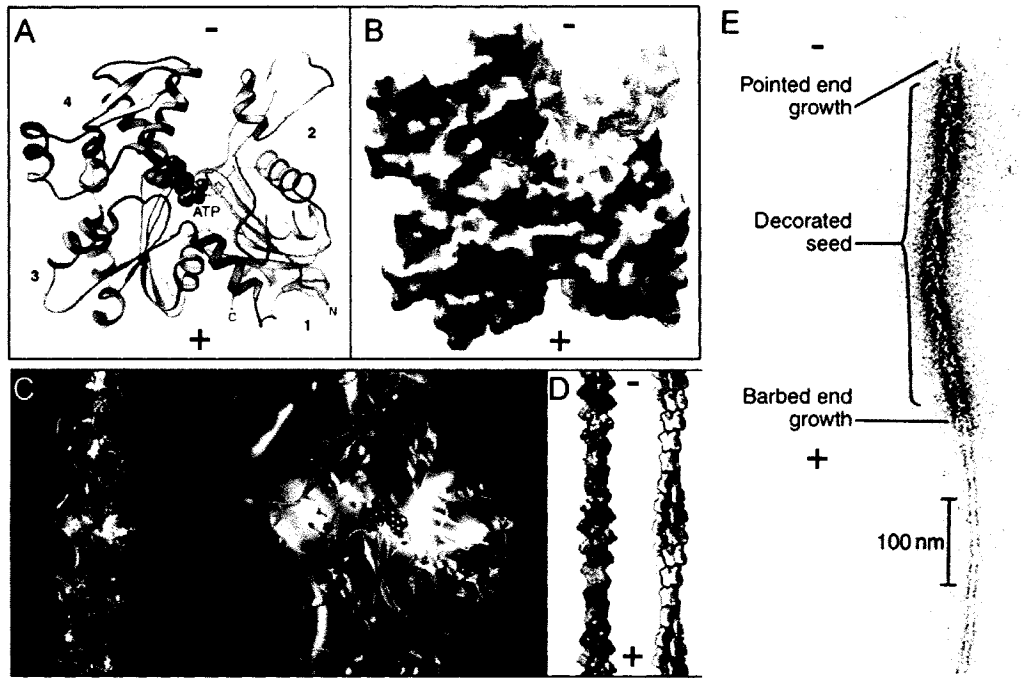
A**B**

Figure 1.3. The Structure of G-actin and F-actin. **A.** A ribbon model of the atomic structure of G-actin is shown. The polypeptide folds and the location of Mg-ATP are clearly illustrated. **B.** Surface rendering of the atomic structure of G-actin is shown. G-actin has four subdomains with the ATP binding occurring deep in the cleft between subdomains 2 and 4. Subdomains 2 and 4 of the actin monomer are oriented towards the pointed (minus) end of F-actin, whereas subdomains 1 and 3 are oriented towards the barbed (plus) end of F-actin. The structure of F-actin is shown in C-E. **C.** Low-resolution (left) and high-resolution (right) reconstruction of an actin filament from electron micrographs with the ribbon models of individual actin subunits indicated in gold. The pointed (-) end of the filament is oriented at the top and the barbed (+) end is oriented towards the bottom. **D.** A topological rendering of the actin filament is shown with subunits in the two long-pitch helical strands indicated (yellow-orange and blue-green). The image on the right outlines individual actin subunits and more clearly illustrates the helical twist in the actin filament resulting in its varying diameter. The topology of the actin filament can change depending on the nucleotide binding status of the actin as well as the binding of other proteins; variations in the local topology of F-actin are exploited by the various actin binding proteins. **E.** An electron micrograph is shown of an actin filament seed, decorated with the S1 fragment of myosin, which was then allowed to undergo further polymerization. The decorated portion of the filament indicates the polarity of F-actin, with faster polymerization occurring at the barbed (+) end and slower growth occurring at the pointed (-) end (images adopted from Pollard and Earnshaw, 2004).

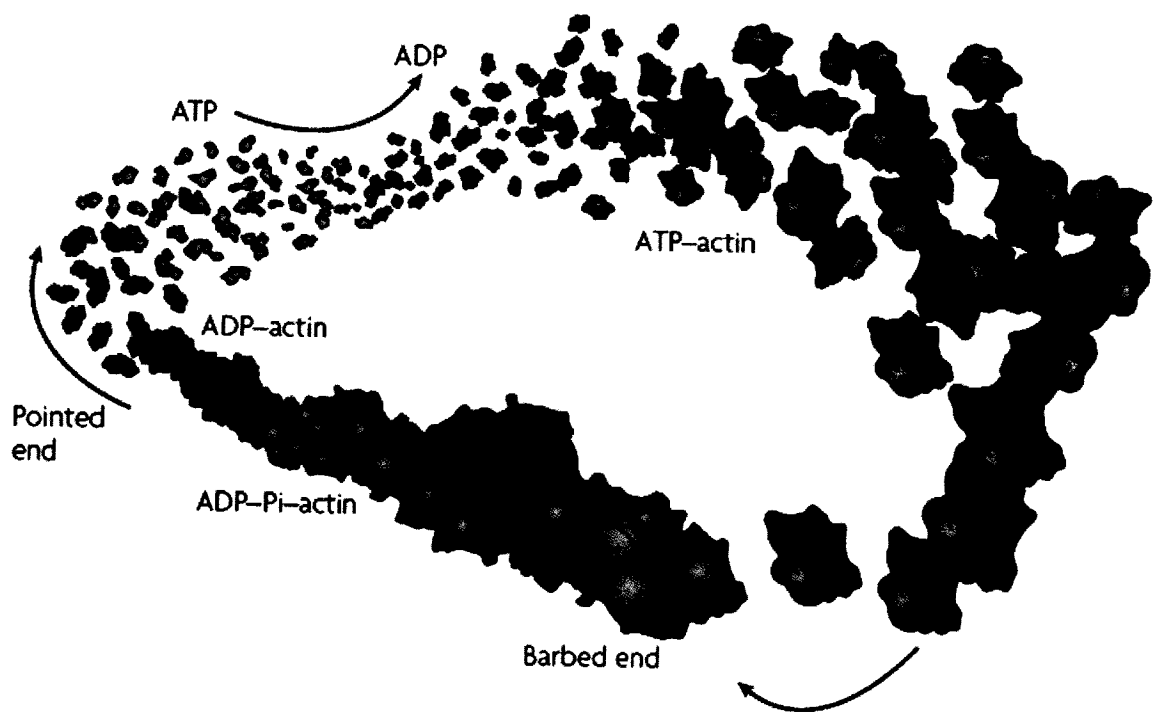


rapidly assembled with G-actin initially added to both ends. As actin assembles and the monomer pool declines, the F-actin reaches a region in which constant polymer mass is maintained (steady state). Because of differences in the equilibrium concentration of monomer necessary to maintain filament growth at each end, one end of the F-actin (pointed) begins to lose subunits under conditions where the other end (barbed) still adds subunits. The kinetic differences results from the nucleotide-binding status of actin monomers in F-actin and this confers a structural and functional polarity to the filament (Carlier, 1990).

The polarity of F-actin was first realized in myosin decoration experiments which showed that when the S1 proteolytic fragment of myosin was added to actin it resulted in an arrowhead-like decoration as viewed by electron microscopy (Figure 4). The pointed end of the arrow-like actin filaments is also called the minus (-) end because it loses subunits when actin monomer concentration has declined to a level that can still support growth of the barbed or plus (+) end. The concentration of G-actin in which the ends of the filament are in equilibrium, called the critical concentration or C_c , is $0.8\mu\text{M}$ at the pointed end, which is high compared to the barbed end, which has a C_c of $0.1\mu\text{M}$. Thus, when monomer concentration is between these values, actin subunits will be added at the barbed end and lost at the pointed end (Carlier, 1990). An individual actin subunit will incorporate at the barbed end, flow through a filament, and disassociate at the pointed end in a process called treadmilling. Treadmilling is an important feature of the actin cytoskeleton underlying cell locomotion and growth cone dynamics.

Treadmilling is reflected by ATP hydrolysis of actin subunits in the filament (Figure 4). After ATP-actin subunits are added to the plus end of the filament, the ATP rapidly hydrolyses although the inorganic phosphate (P_i) does not immediately dissociate resulting in ADP- P_i bound actin subunits. Eventually, the P_i dissociates resulting in ADP bound actin accumulating towards the minus end of the filament. Thus, the nucleotide binding status of actin subunits results in a molecular “aging” with three strata: 1. ATP bound subunits which are very young; 2. ADP- P_i subunits which are middle-aged; and 3. ADP-bound subunits which are old. In a filament at steady state growth, the three strata are kept in a quasi-equilibrium (Figure 4). This stratified polarity of an actin filament results in a

Figure 1.4. Actin treadmilling. Actin can undergo spontaneously nucleated self-assembly into a polarized, non-equilibrium, bi-helical filament. As a monomer and within filaments, actin subunits are non-covalently associated with an adenine nucleotide, forming an actin-nucleotide complex. *In vitro*, ATP-actin complexes are preferentially added to the barbed end, and barbed end incorporation is even more heavily favored in cells. Rapidly after subunit incorporation, the non-covalently bound ATP is hydrolyzed into ADP-Pi, with release of the Pi being much slower on purified actin. ATP hydrolysis occurs ~1-2 sec on average after incorporation and Pi release occurs ~600 sec on average; however, both processes are stochastic for each subunit. Thus, even when the monomer pool consists only of ATP-actin and given a sufficient amount of time to reach a steady state, an assembled actin filament will eventually consist of three actin-nucleotide complexes: ATP-actin, ADP-Pi-actin, and ADP-actin. Based on the kinetics of ATP hydrolysis and Pi release, ATP-actin subunits are preferentially located at the tip of the barbed end whereas ADP-Pi-actin and ADP-actin subunits make up the remainder of the filament. The two ends of an actin filament maintain different minimal monomer concentrations for assembly, which are referred to as the critical concentrations. When the monomer concentration rests between the two different critical concentrations, net assembly occurs at the barbed end and net disassembly occurs at the pointed end in a process called treadmilling. Thus, at steady state, the barbed end is the favored site for ATP-actin addition, while the pointed end is the favored site for ADP-actin loss both *in vitro* and in cells. In cells, actin turnover is enhanced >100 fold by actin binding proteins that sever filaments, disassemble subunits faster from the filament pointed end, sequester subunits and facilitate ATP-for-ADP nucleotide exchange on free actin subunits (Modified from Pak et al., 2008).



molecular scaffold for different actin binding proteins that have different affinities for a specific nucleotide-bound actin subunits or particular strata (Pak et al., 2008). The intrinsic heterogeneity of actin filaments are exploited by different actin binding proteins, which can compartmentalize in specific regions of actin networks and, perhaps, underlie actin superstructures in cells. This organization has important implications in neuronal growth cones (see below).

ADF/Cofilin (from Flynn et al, 2006)

ADF/Cofilin expression and activity

ADF and cofilin belong to a family of structurally and functionally related proteins, ~19 kD in size, collectively known as the ADF/cofilin (AC) family (Figure 5). AC proteins are expressed in all eukaryotic organisms. Yeast and other unicellular eukaryotes carry only one gene for AC, which is essential for viability. Metazoans typically have multiple genes encoding AC proteins (Lappalainen et al., 1998). In mammals, there are three separate genes encoding AC proteins: actin depolymerizing factor (ADF), the ubiquitously expressed non-muscle cofilin (cof1), and the muscle-specific cofilin (cof2b). Cof-2 mRNA can undergo alternative splicing to yield a minor isoform (cof-2a), which is expressed in some non-muscle cells (Thirion et al., 2001). The proteins encoded by cof2a and cof2b mRNAs are identical.

ADF was the first member of this family identified. Isolated from embryonic chick brain, ADF was characterized as an actin-binding protein that depolymerizes actin filaments (Bamburg et al., 1980). Cofilin was later identified and named from its ability to form cofilamentous structures with actin (Nishida et al., 1984). Shortly thereafter, ADF and cofilin were discovered to share sequence homology with other related proteins across phylogeny, and have more recently been referred to as the ADF/cofilin or AC protein family (Bamburg, 1999). The AC proteins bind to actin in a 1:1 stoichiometry (Giuliano et al., 1988; Nishida, 1985) but exhibit a higher affinity for ADP-actin than for ATP- or ADP-Pi-actin subunits either in F-actin or as monomers (Carlier et al., 1997; Maciver and Weeds, 1994; Rosenblatt et al., 1997). AC proteins bind filamentous ADP-actin subunits in a self-cooperative manner;

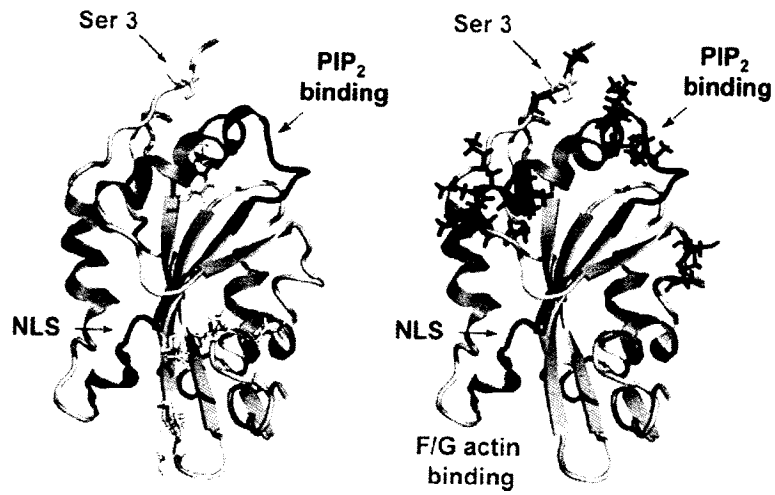
the binding of cofilin promotes further cofilin binding to the same filament. This is thought to occur because cofilin stabilizes a 'twisted' topology of the actin filament, and creates a surface environment that favors more cofilin binding (Figure 5; Pak et al., 2008). The AC proteins enhance actin dynamics by two mechanisms; they facilitate monomer loss from the actin filament pointed end and induce severing of the filaments into shorter oligomers (Figure 6; (Carlier et al., 1997; Maciver, 1998). Although ADF and cofilin are very similar from a functional perspective and each can rescue basic actin-dependent events when expression of the other has been silenced (Hotulainen et al., 2005), they exhibit some nuanced differences that may prove physiologically relevant (Ono and Benian, 1998; Vartiainen et al., 2002; Yeoh et al., 2002; Chen et al., 2004; Yamashiro et al., 2005; Estornes et al., 2007). For example, in vitro, ADF enhances pointed end monomer loss more efficiently and maintains a larger unassembled actin pool, whereas cofilin severs F-actin more efficiently, and when present at high stoichiometry with actin, nucleates actin assembly (Chen et al., 2004; Andrianantoandro and Pollard, 2006). Thus, activation of AC within a cell may lead to depolymerization of actin filaments in one region and a net assembly of F-actin in another region, depending on the localized pools of actin monomer, actin sequestering proteins, and barbed-end capping proteins available in each locale. As a result, the AC proteins should be considered actin dynamizing proteins (Figure 6; Carlier et al., 1997) that can disassemble the existing actin infrastructure to allow for the resurrection of a newer one.

Mechanisms of AC Regulation.

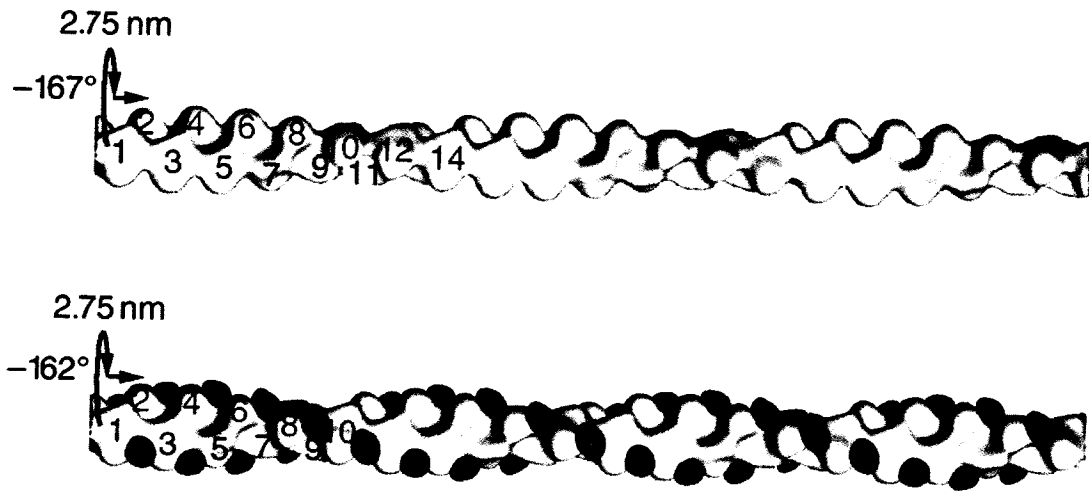
There are multiple mechanisms for regulating the AC proteins, which include phosphorylation/dephosphorylation (phosphoregulation), binding to and release from phosphatidylinositol phosphates, sequestering and delivery by 14-3-3 scaffolding proteins, and pH. In addition, the effects of AC on actin dynamics can either be inhibited or synergized by the activities of other actin-binding proteins. Homologues of yeast actin interacting protein 1 (Aip1), also called WD repeat 1 (WDR1) in chicken and mammals and unc78 in *C. elegans*, enhance the severing activity of cofilin (Ono et al., 2004); (Clark and Amberg, 2007), whereas many isoforms of tropomyosin compete with cofilin for binding to F-actin

Figure 1.5. The structure of human cofilin and cofilin decorated actin filaments. A. A ribbon model of the structure of cofilin is shown. All members of the ADF/cofilin (AC) family contain a highly conserved domain, called the ADF homology domain. This domain is highly folded with a mixed β -sheet between two pairs of α -helices. The regulatory phosphorylation site Serine 3 (Ser 3) and PIP_2 binding site (blue) are also indicated. AC proteins have two distinct actin binding surfaces indicated in yellow (F-actin) and red (F-actin and G-actin). When bound to F-actin, AC proteins make contacts with two adjacent actin monomers in the filament (adopted from Funk and Bamberg, 2007). **B.** Cofilin binds to and stabilizes a naturally twisted minor conformation of F-actin and this binding weakens longitudinal contacts between actin protomers. Shown are reconstructions obtained from electron cryomicroscopy of two conformations of F-actin. In the more abundant form of F-actin (top) an actin subunit is related to the adjacent subunit in the filament by an axial rise of 2.75nm and a rotation of -167° . In cofilin (blue ovals) decorated filaments (bottom), the actin filament is twisted approximately 5° per subunit (rotation of -162°) (adopted from Bamberg et al, 1999).

A



B



and reduce filament severing and turnover (Bryce et al., 2003) (Ponti et al., 2005). The dynamics of AC-induced filament turnover are increased by the Srv2/CAP protein, which enhances nucleotide exchange on AC-bound ADP-actin (Moriyama and Yahara, 2002); (Balcer et al., 2003), and by profilin, which enhances nucleotide exchange on G-actin (dos Remedios et al., 2003). However, considering that phosphoregulation has been a dominant point of focus within growth cones, this *section* will devote itself exclusively to this mechanism (Figure 6). By doing so, we do not imply that the other regulatory mechanisms are irrelevant or uninteresting. On the contrary, we hope to encourage future research in these areas, which have been largely overlooked.

The phosphoregulation of AC proteins was first identified by recognizing that dephosphorylated ADF retained its ability to depolymerize F-actin, whereas the phosphorylated species did not (Morgan et al., 1993). The single regulatory site of phosphorylation, serine 3 on the immature mammalian protein, was later identified for both ADF (Agnew et al., 1995) and cofilin (Moriyama et al., 1996). Phosphorylation at this penultimate residue of the demethionated and N-acetylated protein (Agnew et al., 1995; (Kanamori et al., 1998) compromises an important AC-actin interaction without significantly altering AC structure, resulting in the severely reduced ability of AC proteins to bind to F-actin (Blanchoin et al., 2000). Given the importance of AC phosphoregulation, mutants that harbor a disruption of the phosphoregulatory site were designed, which include a serine 3 to alanine (S3A) mutant and a serine 3 to glutamate or aspartate (S3E or S3D) mutant. The unphosphorylatable S3A mutant is considered to be 'in the active state' as it precludes inactivation by phosphorylation, although regulation by other mechanisms (pH, PIP_2 -binding, etc) can still occur. The phosphomimetic S3E or S3D mutant is non-activatable and may exhibit inhibitory effects possibly through its sequestering of regulatory proteins that have a high affinity for phosphorylated AC species, such as 14-3-3 proteins (Gohla et al., 2005) or the AC phosphatases. From a naïve perspective, the S3A and S3E mutants are often regarded diametrically and are utilized and interpreted in such a context. However, in particular situations, the S3A and S3E mutants may actually induce comparable effects, or the S3E mutant may have no effect at all. Therefore, the most reliable means of probing the

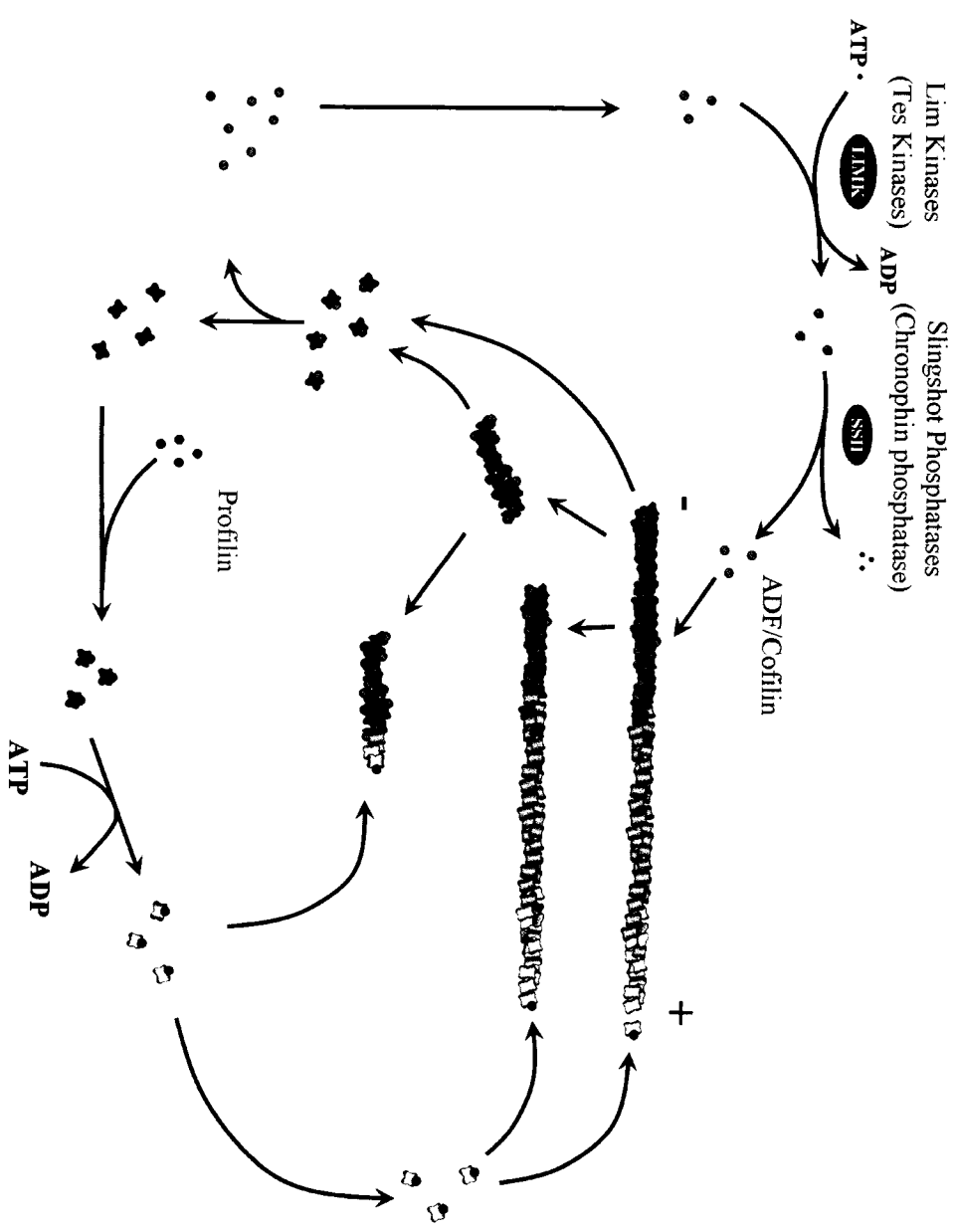
effects of prolonged AC inactivation is accomplished by the experimental downregulation or genetic loss of function of endogenous AC proteins. The S3A, S3E, and S3D mutants will be collectively referred to as the phospho-mutants.

Phosphorylation (inactivation) of AC proteins is subserved by two AC specific protein kinase families: the LIM kinases (LIMK) and the Tes kinases (TESK). However, of these kinases, only the two isoforms of the LIM kinases, LIM kinase 1 (LIMK-1) and LIM kinase 2 (LIMK-2), have been demonstrated to be appreciably expressed in neurons. In fact, the highest level of LIMK mRNAs is found in the brain (Mizuno et al., 1994). The LIM kinases contain two repeated LIM domains and a PDZ domain. The LIM (*lin-11*, *isl-1*, and *mec-3*) domain is a stretch of 50 to 60 amino acids rich in cysteines and histidines, which organize into double zinc fingers (Dawid et al., 1998). The PDZ (*PSD-95*, *Discs-large*, and *ZO-1*) domain contains two important sub-motifs, a guanylate kinase-like and SH3 motif (McGee and Brecht, 1999). Importantly, both the LIM and PDZ domains mediate protein-protein interactions. For the LIM kinases, the LIM domain proves especially critical for its self-association into a dimer complex (Hiraoka et al., 1996). Many signaling mechanisms exist to regulate the LIM kinases. In growth cones of cultured primary hippocampal neurons, LIM kinase 1 is regulated in part by ubiquitination through the ubiquitin ligase, Rnf6 (Tursun et al., 2005). In addition, the LIM kinases are activated by two upstream kinase families, the Rho kinases (ROCK) and the p21-activated kinases (PAK) (Maekawa et al., 1999); (Edwards et al., 1999). The ROCK and PAK family of kinases are stimulated by the Rho family of small GTPases (Manser et al., 1994); (Leung et al., 1995)). These participants comprise a complete signaling mechanism that eventually leads to AC protein inactivation by phosphorylation.

Dephosphorylation (activation) of the AC proteins is subserved by two AC protein phosphatases: the slingshot phosphatases (SSH; (Nagata-Ohashi et al., 2004)) and the chronophin phosphatases (Figure 6; Gohla et al., 2005). Though AC specific protein phosphatases have been identified, nonspecific protein phosphatases may also be capable of dephosphorylating the AC proteins (Samstag and Nebl, 2003). Regrettably, considerably less is known regarding dephosphorylation signaling mechanisms. Only within the last year has

Figure 1.6. ADF/Cofilin activity and Phosphoregulation. ADF and cofilin enhance actin dynamics by severing and increasing the off-rate of actin monomers from the pointed (-) end of actin filaments. In an actin filament undergoing treadmilling, ATP-actin (white) incorporates at the barbed (+) end of the filament and undergoes rapid hydrolysis becoming ADP-Pi-actin (tan actin). Pi release eventually occurs resulting in ADP-actin (brown actin) dominating the composition of the filament near the pointed (-) end. ADF/cofilin binds preferentially to ADP-actin subunits in actin filaments and leads to increased depolymerization and severing. LIM or TES kinases phosphorylate and inactivate ADF/cofilin; slingshot or chronophin phosphatases remove the phosphate and reactivate ADF/cofilin. 14-3-3 (not shown) binds to phosphorylated ADF/cofilin and limits the accessibility of some phosphatases, restricting dephosphorylation. ADP-Actin monomers released from the pointed ends of filaments can be recycled into a polymerization competent pool of G-actin. Profilin (and Srv2/CAP1) can bind to ADP-actin monomers and enhance the rate of ADP/ATP exchange. ATP-actin monomers are then poised for incorporation onto the plus (+) end of existing filaments. Furthermore, the severed actin filaments created by ADF/cofilin can also serve as new sites of actin assembly and filament growth.

ADF/Cofilin Activity and Phospho-regulation



there been some insight in the signaling mechanisms that regulate chronophin. Chronophin is regulated by hsp90 and probably requires ATP-dependent binding and release from hsp90 for activity (Gary Bokoch, personal communication). It is recruited to the membrane of non-neuronal cells in a PI3-kinase and Rac1-dependent manner (DerMardirossian, Delorme, Gohla and Bokoch, personal communication). Even for the slingshot phosphatases, regulatory mechanisms have been elucidated that affect only the SSH-1L isoform. Though a comprehensive map of regulatory mechanisms that activate or inactivate the entire family of SSH phosphatases is lacking, it still appears that regulation of SSH-1L operates through divergent but parallel pathways. SSH-1L is activated in a Ca^{2+} /calmodulin-dependent manner by calcineurin, also known as protein phosphatase 2B (PP2B), and is inhibited by binding of 14-3-3 (Nagata-Ohashi et al., 2004). Both of these mechanisms possibly affect the ability of SSH-1L to bind to F-actin, which is required for its activity (Nagata-Ohashi et al., 2004; (Soosairajah et al., 2005)). SSH-1L is negatively regulated *in vitro* through phosphorylation by PAK kinase 4 (PAK4) (Soosairajah et al, 2005). Active SSH-1L also dephosphorylates (inactivates) LIMK1 *in vitro*. Therefore, in some cells, PAK4 may function as a master switch downstream of the Rho family of small GTPases, leading to phosphorylation (inactivation) of AC proteins by the concomitant activation of the LIMK1 and inactivation of SSH-1L phosphatase. Less is known regarding the regulation of other SSH isoforms. However, it appears that other SSH isoforms have distinct sub-cellular localizations; SSH3, for example, is enriched in and around the trans-Golgi (Oneil Wiggan, personal communication). Thus, different SSHs may have unique regulatory mechanisms for specific regulation within the region of the cell in which each of these resides.

Other Actin Binding proteins

There are a plethora of actin binding proteins in eukaryotic cells, many of which have been identified in neurons. For practical purposes, here I will only briefly review those that have been implicated in important roles in regulating neuronal actin structures. Actin binding proteins can be characterized based on function, which will be the approach employed here:

actin nucleators, actin dynamizing proteins, motor proteins (myosins), actin cross-linking proteins, and lastly, a more generic classification of actin organizing proteins. After concise reviews of these proteins, we will briefly address how some of these actin binding proteins interact with and define actin superstructures in neuronal growth cones. Actin binding proteins also exhibit a binding preference to one of the three strata in an actin filament, which also confers differences in the local topology of the filament: ATP-actin, ADP-Pi-actin, and ADP-actin (Figure 7). The exploitation of the heterogeneity of the actin filament by actin binding proteins may have important functional consequences in neuronal growth cones.

Actin Nucleators Four classes of *de novo* actin nucleators that exist in neurons have been characterized: the Arp2/3 complex, formin proteins, Spir proteins, and cofilin (Mullins et al., 1998); (Pruyne et al., 2002); (Quinlan et al., 2005); Andrianantoandro and Pollard, 2006). There are important differences between these classes of actin nucleators, which shall only be considered briefly here (reviewed in (Kerkhoff, 2006); Andrianantoandro and Pollard, 2006). Most importantly, each class nucleates actin filaments through a distinct mechanism, which suggests that they participate in the assembly of different actin structures and possibly operate within distinct micro-domains of the growth cone.

A composite of seven protein subunits including two actin-related proteins and other arc proteins form the core of the Arp2/3 complex (Mullins et al., 1998). By mimicking a lateral actin dimer, the Arp2/3 complex forms a base for actin polymerization. It is widely assumed that Arp2/3 complex cannot function without a pre-existing “mother” actin filament to which it binds and initiates a branched “daughter” filament. The actions of Arp2/3 gives rise to the canonical dendritic array of branched actin filaments at the leading edge of migrating cells. The role of Arp2/3 complex in the neuronal growth cone is somewhat controversial due to conflicting data. In hippocampal neurons, this complex has been shown to localize predominately in the central domain of growth cones and Arp2/3 complex activity dampens neurite elongation, perhaps by increasing F-actin content in the central domain which can attenuate microtubule advance, the driving force behind outgrowth (Strasser et al., 2004). In rat sympathetic neurons, NGF treatment increases recruitment of Arp2/3

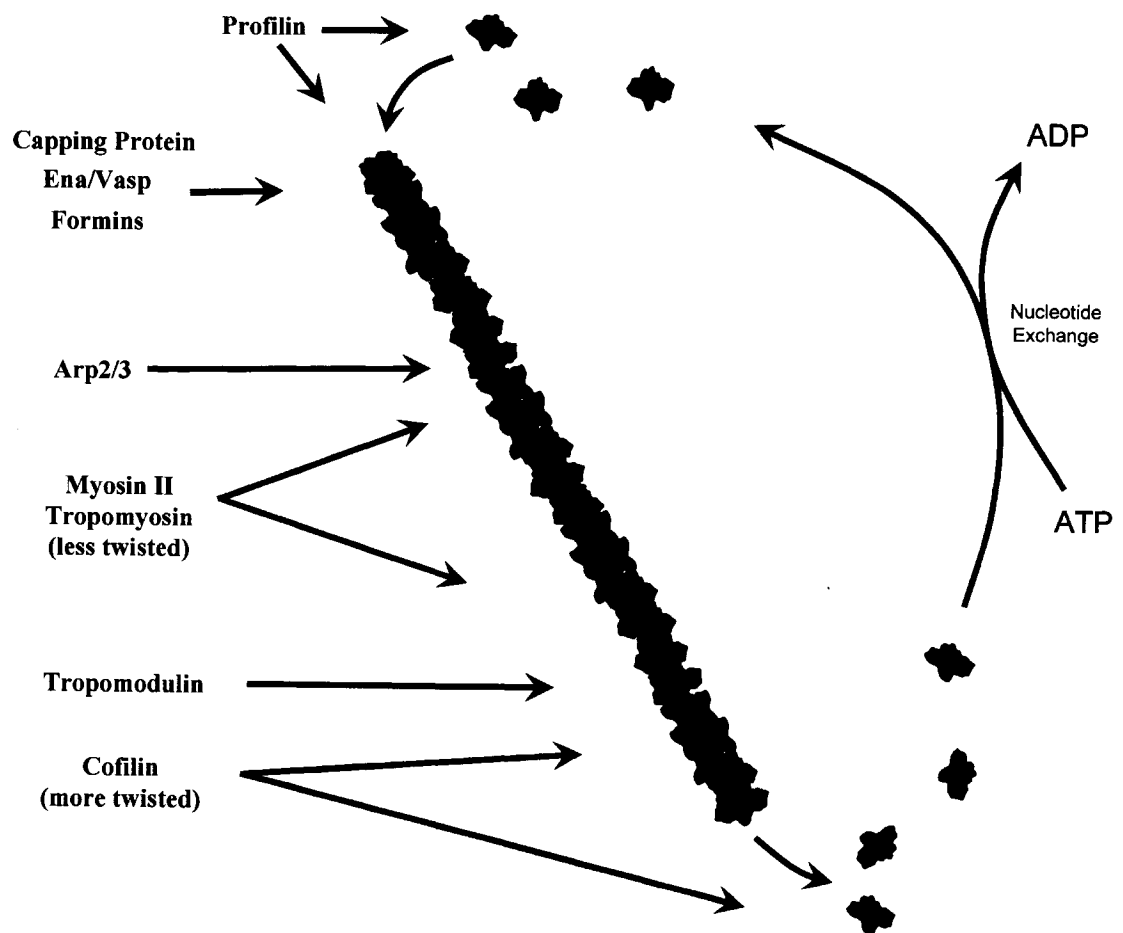
complex to the leading edge of the growth cone (Goldberg et al., 2000). Arp2/3 complex also localizes to the leading edge of chick dorsal root ganglion neurons, where it is responsible for branched actin structures similar to fibroblast lamellipodia (Mongiu et al., 2007). The differences in Arp2/3 complex localization and function may reflect intrinsic differences in different neuronal cell types.

Formins are large multidomain proteins that affect microtubules and actin. Formins are hinged dimers that bind to and stabilize two actin monomers in a conformation favorable for additional monomer incorporation (reviewed in Faix and Grosse, 2006). Instead of remaining with the pointed ends of actin as for other nucleators, formins track with the barbed ends of polymerizing actin filaments (Kovar and Pollard, 2004). There has been only one study implicating a role for formins in neuronal growth cones. In this study, mDia (mouse Diaphanous family of formins) was found to play a role in SDF-1, a neuronal cytokine, induced axon elongation in cerebellar neurons. CA-mDia over-expression mimicked SDF-1 treatment whereas DN-mDia expression or siRNA-mediated mDia knockdown suppressed SDF-1-induced outgrowth (Arakawa et al., 2003).

Spir is another actin nucleator. There is little known about the role of this protein in neurons, but its expression in neuronal tissues (Schumacher et al., 2004) suggests an important role in actin dynamics. Spir is the most recently discovered class of actin nucleators and it nucleates actin via a unique mechanism. Spir binds to four actin monomers, forming a longitudinal tetramer, which then combines with another tetramer forming an octamer nucleus (Kerkhoff, 2006). It remains associated with the pointed end of actin filaments after polymerization commences. Over-expression studies suggest spir proteins regulate Golgi dynamics and vesicle trafficking and delivery to membranes, although its role in leading edge actin has not been elucidated.

It had been postulated that through its F-actin severing activities cofilin can indirectly support actin assembly by generating new barbed ends available for nascent actin monomer growth. Indeed targeted activation of photo-caged cofilin stimulates lamellipodial protrusions (Ghosh et al., 2004). More recent evidence suggests that cofilin may directly stimulate actin assembly *de novo* ((Chen et al., 2004); Adrinantoandro and Pollard, 2006). In

Figure 1.7. Actin binding proteins prefer different strata of an actin filament. The molecular 'aging' of a filamentous subunit that results from ATP hydrolysis and Pi release produces an actin filament that can be stratified based on the enrichment of specific actin-nucleotide complexes: ATP-, ADP-Pi-, or ADP-actin complexes. In a filament that has reached steady state growth, these three 'strata' are maintained in a quasi-equilibrium state along with concomitant changes in the local topology of the filament (Galkin et al., 2003). The resulting polarized and non-equilibrium nature of an actin filament results in a multi-compartmental molecular scaffold for the actin binding proteins. Actin binding proteins as a group have evolved to exploit the differences in the topology of an actin filament and are able to bind with considerable specificity and affinity to a specific stratum along the filament. Differential binding for specific subunits or stratum can occur in the absence of external signaling. For instance, cofilin binds with higher affinity to ADP-actin subunits within filaments; therefore, it is enriched nearest the filament pointed ends. Tropomodulin also associates with the ADP-actin stabilizing the pointed ends of filaments. Arp2/3 complex, which can act as a side binding actin nucleator, binds preferentially to Pi bound actin. Profilin, capping proteins, and formins all bind preferentially to ATP-actin at the barbed end of actin filaments. Tropomyosins, which recruits myosin, binds all along 'untwisted' actin filaments, without any preference for nucleotide-binding status of the actin.



these studies, a high cofilin ratio to actin was required for actin nucleation. The mechanism of cofilin's nucleating activity remains ambiguous, although it has been shown that rapid actin polymerization occurs at the leading edge of EGF stimulated carcinoma cells and this requires active cofilin, but it does not arise from local dephosphorylation of phospho-cofilin (Song et al., 2006).

Other actin dynamizing proteins

Ena/Vasp proteins regulate actin dynamics by antagonizing the activity of barbed-end capping proteins and by promoting filament bundling (Barzik et al., 2005); (Bear et al., 2002). These proteins are critical for filopodia formation in fibroblasts and neuronal growth cones and may be important downstream of guidance cues such as netrin (LeBrand et al., 2002).

Gelsolin is a barbed end capping and severing protein. It is thought that the binding of gelsolin to the plus end changes the conformation of the actin subunits in the filament, causing the breakage of intersubunit bonds. In mice, the knockout of gelsolin does not result in drastic abnormalities (Witke et al., 1995). The growth cones of neurons from gelsolin knockout mice can extend filopodia normally, but exhibit delayed retraction (Lu et al., 1997)

Profilins are ~19kDa actin monomer binding proteins that are highly expressed throughout the cytoplasm (Dos Remedios et al., 2003). They bind actin monomers with high affinity, catalyze the exchange of ADP for ATP, promote actin filament assembly, and can enhance actin filament turnover in the presence of cofilin. When bound to actin, profilin inhibits the hydrolysis of ATP bound to actin, thus contributing to a condition where actin monomers have a high affinity for growing plus ends of actin filaments. The assembly of actin from the profilin-ATP-actin pool is enhanced by formins, which are localized at the barbed ends of filaments (Romero et al., 2004). In mammals profilin I is ubiquitous, but profilin II is highly expressed in the nervous system (Witke et al., 1998). Mutations in profilin have been shown to disrupt growth cone advance in drosophila motor neurons (Wills et al., 1999).

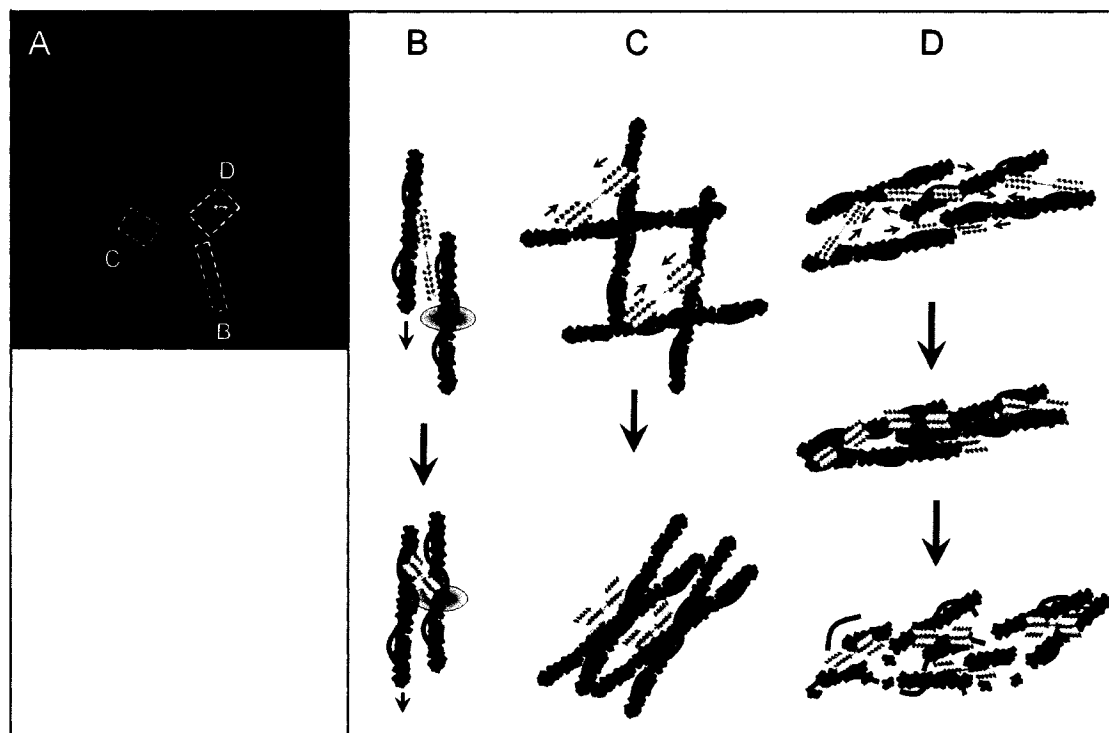
Motor Proteins

The only known actin binding motor proteins are the myosins. Of the 13 known isoforms only a four (I, II, V, VI) have been shown to exist in neurons, with myosin II isoforms being the most extensively studied. A plethora of new data suggests a prominent role for myosin II in neurite formation, extension, axonogenesis, and growth cone pathfinding (Brown and Bridgman, 2003; Gallo, 2006; Kim and Chang, 2004). This conventional myosin is composed of two heavy chains and two different light chains (essential and regulatory). It functions as a dimer in which the α -helical tails that associate in a long coiled-coil structure and the heads bind to and exert sliding force on actin in an ATP-dependent manner. In growth cones, there are three major types of actin networks: gels, bundles and actin arcs. Myosin II may act differently on these actin structures (Figure 8). In gels, myosins may cause actin networks to deform or stretch; in bundles, the actin filaments would slide relative to one another; and in arcs, myosins compresses actin filaments to form the actin arcs in the transition zone potentiating their severing. In a new study, myosin II was shown to act directly in actin depolymerization via the contractile forces they exert on actin filaments (Figure 8D). In *Aplysia* growth cones, myosin II is localized in the transitional domain of growth cones and its activity, in a ROCK independent manner, is responsible for about 50% of the observed retrograde F-actin flow in the periphery (Zhang et al., 2003; Medeiros et al., 2006)). Treatment of growth cones with the myosin II inhibitor blebbistatin caused filaments to double in length and reduced the compression of the actin networks into actin arcs. This activity is ROCK-dependent. When actin is stabilized with jasplakinolide, myosin II activity can lead to neurite retraction (Gallo et al., 2002), presumably by the prevention of microtubule advance by a contracting actin network.

Actin Cross-linking proteins

Actin crosslinking proteins resolve the two basic actin superstructures: actin gels and actin bundles. These semi-autonomous superstructures underlie the largely distinct structural features common to growth cones: lamellipodia and filopodia. Actin gels are cross-linked

Figure 1.8. Myosin II activity in growth cones. Although the overall activity of myosin II is to restrain growth cone advance, myosin II may have different functions in growth cone depending on their substratum attachment. **A.** Shown is an axonal growth cone stained for tubulin (red) and actin (green). Actin filaments undergo a constant retrograde flow in growth cones, which is partially due to myosin II activity. When actin filaments become tethered to substratum (a 'clutch' is engaged), a traction force develops that can lead to protrusive activities of filopodia and lamellipodia. Retrograde flow occurs at maximal rates when there are limited cross-linkages between the actin network and the substratum. Myosin II activity has been implicated in the generation of the traction forces in growth cones. Furthermore myosin II activity in different actin structures of the growth cone may have different consequences on growth cone morphology. **B.** In filopodia (and other parallel actin bundles), the action of myosin can cause actin filaments to slide relative to each other. This could result in the retrograde flow of actin or, depending on the linkages to the substrate, to filopodial protrusions. **C.** In lamellipodia, which contain branched actin filaments, myosin II activity can compress actin filaments, changing the density and alignment of F-actin. Again, depending on attachments with the substratum, this could lead to leading edge protrusions or retractions. **D.** In the transitional domain, myosin activity is responsible for the compaction of actin filaments into arcs and can lead to their severing and depolymerization via mechanical stress of myosin-based contraction.



meshworks, which have high viscoelasticity resembling a gel-like composition. Bundles are more rigid, tightly packed parallel arrays providing structural rigidity necessary for the thin protrusions of filopodia.

Filamin binds actin filaments into a cross-linked 3-dimensional meshwork. The network formed by actin cross-linked by filamin is a deformable with the viscoelasticity of a gel-like material. Filamin can also tether actin to the membrane via interactions with transmembrane proteins. In humans, mutations in filamin result in perturbations in neuronal migration in the cortex resulting in malformation underlying epilepsy as well as other neurological disorders (Fox et al., 1998; Sheen et al., 2003; Nagano et al., 2004). The role of filamin in growth cones is unknown.

Fascin binds longitudinally along two actin filaments conferring a parallel bundle arrangement. Fascins may be crucial to the formation and maintenance of actin filament bundles in growth cones, including those underlying filopodia (Cohan et al., 2001).

In vitro studies have shown that simply changing the concentrations of fascin and filamin in a solution with actin can determine if actin forms into gels or bundles (Tseng et al., 2002; Tseng et al., 2004). In cells, local changes in the concentrations of these proteins can underlie changes in cell morphology and motility. Thus, localized alterations in fascin and filamin concentrations and activity could influence growth cone behavior and, consequently, neurite growth.

Actin-organizing proteins

Tropomyosins (TMs) are rod-like proteins that bind in a spiral manner along the α -helical groove of actin filaments and are involved in actin filament stability. In neurons there are two genes that, through alternative splicing, give rise to over ten isoforms (Gunning et al., 2005). The understanding of the expression patterns, regulation, and effects of TM isoforms on microfilaments is a massive undertaking in and of itself. Thus, here, we will resort to generalities to provide a basic conceptual understanding of how TMs can influence the organization of actin structures. As previously mentioned, there are

structurally and functionally distinct microfilament populations associated with different cellular compartments in different regions of neurons. Notable actin structures include stress fibers, mesh-like actin networks of lamellipodia, and actin bundles in filopodia. These different populations are not only composed of different actins, but also of different TM isoforms. Although there is some degree of functional redundancy, these different TMs can differentially influence the behavior of the microfilament to which they are bound. For example different TMs may confer upon actin structures different myosin mechanochemistry, actin turnover stability, and different levels of protection against actin severing proteins (Bryce et al., 2003; Gunning et al., 1998; Bernstein and Bamburg, 1982; Ishikawa et al., 1989).

Microtubules

Microtubules are reviewed here only in the detail necessary for understanding their role in neuronal morphology, neurite growth, and growth cone dynamics. Later we will review how the microtubule stability and dynamics may underlie important features of neuronal development including the establishment of neuronal polarity.

Microtubule Structure and Function

Microtubule dynamics play important roles in many cellular functions, none more studied than mitosis (Verhey and Gaertig, 2007). The onset of mitosis is conspicuous by remarkable changes in microtubule organization and dynamics leading to the formation of a mitotic spindle from which microtubules radiating from opposite poles capture chromosomes and aid in their proper segregation into daughter cells. Microtubules also serve as tracks for intracellular transport where molecular motors haul proteins, organelles, and RNA-containing complexes throughout the cell. Intracellular transport is of great consequence in neurons, some of which have axons with lengths that are 50,000 times the diameter of the soma. At the distal end of the axon, the terminal bouton is reliant on intracellular

transport for providing the molecular cargo necessary for proper synaptic function. Problems in maintaining the proper trafficking of materials in neurons may have devastating consequences to neuronal function, possibly underlying degenerative diseases such as amyotrophic lateral sclerosis (ALS) (Boillee et al., 2006). Microtubules also engage in various cellular movements, including the beating of cilia and flagella, directed cell migration and in neurite outgrowth and axon guidance.

Microtubules are assembled from soluble tubulin dimers, which, like actin monomers, can self-assemble (reviewed in Desai and Mitchison, 1997). The soluble tubulin heterodimer consists of α - and β - tubulin, which are products from two separate genes and share ~ 50% amino acid homology. There is an additional tubulin isoform, γ -tubulin, localized to microtubule organizing centers (MTOCs) or centromeres where it forms a ring complex that can nucleate microtubule assembly. Microtubules usually consist of 13 protofilaments interacting laterally to form a 24 nm hollow cylinder. The protofilaments themselves consist of dimeric $\alpha\beta$ -tubulin subunits in longitudinal association and grow and shrink by subunit addition or loss from the ends of the cylinder.

As with F-actin, microtubules exhibit a functional and structural polarity having a minus (-) and a plus (+) end. The (-) end of microtubule is usually localized to a microtubule organizing center (MTOC), a nucleator of microtubule growth. The (+) end, which is typically free in the cell, is the dynamic end of the microtubule and usually occurs distal to the MTOC (Figure 9). Microtubules can also undergo assembly and disassembly in a manner analogous to actin filaments. At concentrations above the critical concentration (C_c), $\alpha\beta$ -tubulin dimers will polymerize into microtubules and at concentrations below C_c microtubules depolymerize. The (+) and (-) ends of microtubules have different dimer equilibrium concentrations such that the (+) end grows about twice as fast as the (-) end. Although microtubules can treadmill at tubulin dimer concentrations between the critical concentrations for the (+) and (-) ends, microtubules differ from actin in their disassembly kinetics; at concentrations below C_c disassembly occurs twice as fast at the (+) end. Thus, both assembly and disassembly occur preferentially at the (+) end of microtubules, and

because the (-) end is often bound to nucleation complexes, it is the dynamics of the (+) end that gives microtubules their unique behavior. Observations *in vitro* (Walker et al., 1991; Mandelkow et al., 1991) and *in vivo* (Sammak and Borisy, 1988) have revealed that microtubules oscillate between periods of slow growth and more rapid shortening events called catastrophes (Figure 9). This behavior, coined dynamic instability, is due to weakening of the lateral interactions between protofilaments at the end of the microtubule. Dynamic instability is intimately related to C_c , where the growth and shrinkage of microtubules reflect the local fluctuating tubulin concentrations around C_c , but dynamic instability is also dependent on a tubulin conformation change that occurs upon hydrolysis of the GTP bound to the β -tubulin subunit. Each subunit of the α,β -tubulin dimer has a bound GTP, but following incorporation into a microtubule, the GTP is hydrolyzed to GDP only on the β subunits. This results in a GTP-tubulin “cap” on the exposed microtubule (+) end, which is protective against catastrophe. However, depending on the availability of soluble tubulin, the GTP hydrolysis can encroach upon the (+) end of the microtubule. When the GTP hydrolysis reaches the tip, a catastrophe occurs: lateral interactions between the protofilaments are compromised and protofilaments peel away and depolymerize (Figure 9).

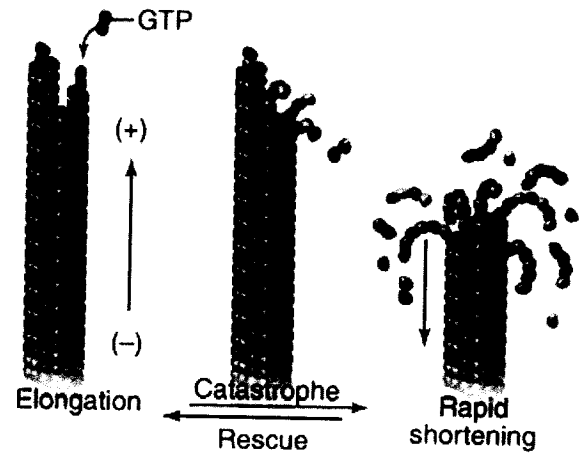
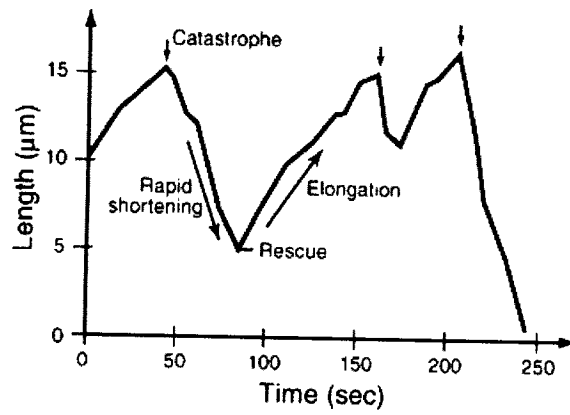
Microtubule binding proteins

There are various microtubule binding proteins found in cells that have specific and important functions, especially in neurons. Indeed, several microtubule binding proteins are found exclusively in neurons. Here we will only briefly consider those microtubule binding proteins relevant for neurite elongation, neuronal polarity and growth cone motility. These include microtubule cross-linking proteins, tubulin dynamizing proteins, microtubule motors and plus-end binding proteins (Figure 10).

Microtubule Cross-linking Proteins

MAP is a generic acronym for **m**icrotubule **a**ssociated **p**roteins (reviewed in Maccioni and

Figure 1.9. Microtubule dynamics. Microtubules are hollow cylinders of 13 protofilaments which are made up of $\alpha\beta$ tubulin dimers in longitudinal association. The minus (-) end (not shown) is usually associated with γ -tubulin at the MTOC from which microtubules assemble. The polymerization of microtubules occurs at the plus (+) ends. Free tubulin dimers with GTP-bound to the β -subunit are added to the plus end. Shortly after incorporation of a dimeric subunit into the microtubule, the GTP is hydrolyzed to GDP. When polymerization is faster than the rate of GTP hydrolysis, a GTP cap is generated at the (+) end and this provides some structural stability. When the rate of GTP hydrolysis is faster than the rate of assembly (in a situation where free tubulin dimers are unavailable) a catastrophe occurs and the microtubules depolymerize rapidly. A shortening microtubule can be 'rescued' and begin polymerizing again when GTP-tubulin dimers become available.



Cambiaso, 1995). High fidelity *in vitro* isolation of tubulin led to the identification of MAPs which co-purified in a fixed stoichiometry with tubulin. One major family of MAPs, the assembly Maps, are responsible for cross-linking microtubules into bundles in cells. There are two major subgroups of Maps based on sequence analysis: 1) Type I including Map1A and Map 1B, and 2) Type II Maps including Map2, Map4, and Tau. Type I Maps are positively charged and are thought to counteract the charge repulsion of negatively-charged tubulin. Type II Maps also form cross-bridges between microtubules and can regulate the lateral spacing between parallel microtubules. Maps also are stabilizing factors, bundling microtubules to help maintain their structural integrity, but they can also accelerate the polymerization of tubulin subunits. MAPs display differential expression patterns and subcellular localization, which may impart important differences in the microtubule structures. For example, MAP2 is asymmetrically distributed in dendrites and in the axon proximal segment, whereas Tau is localized to axons. This differential distribution of MAPs may be crucial to neuronal development since different MAPs may confer different microtubule structural properties. For example, axons have much longer microtubules, which act as highways for transport and may also prevent neurite retraction (Baas and Buster, 2004).

Microtubule dynamizing proteins

CRMP-2, the collapsin-response mediator protein 2, was first identified for its role in semaphorin-mediated growth cone collapse. Recent biochemical data have demonstrated that CRMP proteins bind to tubulin heterodimers and promote microtubule polymerization *in vitro* (Amano et al., 1998). CRMP-2 also seems to bind Sra-1/Wave which may lead to a regulation of actin stability (Kawano et al., 2005). CRMP-2 is highly expressed in the developing nervous system (Goshima et al., 1995; Wang and Strittmatter, 1996), particularly in growing axons (Inagaki et al., 2001).

SCG-10 and Stathmin are related microtubule heterodimer binding proteins that, unlike CRMP-2, are considered destabilizing proteins, preventing dimer association with the plus ends of microtubules (Grenningloh et al., 2004). SCG-10 and stathmin are found in

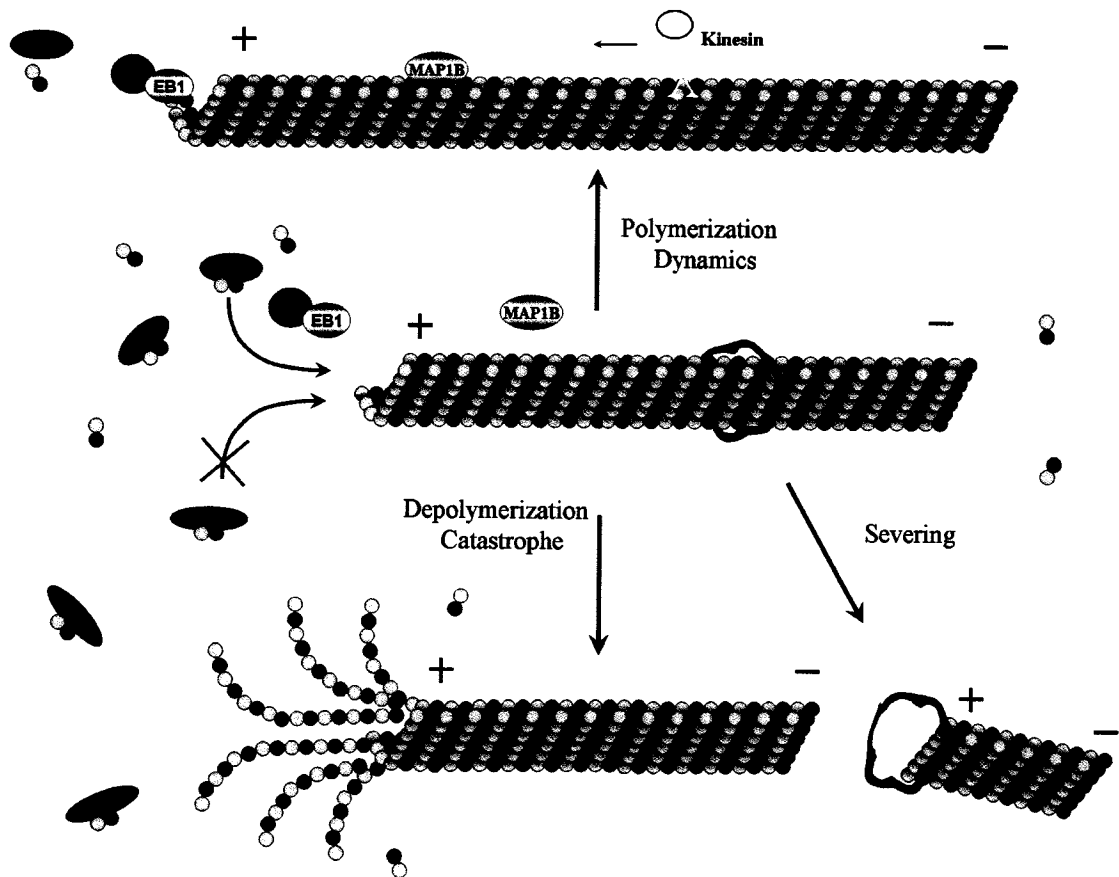
neurons and differ in that SCG-10 has an additional 30-35 amino acids at the N-terminus that contains a double cys motif, which directs palmitoylation and membrane association of this isoform. Increasing phosphorylation by different kinases on multiple sites has a proportional effect on diminishing SCG-10/stathmin activity. The tight regulation of SCG-10/stathmin may be important for regulating neurite growth.

Katanin is an ATP-dependent microtubule severing protein. Neurons contain higher levels of katanin than other cell types. Katanin may be involved in releasing microtubules from the centrosome in the soma, and also for regulating the length of the microtubules after their release (Ahmad et al., 1999). These fragmented microtubules then can be efficiently transported throughout the cell to support microtubule-dependent processes, such as neurite growth. Excessive katanin activity, however, results in neurite retraction, due to dissolution of microtubules (Karabay et al., 2004). Interestingly, axonal microtubules are more resistant to katanin-mediated severing than those in the dendrites or cell body which may be partly due to the protective properties of tau binding (Qiang et al., 2006).

Motor proteins

There are two major types of microtubule motor proteins: kinesins and dyneins (Hirokawa, 1998). Kinesins are usually (+) end directed motors whereas dyneins are (-) end directed motors. These motors are responsible for the transport of various molecular cargos (proteins, organelles and vesicles), playing particularly important functions in large complex cells such as neurons. For kinesins, the dimeric head domain binds the microtubule and ATP, which is utilized for energy, while the tail domain binds specific types of cargo. Dynein requires large complexes of microtubule binding proteins, such as dynactin, to bind cargo. In neurons, dynein is largely responsible for retrograde (toward the soma) transport while kinesin is responsible for anterograde (away from the soma) transport. In addition to a role in transport, specific isoforms of these motors may also have a neuronal specific function. Kinesin 5, for example, may act to constrain excessive neurite growth by generating forces on axonal microtubules (Myers and Baas, 2007).

Figure 1.10. Microtubule associated proteins (MAPs) can stabilize or destabilize microtubules. A growing number of proteins bind to and regulate microtubule assembly and architecture. Here, only a subset of MAPs is presented that have functional implications in neurons. Map1B is heavily expressed in developing neurons and promotes microtubule stability and assembly. The end-binding proteins APC and EB-1 bind to the (+) ends of microtubules and promote microtubule polymerization. CRMP-2 also can facilitate microtubule assembly, but does so by binding tubulin dimers and guiding them to the (+) ends of microtubules. Destabilizing MAPs include stathmin and its membrane associated relative, SCG-10, and Katanin. Stathmin can destabilize microtubules by binding to and sequestering tubulin dimers, preventing their association with the (+) ends of microtubules. The ATPase, Katanin is a heterodimeric protein that severs microtubules into shorter fragments, which then can depolymerize into tubulin dimers. The tubulin dimers generated by katanin are capable of reassembling into microtubules, so in certain situations katanins may also facilitate microtubule growth.



Plus-end binding proteins (+ TIPs)

There are a large number of disparate proteins that bind to growing microtubule plus ends. Here, we only review a few +TIPs that have been implicated in the development of neuronal polarity.

EB1 (end binding) is one of three members (EB2 and EB3 being the others) of a family of (+) end microtubule binding protein that are emerging as a core component of +TIPs activities (reviewed in Morrison, 2007). Although it is not known exactly how EB1 binds preferentially to microtubule + ends, it may take advantage of conformational differences in GTP-bound tubulin at the + ends versus GDP-bound tubulin in the more proximal microtubule. Various proteins characterized as + TIPs may “piggy-back” microtubule plus ends via EB1 interactions. EB1 can promote microtubule growth *in vitro*, but only in the presence of other binding partners (e.g. APC), perhaps due to a release of an autoinhibitory conformation.

APC (adenomatous polyposis coli) is well-known for its role in the degradation of β -catenin in the Wnt signaling pathway. There is also growing evidence for its role as a regulator of microtubule dynamics. APC binds to microtubules, through EB1 interactions (Morrison, 2007), and promotes microtubule assembly and bundling *in vitro* (Munemitsu et al., 1994). It moves along growing microtubules in cells, especially at actively protruding membranes and the leading edge of migrating cells (Barth et al., 2002). APC can also form a complex with KAP3 and KIF3, which suggests a role in the transport of cargos carried by KIF3 motors along microtubules (Jimbo et al., 2002). APC also has an actin binding domain and this domain can promote actin assembly (Moseley et al., 2007), which could be of importance in the microtubule-F-actin interaction within the growth cone peripheral domain.

Rho Family GTPases

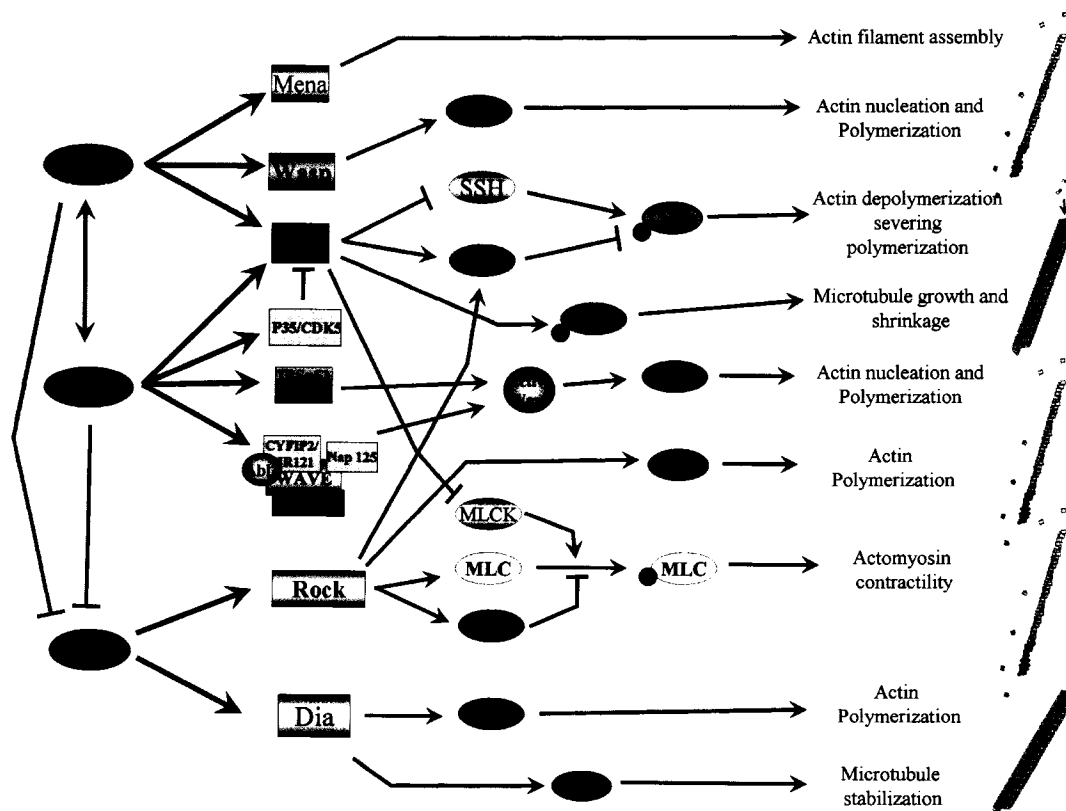
The Rho family GTPases are low molecular weight guanine nucleotide binding proteins that include at least 16 members. Since they are critical to many cellular functions, the Rho GTPases are esteemed as decisive pivotal signaling proteins linking membrane receptors

to proteins effecting cell morphology and motility as well as gene expression. In neurons, Rho GTPases play a crucial role in various aspects of neuronal development including cell migration, neuritogenesis, axon differentiation and growth, neurite branching and dendritic spine development (Govek et al., 2005). The canonical Rho GTPases include RhoA, Rac1, and Cdc42, which play a role in various aspects of cell physiology including actin and microtubule organization, Golgi dynamics, and endo- and exocytosis. In terms of actin structures, pioneering work performed by Alan Hall and associates suggested that each of these GTPases controlled distinct actin structures: Rho, Rac, and cdc42 regulate stress fibers, lamellipodia, and filopodia, respectively. Although very over-simplistic, this general characterization is at least partially true. We now know that these proteins exhibit substantial cross-talk and even have common downstream effectors. Many of the signaling pathways involving the Rho GTPases have been mapped (Figure 11). Thus, considering these proteins as independent signaling entities is sometimes misleading, because they need to be considered as parts of an interdependent signaling network, at least under most conditions in most cell types. However, in some cell types the Rho GTPases may exhibit less interdependence. For example, in hippocampal neurons, the removal of cdc42 does not affect the activity of the either Rac or Rho (Garvalov et al., 2007).

The activity of Rho GTPases is effected downstream of various transmembrane receptors including G-protein coupled receptors and receptor tyrosine kinases. Downstream of these receptors are proteins that directly affect Rho GTPase activity. The Rho GTPases function as binary switches, cycling between an active GTP bound state and an inactive GDP-bound state. Their activity is determined by the ratio of GTP to GDP in the cell and modulated by various regulatory molecules. Guanine nucleotide exchange factors (GEFs) activate Rho GTPases by facilitating the exchange of GTP for GDP. GTPase activating proteins (GAPs) increase the low intrinsic GTPase activity of Rho proteins, thereby increasing the rate of their inactivation.

Rho GTPases exert their influence on multiple effectors through direct binding (Bishop and Hall, 2000). Rho Activated Kinase (ROCK), as it name implies, is activated by Rho binding leading to changes in other downstream actin binding proteins including myosin

Figure 1.11. Signaling pathways downstream of Rho GTPases affect actin and microtubule dynamics. This simplified diagram illustrates major signaling pathways downstream of the canonical GTPases, Rho, Rac and cdc42, which may be involved in the regulation of growth cone cytoskeleton. The Rho GTPases themselves are thought to display significant cross-talk, which plays important roles in modulating and coordinating the downstream signaling responses. This cross-talk may occur via the modulation of the activity of GAPs and GEFs (not shown) that control other Rho GTPases. Furthermore, the ability for multiple Rho GTPases to interact with common effectors allows for further cross-talk. Cdc42 controls actin assembly and disassembly through multiple downstream effectors including IRSp53-Mena, Wasp, and Pak. Mena activation causes actin filament assembly, Wasp activates Arp2/3 complex, which is responsible for actin nucleation and formation of branched actin networks, and Pak can lead to modulation of ADF/cofilin activity through Lim kinases and slingshot phosphatases. Pak can modulate microtubule assembly via activation of SCG-10 (Stathmin), a tubulin dimer sequestering protein. Pak is also a downstream effector of Rac. Other downstream effectors of Rac include IRSp53-Wave and a separate multi-component Wave complex. Activated Wave also stimulates actin filament assembly via Arp2/3 complex. RhoA affects actin filament dynamics via Rho-Kinase (ROCK), which, in turn, has multiple downstream effectors. Profilin activation by ROCK can lead to actin filament polymerization. ROCK inhibits ADF/cofilin activity via LimK. ROCK can also affect actomyosin contractility via either direct phosphorylation of MLC and phosphorylation (inhibition) of MLC. Another Rho-effector, Dia can impinge upon actin filament assembly by directly nucleating new filaments. Dia also impacts microtubule stability via interactions with APC.



II, profilin and cofilin, generally leading to increased actin stabilization. P21 activated kinase (PAK), a downstream target of both cdc42 and rac-1, can affect the activity of actin binding proteins such as cofilin and myosin II generally leading to increased actin dynamics (Figure 9). PAK activity can also increase microtubule polymerization via the phosphorylation of Stathmin/SCG-10 proteins. In addition, cdc42 has been shown to affect the activity of the Par3/Par6/aPKC complex which regulates microtubules through GSK 3 β phosphorylation of various proteins including APC, tau and CRMP2 (Etienne-Manneville and Hall, 2003).

As shown in Figure 8, the signaling networks involving the Rho GTPases are extremely complex affecting various downstream effectors that modulate microtubules and actin. Thus, in experiments where Rho GTPase activity is manipulated, one has to be careful with interpretation and realize that the overall change in cell structure, motility and physiology may be due to changes in molecules beyond those under study.

Cytoskeletal Dynamics in Growth Cone (*from Flynn et al, 2006*)

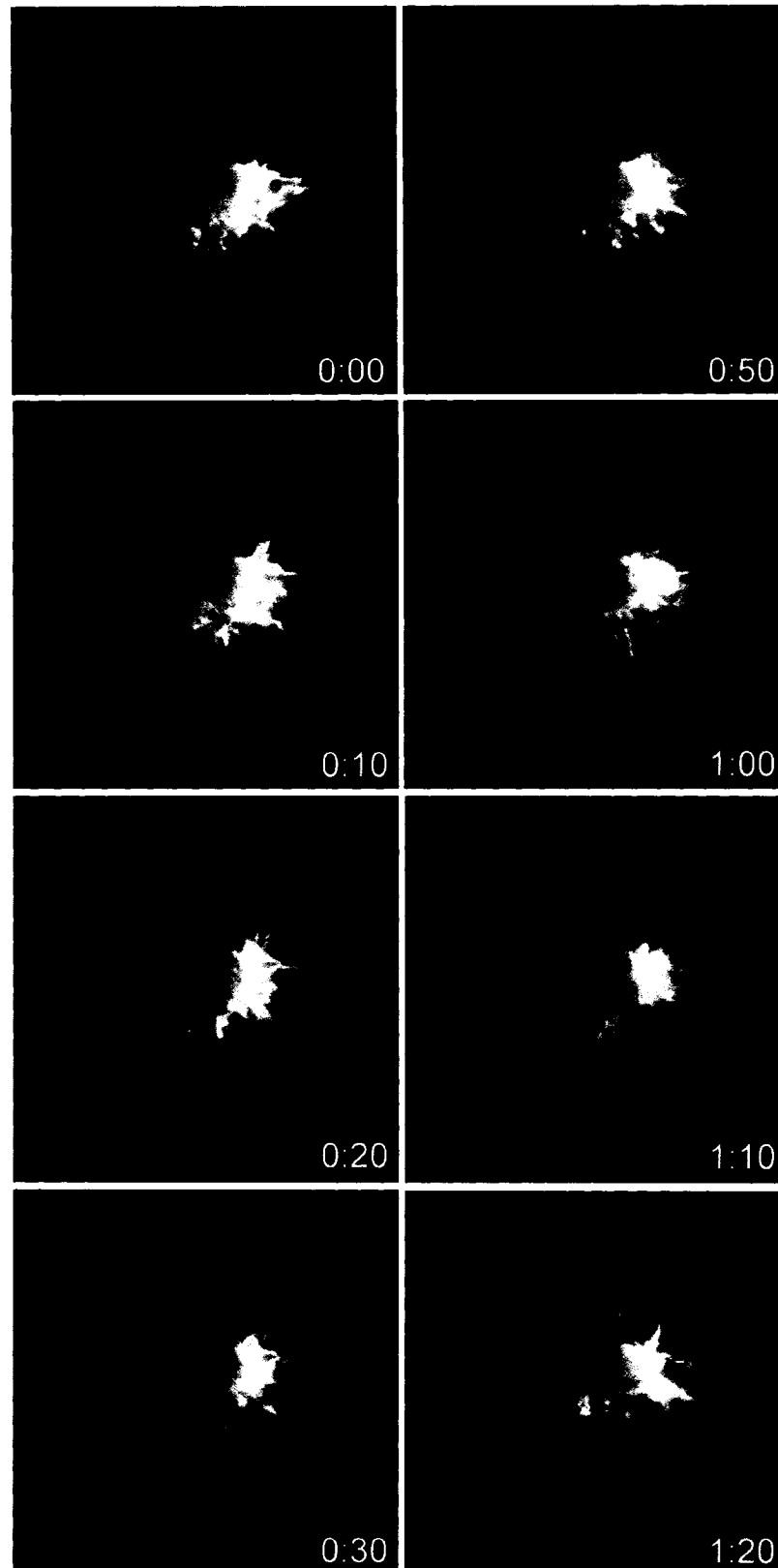
Cytoskeletal Features of growth cone

Growth cones are labile, pleiomorphic protrusions at the distal tips of axon and dendrites, which on a flat substratum often have a 'hand-like' morphology (Goldberg and Burmeister, 1989). The growth cone is classically subdivided into two distinct domains based on the segregation of filament networks and cytoplasmic organelles (Figure 2, Bridgman and Dailey, 1989; Forscher and Smith, 1988; Smith, 1988; Lin and Forscher, 1995). The most proximal portion or 'palm' of the growth cone is referred to as the central domain or C-domain. The C-domain is contiguous with the neurite proper ('wrist') and therefore contains a sheath of densely bundled microtubules most of which terminate within this domain (Dailey and Bridgman, 1991; Forscher and Smith, 1988; Letourneau, 1983; Tanaka and Kirschner, 1991). The C-domain also contains and corrals cytoplasmic organelles (Tsui et al., 1983; Dailey and Bridgman, 1991). Surrounding the C-domain is the peripheral domain or P-domain. The P-domain is highly structured, containing both actin-based filopodia and lamella (Forscher and Smith, 1988). Protrusive, spike-like bundles of actin, sometimes referred to as ribs,

radiate outward from the distal circumference of the C-domain into the P-domain where they often extend like ‘fingers’ radiating away from the growth cone as filopodia (Bray and Chapman, 1985; Forscher and Smith, 1988). Broad, sheet-like lamella enjoin the regions between filopodia as a thin ‘veil’ much like the webbing on duck feet (Forscher and Smith, 1988). The distinct structures of filopodia and lamella are attributed to the cytoskeleton and the extracellular matrix to which the growth cone is adhered. Filopodia are composed of parallel, filamentous actin (F-actin) bundles that have most if not all of the filament barbed (plus) ends at their distal tips (Svitkina et al., 2003; Vignjevic et al., 2003). The lamella, in contrast, contains an entangled meshwork of F-actin, with the majority of filaments angled to grow outward (Lewis and Bridgman, 1992; Svitkina et al., 1997). Microtubules are mostly excluded from the P-domain, although occasionally and importantly microtubules may penetrate into this region guided by F-actin cables (Letourneau, 1983; Zhou et al., 2002). Microtubule penetration into the P-domain promotes leading edge extension of the growth cone (Zhou and Cohan, 2003; Lee et al., 2004). A third domain has also been described that exists at the interface between the C-domain and the P-domain, referred to as the transition zone (T-zone) (Schaefer et al., 2002). F-Actin, assembled into ribs and meshwork of the lamellipodium, undergoes retrograde transport into the T-zone and undergo compression, creating a population of transversely oriented actin filaments called actin arcs (Lin and Forscher, 1995; Lin et al., 1996; Schaefer et al., 2002). Actin disassembly also occurs within this region. The retrograde translocation of actin arcs into the C-domain contributes to the packing of C-domain microtubules and inhibits microtubule penetration (Schaefer et al., 2002).

Growth cones are extremely dynamic. For instance, growth cone lamella and filopodia extend and retract at a rate up to ten times faster than axon extension (Figure 12, Movie 1.1). These dynamic changes require a highly dynamic actin cytoskeleton system, which is maintained by constant recycling (Okabe and Hirokawa, 1991). Turning over the actin network in growth cones requires both new actin assembly and disassembly, which are important for maintaining the extant growth cone structure. Inhibiting new actin assembly with cytochalasin B resulted in collapse of the growth cone due to the loss of lamella and

Figure 1.12. Growth cones are extremely dynamic structures. A time-lapse series is shown of an axonal growth cone expressing RFP-actin. Time is indicated in lower right corner (minutes:seconds). Notice that the growth cone is extending and retracting filopodia and lamellipodia at a rate more rapid than neurite extension. The actin is undergoing rapid turnover, with assembly and disassembly determining the dynamics of the growth cone (See Movie 1.1).



filopodia (Marsh and Letourneau, 1984; Forscher and Smith, 1988). Likewise, inhibiting actin disassembly with jasplakinolide also resulted in collapse of the growth cone due to a myosin-dependent retraction of the stabilized actin network (Gallo et al., 2002). In addition to its role in the maintenance of growth cone structure, actin disassembly is also important for neurite growth and growth cone guidance. Although neurite elongation per se does not require the actin filament system, as it can be driven entirely by a microtubule-based process (Marsh and Letourneau, 1984), the rate and direction of neurite growth are regulated by the focal disassembly of an organized actin cytoskeleton (Bentley and Torion-Raymond, 1986; Zhou et al., 2002). For example, focal disassembly of actin bundles can induce growth cone turning by reorienting microtubule growth away from the affected region. In fact, the coincident global loss of actin bundles and leading edge actin actually leads to growth cone collapse. Therefore, the global or localized disassembly of actin bundles may represent a general mechanism for growth cone collapse or repulsive growth cone turning, respectively. However, actin disassembly may additionally contribute to growth cone guidance by promoting filopodia dynamics, which may require recycling of assembled actin.

Filopodia likely operate as environmental sensors that when stabilized can direct directional growth. For example, more filopodia are observed on the growth cone edge that faces towards the direction of a glutamate gradient than away from it and the increase in filopodia is necessary for attractive turning (Zheng et al, 1996). Although contact with a guidepost cell induces an increase in both number and length of filopodia on grasshopper limb pioneer growth cones, a single filopodial contact is sufficient to reorient growth cone advance (O'Connor et al., 1990). In fact, loss of filopodia in these growth cones disrupts pathfinding (Bentley and Toroian-Raymond, 1986; Chien et al., 1993). Therefore, promoting filopodia extension may equally represent a complementary mechanism for attractive growth cone turning. Thus, regulation of actin disassembly by the various guidance molecules may act through both mechanisms to ensure proper growth cone guidance and neurite growth.

Regulation of actin binding proteins during growth cone guidance (*from Pak et al., 2008*)

Because actin assembly, organization, and turnover are inter-dependent and recursive,

perturbations of any one of these steps may impact subsequent steps in subtle or fatal ways. Each of these steps also critically depends on the activities of unique classes of actin binding proteins, and thus numerous 'pressure points' can be targeted to regulate growth cone translocation or turning. Nearly every actin binding protein may be regulated by direct post-translational modification. However, whereas intrinsic regulation (protein structure) generally governs the spatial binding of an actin binding protein relative to an actin filament or a superstructure stratum, post-translational modification (extrinsic regulation) generally regulates its temporal binding. This is an important contention because the ratio of bound/unbound proteins to actin in a localized region can be inherently regulated simply by controlling the kinetics of actin binding in that region. For some actin binding proteins that only require actin binding to function, such as myosin II and cofilin, regulating the kinetics of binding also controls their activity. However, there are important exceptions to this paradigm, such that a certain actin binding protein may remain inactivated while being bound to a filament. The extrinsic regulation of actin binding proteins is particularly important during guidance decisions, and *in vivo*, growth cone turning likely relies on the regulation of many actin binding proteins through multiple signaling gradients where multiple extracellular guidance cues are often presented at the same time (Song and Poo, 1999). However, even a single extracellular guidance cue can trigger multiple overlapping signaling gradients to increase the potential responses of the growth cone. Overlapping signaling gradients have already been demonstrated for two guidance cue systems: myelin-associated glycoprotein (MAG)-induced Ca^{2+} /cAMP, and Semaphorin 3B-activated MAPK/Src kinase (Henley et al., 2004; Falk et al., 2005). Yet, as was recently demonstrated in cultured neurons, the extrinsic regulation of only a single actin binding protein is sufficient to support either an attractive (towards a source) or repulsive (away from a source) turn.

Spinal neuronal growth cones from stage 20-22 *Xenopus* embryos are first attracted to a gradient of bone morphogenetic protein (BMP)-7 4-8 hours after plating; however, the same neuronal growth cones are repelled by BMP7 after overnight culturing (Wen et al., 2007). Either response to the same ligand is mediated by the same actin binding protein, cofilin, and the bi-directional modification of its regulatory phosphorylation site. Cofilin

can be phosphorylated on serine-3, which through charge-repulsion prevents its binding to actin monomers and filaments. When dephosphorylated at this residue, cofilin can bind to filaments, enhancing their severing and depolymerization.

The initial attraction towards a BMP-7 point source is mediated by the biased phosphorylation of cofilin in the region of the growth cone nearest the source. This occurs through the activation of LIM kinase, creating a gradient of inactivated cofilin highest nearest the source. Conversely, BMP-7 repulsion is mediated by the biased dephosphorylation of cofilin by slingshot also in the region of the growth cone nearest the source. This effectively reverses the gradient established by the LIM kinases. Slingshot phosphatase can also inactivate LIM kinase *in vitro*, although this mechanism has not been investigated (Soosairajah et al., 2005).

An imbalance in cofilin phosphorylation and dephosphorylation ultimately results from the generation and maintenance of asymmetrical signaling gradients across the perpendicular axis of migration for the growth cone. In the case of attractive turning for same-day cultures, LIM kinases are likely activated by release from the BMPRII receptor (Foletta et al., 2004) and/or perhaps a Rho GTPase-dependent signaling gradient (Arber et al., 1998; Yang et al., 1998)), although these have not been investigated. In the case of repulsive turning for overnight cultures, the LIM kinase signaling gradient does not disappear; instead, the overlapping presence of a Ca^{2+} -dependent signaling gradient dominates to cause a repulsive turn. Thus, by inhibiting Ca^{2+} -dependent signaling, attractive turning resumed because of the still-present LIM kinase signaling gradient (Wen et al., 2007). The ' Ca^{2+} switch' is observed in overnight cultures but not in same-day cultures because of the delayed expression of a transient receptor potential (TRP) channel. TRP channels have been implicated in Ca^{2+} -dependent neurite outgrowth (Greka et al., 2003), and in guidance by netrin-1, BDNF, and MAG *in vitro* and *in vivo* (Wang and Poo, 2005; Shim et al., 2005; Li et al., 2004). Interestingly, under either attractive or repulsive turning, the different signaling gradients are highest nearest the source; therefore, BMP7-mediated signaling to cofilin is experimentally unique in that it is the only system to show that the bi-directional regulation of the same spatial pool of a single actin binding protein is sufficient to mediate either an

attractive or repulsive turning response.

The ability of cofilin to mediate either attractive or repulsive turning suggests that actin binding proteins can function as effective signal integrators. As mentioned before, there are many signaling pathways in growth cones that can bridge receptor occupancy to the regulation of numerous actin binding proteins. Therefore, the capacity for a single actin binding protein to support bi-directional turning is not unique to cofilin. For instance, regulation of myosin II has already been shown to mediate either attractive or repulsive turning to adhesion-based guidance cues, although different spatial pools of myosin II are likely used (Turney and Bridgman, 2005). The ability of a single actin binding protein to profoundly affect growth cone motility is an important consideration in the search for broad and effective therapeutics for motility-based disorders.

Actin superstructures in growth cones (from Pak et al., 2008)

Distinct but spatially overlapping actin superstructures exist beyond the general characterizations such as lamellipodia and filopodia . With the advent of fluorescent speckle microscopy (FSM), dynamic characteristics of actin superstructures can be measured and used to identify distinct but spatially overlapping superstructures. At the leading edge of newt lung and potoroo kidney (PtK1) epithelial cells, FSM revealed two distinct populations of actin speckles, which have different lifetimes and distinct rates of retrograde movement away from the leading edge membrane (Ponti et al., 2003). From these observations, it was reasoned that two distinct superstructures actually comprised leading edge actin, which have since been demonstrated to make up the cellular protrusions of the lamellipodium and lamellum. This finding was also experimentally supported by treating PtK1 epithelial cells with microinjected skeletal muscle tropomyosin, which resulted in the loss of the lamellipodium but left the lamellum relatively intact (Gupton et al., 2005). The existence of spatially overlapping but distinct actin superstructures within certain types of growth cones should also be considered but this has not yet been empirically demonstrated, even though two distinct zones of actin retrograde (kinetic) movement have been described in *Aplysia* growth cones using FSM (Schaefer et al., 2002). However, because the lifetimes of

individual actin speckles within the *Aplysia* growth cone were not measured, it is uncertain whether the two zones of actin retrograde flow actually represent two distinct superstructures that spatially overlap. Nevertheless, in addition to possibly underestimating the unique types of superstructures utilized by different growth cones, spatially overlapping superstructures might be functionally redundant (Gupton et al., 2005).

The intricate complexities of maintaining spatially overlapping but distinct superstructures has limited their study; nevertheless, ABP-dependent regulation of other actin binding proteins represents a fundamental mechanism to the generation or maintenance of spatially overlapping superstructures. The tropomyosin proteins are centrally important in that they can preclude or even facilitate the binding of other actin binding proteins to actin filaments. ABP-dependent regulation of actin binding is distinguished from extrinsic regulation in that another actin binding protein must be involved. Tropomyosins are cylindrical alpha-helical coiled-coil proteins that bind cooperatively in a head-to-tail manner along actin filaments (reviewed in Gunning et al., 2005). TM isoforms can be classified as high molecular weight (HMW) TMs (~284 amino acids), or low molecular weight (LMW) TMs (~248 aa). As suggested already, different TM isoforms can either antagonize or synergize the activities of other actin binding proteins (Bryce et al., 2003; Bernstein and Bamburg, 1982; Nishida, 1985). In fact, the selective localization of HMW TMs to the subpopulations of filaments and exclusion from others in non-neuronal cells defines these overlapping superstructures. As a result, myosin II motors are recruited to the lamella by HMW TMs, whereas, cofilin competes with HMW TMs in the lamellipodium (DesMarais et al., 2002; Ponti et al., 2005). Though overlapping actin superstructures have not been demonstrated in growth cones, the TM proteins are necessary for superstructure organization, since different isoforms differentially regulate growth cone size, shape, and myosin heavy chain IIB recruitment to the leading edge of mouse cortical neurons (Figure 13; Schevzov et al., 2005). For non-neuronal cells and growth cones, understanding how TM proteins are recruited to different populations of actin filaments will represent a key step in understanding how spatially overlapping actin superstructures are generated or maintained. Interestingly, the binding of TM isoforms to actin filaments is also likely intrinsically regulated by their

Figure 1.13. A model for actin dynamics at the leading edge of growth cones. In motile cells, actin filaments at the leading edge are organized into either cofilin-rich (red) or tropomyosin-myosin rich (green) subpopulations (superstructures). Although it has not been proven, the same organization likely exists in growth cones: all the relevant actin binding proteins are present and myosin II accounts for 50% of retrograde actin flow and actin turnover accounts for the other 50% of retrograde flow (Mederios et al., 2006). Although distinct, these superstructures overlap and comprise the peripheral domain of growth cones. Myosin II can reorganize actin by sliding filaments relative to each other, deforming branching actin networks, and by compacting actin into arcs; myosin II –induced mechanical shearing can lead to the dissolution of F-actin. The actions of cofilin lead to increased F-actin severing and depolymerization, which can enhance the turnover of actin filaments. Arp2/3 and/or other actin nucleators may also contribute to actin filament turnover. Both types of actin superstructures may be required for normal growth cone navigation. The activity of either myosin II or cofilin is sufficient to stimulate a turn of the growth cone (Turney and Brigman, 2005; Wen et al., 2007).



structures, since their localization can be dispersed by disassembling actin superstructures and restored by rescuing superstructures (Schevzov et al., 1997).

Aside from the tropomyosin proteins, multivalent complexes of actin binding proteins might also be necessary for the correct localization of actin binding proteins. For instance, in addition to its ability to efficiently bind F-actin, cortactin localization to the front of leading edge actin superstructures likely also relies on its interaction with subunits of the Arp2/3 complex (Weed et al., 2000). Also, the actin binding proteins coronin 1B, Slingshot-1L, and the Arp2/3 complex form a ternary complex in Rat2 fibroblasts, and the downregulation of coronin 1B disrupts the normal localization of Slingshot-1L to the leading edge (Cai et al., 2007).

The Development of Neuronal Polarity

In humans, millions and millions of intricate interconnections make up the complex machine that is the nervous system. From a developmental perspective, the correct wiring the nervous system is monumental task in scope as well as detail. Despite the enormity and mind-boggling complexity of wiring the nervous system, a developmental program proceeds in most cases with relatively few errors. Neurons extend projections in a precise manner to create circuits that, although plastic and subject to modification, can exist and function throughout an organism's existence. Given the importance of the correct wiring of the nervous system in the maintenance of normal physiology and an organism's ability to interact with its environment, it is not surprising that major problems in neurite growth and pathfinding may result in mental retardation, neuromuscular disorders, epilepsy and even lethality (ten Donkelaar et al., 2004; Setola et al., 2007; Ponnio and Conneely, 2004).

The processes that a neuron extends during development become specialized in morphology, molecular composition and physiological properties. Although there is extreme diversity among neurons in the nervous system, varying in shape and size, they all polarize and develop discrete functional domains. The specialization of the somatodendritic

compartment and the axon is the broadest level of polarization common to nearly all neurons. This basic polarity is essential to neuronal function (and the function of the nervous system as a whole), where there is unidirectional information flow: signals are received in the somatodendritic compartment and are transmitted via the axon to the postsynaptic cell (Figure 1). Furthermore, polarization of processes into the axon and dendrites has an important role in the correct wiring of the nervous system; growing axons and dendrites from the same neuron will respond differently to the same guidance cue potentially targeting these processes to distinct regions of the developing brain (Shibata et al., 1998). Thus, the early establishment of neuronal polarity is not only crucial for the proper function of mature neurons but also important for the correct connectivity of the nervous system. Furthermore, in injury and disease, the axon is often compromised, whereas dendrites are spared. Therefore determining how neuronal polarity is established can not only improve our understanding of development but also may have clinical relevance for improving nerve regeneration.

Hippocampal neurons are a model system for neuronal polarity

As widely employed model system, hippocampal neurons in culture undergo a stereotypical developmental progression, in a manner that is presumably similar to their *in vivo* development (Dotti et al., 1988; Craig and Banker, 1994). This progressive development has been divided into five different stages which occur at roughly the same time frame from culture to culture (Figure 14). Within hours after seeding, hippocampal neurons extend broad lamellipodia with active ruffling and filopodial dynamics assuming a “fried-egg” morphology (stage 1). After 3-12 hours the lamellipodium collapses in discrete regions around the periphery of the cell and the remaining lamellipodia become the growth cones of nascent neurites (stage 2). The regulation of actin dynamics (actin bundles) resulting in filopodia are crucial to the stage 1-2 transition; inhibition of filopodia inhibits neurite formation (Dent et al., 2007). These actin bundles serve as tracks on which microtubules converge and condense in a Map1C-dependent manner (Dehmelt et al., 2003) to form the neurite proper. Stage 2 hippocampal neurons typically have multiple undifferentiated neurites or “minor processes.”

The growth cones of these neurites undergo dynamic changes in size, shape, extension and retraction (see movie 1). There is often an engorgement of one neurite's growth cone concomitant with the contraction of the other growth cones. This gives the appearance of a tug-of-war type of competition amongst the neurites. Immediately prior to axon formation, the neurite with the engorged growth cone becomes the axon (Bradke and Dotti, 1997; Bradke and Dotti, 1999; Kunda et al., 2001). A stage 3 neuron has multiple minor processes and one rapidly extending axon. The minor processes later display increased outgrowth and arborization developing into dendrites (Stage 4). After a few weeks in culture, hippocampal neurons will mature, develop dendritic spines and make functional synaptic contacts (Stage 5).

As *in vivo*, in culture, the polarized functional domains (ie. the somatodendritic and axonal compartments) are founded on a segregation of various molecular components that facilitate the function of the respective domains. The axon, for example, is enriched in voltage-gated sodium and potassium channels which are required for the generation and propagation of action potentials. Conversely, dendrites are largely devoid of voltage-gated channels but contain increased numbers of neurotransmitter-gated receptors which are necessary for the receiving chemical messages from the pre-synaptic cell. There are various other important lipid and protein components that are segregated into different compartments of a mature neuron. The maintenance of this differential distribution relies not only on transport mechanisms, but also on diffusion barriers in the membrane that corral membrane components in particular subdomains (Winckler et al., 1999, Nakada et al., 2003). The maintenance of polarization in mature neurons over the period of an organism's life (in humans up to and exceeding one hundred years) is a wondrous feat. This is an important issue and one of clinical relevance, given that neurological diseases such as Amyotrophic Lateral Sclerosis (ALS) and Huntington's disease may involve problems with maintaining proper transport of key molecular components to allow the proper function of neurons (Teuling et al., 2007; Cowan and Raymond, 2006).

The work embodied in this dissertation focuses much earlier, at the initial stages of developing a functional polarized neuron, which begins with the specification of the axon.

There are various molecular mechanisms involved in the establishment of neuronal polarity including intracellular trafficking, membrane specialization and cytoskeletal dynamics.

Although the focus of this work is the regulation of the cytoskeleton, to some extent, this dissertation will contain work that touches upon all of these mechanisms.

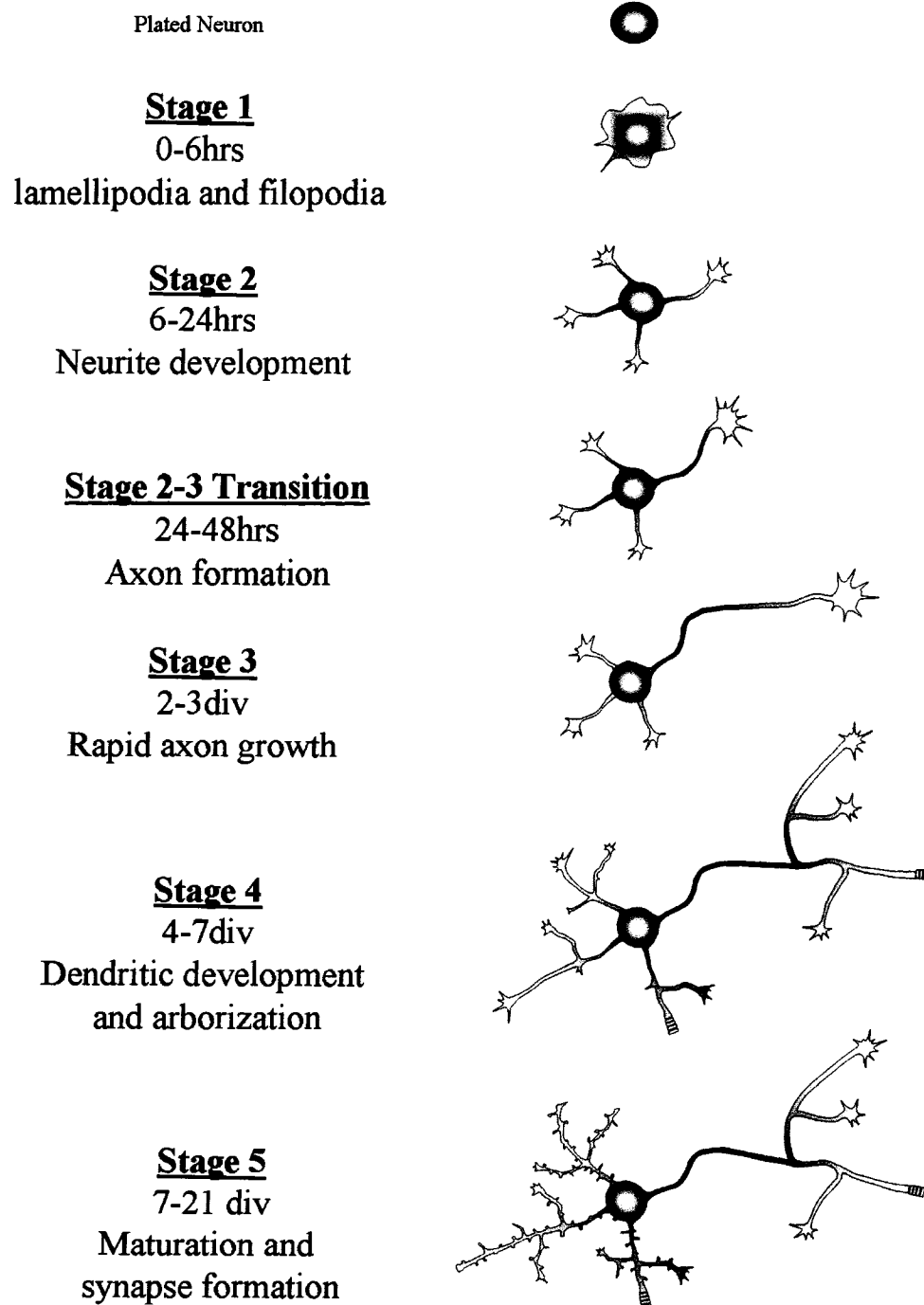
Intracellular Trafficking and Neuronal Polarity

The establishment and the maintenance of neuronal polarity involve the regulation of intracellular trafficking (Horton and Ehlers, 2003). As already mentioned, during the stage 2-3 transition of hippocampal neurons the axon rapidly elongates from one of several immature processes. This requires the delivery of materials necessary to support such growth. Consequently, at a fundamental level, there must be a differential increase in net anterograde transport of materials in the developing axon versus the other processes. Furthermore, we have also seen that neuronal polarization requires the establishment of sub-cellular membrane domains with distinct molecular components. Exactly how intracellular trafficking is regulated during axon formation and how molecular constituents are trafficked and segregated in neurons remain daunting questions in cellular neurobiology. An even more elusive question is how actin is transported in neurons. In this section we will consider these issues.

Intracellular trafficking during axonogenesis

To support rapid elongation of the axon an escalation in the amounts of cytosolic and membrane components need to be transported into the axon. Thus, it is not surprising that a general increase in axoplasmic flow has been observed in the growing axon compared to the slower growing minor neurites (Figure 15; Bradke and Dotti, 1997). During the stage 2-3 transition, axon extension is preceded by an increase in growth cone size, coincident with greater transport of organelles and mitochondria, polarized delivery of Golgi-derived vesicles, and increasing concentrations of cytosolic proteins and ribosomes (Bradke and Dotti, 1997). The appearance of polarized transport is markedly different from the situation

Figure 1.14. The developmental progression of hippocampal neurons in culture. This figure indicates the 5 stages of development, the timing of these events in culture, and the major morphological changes that occur during that stage. Dissociated rodent hippocampal neurons follow a stereotypical program of development. Shortly after plating, the initially round cell body extends lamellipodia and filopodia and assumes a “fried egg” morphology (Stage 1). There is localized collapse of lamellipodia and engorgement and extension of filopodia leading to the formation of multiple neurites that are indistinguishable (Stage 2). All of the neurites of a Stage 2 neuron have the potential to become the axon. Nevertheless, in the cell culture environment without any graded external polarization signals, a stochastic process occurs where one process eventually assumes the axonal identity. 24-48hrs in culture, during the Stage 2-3 transition, one of the growth cones of these processes becomes enlarged and displays increased dynamics relative to the growth cones on other neurites; this neurite begins elongating at a more rapid rate than the remaining processes. 2-3 days in culture, the developing axon continues to grow at a faster rate than the other minor processes (Stage 3). Later in culture, the remaining processes begin to grow and arborize, acquiring the characteristics of dendrites (Stage 4). In between 1 and 3 weeks in culture, the hippocampal neurons form dendritic spines and functional synaptic connections (Stage 5).



in stage 2 neurons, where multidirectional transport of organelles, proteins, and lipids occurs roughly equally in all of the minor processes.

An early signal for polarization is the positioning of the centrosome and Golgi apparatus adjacent to the process that eventually develops into the axon (de Anda et al., 2005). Although this could set into motion the eventual increased transport in the developing axon, transport in stage 2 neurons is uniformly multidirectional when the position of the Golgi is presumably stable until the axon rapidly elongates. Thus it seems a change occurs to shift the trafficking of trans-Golgi network (TGN)-derived vesicles into the developing axon. The situation becomes more complex later in neuronal development in stage 4-5 neurons when Golgi positioning is altered, rotating in the soma from a region juxtaposed to the axon to a region adjacent the base of dendrites. Concomitant with this translocation of the Golgi, TGN derived vesicles are asymmetrically trafficked to the dendritic processes (Horton and Elhers, 2003; Horton et al., 2005). How Golgi translocation occurs is unknown, but may be a crucial aspect for understanding neuronal polarity. The position of the Golgi and its integrity is absolutely necessary for axonogenesis early in neuronal development but also crucial for dendritic development later on. Brefeldin A (BFA) is a drug that blocks endoplasmic reticulum (ER) to Golgi vesicle trafficking but not Golgi to ER trafficking, and thus causes the resorption of the Golgi back into the ER. Treatment of stage3 neurons with BFA diminishes axon growth, while minimally affecting the minor processes (Jareb and Banker, 1997). Stage 4-5 neurons treated with BFA have reduced dendritic growth and arborization (Horton et al., 2005).

Work from the 1980's and 1990's showed axon-specific proteins such GAP-43, synapsinI, and synaptophysin accumulated in developing axons (Goslin and Banker, 1990; Goslin et al., 1988; Goslin et al., 1990; Fletcher et al., 1991). These results suggested a molecular sorting program was involved in the determination of neuronal polarity. However, it was later observed that proteins that are dendrite-specific in mature neurons, such as glutamate receptor subunits, also accumulate in the developing axon early in neuronal development (Craig et al., 1993; Bradke and Dotti, 2000). These results suggest that there is a polarized, albeit unspecific, increase in intracellular transport into the developing axon

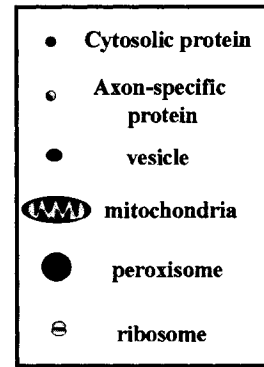
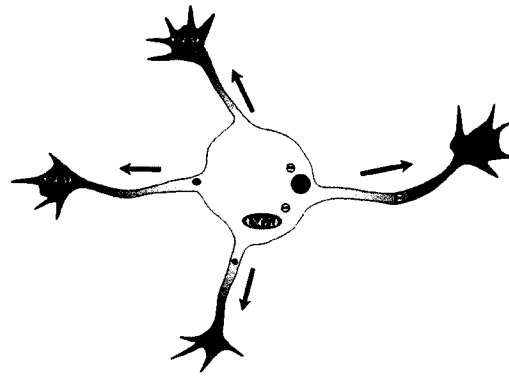
and that it is only after the initial establishment of neuronal polarity that axonal and dendritic functional domains are established to give rise to a mature neuron.

Therefore, in the case of stage 2-3 neurons, axon formation may involve bulk flow of some materials rather than purposeful, directed transport. Yet for other intracellular proteins, directed transport along microtubules via kinesin and dynein motors may be important for their appropriate localization and the development of neuronal polarity. The observation that kinesin 1, but not kinesin 3, accumulates in the developing axon suggests that the selective binding of molecular cargos to kinesin 1 ensures the transport of materials necessary for axon specification (Jacobson et al., 2006). However, this is certainly not the only mechanism, given the observations on other molecules involved in axonogenesis. The Par3/Par6/aPKC complex is considered an evolutionarily conserved polarization signal in various organisms and cell types (Wodarz, 2002). In neurons, Par3 and Par6 initially localize to all growth cones in stage 2 neurons, but then are lost in minor processes but maintained in the developing axon of stage3 neurons (Shi et al., 2003). Par3 is transported to the distal part of neurites via kinesin 2, but not kinesin 1, through an interaction with KIF3A (Nishimura et al., 2004). Thus, selective transport alone cannot explain the differential concentration of Par3, which may also require selective degradation or destabilization of Par3 in the nascent dendrites but not in the axon. There is recent evidence that selective degradation may be a mechanism for the concentration of at least some proteins important to axon specification. Rap1B, a small Rho GTPase that is necessary for axonogenesis (Schwamborn and Puschel, 2004) undergoes ubiquitination, targeting its degradation in minor processes while it is retained in the axon (Schwamborn et al., 2007).

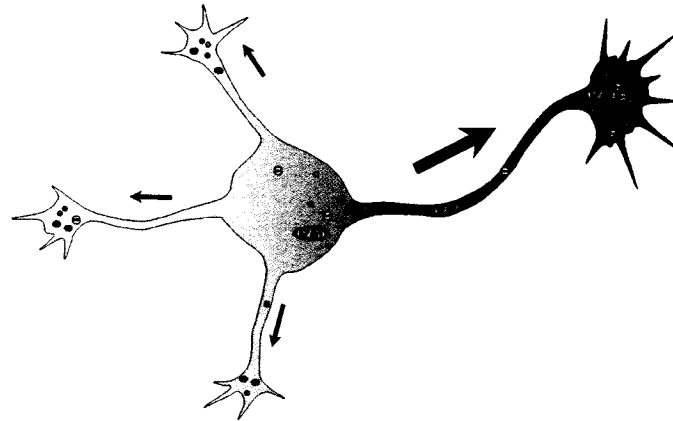
Another possible mechanism that has received much less attention is that growth cone-like waves originating at the cell body propagate down neurite processes (Ruthel and Banker, 1998; Ruthel and Banker, 1999) carrying newly synthesized proteins to the axon and thereby supporting axon development. Various molecules involved in axon development have been localized to wave structures along axonal shafts including Lim kinase, NgCAM, (Rosso et al., 2004) and Shootin (Toriyama et al., 2006). In stage 3 hippocampal neurons, waves travel down both dendrites and axons and result in “bursts” of outgrowth (Ruthel

Figure 1.15. Polarized intracellular trafficking during axonogenesis. A. During Stage 2, there is uniform delivery of materials to all the neurites. At this stage, all of the neurites have the potential to become the axon and have equal distributions of the organelles and proteins that facilitate axon formation. During the Stage 2-3 transition there is increased trafficking of organelles, cytosolic proteins, and ribosomes into one neurite. The growth cone of this neurite becomes larger and more dynamic as a result. Although some specialized delivery mechanisms are certainly working to ensure proper delivery of some axon specific proteins, the bulk delivery of materials ensures the stage 2-3 process has the means to support rapid out growth. This polarized, indiscriminate delivery continues to occur in stage 3 axons. Molecular sorting mechanisms are established later in stage 4 and stage 5 neurons leading to the maturation of the functional sub-domains necessary for neuronal function.

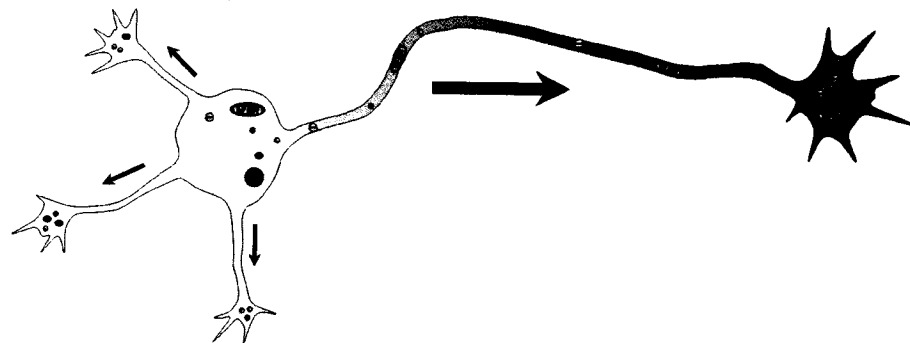
Stage 2



Stage 2-3



Stage 3



and Banker, 1998). It was proposed that these waves are a mechanism for actin transport, although the hypothesis was never directly tested. Actin is known to be part of slow component b of axonal transport, but how it is transported in axons remains an elusive question (Mills et al., 1996). One possibility is that the transport of β -actin mRNA into the axon and local translation supplies the actin to the distal neurite (Piper and Holt, 2004). Although the local translation of actin may be important for mature neurons, the inhibition of actin translation in axons did not affect axon elongation (Eng et al., 1999), suggesting that the delivery of actin from the soma is crucial for axon growth. It is possible that waves represent a mechanism for supplying actin and/or other factors that are crucial during the rapid elongation of the axon.

Evolving functional domains in neurons

How then is the segregation of protein and lipid repertoires achieved to give rise to distinct sub-domains in neurons? For young neurons, bulk transport mechanisms and some biased transport involving kinesin motors are sufficient to initiate the morphological specification of the axon. The maturation of distinct sub-domains in neurons is likely a gradual process and true functional polarization does not occur until later maturation. Accumulating evidence suggests that functional specialization of neuronal subdomains is through the combined effects of various “sorting” mechanisms. In neurons, as in other cells, membrane specialization is the essence underlying neuronal polarity, with distinct lipid and protein repertoires in the somatodendritic membrane and axonal membrane. This is the first basic level of membrane specialization. Axonal membranes, for example, can be dissected further into different functional domains such as the axon initial segment, the nodes of Ranvier, and terminal boutons. Dendrites also have additional regional specializations with distinctions in apical and basolateral dendrites. These region specializations further complicate the issue of axonal and dendritic membrane vesicle trafficking during polarization.

Multiple factors are at work to evolve locales within the neuronal membrane that are distinct in molecular composition. These include selective targeting of proteins along

secretory and endosomal pathways (Jacob and Naim, 2001), stabilizing protein complexes by scaffolding proteins (Harris and Lim, 2001), establishing barriers to lateral diffusion (Kobayashi et al., 1992; Winckler et al., 1999; Nakada et al., 2003), and selectively degrading protein (Schwamborn et al., 2007). These mechanisms likely are at work not only during the development of specialized membrane domains, but also in maintaining these domains in mature neurons.

Selective targeting of proteins involves the recognition, sorting and targeting of proteins to proper localizations. Exactly how proteins are specifically targeted to dendritic and axonal compartments is still a contentious issue. Nevertheless, we can draw inferences from work in other systems, such as polarized epithelial cells. Membrane proteins typically are sorted and trafficked to the cell membrane via secretory and/or endocytic pathways. In the secretory pathway, proteins are trafficked from the Trans-Golgi network to the plasma membrane, as well as lysosomes, endosomes or back to the endoplasmic reticulum. One intrinsic mechanism for sorting proteins is utilizing different cytoplasmic amino acid motifs (tyrosine- and dileucine-based motifs for example) which act as targeting signals to plasma membrane domains or intracellular organelles. In epithelial cells, these signals seem to help localize proteins by directly binding to coat protein components, such as one of the multi-subunit adaptor protein complexes (APs), at the cytoplasmic face of membranes (Bonifacino and Traub, 2003). In neurons, transferrin receptors have been shown to be trafficked to dendrites via a cytoplasmic tyrosine-based signal (Burack et al., 2000), whereas NgCAM seems to be targeted to axons via extracellular fibronectin-like repeat motifs (Sampo et al., 2003).

Membrane proteins can also be trafficked to the plasma membrane in non-descript locations, internalized in a clathrin-dependent manner and transported via transcytosis in an endocytic pathway to specific membrane domains (Tuma and Hubbard, 2003). In some cells, such as hepatocytes, it appears transcytosis is a major mechanism for targeting proteins to specific membrane regions. Although it is unclear how important endocytic pathways are in distributing proteins in discrete regions of the neuronal membrane, endocytosis occurs frequently in active dendrites (Prekeris et al., 1999). This suggests that endocytic pathways

may be important for targeting membrane proteins in neuronal sub-domains. Indeed, recent data supports this hypothesis. VAMP2, a vSNARE, accumulates at axon terminals, but reaches the surface of dendrites as well and is transcytosed in a manner dependent upon its C-terminus, which contains a known endocytosis signal (Sampo et al., 2003). Exactly why VAMP2 is endocytosed in the dendritic membrane while retained in the axon is unknown.

Cellular signaling pathways that modulate actin and microtubule during axon formation

Signalling to the RhoGTPases

Various signaling molecules involved in axonogenesis have been identified recently including factors that impact the actin cytoskeleton. For example, the Rho GTPases Cdc42, Rac-1, and RhoA all play distinct roles in axon specification. However, the identification of actin binding proteins that execute changes in actin dynamics downstream of the Rho GTPases are only now beginning to be characterized. Furthermore, microtubules and microtubule regulating proteins are also important in axonogenesis. Thus, the consideration of signaling pathways affecting cytoskeletal dynamics as a whole, including actin and microtubules, are needed for a more complete understanding of the development of neuronal polarity (reviewed in Yoshimura et al., 2006, Figure 16).

Most of our current understanding of the molecular players involved in axonogenesis comes from studies in cultured neurons, where axon fate is intrinsically specified due to a uniform environment (Craig and Banker, 1994). Conversely, *in vivo*, extrinsic signals probably play a crucial role in axon specification. Although the role of extracellular cues in axonogenesis have not been extensively studied *in vivo*, extrapolations from expression patterns of molecules in developing brain have identified molecules that are potential players involved in axon formation. For example, the extracellular matrix protein laminin is highly expressed transiently in the developing hippocampus (Gordon-Weeks et al., 1989). When neurons are plated on a two dimensional substrate coated with alternating stripes of

polylysine and laminin, axon formation occurs preferentially on laminin substrate (Esch et al., 1999), suggesting a role for laminin *in vivo*. Neurotrophins have been widely studied for their role in supporting neuronal survival, but their role in promoting neurite growth and as potential guidance cues have also been noted (Lykissas et al., 2007). In the hippocampus, Brain Derived Neurotrophic Factor (BDNF) and Neurotrophin 3 (NT-3) are highly expressed during development (Friedman et al., 1991) and induce increased axon growth and branching of hippocampal neurons in culture (Labelle and Leclerc, 2000; Yoshimura et al., 2005). Nerve growth factor (NGF), which is expressed only at low levels in the hippocampal formation does not affect axon growth of cultured hippocampal neurons (Labelle and Leclerc, 2000).

These extracellular cues that affect axon development all have been shown to cause changes in the activity of RhoGTPases, which may be pivotal for the divergence of signals affecting actin and microtubules. PI3-kinase is activated downstream of many guidance cues and, through PIP₃ interactions with Rho guanine nucleotide exchange factors (GEFs), regulate the activity of Rho GTPases (Yoshimura et al., 2006). Broadly speaking, Rho activity is considered inhibitory to neurite outgrowth, whereas Rac and Cdc42 are thought to be supportive. Although these generalizations are helpful, the situation is complicated by the fact that dominant negative (DN) and constitutively active (CA) Rho GTPase mutants often produce similar, rather than opposite, effects on neurite elongation (Luo et al., 1994; Kuhn et al., 1998; Ruchhoeft et al., 1999). In neuronal cell lines, neurite outgrowth depends on rac and cdc42, because DN mutants of either of these GTPases inhibits neurite extension (Sarner et al., 2000; Aoki et al., 2004). Furthermore, in rat cortical neurons, DN versions of both Rac1 and cdc42 decrease neurite outgrowth (Threadgill et al., 1997), and at least in some cases the expression of CA-cdc42 induces neurite outgrowth (Kuhn et al., 2000). The converse is true of RhoA; CA Rho expression prevents neurite growth (Kranenburg et al., 1999; Amano et al., 1998; Satoh et al., 2003) while inhibition of RhoA with C3 exoenzyme or DN Rho expression induced neurite growth ((Kozma et al., 1997; Kranenburg et al., 1999). Although these experiments did not study the development of neuronal polarity *per se*, the results suggest that Rac and Cdc42 positively regulate axon development while Rho

inhibits it. This was an attractive interpretation, especially given the prevalent view that axon differentiation was directly related to neurite length; in neurons with multiple processes, such as hippocampal neurons, the neurite that grows the longest becomes the axon (Goslin and Banker, 1989; Bradke and Dotti, 2000). Later work has corroborated this hypothesis.

The first direct evidence for the role of Rho GTPases in the development of neuronal polarity comes from studies where Stage 2 hippocampal neurons were treated with the Clostridium toxin B, an inhibitor of Rho GTPases (Bradke and Dotti, 1999). Treatment with toxin B caused a reduction of F-actin and produced multiple axons. Since toxin B inhibits all Rho GTPase members, the contributions of individual members of the Rho GTPases could not be assessed from these studies.

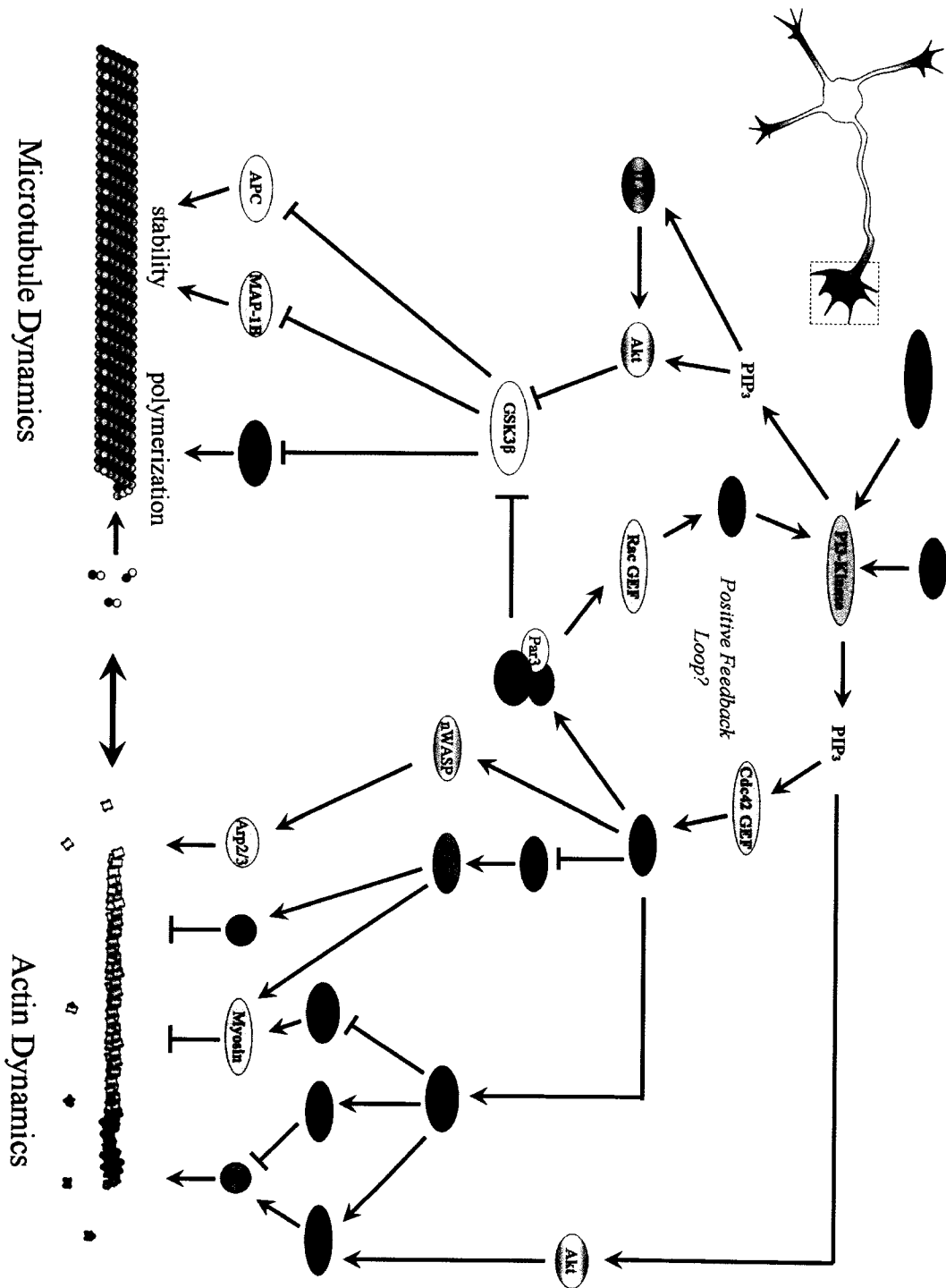
The roles of individual Rho GTPases in axon polarity have been investigated during the past few years. The Rac1 GEF Tiam1 localizes in the developing axon and presumably activates rac1 contributing to axon development (Kunda et al., 2001). Overexpression of Tiam1 induced the formation of multiple axon-like processes whereas antisense RNAs targeting Tiam1 attenuates axon development (Kunda et al., 2001). In addition, the cytoplasmic dynein light chain TcTex-1 functions in axon formation acting through Rac1 (Chuang et al., 2005). However, conflicting results regarding the role of Rac1 in the development of axons and dendrites have also been published (Schwamborn and Puschel, 2004; Gualdoni et al., 2007). In one study it was suggested that Rac was more important for the development of dendrites, because the depletion of Rac with siRNA had no effect on axon length but decreased dendritic length (Gualdoni et al., 2007). In the other work, overexpression of either CA Rac or CA cdc42 did not significantly alter neuronal polarity phenotype. However, the expression of a mutant cdc42 that cycles constitutively between an active (GTP-bound) and inactive (GDP-bound) state induced supernumerary axons. Cdc42 was found to be essential in axon specification downstream of another GTPase, Rap1B (Schwamborn and Pulchel, 2004). This work did not examine the effect of expressing a cycling Rac mutant on neuronal polarity and this may be crucial for determining Rac's effect on axon growth since FRET studies have shown that Rac and cdc42 undergo localized activity cycling during NGF mediated neurite growth in PC12 cells (Aoki et al., 2004).

In hippocampal neurons, the over-expression of active Rho (RhoAV14) leads in some studies to an inhibition of axon differentiation (Da Silva et al., 2003; Schwamborn and Puschel, 2004) and in other studies inhibits neuritogenesis altogether (Kim and Chang, 2004). DN RhoA expression (RhoAV12) increases neurite lengths but does not cause the development of supernumerary axons (Schwamborn and Puschel, 2004). Again, these studies did not examine the expression of a constitutively cycling Rho, which may exhibit different effects than the DN-Rho or CA- Rho.

What signaling cascades are important for axon development downstream of the Rho GTPases? From studies on cell motility and neuronal pathfinding in different systems various signaling proteins that are downstream effectors of the Rho GTPases have been identified (Song and Poo, 2002) that may also play a role in the development of neuronal polarity. Dissecting these signaling pathways is no trivial feat given the complexity of the interactions between these proteins and the divergence and convergence of cell signaling cascades (see Figure 16). Nevertheless, there is sufficient evidence demonstrating that signals that affect axon specification impact actin and microtubules (Yoshimura et al., 2006).

The highly motile growth cones of rapidly growing neuronal processes require drastic dynamic rearrangements of the underlying actin and microtubule cytoskeletons. Actin instability (i.e. dynamics) is markedly increased in one of the neurite growth cones of an unpolarized stage 2 hippocampal neuron and the application of the actin destabilizing drug cytochalasin D induces axons to form, implying a direct role for increased actin reorganization and dynamics during axon formation (Bradke and Dotti, 1999). It was hypothesized in these studies that the increased actin dynamics would permit increased microtubule polymerization, the driving force behind neurite extension (Figure 17). Indeed, Forsher and Smith (1988) showed that increasing actin disassembly with cytochalasin allows microtubule penetration into peripheral regions of the growth cone and leads to rapid neurite growth. Thus, it appears some mechanical linkage or steric interaction is present in growth cones between actin and microtubules, such that the actin cytoskeleton is restrictive for microtubule growth. Recent work has identified molecules that bind actin and microtubules which may be important for axon growth.

Figure 1.16. Signaling pathways involved in axonogenesis. This simplified diagram illustrates major signaling pathways involved in the regulation of the growth cone cytoskeleton during the development of neuronal polarity (see details in text). The Rho GTPases are at the center of the polarity pathway, exhibiting crosstalk which may account for the proposed feedback loop involved in the initial symmetry breaking during axon formation. This feedback loop may involve the generation of PIP_3 , which can activate cdc42 via GEFs. Cdc42 activity can regulate Par3/Par6/aPKC, which affects Rac activity via GEFs. Rac can feedback to PIP_3 -Kinase, leading to further increases in PIP_3 . PIP_3 can also activate RhoGTPase-independent pathways that affect GSK3 β activity via Akt. GSK3 β represent another site of divergence in the signaling pathway affecting multiple proteins, including microtubule polymerization and stability. Downstream of RhoGTPases are multiple signaling proteins, such as ROCK and PAK, that can affect actin dynamics through a variety of actin binding proteins.



Microtubules were first shown to be crucial for neurite extension in studies using drugs such as nocodazole that caused microtubule depolymerization, as well as drugs such as taxol that increased microtubule stability, both of which inhibited outgrowth (Rochlin et al., 1996; Rochlin et al., 1999). These early studies used relatively high levels of these drugs leading to dramatic effects on the microtubules. More recent studies using lower concentrations of taxol and nocodazole have demonstrated that the tight regulation of microtubule stability is required for axon formation (Witte et al., 2008). When low concentrations of taxol was applied to a stage 2 neuron, multiple axons formed and the number of stable microtubules (Glu-tubulin) increased in the supernumerary axons. Low levels of nocodazole did not prevent axon formation, but did reduce the number of minor processes, suggesting that the axon is unaffected by nocodazole because it contains more stable microtubules (Witte et al, 2008). Thus, it appears microtubule stability is paramount to axon formation. The more stable microtubules may not only serve as tracks for kinesin motors to delivery molecular cargo, but also as sites for increased microtubule polymerization. The microtubule array in the neurites is established through two mechanisms: the transport of microtubule polymers preassembled in the soma and via microtubule polymerization at the plus ends of microtubules (Baas, 1997).

Signaling to Actin

Downstream targets of Rho GTPases modulate the actin cytoskeleton. Activation of the Rho effector, ROCK, counteracts axon development. Treating stage 2 neurons with the ROCK inhibitors H1192 or Y21372 increases neurite growth and the percentage of neurons with supernumerary axons (Kim and Chang, 2004; Da Silva et al., 2003). ROCK is known to regulate actomyosin contractility via myosin II activity through phosphorylation and activation of myosin light chain kinase (MLCK) and by inhibition of MLC phosphatase (MLCP) (Totsukawa et al., 2000). Myosin inactivation may facilitate the formation of axons (Kim and Chang, 2004,), suggesting increased myosin activation would attenuate axon formation. ROCK activation can also decrease actin turnover by inhibiting ADF/cofilin activity through Lim kinase activation (Maekawa et al., 1999), which may be important in

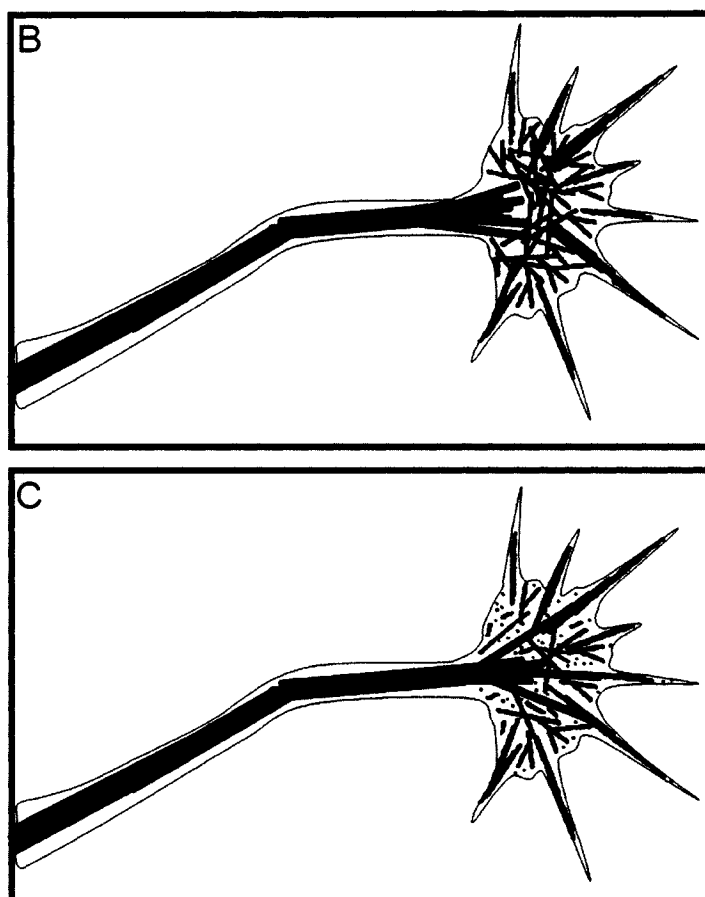
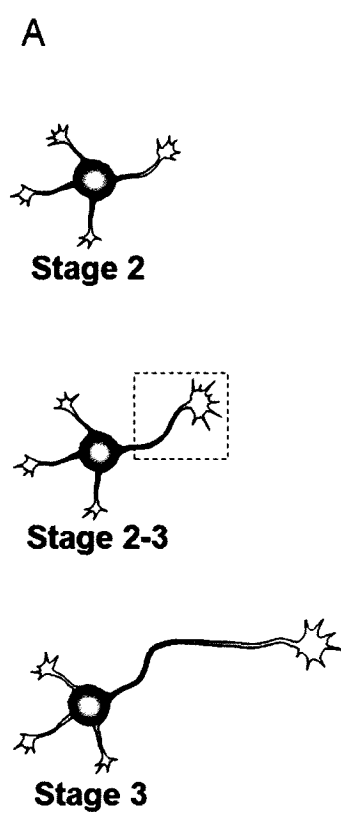
neurite growth (Zhang et al., 2006). Profilin is also activated downstream of ROCK, and this has been speculated to be unfavorable for neurite growth and axon differentiation (DaSilva et al., 2003). The downstream effects of Rho exemplifies the complexity GTPase signaling, since here we have discussed four actin binding proteins whose activity is modulated by Rho, and undoubtedly there are others. Nevertheless, we can begin to understand how Rho may lead to decreased axon growth via these downstream effectors which all could contribute to the increased stability of a contractile actin network.

Other work has recently shown that p21-activated kinase (PAK), a downstream effector of rac and cdc42, also plays a role in the development of neuronal polarity (Jacobs et al., 2007). The over-expression of an active, membrane-targeted PAK leads to a disruption in neuronal polarity; neurons did not display a single axon, but rather had numerous long axon-like neurites. Interestingly, the expression of rac and active cofilin partially rescued a normal, one-axon phenotype. Since microtubules were also disrupted, the authors speculated that perhaps the downstream effector stathmin may also be regulated by PAK during the establishment of neuronal polarity (Jacobs et al., 2007, see below).

Other actin binding proteins also may function downstream of the RhoGTPases during the establishment of neuronal polarity. For example, Ena/Vasp proteins are crucial for filopodia formation and dynamics in axonal growth cones, perhaps explaining their role in axon guidance (Lebrand et al., 2004). Analysis of brains from the triple Ena/Vasp/EVL knockout have revealed disruptions in axon tract formation in the cortex and blocked neuritogenesis in culture (Kwiatkowski et al., 2007). It was unclear from this study if there were perturbations in axon specification in the Ena/Vasp/EVL nulls. Laminin treatment fully rescued neuritogenesis, but there was only a partial rescue of neurons with an axon (Dent et al., 2007). Arp2/3 complex activity reduces axon outgrowth and also probably plays a role in growth cone guidance (Strasser et al., 2004), but its contribution to axon specification has not been studied. In addition, the formin mDia promotes axon growth in cerebellar neurons (Arakawa et al., 2003) and can increase neurite growth and axon development in Ena/Vasp/Evl knockout neurons (Dent et al., 2007).

Tropomyosins are another family of actin binding proteins likely involved in the

Figure 1.17. Increased growth cone actin dynamics precedes axon formation. **A.** The growth cones of stage 2 neurons have similar sizes and dynamics. During neuronal polarization (Stage 2-3) the growth cone of one of the minor neurites grows larger and becomes more dynamic. This growth cone's neurite begins to rapidly extend, forming the axon (Stage 3). **B.** Before axon formation, the growth cone of the presumptive axon is similar to the other growth cones of the minor neurites. The growth cone contains actin filaments comprising the peripheral domain that are less dynamic than during stage 2-3 and act as a barrier for microtubule growth. **C.** During the stage 2-3 transition the developing axonal growth cone becomes more dynamic with increased F-actin disassembly and turnover. This increased dynamics of the actin cytoskeleton releases inhibitory constraints on the microtubules, which can polymerize more distally into the peripheral growth cone. These cytoskeletal changes continue in stage 3 neurons as the axon rapidly elongates (figure based on Bradke and Dotti, 2000).



development of neuronal polarity. Despite the complexity of gene expression of the TM proteins, recent progress has been made in identifying and characterizing how specific TMs regulate specific actin structures in neurons and how TMs contribute to axon development and growth cone dynamics. It was recognized years ago that TMs were spatially segregated in specific regions of developing and mature neurons (reviewed in (Gunning et al., 1998). For example, TM5NM 2 from the γ Tm-gene is highly enriched in the axon, but is absent from the growth cones and dendrites. On the other hand, TM5NM 1, as well as Tm4 are localized to growth cones of developing neurons. The over-expression of TM5NM1 resulted in enlarged growth cones and longer axons with increased branching, but also increased the number of dendrites (Schevzov et al., 2005). The non-neuronal Tm3 over-expression reduced dendrite number and length. These findings support the hypothesis that the differential expression and spatial segregation of TM isoforms may lead to the formation of different actin populations with different kinetics and specific functions; this role of TMs may be crucial for the development of neuronal polarity (Gunning et al., 1998).

Signaling to Microtubules

Rho GTPases signaling to microtubules also appears to play an important role in the development of neuronal polarity. However, Rho GTPase-independent signaling to microtubules are present in neurons that influence axon development. Both Rho GTPase-dependent and -independent signaling influence microtubule binding proteins that regulate microtubule stability and polymerization-depolymerization kinetics.

As previously mentioned, PI3-kinase and its lipid product PIP_3 is important in the determination of cell polarity in various cell types (Iijima et al., 2002; Janetopoulos and Devreotes, 2006) including neurons (Shi et al., 2003; Yoshimura et al., 2005). PIP_3 represents a divergence point for Rho GTPase-dependent (via activation of GEFs) and -independent signaling during axonogenesis. For the latter, PIP_3 is necessary for the localization of Akt at the plasma membrane, where it is phosphorylated by PDK, IDK, as well as other kinases (Hannigan et al., 2005). When active, Akt phosphorylates GSK-3 β , which inhibits its kinase activity against primed substrates (those that require a prior

phosphorylation; (Cohen and Frame, 2001). GSK3 β can also be regulated downstream of the Rho GTPases via Par3/Par6/aPKC complex (Hall, 2005). Inhibition of GSK-3 β with drugs or knock-down of GSK-3 β with siRNA induces the formation of multiple axons, whereas the expression of CA-GSK-3 β inhibits axon formation (Jiang et al., 2005; Yoshimura et al., 2006). Of the various substrates for GSK-3 β , many are key microtubule binding proteins, including MAP1B, MAP2, APC, tau, and CRMP-2.

These microtubule binding proteins have all been shown to play a role in neurite growth and potentially in axon specification. MAP1B, which does not require priming, is phosphorylated by GSK-3 β and this activates its binding to microtubules (Goold and Gordon-Weeks, 2004, Goold and Gordon-Weeks, 2005). Hippocampal neurons isolated from the MAP1B knockout display a drastic attenuation of axon development (Gonzalez-Billault et al., 2001). These effects are presumably because of altered microtubule stability, which can influence microtubule assembly that is crucial for axon development. Support for this comes from a recent study where the expression of EB-1, which promotes microtubule assembly, can rescue polarity defects in the MAP1B KO neurons (Jimenez-Mateos et al., 2005).

MAPs may also regulate neuronal polarity by other means. The differential expression pattern of MAPs in developing neurons may also help regulate axon specification by their different abilities to protect microtubules against the actions of severing proteins such as katanin (Qiang et al., 2006). Tau expression in the axon seems to confer decreased sensitivity to katanin severing than other Maps, such as Map1B. Interestingly, katanin expression increases in neurons undergoing axonogenesis, suggesting a role for severing in microtubule dynamics during axon formation. Indeed, the tight regulation of katanin levels and activity may be crucial for axon growth since DN-katanin inhibits axon growth as does excessive over-expression of wt-katanin (Karabay et al., 2004). The protection of axonal microtubules may ensure a suitable level of microtubule severing to promote growth, whereas the less protected microtubules in the minor processes leads to an environment with excessive severing, one unfavorable for outgrowth.

Another GSK3 β substrate that does require priming, APC, has also been shown to

play a role in axon formation (Shi et al., 2004). APC over-expression reduced neuronal polarity, which the authors speculated was due to Par3 mis-localization, however, it also could have been due to abnormal microtubule polymerization.

CRMP-2 is highly and specifically expressed in the developing nervous system (Goshima et al., 1995; Wang and Strittmatter, 1996). GSK-3 β phospho-regulation of CRMP-2 activity is an important determinant of axonal fate in hippocampal neurons (Yoshimura et al., 2005). Active CRMP-2 localizes to developing axons and the over-expression of CRMP-2 induces the formation of multiple axons. Conversely, its inhibition attenuates axonogenesis (Ignaki et al., 2001). It is likely that CRMP-2's promotion of microtubule polymerization is a crucial aspect of its promotion of axon specification.

Another microtubule regulating protein that is of importance during the establishment of neuronal polarity is stathmin/SCG-10. Pak1, which plays an important role in axonogenesis (Jacobs et al., 2007), can phosphorylate and inhibit stathmin proteins (Wittmann et al., 2004). The expression levels of SCG-10 have different effects on neurite outgrowth; siRNA-mediated silencing of SCG-10 expression decreases neurite outgrowth and moderate over-expression increases neurite outgrowth; however, robust over-expression also reduces outgrowth (Morii et al., 2006). The resulting perturbations in neurite outgrowth were mirrored by alterations in microtubule stability; knockdown of SCG-10 increases microtubule stability whereas the modest over-expression of SCG-10 results in increased microtubule dynamics, but excessive over-expression results in microtubule depolymerization. Stathmin inhibition downstream of Rac1 is necessary for microtubule stabilization specifically during axon formation, since the expression of a CA-stathmin inhibited axon induction by Dock (a Rac-activating GEF) expression (Watabe-Uchida et al., 2006). Thus, the tight regulation of stathmin/SCG-10 activity downstream of the Rho GTPases also contributes to axon formation.

Summary

In this review of these cytoskeletal regulators we can identify certain trends in the combined effects of the various proteins on actin and microtubules. Generally, the activities

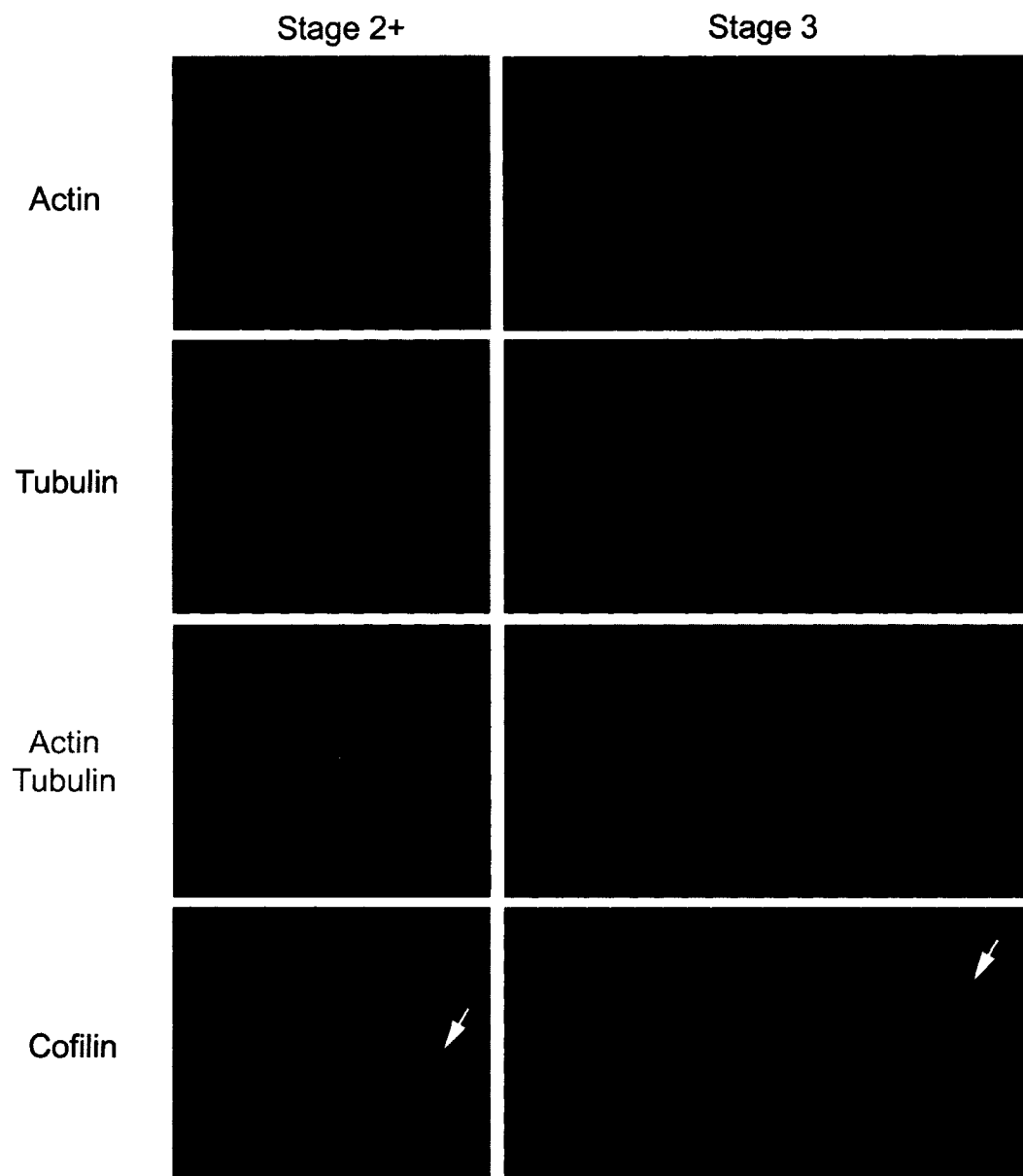
of the cytoskeletal regulating proteins reflect the results from the aforementioned drug studies. For microtubules, simply put, there needs to be a positive potential for microtubule polymerization. In neurons, this can be achieved by the tight regulation of microtubule binding proteins that modulate the stability of microtubules in the axon as well as activating molecules that aid in the addition of microtubule to the plus ends.

For actin, overall it is clear that signaling pathways favoring increased actin turnover and dynamics are activated in the developing axonal growth cone. The coordinated regulation of the activity of a repertoire of actin binding proteins can achieve this end; the activity of proteins that favor actin stability and contractility are down-regulated whereas actin dynamizing proteins exhibit increased activation.

One such family of proteins that favors increased actin dynamics is the ADF/cofilin family. At the time I began my research for this dissertation, there had been no direct examination of the role of ADF/cofilin in the development of neuronal polarity. We recognized early on that the high level of cofilin in developing axonal growth cones could be crucial to neuronal polarization (Figure 18) Our work presented in Chapter 2 has described a niche for cofilin downstream of cdc42 in the regulation of axon formation (Garvalov et al., 2007). Other groups, although not directly examining ADF/cofilin or utilizing different systems, have largely corroborated our findings (Ng and Luo, 2004; Rosso et al., 2004; Jacobs et al., 2007). In our work we found that ADF/cofilin could not rescue the polarity in cdc42 KO neurons; this suggests the potential involvement of other actin binding proteins downstream of cdc42. Therefore, we began studies looking into a potential role of myosin II and how myosin II inhibition may work synergistically with cofilin activation to specify axon formation (Chapter 3). We identified that myosin II inhibition resulted in increased axonogenesis, an effect that was enhanced by increased cofilin activation. Furthermore, active myosin was seen to localize to neurite shafts where it plays a role in limiting the formation of collateral branches.

In our live-cell imaging studies we recognized an interesting correlation of propagating growth cone-like waves in axon formation and neurite branching. We found that these waves were enriched in proteins involved in axonogenesis that regulate actin, including

Figure 1.18. The distribution of actin, microtubules and cofilin in developing hippocampal neurons. Cultured hippocampal neurons were fixed and immunostained for tubulin (second row) and cofilin (bottom row). Actin filaments were visualized with fluorescent phalloidin (top row). The presumptive axon of a stage 2-3 neuron (left column) has an enlarged growth cone relative to the other processes. Notice that microtubules penetrate deep into the growth cone and splay within the F-actin rich peripheral domain. There is a high level of total and putatively active cofilin in the enlarged growth cone. Stage 3 neurons (right column) have a single long axon with a large growth cone. The axonal growth cone also has penetrating microtubules and a high level of cofilin.



ADF/cofilin. In Chapter 4, we describe the potential role of waves in axon formation and the transport of actin (and potentially other proteins involved in axon growth) to the growth cones of developing neurons. Furthermore, we show that waves occur in hippocampal slice cultures, an *in vivo*-like environment, suggesting that waves are physiologically relevant contributors to neuronal development.

The significance of the findings presented in the work embodied here is discussed in Chapter 5. A unified model of the combined effects of cdc42, cofilin, myosin II and waves during axonogenesis is presented with an emphasis on the regulation of distinct, though overlapping actin superstructures. Finally, we will consider future avenues of research that can stem from this dissertation.

Chapter 2

Cdc42 regulates cofilin during the establishment of neuronal polarity

Preface and Acknowledgements

The work presented in this chapter was published in the Journal of Neuroscience (Garvalov et al., 2007). The list and order of authors are as follows: Boyan K. Garvalov, Kevin C. Flynn, Dorothee Neukirchen, Liane Meyn, Nicole Teusch, Xunwei Wu, Cord Brakebusch, James R. Bamberg, and Frank Bradke. Boyan Garvalov and Kevin Flynn were co-first authors. The authors would like to thank the animal facilities of the MPI of Neurobiology, as well as Alisa Shaw for technical assistance. We are very grateful to Barbara Bernstein, Magdalena Götz, Pankaj Goyal, Françoise Helmbacher, Rüdiger Klein, Mike Maloney, Thomas Mayer, Chi Pak, Dharmendra Pandey, Gaia Tavosanis, Hans Thoenen, and O'Neil Wiggan for helpful comments and suggestions on the manuscript. We also thank Gergana Dobрева for assistance with histological analysis, Andreas Püschel for the pEGFP-Cdc42 construct, Gerhard Schratt and Michael Greenberg for the phospho-PAK antibody, Walter Witke for the profilin II antibody, Martin Vogelsang and Klaus Aktories for the C2-C3 fusion toxin. We gratefully acknowledge support from the Max Planck Society (F.B.) and grant SFB 391 from the Deutsche Forschungsgemeinschaft (F.B.), as well as from the National Institutes of Health, grants NS40371 and DK69408 (J.R.B.), NS43115 (J.R.B. and K.C.F.), and NS48660 (K.C.F.). F.B. is a recipient of a Career Development Award from the Human Frontier Science Program.

Abstract

The establishment of polarity is an essential process in early neuronal development. Although a number of molecules controlling neuronal polarity have been identified, genetic evidence about their physiological roles in this process is largely lacking. We analyzed the

consequences of loss of Cdc42, a central regulator of polarity in multiple systems, on the polarization of mammalian neurons. Genetic ablation of Cdc42 in the brain led to multiple abnormalities, including striking defects in the formation of axonal tracts. Neurons from the Cdc42-null animals sprouted neurites, but had a strongly suppressed ability to form axons both *in vivo* and in culture. This was accompanied by disrupted cytoskeletal organization, enlargement of the growth cones and inhibition of filopodial dynamics. Axon formation in the knockout neurons was rescued by manipulation of the actin cytoskeleton, indicating that the effects of Cdc42 ablation are exerted through modulation of actin dynamics. In addition, the knockouts showed a specific increase in the phosphorylation (inactivation) of the Cdc42 effector cofilin. Furthermore, the active, non-phosphorylated form of cofilin was enriched in the axonal growth cones of wild type, but not of mutant neurons. Importantly, cofilin knockdown resulted in polarity defects quantitatively analogous to the ones seen upon Cdc42 ablation. We conclude that Cdc42 is a key regulator of axon specification, and that cofilin is a physiological downstream effector of Cdc42 in this process.

Introduction

The establishment of neuronal polarity is manifested in the differentiation and functional specialization of distinct processes, the axon and the dendrites (Craig and Banker, 1994). A number of molecules involved in neuronal polarization have been delineated in recent years, many of which regulate cytoskeletal dynamics (reviewed in Arimura and Kaibuchi, 2007). Of particular interest among those are small GTPases of the Rho family, which are key regulators of the cytoskeleton (Ng and Luo, 2004; Govek et al., 2005; Jaffe and Hall, 2005). However, no loss-of-function data in a vertebrate organism supporting a role of Rho GTPases in neuronal polarization have been reported. It is also unclear which downstream effectors of Rho GTPases are important under physiological conditions.

Among the Rho GTPases, Cdc42 is of particular interest with respect to neuronal polarization, since it is crucial for axon growth in *Drosophila* (Luo et al., 1994) and has been implicated in the establishment of polarity in neuronal cultures, downstream of another small GTPase, Rap1B (Schwamborn and Püschel, 2004). Interestingly, the generation of Cdc42-

deficient mammalian fibroblastoid cells has demonstrated that Cdc42 is not essential for functions such as filopodia formation, cell polarization or directed migration (Czuchra et al., 2005), which have hitherto been assumed to be Cdc42-dependent. Moreover, constitutively active and dominant negative Rho GTPase mutants usually produce similar, rather than opposite effects on neurite extension in a variety of systems (Luo et al., 1994; Kuhn et al., 1998; Ruchhoeft et al., 1999). This underscores the importance of examining the consequences of Cdc42 ablation on the establishment of neuronal polarity.

Cdc42 has a large number of downstream effectors that control polarity-related events (Etienne-Manneville, 2004; Arimura and Kaibuchi, 2007). One pathway, shared between Cdc42 and other members of the Rho family, is the ADF (actin-depolymerizing factor)/cofilin-dependent control of actin dynamics. Cofilin/ADF is the major cellular factor enhancing the turnover rate of actin filaments (Carrier et al., 1997; Rosenblatt et al., 1997). It possesses concentration-dependent actin filament severing, filament stabilizing, and filament nucleating activities (Bamburg, 1999; Andrianantoandro and Pollard, 2006), which are inhibited upon phosphorylation of the protein on Ser³ (Agnew et al., 1995; Nagaoka et al., 1996). Cofilin activity is important for sustaining neurite outgrowth (Meberg and Bamburg, 2000), growth cone dynamics in cultured neurons (Endo et al., 2003), and pathfinding in response to guidance cues (Wen et al., 2007). In addition, BDNF-stimulated filopodial dynamics in retinal cells is mediated by cofilin (Gehler et al., 2004), through mechanisms that are thought to involve Cdc42 (Chen et al., 2006). However, none of the studies so far has addressed the role of cofilin in the establishment of polarity *per se*, nor the relationship between the activities of Cdc42 and cofilin in this process.

Here we used a genetic knockout strategy to ablate the Cdc42 protein in mouse brain in order to investigate its physiological role and downstream effectors in axonogenesis. We show that loss of Cdc42 strongly suppressed axon formation *in vivo* and in culture and that cofilin is an important downstream effector in this process

Materials and Methods

Cell culture and transfection: Primary hippocampal neurons from E16.5-17.5 mouse embryos were cultured essentially as described (de Hoop et al., 1998). For the mixed wild-type (GFP-positive)/Cdc42 knockout (GFP-negative) cultures, the hippocampi of embryos from a *Nestin-Cre^{+/-}*, *Cdc42^{fl/wt}* × *Cdc42^{fl/fl}* cross were dissected, trypsinized and dissociated individually for each embryo. In parallel, hippocampi from wild type, GFP positive embryos expressing GFP under the ubiquitous “CAG” promoter, (composed of the CMV enhancer, a fragment of the chicken β -actin promoter and rabbit β -globin exons) (Okabe et al., 1997; Ikawa et al., 1998) were dissected, trypsinized and dissociated. The cells were then washed in Hank’s balanced salt solution (HBSS), containing 7 mM HEPES, pH 7.25, and $60\text{--}65 \times 10^3$ wild type cells were plated together with $80\text{--}90 \times 10^3$ Cdc42 knockout cells onto polylysine coated glass coverslips in 6 cm tissue culture dishes, containing minimal essential medium and 10% heat-inactivated horse serum. For transfection, $3\text{--}6 \times 10^5$ cells were electroporated following the manufacturer’s instructions (Amaxa). The pEGFP-Cdc42 plasmid was a generous gift of A. Püschel. The cultures were grown in a humidified tissue culture incubator at 36.5 °C, 5% CO₂, and after 12-20 hr the coverslips were flipped in 6 cm dishes containing astrocytes in N2 medium. E16.5 mouse hippocampal neurons used for the experiments with adenoviral-mediated expression in neurons were cultured as described (Meberg and Miller, 2003).

Live cell imaging: Long-term time lapse imaging for analysis of neurite growth rates was performed in T-25 flasks to which photo-etched number 1 glass coverslips (Electron Microscopy Sciences, Washington, PA) had been sealed. Mixed GFP wild-type and cdc42KO neurons were cultured in 10 ml Neurobasal medium, containing B27 supplement (Invitrogen, San Diego, CA) and 2 mM glutamine, which was pH equilibrated in 5% CO₂ incubator prior to imaging. The flask was sealed for the duration of the imaging and there was no noticeable change in the pH of the media over a 48hr period. Images were acquired every 60-120 minutes using a Metamorph controlled CCD camera at ~37°C.

Short term time lapse imaging for analyzing growth cone dynamics was done in HBSS/

HEPES-containing closed metal chambers at ~37 °C (Bradke and Dotti, 1997).

Drug treatments: The general inhibitor of caspase-1/caspase-3 family proteases, Z-Val-Ala-DL-Asp(OMe)-fluoromethylketone (Z-VAD-fmk; Bachem), was dissolved in DMSO at 100 mM and applied to the neuronal cultures at a final concentration of 100 μ M 0-6 hr after plating. After flipping the coverslips in N2 medium, fresh Z-VAD-fmk was added to a final concentration of 100 μ M. For depolymerization of actin filaments, the barbed end binding compound cytochalasin D (Cooper, 1987; Sigma) was dissolved in DMSO at 10 mM and applied to the neuronal cultures 24 hr after plating at a final concentration of 1 μ M. For the washout experiment, cytochalasin D was applied 24 hr post plating, washed 24 hr later and the neurons were allowed to grow for another 24-48 hr in the absence of the drug before fixation. The Rho kinase inhibitor H-1152 (Calbiochem) was dissolved in water at a concentration of 5 mM and applied to the neuronal cultures 2 hr after plating at a final concentration of 500 nM. The GSK-3 inhibitor SB415286 (Tocris Bioscience) was dissolved in DMSO at a concentration of 25 mM and applied 4 hr after plating at a final concentration of 20 μ M. The PAK inhibitory and control peptides (Kiosses et al., 2002) were dissolved in water at a concentration of 10 mg/mL and applied 4 hr after plating at a final concentration of 100 μ g/mL.

Immunocytochemistry: For immunofluorescence staining, neuronal cultures were fixed with 4% paraformaldehyde, 4% sucrose in phosphate-buffered saline (PBS) for 20 min, quenched with 50 mM ammonium chloride in PBS for 10 min and extracted with 0.1% Triton X-100 in PBS for 5 min. The coverslips were blocked in 2% fetal bovine serum (Gibco), 2% bovine serum albumin (Sigma), and 0.2% fish gelatin (Sigma) in PBS. The following primary antibodies were used: mouse anti-Tau-1 monoclonal antibody, clone PC1C6 (Chemicon), anti-class III β -tubulin monoclonal antibody, clone TUJ1 (Covance), anti-MAP2 monoclonal antibody, clone HM-2 (Sigma), and anti- β -tubulin monoclonal antibody, clone B-5-1-2 (Sigma). The secondary antibody was Alexa Fluor 568 goat anti-mouse IgG (Molecular Probes). For visualization of actin filaments, neurons were stained with rhodamine phalloidin (Molecular Probes). Images were acquired on Axiovert 135/135 TV inverted microscopes (Carl Zeiss), equipped with standard

filters for GFP and Texas Red fluorescence (Zeiss and AHF analysentechnik), using a High performance CCD Camera 4912 (COHU) and Scion Image 4.0.2 software. Adobe Photoshop and Adobe Illustrator were used for processing and annotation of the images. Process lengths and growth cone areas were measured using Scion Image, ImageJ and Metamorph software.

Ratio imaging of total cofilin/phospho-cofilin: All neurons were fixed for 30 min in 4% formaldehyde in cytoskeletal preservation buffer containing 10 mM MES pH 6.1, 138 mM KCl, 3 mM MgCl₂, 10 mM EGTA, and 0.32 M sucrose. Cells were washed 3x in PBS and permeabilized in 0.5% Triton X-100 for 10 minutes. After blocking for 1 hr in 1% Bovine Serum Albumin (BSA) and 2% goat serum in PBS, cells were immunostained for total cofilin with 14.8 µg/ml mouse monoclonal antibody (MAb22; Abe et al., 1989) and for phospho-cofilin with 1.1 µg/ml affinity purified rabbit antibody (Meberg et al., 1998) in blocking buffer at 4 °C overnight. Cultures were then washed in PBS and incubated with secondary antibodies diluted 1:400 in 1% BSA-PBS for 1-2 hrs. IgG secondary antibodies (Molecular Probes, Eugene, Oregon) were Fluorescein goat anti-mouse IgG, Texas Red goat anti-rabbit, and Alexa 350 goat anti-mouse. Coverslips were mounted with Prolong Anti-fade (Molecular Probes).

Images were acquired with a Nikon Diaphot inverted microscope using a 40x oil immersion objective and a Coolsnap ES CCD camera (Roper Scientific, Tucson, AZ). Metamorph software (Universal Imaging, Westchester, PA) was used for image acquisition and analysis. Background fluorescence was subtracted from the raw images, which were then overlaid as a stack. After alignment, the ratio of the total cofilin image over the phospho-cofilin image was obtained with the ratio images option in the Metamorph software. Intensities of the ratio images were compared between growth cones from the same neuron. Quantitative comparisons between images from growth cones of Cdc42 knockout neurons and wildtype neurons were only made between neurons from the same coverslip where images were acquired under identical conditions.

Histological analysis: The heads of E18.5 mouse embryos or P0 pups were fixed in 4% paraformaldehyde, 4% sucrose in PBS overnight and Nissl stained following standard

procedures. Briefly, the heads were dehydrated in a series of 30%-100% ethanol solutions, followed by incubation in xylene and paraffin embedding. 12 μm thick paraffin sections were deparaffinized by warming to 62 °C for 30 min, incubating consecutively in 2 changes of xylene, 100% EtOH, 70% EtOH and H_2O , followed by a 15 min staining with a 0.2% cresyl violet solution, dehydration in 70%-100% EtOH solutions and xylene, and mounting. For immunohistochemistry, paraffin sections were stained with the Tau-1 mouse monoclonal antibody (Chemicon) and developed using an ABC Vectastain kit, following the manufacturer's recommendations (Vector Laboratories).

For DiI tracing, heads from E18.5 embryos were dissected and immediately fixed overnight in 4% paraformaldehyde (PFA), 4% sucrose in PBS. Dry crystals of 1,1'-dioctadecyl-3,3,3',3'-tetramethylindocarbocyanine perchlorate (DiI; Molecular Probes) were injected with a glass capillary into the cortex of the dissected brains, laterally of the longitudinal fissure, and allowed to diffuse for at least 1-2 weeks at room temperature. Care was taken to inject crystals of similar size into corresponding regions of wild type and knockout cortices. The brains were subsequently cut into 50-100 μm -thick sections with a vibratome and imaged using a TCS NT confocal microscope (Leica).

DiOlastic labeling of 250-300 μm thick vibratome sections of PFA fixed E18.5 cortices was done with DiO-coated 1 μm tungsten microcarriers, as previously described (Gan et al., 2000).

Protein extraction, immunoprecipitation and Western blotting: Dissected cortices or hippocampi from E18.5 embryonic brains were resuspended by pipetting in cold extraction buffer (1% Triton X-100, 0.5% Nonidet P-40, 25 mM Tris.HCl pH7.5, 100 mM NaCl) supplemented with 1x Complete, EDTA-free protease inhibitor cocktail (Roche), 50 $\mu\text{g}/\text{mL}$ 4-(2-aminoethyl)benzenesulfonyl fluoride hydrochloride (AEBSF, Sigma) and 1 mM sodium orthovanadate (Sigma). After mixing for 30 min at 4 °C, the samples were centrifuged for 10 min at 16100 g and the supernatant was transferred to a fresh tube. The protein concentration was measured using a protein microassay (BioRad). Sodium dodecyl sulfate polyacrylamide gel electrophoresis (SDS PAGE) sample buffer was added to the extracts, followed by heating

at 95 °C for 5 min. For the LIM kinase and phospho-LIM kinase blots lysates were prepared by resuspending dissected cortices in 20 µl/mg wet tissue weight of the following buffer: 10 mM Tris pH7.5, 1% SDS, 0.5 mM DTT, 2 mM EGTA, 20 mM NaF, 1 mM Na₃VO₄ and protease inhibitors as above. After sonication for 3 sec the lysates were plunged in a boiling water bath for 10 min. Equal amounts of protein were separated by SDS PAGE and analyzed by Western blotting, using the following primary antibodies and dilutions: anti-Cdc42 mouse monoclonal antibody, clone 44 (BD Transduction Laboratories) at 1:500, anti-Rac mouse monoclonal antibody, clone 23A8 (Upstate) at 1:1000, anti-β-tubulin mouse monoclonal antibody, clone B-5-1-2 (Sigma), at 1:100000, anti-Rho mouse monoclonal antibody (clone 26C4, Santa Cruz) at 1:200, anti-PAK rabbit polyclonal antibody (C-19, Santa Cruz) at 1:10000, anti-phospho LIMK1/LIMK2 (Thr^{508/505}) rabbit polyclonal antibody (Cell Signaling) at 1:1000, anti-LIMK mouse monoclonal antibody, clone 42 (BD transduction Laboratories) at 1:300, anti-phospho-cofilin (Ser³) rabbit polyclonal antibody (Cell Signaling) at 1:500, anti-cofilin mouse monoclonal antibody, clone 32 (BD Transduction Laboratories) at 1:2000, anti-Par3 rabbit polyclonal antibody (Upstate) at 1:1000, anti-PKCA rabbit polyclonal antibody (C-20, Santa Cruz, sc-216) at 1:200, anti-LIMK2 rabbit polyclonal antibody (H-78, Santa Cruz, sc-5577) at 1:200, and anti-phospho-GSK-3β (Ser9) (Cell Signaling #9336) at 1:1000. The anti-phospho-PAK (Ser^{198/203}) antibody was a kind gift from Gerhard Schratt and Michael Greenberg (Harvard Medical School) and the anti-profilin II antibody was a kind gift from Walter Witke (EMBL Mouse Biology Unit, Monterotondo). The secondary antibodies were goat anti-mouse or anti-rabbit IgG-HRP (Santa Cruz), and the blots were developed using ECL Plus Western Blotting Detection System (GE Healthcare).

Extracts from cultured neurons and Swiss 3T3 cells were prepared by rapidly rinsing the cultures 4-5 times in cold PBS, adding SDS lysis buffer (Morgan et al., 1993) or SDS sample preparation buffer (Laemmli, 1970) and heating to boiling for 5 min. Protein concentration was determined using a filter paper dye binding assay (Minamide and Bamburg, 1990). SDS-polyacrylamide gel electrophoresis was performed on 12.5% and 15% polyacrylamide gels and Western blotting was onto PVDF. Antibodies against cofilin (MAb22; Abe et al., 1989), phospho-ADF/cofilin (Meberg et al., 1998), and a common epitope encompassing amino acids

52-54 of mouse ADF and cofilin (rabbit 1439; Shaw et al., 2004) were used.

Immunoprecipitation was carried out using Rabbit or Mouse IgG TrueBlot Sets, following the manufacturer's instructions (eBioscience).

Phosphatase assay: Phosphatase activity of cortical extracts was assayed in 96-well microtitre plates using a serine/threonine phosphatase assay system (Promega, Madison, WI) following the manufacturer's recommendations. Purified PP2A (0.5 U), included as a control, was also purchased from Promega. Extracts were either incubated with 100 μ M of the provided Ser/Thr Phosphopeptide (Promega) or with 100 μ M phospho-cofilin (Ser³) peptide from Upstate. Extracts were incubated with the respective peptides at 30 °C for 15 min. The reaction was quenched by the addition of malachite green reagent. The colour was allowed to develop for another 15 min, and released phosphate was determined by measuring A_{620} with a plate reader and extrapolating the values to a phosphate standard curve.

Adenoviral-mediated siRNA transduction: Vectors for expressing small interfering RNAs for mouse ADF, mouse cofilin and human cofilin were made by inserting DNA oligonucleotides (Macromolecular Resources, Fort Collins, CO) in a plasmid expression vector pSuper (Brummelkamp et al., 2002) containing the H1 polymerase III promoter. The oligonucleotide product from the pol III promoter is a double-stranded hairpin RNA (antisense-linker-sense) that is processed into a functional siRNA in the cell. Modified inserts including the H1 pol III promoter from the pSuper vector were excised and ligated into pShuttle and pAdTrack vectors (He et al., 1998). The siRNA sequence used for mouse cofilin is 5'-GGAGGACCTGGTGTTTCATCTT-3' and for mouse ADF is 5'-AAGTGATTGCAATCCGTGTAT-3' (Hotulainen et al., 2005). The siRNA sequence for human cofilin, used as a control in the mouse neurons, is 5'-AAGTCTTCAACGCCAGAGGAG-3'. The pShuttle and pAdtrack siRNA plasmids were then used to make adenoviruses as previously described (Minamide et al., 2003). The ability of the siRNA-expressing adenoviruses to effectively knockdown their targeted mRNAs was tested in mouse hippocampal neurons and Swiss 3T3 cells, and in the human Saos-2 cells.

Adenoviruses expressing human cofilin constructs were made using the AdEasy system as previously described (Minamide et al., 2003). The human cDNA sequence was isolated from pET vectors (a kind gift from Alan Weeds) using PCR and cloned into pmRFP-N1 vectors (Clontech) which were subsequently used to clone into pShuttle vectors for virus production. The Serine-3-Alanine (A3) and Serine-3-Glutamate (E3) cofilin constructs were made by introducing these mutations in the primers used for PCR.

Cell Infections: Hippocampal neurons were infected at a multiplicity of infection (MOI) of 150-300 in neurobasal medium with B-27 supplements and 5% fetal bovine serum (FBS) in 500 μ l volume. Neurobasal medium with B27 supplements (1.5 ml) was added 2-3 hr post-infection and approximately half the medium was exchanged 12-16 hr later. The neurons selected for analysis were of low to moderate GFP fluorescence and had neurites of 20 μ m or longer. In experiments testing the efficacy of siRNAs (Fig. 12C-H), hippocampal neurons were infected in the same manner but at an MOI of 500 after 48 hr in culture. Under these conditions, approximately 50-60% of the neurons were infected, as determined by GFP co-expression from a separate CMV promoter in the same adenoviral vectors. In experiments where cofilin mutants were expressed the neurons were pre-plated on untreated glass coverslips for 16-18hrs and infected at an MOI=150. During this time, the neurons become attached, but do not sprout long neurites. The cells were trypsinized and re-plated on polylysine coated coverslips where they were cultured for an additional 72 hr. This procedure allowed for earlier transgene expression (visible within hours of plating), which typically peaks 48-72hrs post-infection (Meberg and Bamberg, 2000). This would allow for transgene expression in a time-course that could impact axonogenesis. For time-course studies testing siRNA function, infections were performed in Swiss 3T3 cells at an MOI of 1000-1500 in LG-DMEM + 0.1% FBS. Under these conditions, 100% of the cells were infected as indicated by fluorescent protein expression. The medium was exchanged 12-16 hr later with LG-DMEM + 10% FBS. In experiments testing the efficacy of human cofilin siRNA expressing adenoviruses, Saos-2 cells were infected in HG-DMEM-10% FBS at an MOI of 100-200 (100% infected).

Results

Deletion of Cdc42 in the nervous system

To ablate Cdc42 in the nervous system, we used a mouse carrying a floxed Cdc42 allele (Wu et al., 2006) and crossed it with strains expressing Cre recombinase under the control of different nervous system promoters, including NEX (Goebbels et al., 2006), Tau (Korets-Smith et al., 2004) and nestin (Graus-Porta et al., 2001). Only Cre expression driven by the nestin promoter led to complete depletion of the Cdc42 protein in the cortices and hippocampi of homozygously floxed embryos by late gestation (Figure 1A and B and data not shown). Therefore we performed our analysis using embryos from the cross with the nestin-Cre line.

The knockout embryos were produced at the expected ratio, but died on the day of birth. Histological staining of sectioned brains revealed that knockout embryos and P0 pups displayed a range of abnormalities (Figure 1C-F). These included a dramatic decrease in cortical mass, enlargement of the lateral ventricles, and widespread reduction or loss of axonal tracts, as seen for instance in the cortex or the striatum (Figure 1C-F). To characterize the effect of Cdc42 ablation on axonal formation and growth, we injected DiI tracer in E18.5 cortices. The axonal tracts labeled in the cortex of wild type embryos were long, sharply defined and fasciculated (Figure 1G). By contrast, Cdc42 knockout cortices had much fewer, shorter and sparser fibres (Figure 1H).

The analysis of the effect of Cdc42 depletion on neuronal development in the brain was complicated by the severity of the *in vivo* phenotype and the possibility that multiple factors could contribute to the observed defects, e.g. aberrations in neuronal generation, migration, survival, polarization, cell-cell or cell-matrix adhesion and signaling. Therefore we assessed whether the defects in axonal growth were cell intrinsic. To this end we focused our study on the analysis of neuronal polarization in the well established tissue culture system of hippocampal neurons (Dotti et al., 1988).

Analysis of neuronal polarity in mixed cultures of Cdc42 knockout/wild type hippocampal neurons

We aimed to use a system where the wild type and the Cdc42 knockout neurons

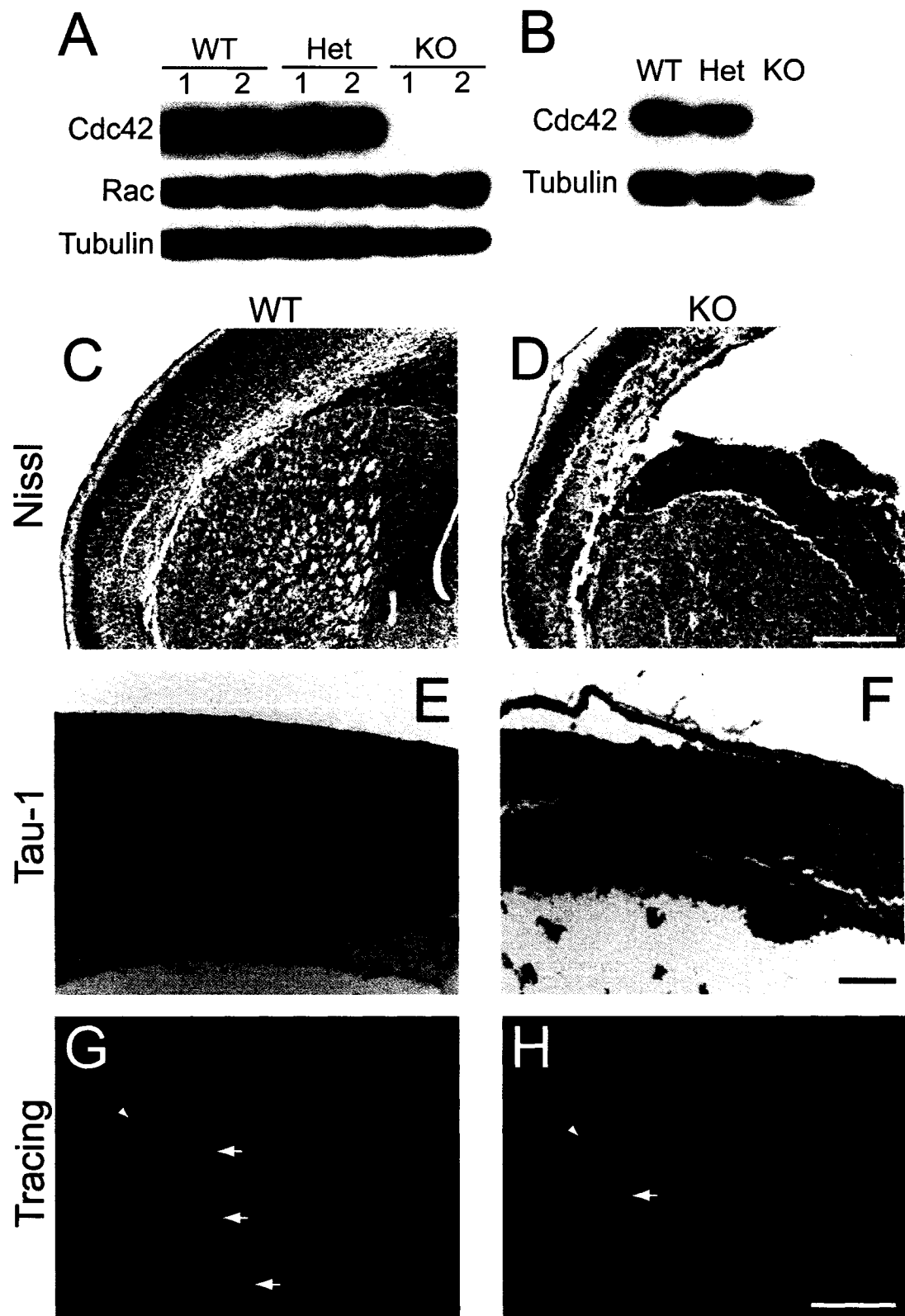
Figure 2.1. Cdc42 depletion *in vivo*

(A–B) Depletion of the Cdc42 protein in embryonic cortices and hippocampi. Mice double heterozygous for Nes-Cre and a floxed Cdc42 allele (*Nes-Cre*^{+/+}, *Cdc42*^{fl/wt}) were crossed with homozygously floxed Cdc42 mice (*Cdc42*^{fl/fl}). The resulting embryos were dissected at E16.5 and protein extracts were prepared from the brain cortex (A) or from isolated hippocampi (B). Equal amounts of protein from each embryo were loaded on an SDS PAGE gel and analyzed by Western blot with antibodies against Cdc42 and Rac1. A tubulin antibody was used as a control for equal loading. The Western blot in A shows the protein levels in two separate wild-type embryos (WT: *Nes-Cre*^{+/+}, *Cdc42*^{fl/wt} or *Nes-Cre*^{+/+}, *Cdc42*^{fl/fl}), two separate heterozygous embryos (Het: *Nes-Cre*^{+/+}, *Cdc42*^{fl/wt}) and two separate Cdc42 knockout embryos (KO: *Nes-Cre*^{+/+}, *Cdc42*^{fl/fl}). The blots shown are representative of at least 3 independent experiments.

(C, D) Nissl staining of paraffin sections of E18.5 embryonic brains. Coronal sections at the level of the striatum of wild-type (C) and knockout (D) brains are shown. Scale bar: 200 μm.

(E, F) Immunohistochemical staining of paraffin-embedded, E18.5 coronal sections with a Tau-1 antibody. Abundant Tau-1-positive axonal tracts are seen in the intermediate zone (IZ) in wild type cortices (E), but very few are apparent in knockout animals (F). Thinning and disorganization are also observed in other cortical layers, including the marginal zone (MZ), cortical plate (CP) and subventricular/ventricular zones (SV/VZ). Scale bar: 100 μm.

(G–H) DiI tracing of cortical axonal tracts. Fixed brains from wild-type (G) and knockout (H) E16.5 embryos were injected with DiI crystals. After diffusion of the dye, the labeled fibres in coronal sections at the level of the striatum were imaged by confocal microscopy. The axonal tracts were visualized inside the cortex (arrows); some surface labeling resulted from dye diffusion into the pia mater (arrowheads). The images shown are representative of at least 5 injected brains of each genotype; the axonal tracts were shorter and sparser in all knockout animals in all regions of the cortex, compared to the wild type counterparts. Scale bar: 500 μm.



would grow under identical conditions, since we had previously determined that differences in cell density, e.g. resulting from differences in attachment or survival, could significantly influence the proper developmental program of pyramidal neurons in culture (B. G. and F. B. – unpublished observations). In order to be certain that the cells would grow at identical densities we plated the knockout and the wild type neurons together on the same coverslips. To distinguish the knockout from the wild type cells, the latter were isolated from age matched embryos ubiquitously expressing enhanced green fluorescent protein (EGFP) under a “CAG” promoter (Okabe et al., 1997; Ikawa et al., 1998)(Figure 2A-C).

Cdc42 ablation leads to inhibition of axon formation

Using mixed cultures we determined that the Cdc42 knockout neurons attached normally and started to extend several minor neurites in synchrony with the wild type cells (Figure 2A). The knockout neurons were also positive for neuronal markers such as class III β -tubulin (TUBJ-1) at both early (Figure 2A) and later stages of the culture (data not shown). At later stages, however, while wild type, GFP-positive neurons polarized and formed a process positive for the axonal marker Tau-1 (in $69.1 \pm 3.2\%$ of the cases; Figure 2D) only a minor fraction of Cdc42 knock out neurons generated an axon ($29.9 \pm 6\%$; Fig. 2B). Both the knockout and the wild type cells, however, expressed the dendritic marker microtubule-associated protein 2 (MAP2) at comparable levels (Figure 2C). The longest processes of the knockout neurons were also significantly shorter than those of the wild type cells (Figure 2E). These observations were supported by time lapse imaging, which revealed that within the first ~24 hr of culture Cdc42 null neurons extended processes normally, but at later stages the rate of extension of the longest neurites in mutant cells became substantially lower than in the wild type counterparts and similar to the extension rate of the wild type minor neurites (Figure 2F). The length of the minor (non-longest) neurites of Cdc42-deficient and wild type neurons was identical at 3 days in culture (Figure 2G), further supporting the conclusion that the defects were specific for the axons. Moreover, the total number of processes in the knockout was only slightly reduced (Figure 2H), suggesting that the majority of the mutant neurons failed to generate an axon, but formed minor neurites normally. Importantly, to confirm that the defects

observed in culture correspond to developmental abnormalities at the cellular level *in vivo*, we labeled individual cells with lipophilic dyes using a DiOlistic delivery method (Gan et al., 2000). This approach demonstrated that whereas wild type cortical neurons had a typical morphology of a long axon with several minor neurites, the mutant cells usually did not form an extended axon (Figure 2I-J)

The defects in neuronal polarity are cell autonomous and not due to apoptosis

To examine whether the observed polarity defects were cell autonomous and specifically caused by Cdc42 ablation, we expressed wild type Cdc42 fused to EGFP in the Cdc42 null neurons. Mutant neurons that were transfected with EGFP-Cdc42 but not those transfected with EGFP alone (Figure 3A-B) were rescued in their ability to form Tau-1 positive axons (Figure 3C).

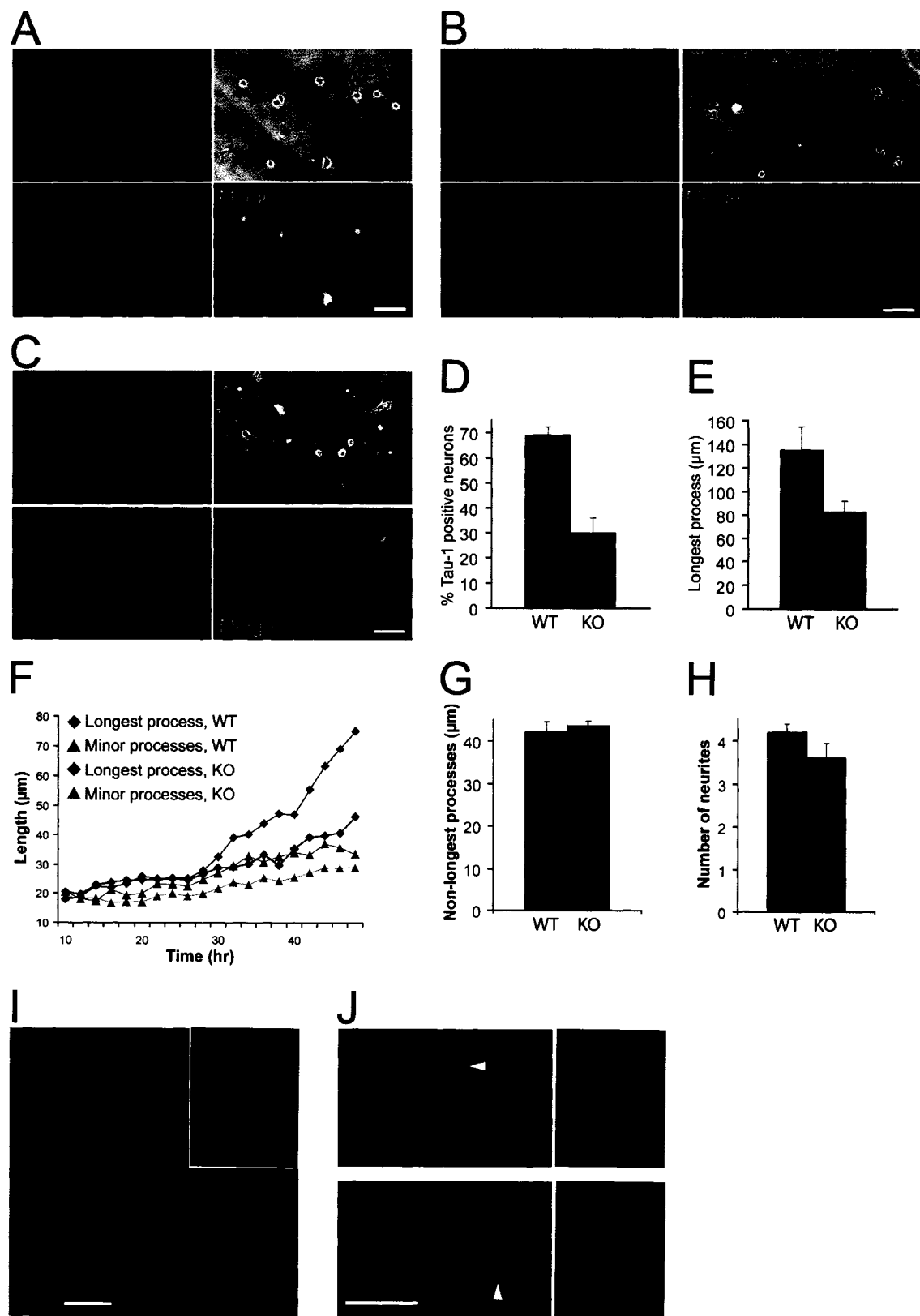
Although Cdc42 knockout neurons attached at normal levels and initiated neurite sprouting (Figure 2A and data not shown), at later stages a significant fraction of the knockout, but not of the wild type neurons was lost (see Figure 3F). Therefore we examined whether the observed polarity deficiencies in the knockout cells may be secondary to a decrease in cell survival. To address this, we treated mixed cultures with the general caspase inhibitor Z-VAD-fmk in order to suppress neuronal apoptosis (Figure 3D and E). Quantification of the vehicle-treated, and the Z-VAD-fmk-treated cells demonstrated that the caspase inhibitor produced a major (2.5 fold) increase in neuronal survival among the mutants (Figure 3F). Importantly, under these conditions the formation of Tau-1 positive axons by the knockout neurons was inhibited to the same extent as under control conditions ($29.2 \pm 2.3\%$ for the DMSO control versus $26.9 \pm 1.1\%$ for the Z-VAD-fmk treatment, Figure 3G), arguing that the polarity defects are separate from the effects of Cdc42 ablation on neuronal survival.

Cdc42 knockout neurons are growth competent

We further wanted to examine whether we could stimulate Cdc42 knockout neurons to produce an axon by manipulating the actin cytoskeleton. To this end we treated mixed cultures with the actin depolymerizing agent cytochalasin D, which has been shown to induce the

Figure 2.2. Analysis of the phenotype of Cdc42 knockout hippocampal neurons

Hippocampal neurons from Cdc42 knockout E16.5 embryos were dissociated and mixed with wild type hippocampal neurons from E16.5 embryos, ubiquitously expressing enhanced green fluorescent protein (GFP) under a “CAG” promoter (Okabe et al., 1997; Ikawa et al., 1998), resulting in mixed cultures of GFP-positive wild-type neurons and GFP-negative Cdc42 knockout neurons. (A) Mixed cultures were fixed 10 hr post plating and stained with an antibody against class III beta-tubulin (TUJ-1) to visualize all neuronal cells. (B) Mixed cultures were fixed at 3 days post plating and stained with an antibody against a dephosphorylated epitope of Tau (Tau-1), to visualize axons. (C) Mixed cultures were fixed at 3 days post plating and stained with an antibody against the microtubule associated protein MAP2. The arrows in (A-C) indicate GFP-negative neurons, derived from Cdc42 knockout hippocampi. All GFP-positive neurons are wild type. (D) Quantification of the neurons having a Tau-1-positive process in mixed cultures. Here and in subsequent quantifications green bars represent wild type, GFP-positive neurons and black bars represent Cdc42 knockout, GFP-negative neurons. The data are from 5 separate cultures (number of cells counted (n) ≥ 1200 per data point, $p < 0.001$). The values on this and all other graphs are averages plus standard deviations. (E) Quantification of the length of the axon/longest neurite in mixed cultures. (5 separate cultures, $n \geq 660$ per data point, $p < 0.001$). (F) Time course of process growth of wild type and Cdc42 knockout neurons imaged live. The graph shows the average length of the longest and minor (non-longest) processes of 8 wild type (GFP positive) and 9 knockout neurons. (G) Length of the minor (non-longest) processes of wild type and Cdc42 knockout neurons (3 separate cultures $n = 75$ per data point, $p = 0.41$). (H) Number of the neurites of wild type and Cdc42 knockout neurons (3 separate cultures, $n = 75$ per data point, $p = 0.07$). (I, J) Brain sections of E18.5 wild type (I) and Cdc42 knockout (J) embryos were labeled with DiO using a ballistic delivery method, to reveal individual neurons in the cortex. The inset in (I) shows a higher magnification of the wild type growth cones. The arrowheads in (J) indicate enlarged growth cones in the Cdc42 knockout neurons, which are shown at higher magnification on the right. Scale bars: 50 μm .



formation of multiple axons per cell (Bradke and Dotti, 1999; Kunda et al., 2001; Schwamborn and Püschel, 2004). Control, vehicle-treated neurons formed one long, Tau-1 positive axon and several shorter minor neurites (see Figure 2B). By contrast, the cytochalasin D-treated neurons displayed the characteristic phenotype (Bradke and Dotti, 2000b), with several long, curved, Tau-1 positive axons after 2 days of treatment (Figure 3H). Importantly, the same phenotype was observed for the Cdc42 knockout neurons (Figure 3I). The number of knockout neurons displaying multiple (two or more) axons rose dramatically – from $1.9 \pm 1.2\%$ under control conditions to $47.1 \pm 1.9\%$ when actin was depolymerized with cytochalasin D, comparable with the percentage of multi-axonal wild type neurons ($53.1 \pm 1.2\%$, Figure 3J). There was a concomitant increase in the total percentage of Cdc42-deficient cells that produced axons (one or more): from $28.0 \pm 5.4\%$ in the DMSO control to $71.1 \pm 5.0\%$ under cytochalasin D treatment (Figure 3J). When cytochalasin D was washed out after one day of application and the neurons were allowed to grow for a further 1 to 2 days (Figure 4A, B), the axon-forming ability of the Cdc42 mutants was again restored (Figure 4C). Under these conditions, however, both the wild type and the knockout neurons usually formed only a single axon and more rarely multiple axons (Figure 4C). In both cases the mutant axons were indistinguishable in length from the wild type counterparts (Figure 4). Based on these experiments we conclude that neurons lacking Cdc42 retain the ability to form axons at nearly wild type levels, but that under normal conditions the absence of Cdc42 dramatically reduces this capacity. It also suggests that Cdc42 is required in the initial step of axon formation but that once an axon extends the process is self-reinforcing and functions in the absence of Cdc42. Our results also support the notion that the organization of the actin cytoskeleton is a crucial downstream determinant for the axon forming capacity of the knockout neurons.

Altered cytoskeleton and arrested filopodial dynamics in Cdc42 knockout neurons

We next assessed the organization of actin filaments and microtubules in the knockout neurons. Staining with fluorescently labeled phalloidin revealed that in the knockout neurons there was no overall disruption of actin filaments, which showed the typical enrichment at growth cones, similar to wild type cells (Figure 5A and B). However, the growth cones of the

longest processes were often greatly enlarged in the knockouts compared to wildtype (Figure 5C-F). The enlarged growth cones in the mutant neurons had no clear filopodial protrusions, showed a more diffuse distribution of actin filaments (Figure 5C, D) and were filled with long, curved microtubules (Figure 6B), whereas wild type growth cones were only partially penetrated by bundled microtubules (Figure 6A). Similar enlarged growth cones were also observed *in vivo* in Cdc42-deficient cortices, but not in wild type cortices (Figure 2I, J). In addition, a substantial fraction of the Cdc42-deficient neurons ($25.9 \pm 11.9\%$) had no filopodia along the shafts of their processes, which was rarely observed in the wild type cells (in $2.2 \pm 3.2\%$ of the cases, Figure 5G). Live cell imaging demonstrated that the growth cones of the knockout neurons were strongly inhibited in the formation of filopodia, and to a lesser degree in filopodia retraction (Figure 5H). Moreover, while most ($87.0 \pm 9.1\%$) growth cones in the wild type were actively motile, a much smaller fraction (27.7 ± 22.2) of the mutant growth cones displayed such activity (Figure 5I).

Increased cofilin phosphorylation (inactivation) in Cdc42 knockout neurons

We next investigated what signaling pathways are disrupted by the lack of Cdc42, leading to the polarity defects we observed. Since Cdc42 has been suggested to crosstalk with both Rho and Rac (Sander et al., 1999), we first examined the activation state of Rac and Rho in cortical extracts, using biochemical pulldown assays (Sander et al., 1998). We failed to observe any consistent increase in the activity of Rac in Cdc42 knockout extracts (Figure 7). The activity of Rho remained below our limit of detection in both knockout and wild-type cortices, although Rho activation was observed in adult CNS tissue (data not shown) and could be induced at similar levels in both wild type and knockout E18.5 extracts by preincubation with GTP γ S (Figure 7B). Consistent with these observations inhibition of Rho with C3 exoenzyme, or of its effector, Rho kinase, with the pharmacological inhibitors H-1152 and Y-27632, did not result in any significant rescue of axonogenesis in Cdc42 knockout neurons (Figure 7C-D and data not shown).

To identify direct Cdc42 effector pathways that may be deregulated in the knockout neurons we examined by immunocytochemistry or co-immunoprecipitation effectors with

Figure 2.3. The polarization defects are rescued by Cdc42 reexpression and actin depolymerization but are not affected by inhibition of apoptosis

(A,B) Cdc42 knockout neurons were transfected with GFP-tagged wild type Cdc42 (B) or with GFP (A) and stained for the axonal marker Tau-1. (C) Quantification of the percentage of Cdc42 knockout neurons having a Tau-1 positive process after transfection with control vector or with GFP-tagged wild type Cdc42 (3 separate cultures, $n \geq 333$, $p < 0.001$). (D, E) Mixed wild type (GFP-positive)/Cdc42 knockout (GFP-negative) neuronal cultures were treated with DMSO (D) or with the general caspase inhibitor Z-VAD-fmk (E). The cultures were fixed 3 days later and stained for Tau-1. (F) Quantification of the average number of neurons per field (normalized) in cultures treated with DMSO or with Z-VAD-fmk (≥ 60 fields counted per data point). (G) Quantification of the neurons having a Tau-1-positive process in cultures treated with DMSO or with Z-VAD-fmk. The error bars are standard deviations ($n \geq 600$ per data point). The data in (F) and (G) are representative of 3 separate cultures. (H, I) Mixed cultures of wild-type, GFP-positive neurons (H) and Cdc42 knockout, GFP-negative neurons (I) were treated with cytochalasin D 24 hr post plating, fixed at 3 days, and stained for Tau-1. Scale bars: 50 μm . (J) Quantification of the wild-type and knockout neurons having processes positive for Tau-1 ("Axons (≥ 1)") or multiple Tau-1 positive axons ("Multiple axons (≥ 2)"). The black bars represent DMSO-treated control cultures and the white bars – cytochalasin D-treated cultures (3 separate cultures, $n \geq 1250$ per data point; * - $p < 0.05$, *** - $p < 0.001$).

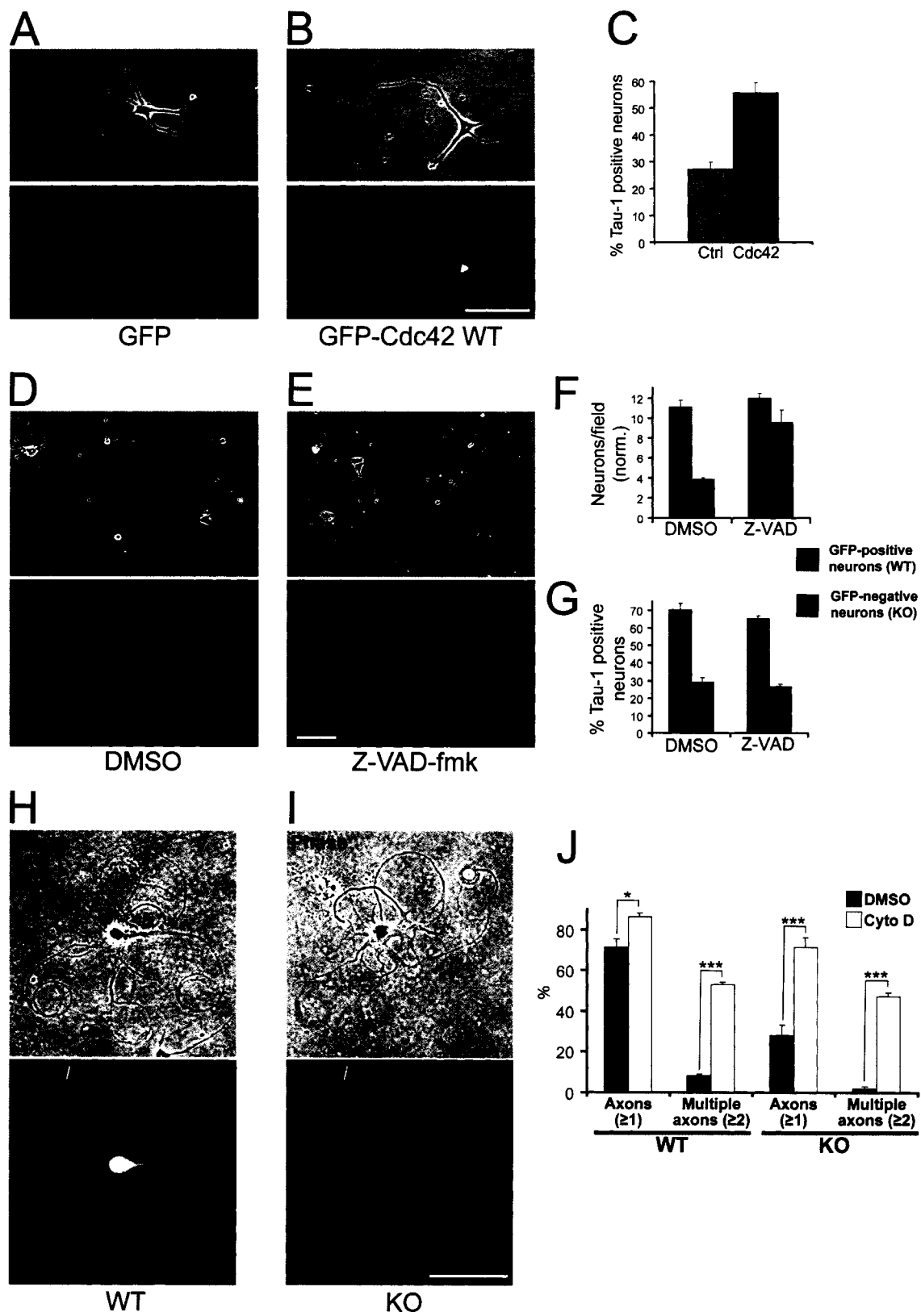
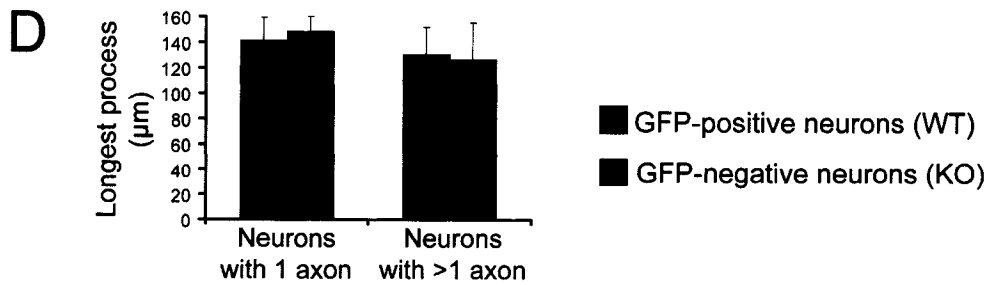
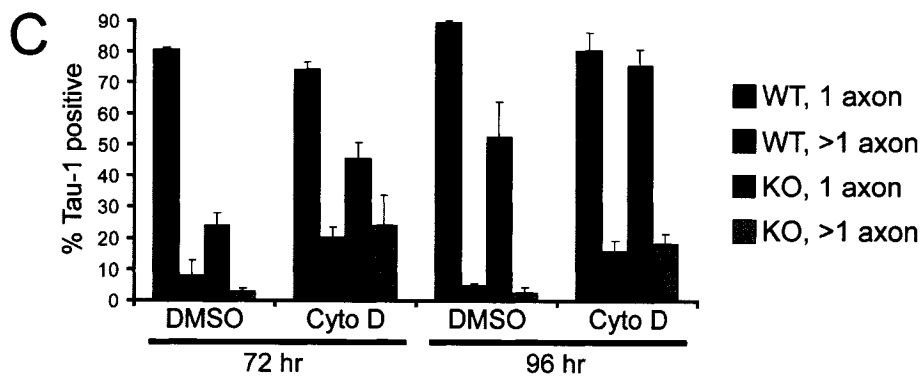
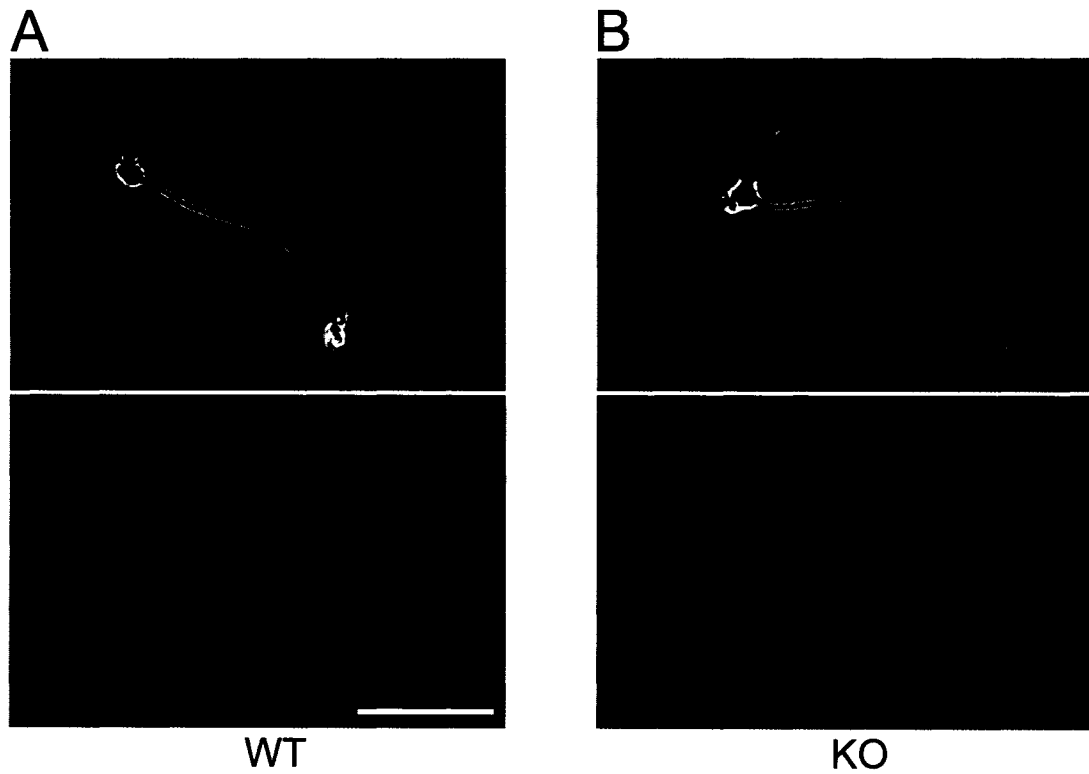


Figure 2.4. Transient actin depolymerization rescues axon formation in Cdc42 knockout neurons

Mixed cultures were treated with 1 μ M cytochalasin D after 1 day in culture. The drug was washed away 24 hr later and the cultures were allowed to grow for a further 24-48 hr. Both wild type, GFP positive neurons (**A**) and Cdc42 knockout neurons (**B**) typically formed a single Tau-1 positive axon. Scale bar: 50 μ m.

(**C**) Quantification of the percentage of neurons forming Tau-1 positive axons after cytochalasin D washout (3 cultures, $n \geq 250$ per condition). (**D**) Quantification of the length of the longest process of 3 day old wild type and Cdc42 knockout neurons after cytochalasin D washout (3 cultures, $n=150$ for wild type and knockout cells).



proposed function in axonogenesis and polarity, including Par3/Par6/aPKC and Arp2/3, but were unable to detect consistent differences between wild type and mutant neurons (Figure 7E and data not shown). Interestingly, however, there was a partial increase in the phosphorylation of GSK-3 β at Ser⁹ (Figure 7F), a modification that leads to inactivation of the kinase for primed substrates (substrates requiring phosphorylation at other sites) but not for unprimed substrates such as Map1B (Zhou and Snider, 2005). We proceeded to analyse whether the lack of Cdc42 had an effect on its downstream effector PAK. We observed a decrease in the phosphorylation of PAK at Ser^{198/203} (Shamah et al., 2001), indicating a reduced activity of the kinase (Figure 8A), as would be expected in the absence of Cdc42. However, contrary to our expectations, when we tested effectors further downstream we observed a strong increase in the phosphorylation of LIM kinase at Thr^{508/505} (Figure 8B), a modification that enhances the capacity of LIM kinase to phosphorylate proteins of the ADF/cofilin family (Edwards et al., 1999). Consistent with the latter result, we also saw a striking increase in the level of cofilin phosphorylation at Ser³ (Figure 8C), which is known to inhibit the F-actin depolymerizing and severing activity of cofilin (Agnew et al., 1995; Bamburg, 1999). This finding was further confirmed by 2D Western blot analysis, demonstrating a major shift toward the phosphorylated form of cofilin (Figure 9A-C). In contrast to cofilin, the phosphorylation of profilin II, another actin-binding protein that has been implicated in neurite growth (Da Silva et al., 2003), was not increased in the knockout (Figure 9D-E).

We further examined whether the activity of cofilin phosphatases was altered in the knockout. First, we assayed the total Ser/Thr phosphatase activity in cortical extracts and found little difference between the wild type and the knockout using a generic phosphorylated peptide as a substrate (Figure 8D). However, when we used phospho-cofilin (Ser³) as a substrate, we saw a significant, $24.4 \pm 6.6\%$ decrease of the specific phosphatase activity in cortical extracts derived from Cdc42 knockout mice (Figure 8E), demonstrating that cofilin phosphatases are inhibited in the absence of Cdc42.

The role of GSK-3, whose phosphorylation/activity was altered in the Cdc42 knockouts, in regulating microtubule dynamics and axonogenesis has been previously studied (Zhou and Snider, 2005), with some divergence in the outcomes (Jiang et al., 2005; Yoshimura et al., 2005;

Kim et al., 2006). Our ability to rescue axon formation in the Cdc42-null neurons using actin destabilizing drugs suggested that pathways which regulate actin dynamics downstream of Cdc42 play a key role. Therefore, we focused our further studies on cofilin, whose involvement in the establishment of neuronal polarity has not been addressed.

Cofilin activity is higher in axonal growth cones

To investigate whether the observed cofilin phosphorylation (inactivation) in Cdc42 knockout neurons could account for the observed polarity defects we first visualized local cofilin activity in different neuronal regions by ratio imaging wild type mouse hippocampal neurons co-stained for total cofilin and Ser³-phosphorylated-cofilin (Figure 10A-F). In cells that only contained minor neurites but one process was thicker and had a larger growth cone than the rest, presumably being on its way to becoming the axon (Bradke and Dotti, 1997) we detected a clear enrichment of active (unphosphorylated) cofilin in the larger growth cone (Figure 10A-C), which had 3.5 ± 0.5 fold higher ratio of total cofilin to phospho-cofilin (Figure 10G). A similar situation was observed in morphologically polarized (stage 3) neurons (Figure 10D-F), which had a 2.9 ± 0.2 fold higher ratio of total cofilin to phospho-cofilin in the growth cones of their axons, compared to minor neurite growth cones (Figure 6H). We also used ratio imaging to examine the activation state of cofilin in the axonal growth cones of wild type neurons and in the growth cones of the longest processes of Cdc42 null hippocampal neurons in mixed cultures (Figure 10I-L). The growth cones of Cdc42 null neurons had ~ 2.5 fold less active cofilin than wild type growth cones (Figure 10M), showing that a high activity of cofilin correlates with axonal growth.

Cofilin is necessary for normal axon formation and promotes axonal growth

To directly test whether cofilin enhances axonal growth, we overexpressed wild type, non-phosphorylatable (non-inactivatable; A3) and pseudophosphorylated (inactive; E3) cofilin constructs (Agnew et al., 1995), as well as RFP (control infection), in wild type neurons through adenovirus-mediated transduction (Figure 11A-F). The overexpression of wild type or A3 cofilin, but not of the inactive E3 cofilin mutant, led to a significant increase in the length of

Figure 2.5. Effects of Cdc42 ablation on the actin cytoskeleton

(A, B) Mixed cultures of wild-type, GFP-positive neurons (A) and Cdc42 knockout, GFP-negative neurons (B) were fixed at 3 days and stained with rhodamine-phalloidin to visualize actin filaments. Scale bar: 50 μm . (C, D) Morphology of growth cones from wild-type neurons (C) and Cdc42 knockout neurons (D) at 3 days in culture, visualized by rhodamine-phalloidin staining. Scale bar: 20 μm . (E) Quantification of the neurons showing enlarged ($>15 \mu\text{m}$ diameter) and smooth (filopodia-free) growth cones (5 separate cultures, $n \geq 660$ per data point, $p < 0.001$). (F) Quantification of the area of the enlarged Cdc42 knockout growth cones compared to the area of wild type growth cones (3 separate cultures, $n \geq 18$, $p < 0.001$). (G) Quantification of the neurons with smooth (filopodia-free) axonal/neurite shafts. (5 separate cultures, $n \geq 660$ per data point, $p < 0.001$). (H) Quantification of the number of filopodia (thin protrusions longer than 3 μm) formed and retracted by wild type and Cdc42 knockout neurons per minute in time lapse observations of live neurons (4 separate cultures; $n \geq 11$ per data point, $p < 0.01$ for newly formed filopodia; $p < 0.02$ for retracted filopodia). (I) Quantification of the percentage of growth cones showing rapid dynamics of filopodial/lamellipodial extension and retraction (active growth cones; 4 separate cultures; $n \geq 11$ per data point, $p < 0.01$)

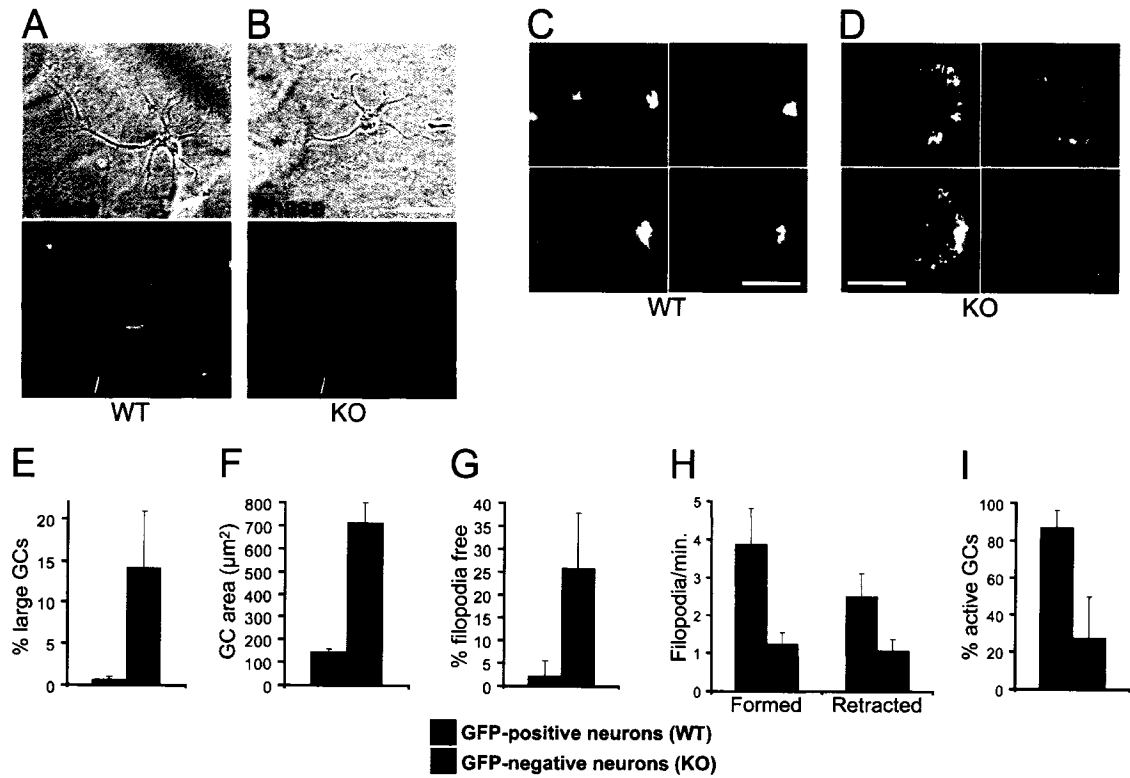


Figure 2.6. Microtubule organization in the enlarged growth cones of Cdc42 null neurons

Mixed cultures of wild type, GFP positive (A) and Cdc42 knockout (B) neurons were fixed at 3 days and stained with an antibody against beta-tubulin to reveal the organization of the microtubules in growth cones (boxed areas, enlarged on the right). Scale bar: 50 μ m.

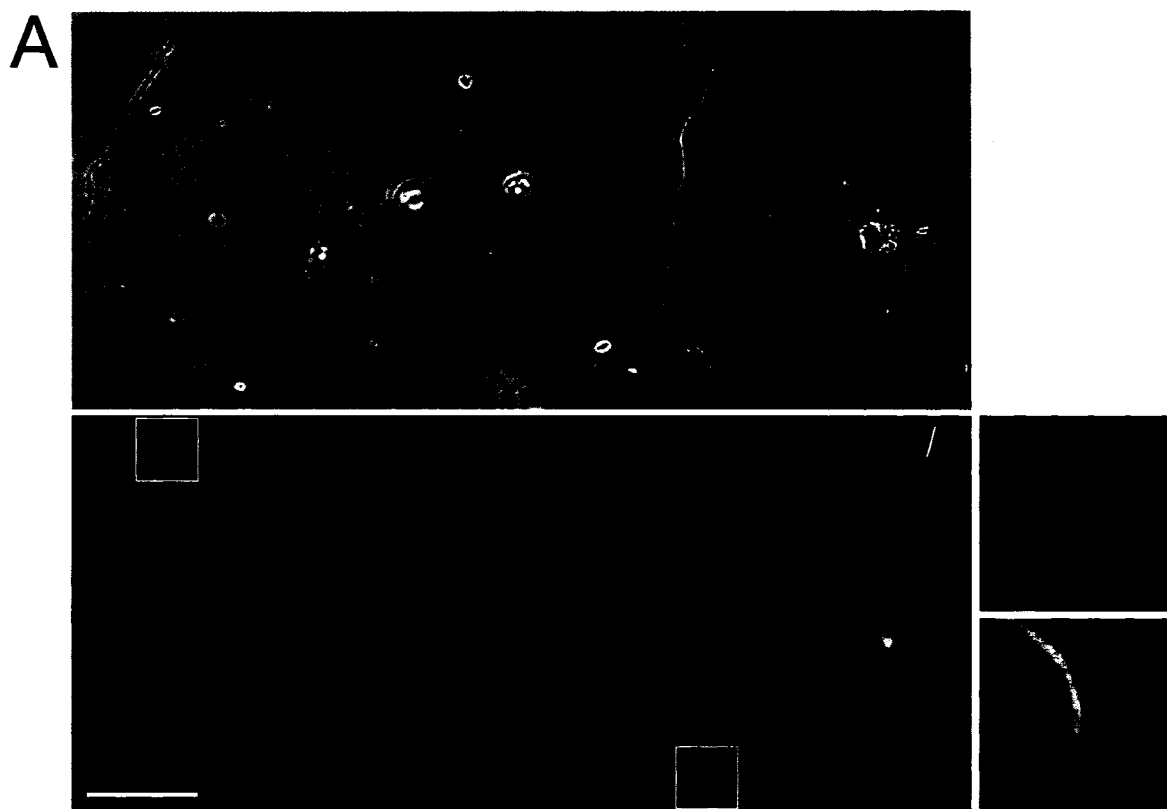
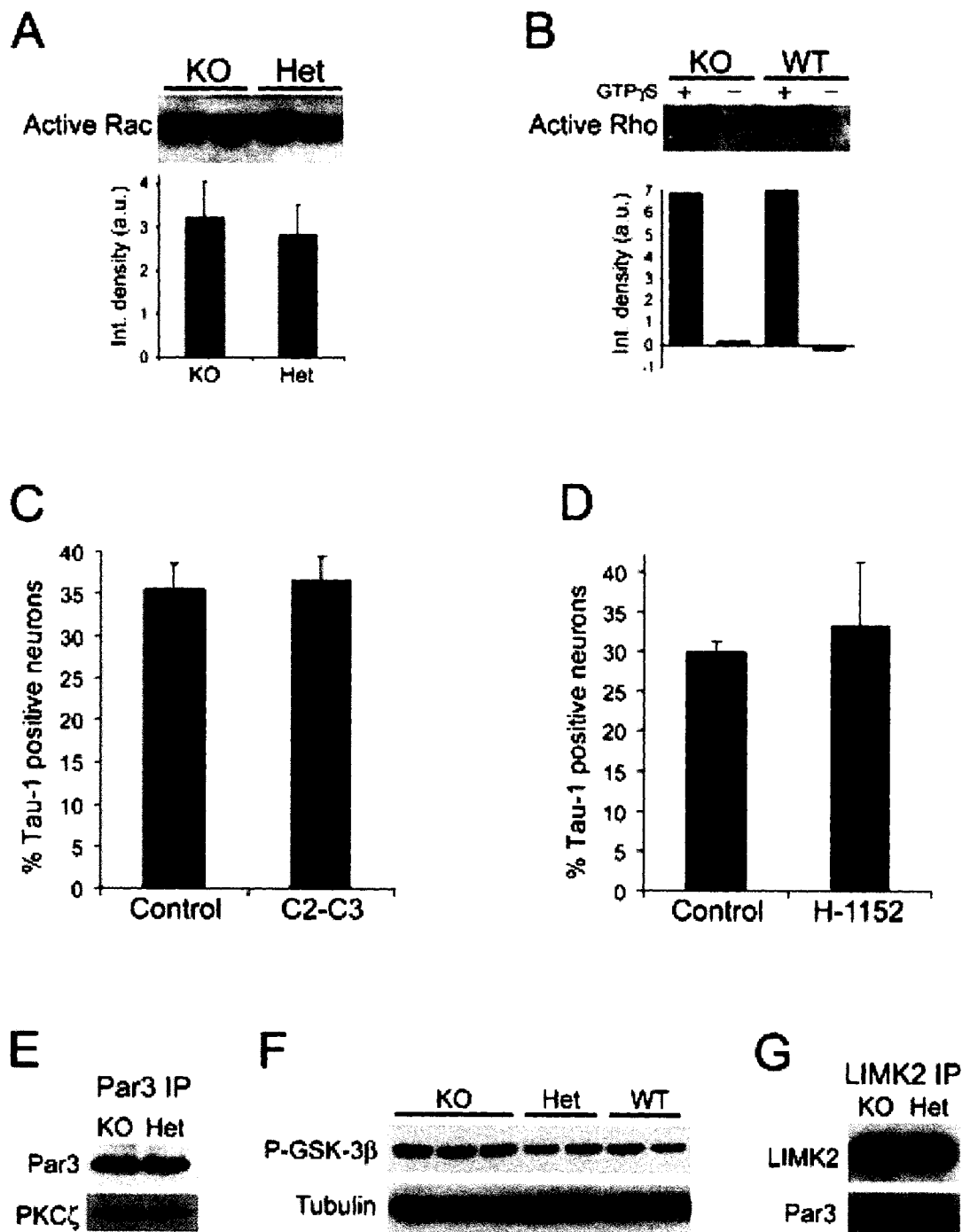


Figure 2.7. Rho and Rac activity and Par polarity complex in wild type and Cdc42 knockout neurons

(A-B) Activity of Rac (A) and Rho (B), as measured by *in vitro* GBD pulldown assays with E18.5 cortical extracts from heterozygous/wild-type and knockout embryos. The endogenous activity of Rho remained below the limit of detection, although a clear signal was observed when the extracts were preincubated with GTP γ S (lower panel). The graph in (A) shows the background-subtracted integrated density of the Rac bands from 4 separate extracts per genotype (average \pm st. dev.; $p > 0.5$). The graph below the blot in (B) shows the background-subtracted integrated signal for the respective lanes in the immunoblot. (C-D) Quantification of the percentage of Cdc42 knockout neurons carrying a Tau-1 positive process after treatment with C2-C3, a cell permeable form of C3 toxin (C) and with the Rho kinase inhibitor H-1152 (D) (3 experiments, $n \geq 800$ per data point, $p > 0.5$). (E) Cortical extracts from Cdc42 knockout and heterozygous E18.5 embryos were immunoprecipitated with an antibody against Par3 and the immunoprecipitates were immunoblotted for Par3 and PKC γ . (F) Cortical extract from separate Cdc42 knockout, heterozygous and wild type E18.5 embryos were probed with antibodies against phosphorylated GSK-3 β and against tubulin as a loading control. (G) Cortical extracts from Cdc42 knockout and heterozygous E18.5 embryos were immunoprecipitated with an antibody against LIM kinase 2 and the immunoprecipitates were immunoblotted for LIMK2 and Par3.



the longest and second longest processes compared to control infected, RFP expressing neurons (Fig. 11G). WT and A3 cofilin overexpressing neurons also showed a small but significant increase in the formation of Tau-1 positive axons compared to controls (Figure 11H).

To assess whether cofilin is necessary for axon formation we depleted the endogenous protein from neurons. Since the complete genetic ablation of cofilin-1, the major isoform which is expressed in neurons, results in lethality before brain development occurs (Gurniak et al., 2005), we knocked down neuronal cofilin using RNA interference. Based on our observation that cofilin is much more highly expressed in mouse hippocampal neurons than its homolog ADF (~12 fold; Figure 12A), we used short interfering RNAs (siRNAs) against mouse cofilin (Hotulainen et al., 2005) and against human cofilin as a control for off-target effects (Figure 12B-H), and expressed them in neurons via adenoviral-mediated delivery. To visualize the neurons where the siRNA was introduced, we used adenovirus that co-expressed GFP under the control of a separate CMV promoter (Figure 13A, C and 14D, F). Neurons expressing the control human cofilin siRNA, which had no effect on cofilin levels in mouse neurons (Figure 12C-E and H), formed Tau-1 positive axons at near normal levels ($50 \pm 2.5\%$ at 72 hr; $64 \pm 7.1\%$ at 96 hr, Fig. 8A, B and E, open bars). By contrast, neurons expressing mouse cofilin siRNA showed a depletion of cofilin (Figure 12C and F-H) and had a dramatically reduced ability to form Tau-1-positive axons ($23.7 \pm 2.8\%$ at 72 hr; $23.8 \pm 2.5\%$ at 96 hr, Fig. 13C, D and E, black bars). Consistently, the length of the longest neurite in the cofilin siRNA-transfected neurons was decreased over 2-fold, compared to the control (Figure 13F). There was no change in the length of the minor neurites (Figure 13G) and the number of processes was only slightly reduced (Figure 13H), indicating that cofilin knockdown specifically attenuates axon formation, rather than generally suppressing neurite growth. In an experiment where mouse ADF siRNA was expressed, there was no obvious decrease in the percentage of neurons with axons (data not shown).

Taken together our data provide evidence that Cdc42 controls the activation state of cofilin/ADF during neuronal development. Cdc42 is required to set cofilin in an active state, which in turn is necessary to support the efficient growth of the axon.

Discussion

Neuronal polarization is a key process during the development of the nervous system and a major effort has been invested in deciphering the molecular players involved (see Arimura and Kaibuchi, 2007). Most of the studies so far have relied on pharmacological treatments or on overexpression/downregulation approaches. What has received very little attention, however, is the role of specific molecules and pathways under physiological conditions. Our study presents the first analysis of the physiological role of a Rho GTPase and its downstream effectors in the establishment of neuronal polarity, based on a conditional knockout mouse model.

Cdc42 ablation disrupts neuronal polarization

Using Cre recombinase expression under the nestin promoter, we achieved complete depletion of the Cdc42 protein in the nervous system in mice homozygous for a floxed Cdc42 allele. A major phenotype that we observed in the Cdc42 null neurons both *in vivo* and in culture was a strong inhibition of the ability to form an axon, although there was little effect on minor neurite growth. Interestingly, this defect was not fully penetrant. It is likely that the lack of Cdc42 can be partially compensated by other highly related GTPases, such as TC10 (Tanabe et al., 2000) or TCL/RhoT (Vignal et al., 2000; Abe et al., 2003). However, Cdc42 is clearly required for the efficient establishment of polarity and growth of the axon.

Importantly, the axonogenesis defects in mutant neurons could be rescued by sustained depolymerization of actin filaments. This indicates that the Cdc42-deficient neurons retain a functional growth machinery, which can support axon formation, but that in the absence of the extra “thrust” provided by actin depolymerization (Bradke and Dotti, 1999) this machinery is suppressed by the lack of Cdc42. A possible explanation of how such machinery could function is that Cdc42 acts upstream of a local actin depolymerizing activity that is required for initial axon formation. Interestingly, transient depolymerization of actin filaments also rescued axon formation. This suggests that Cdc42 activity may be needed only for triggering axonogenesis, but that once axon growth is initiated, it can continue in the absence of Cdc42. A classical model of the mechanisms responsible for singling out one of the undifferentiated neurites for rapid growth proposes the existence of a positive feedback loop that enables sustained axonal

Figure 2.8. The level of cofilin phosphorylation in Cdc42 knockout neurons is increased. (A-C) Protein extracts from several separate E18.5 wild-type (WT), heterozygous (Het) and Cdc42 knockout (KO) cortices were prepared and analyzed in parallel by Western blot. (A) Cortical extracts were probed with an antibody specific for the phosphorylated Ser^{198/203} residues of PAK1 (upper panel) and with a general anti-PAK antibody (lower panel). (B) Cortical extracts were probed with an antibody specific for the phosphorylated Thr^{508/505} residue of LIM kinase 1/2 (upper panel) and with a general anti-LIM kinase (LIMK) antibody (lower panel). (C) Cortical extracts were probed with an antibody specific for the phosphorylated Ser³ residue of cofilin (upper panel), with a general anti-cofilin antibody (middle panel) and with an anti-tubulin antibody as a loading control (lower panel). (D) Phosphatase activity in cortical extracts of wild-type (green bars) and Cdc42 knockout embryos (black bars), measured with a generic phospho-Ser/Thr peptide substrate. The error bars are standard deviations from quadruplicate experiments ($p>0.5$). (E) Phosphatase activity in cortical extracts of wild-type (green bars) and Cdc42 knockout embryos (black bars), measured with a phospho-cofilin (Ser³) peptide substrate. The error bars are standard deviations from quadruplicate experiments ($p<0.02$).

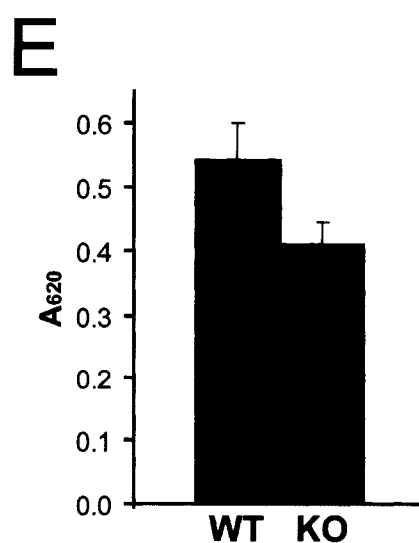
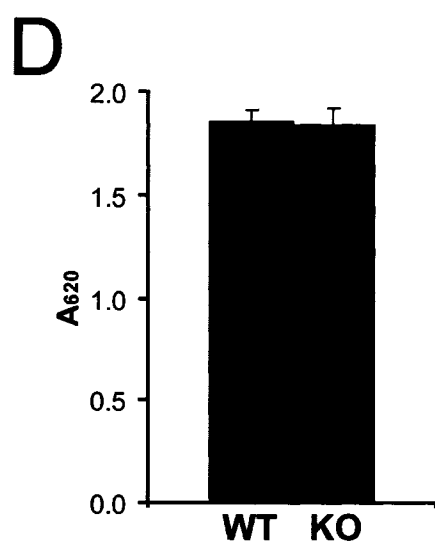
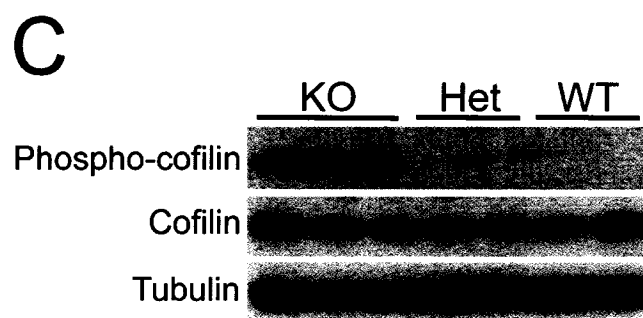
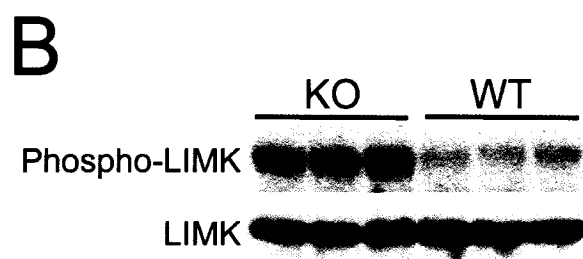
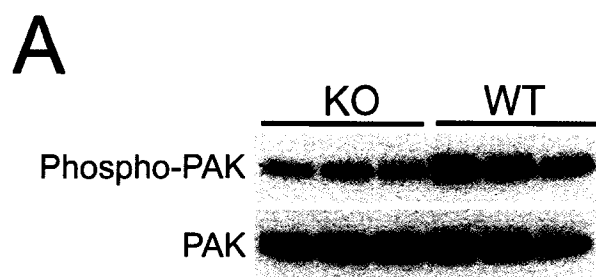


Figure 2.9 The phosphorylation of cofilin, but not profilin II is strongly enhanced in Cdc42 mutants

Cortices from wild type and Cdc42 knockout E18.5 embryos were lysed and subjected to 2D gel electrophoresis and Western blotting with antibodies against total ADF/cofilin (**A**) and phospho-ADF/cofilin (**B**). Spots shown by arrows and arrowheads arise from the cofilin-1 isoform, whereas other minor immunoreactive spots arise from ADF and cofilin-2. (**C**) Quantification of the percentage of phosphorylated cofilin in wild type and Cdc42 knockout cortices from 3 independent experiments. (**D**) 2D Western blot against profilin II from wild type and Cdc42 knockout E18.5 cortical lysates. The arrowheads in (**A**), (**B**) and (**D**) indicate the more basic, unphosphorylated form of the proteins, while the arrows indicate the more acidic, phosphorylated form. (**E**) Quantification of the percentage of phosphorylated profilin II in wild type and Cdc42 knockout cortices from 2 independent experiments.

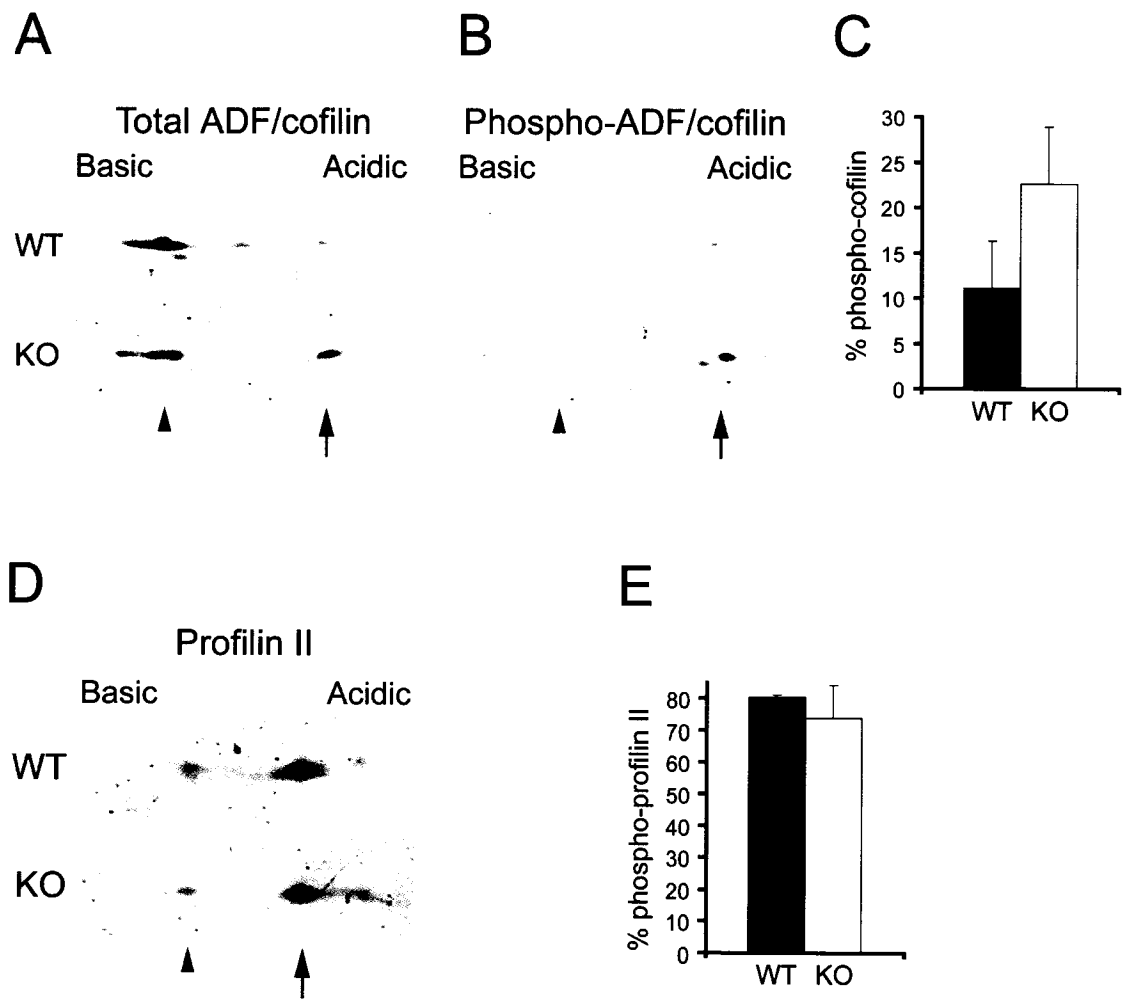


Figure 2.10. Active cofilin is enriched in axonal growth cones.

Mouse hippocampal neurons at stage 2+ (A-C) or stage 3 (D-F) of development were fixed and stained with antibodies against total cofilin (A and D) and Ser³-phosphorylated cofilin (B and E). The ratio of the total cofilin to the phosphorylated cofilin, reflecting the relative amount of active cofilin, is depicted in (C) and (F) using a pseudocolor intensity scale. Insets show higher magnifications of the larger stage 2+ growth cones (C) or of the axonal growth cones at stage 3 (F), along with the next brightest growth cone. Scale bar: 20 μ m. (G) Quantification of the average cofilin/phospho-cofilin ratio in the larger growth cones of stage 2+ neurons (black bar) and in the remaining growth cones (open bar; 3 experiments, $n \geq 70$, $p < 0.001$). (H) Quantification of the average cofilin/phospho-cofilin ratio in the axonal growth cone of stage 3 neurons (black bar) and in the growth cones of minor neurites (open bar; 3 experiments, $n \geq 60$, $p < 0.001$). (I-L) Mixed cultures of wild type hippocampal neurons expressing GFP (K) and Cdc42 null neurons (GFP-negative) were stained for total cofilin (I) and phospho-cofilin (J). The intensity ratio of the total cofilin/phospho-cofilin staining is shown in a pseudocolor scale in (L). The arrow indicates the growth cone of the longest process of a Cdc42 knockout (GFP-negative) neuron. Scale bar: 20 μ m. (M) Quantification of the total/phospho-cofilin ratio (4 experiments, $n \geq 60$, $p < 0.001$).

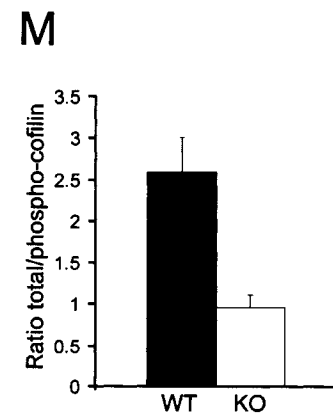
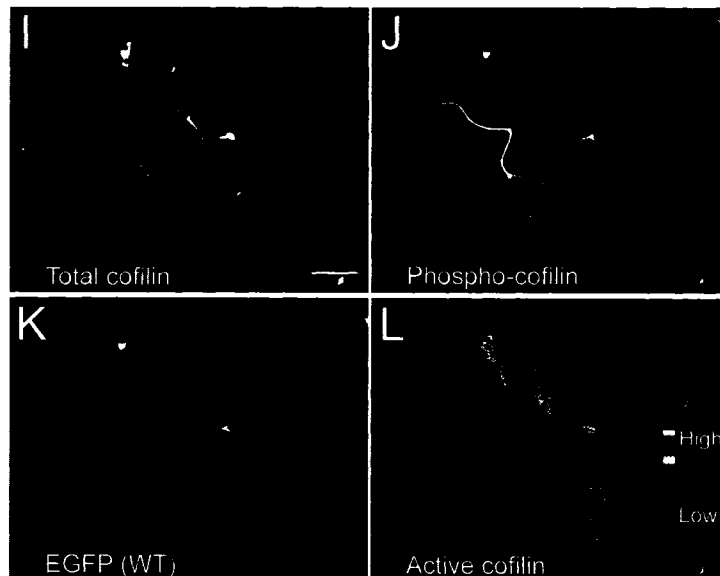
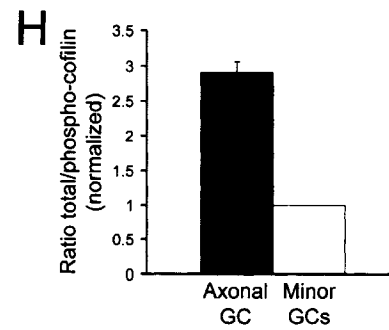
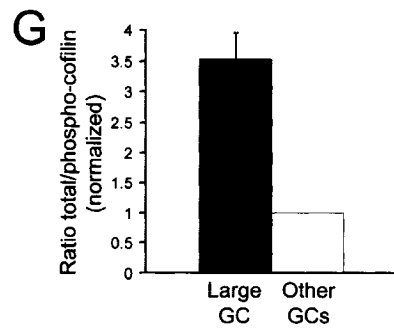
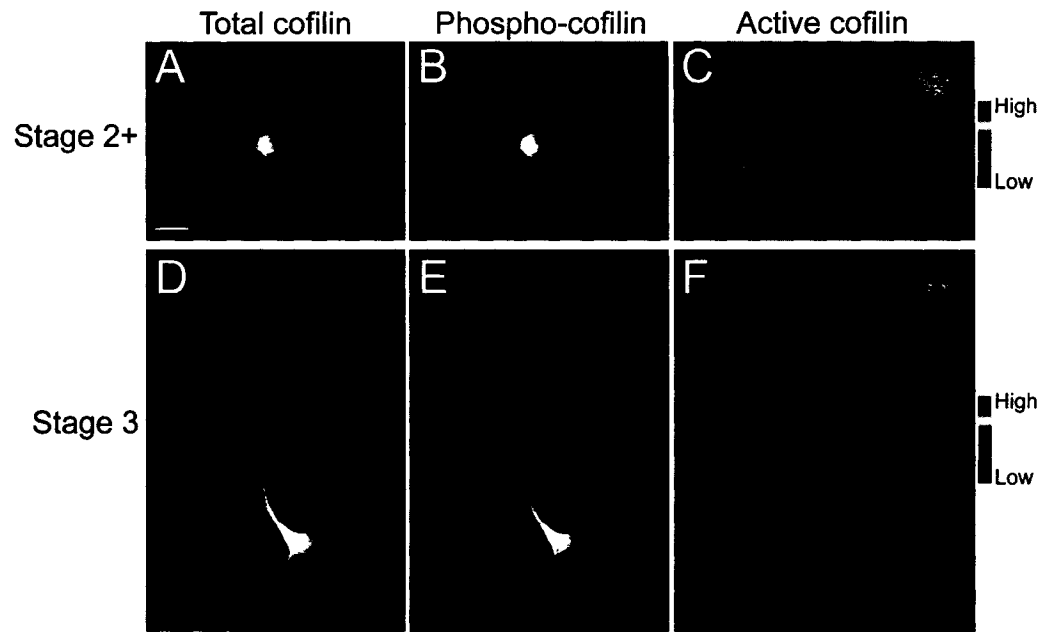
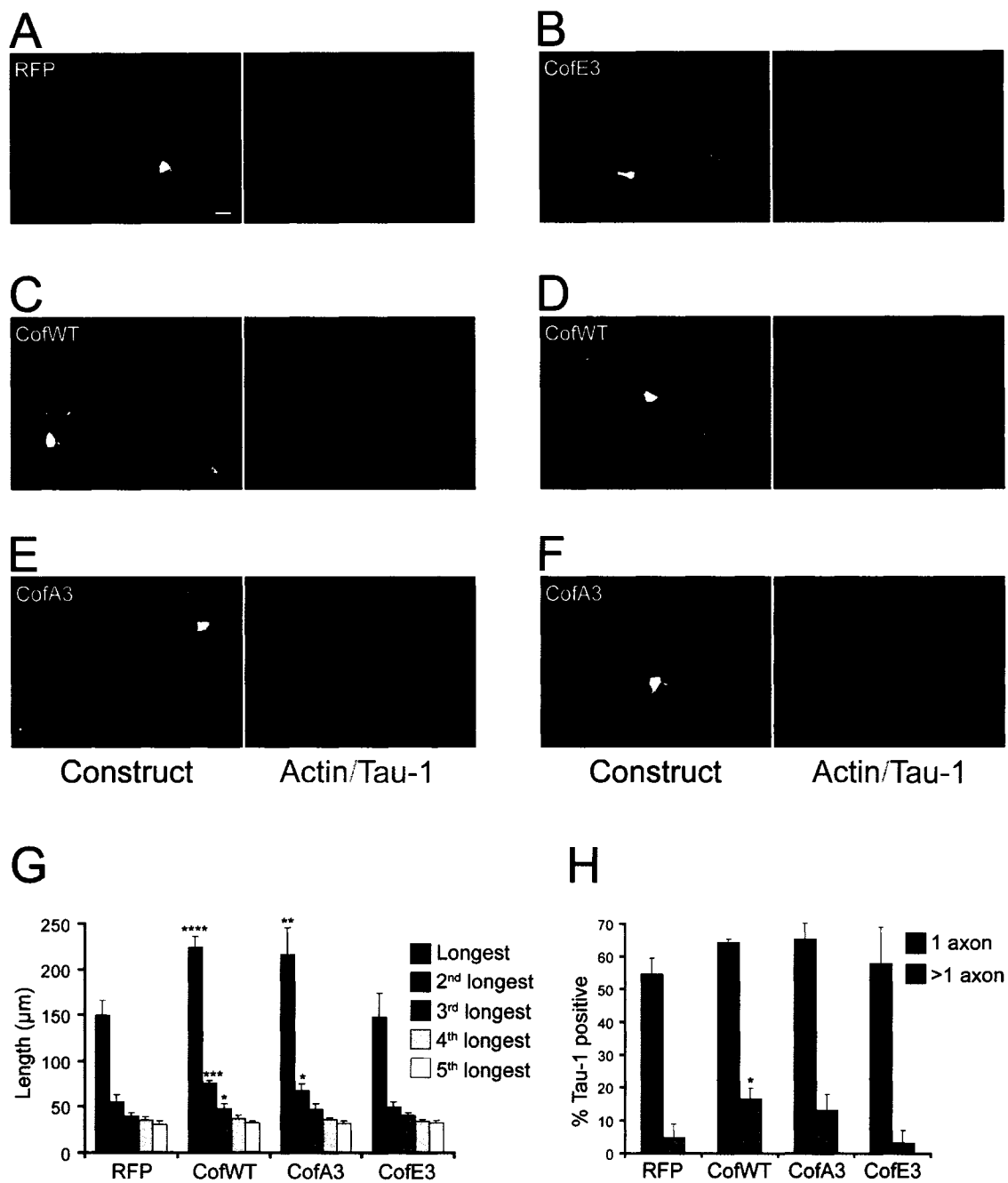


Figure 2.11. Wild type and unphosphorylatable cofilin enhance axonogenesis

Mouse hippocampal neurons were infected with adenoviruses expressing RFP (A) or RFP fused to cofilinE3 (B, C) and cofilinA3 mutants (D, E) or to cofilin wild type (E, F). The cells were stained with phalloidin to reveal actin filaments and with a Tau-1 antibody to label the axons. Scale bar: 20 μ m The length of the individual processes (G) and the percentage of cells having Tau-1 positive axons (H) were quantified (3-4 cultures, $n \geq 35$;, * $p \leq 0.05$, ** $p \leq 0.01$, *** $p \leq 0.005$, **** $p \leq 0.001$)



growth once axon formation is triggered (Andersen and Bi, 2000; Bradke and Dotti, 2000a; Arimura and Kaibuchi, 2007). Our data indicate that an initial Cdc42-dependent triggering event may be sufficient to specify the axon; if a positive feedback loop is indeed involved in maintaining axonal growth after it has been triggered by Cdc42, Cdc42 itself is not a part of that loop.

In addition to defective polarization, the Cdc42 null neurons were also characterized by strongly suppressed dynamics of filopodia formation and retraction. This prominent effect on filopodia in neurons is notable, since the absence of Cdc42 has not been found to affect filopodia formation in other cell types (Czuchra et al., 2005).

Increased cofilin phosphorylation in the absence of Cdc42

To investigate the molecular mechanisms through which Cdc42 depletion results in the observed polarity defects we analyzed different effector pathways that could be affected in the absence of Cdc42, including Arp2/3, the Par3/Par6/aPKC complex, Rho and Rac (Fig. 7 and data not shown), but were unable to detect any consistent differences between knockout and wild type neurons. These findings suggest that other Cdc42 targets may be more physiologically relevant for the establishment of polarity and highlight the significance of testing the role of molecules implicated in neuronal polarity in a physiological setting.

Importantly, we show that in Cdc42 knockout cortices, the Ser³ phosphorylation (inactivation) of the actin depolymerizing protein cofilin was highly increased, presumably due to the enhanced activation of LIM kinase. In addition, the cofilin dephosphorylating activity in knockout extracts was decreased, suggesting that cofilin phosphatases such as slingshot (Niwa et al., 2002; Soosairajah et al., 2005) or chronophin (Gohla et al., 2005), could be affected in the absence of Cdc42. The mechanisms leading to LIM kinase phosphorylation/activation, as well as those resulting in a diminished activity of cofilin phosphatases remain to be fully clarified. One proposed mechanism for the regulation of LIM kinase activity is the association of LIMK2 with Par3 (Chen and Macara, 2006). However we could not detect any substantial differences in this interaction between wild type and Cdc42 knockout conditions (Fig. 9G). LIM kinase can be phosphorylated by PAK (Edwards et al., 1999), which is specifically activated

in axons and affects the establishment of neuronal polarity (Jacobs et al., 2007). However, the activity of PAK in the knockout was actually reduced, as could be expected in the absence of its upstream activator Cdc42, but inconsistent with the involvement of a PAK-dependent pathway in stimulating LIM kinase. In line with our finding that cofilin is phosphorylated in spite of a decreased PAK activity, recent studies have suggested that cofilin-related functions can be regulated in a PAK-independent manner in *Drosophila* neurons (Ng and Luo, 2004). Regarding the activity of cofilin phosphatases, it has been reported that slingshot activity can be affected by actin filaments (Nagata-Ohashi et al., 2004; Soosairajah et al., 2005). Thus, it is conceivable that differences in actin filament distribution in the mutant neurons may contribute to the observed inhibition of cofilin phosphatases. Importantly, this decreased phosphatase activity may also explain the increased levels of LIM kinase phosphorylation, since the cofilin phosphatase SSH can dephosphorylate LIMK (Soosairajah et al., 2005).

Cofilin activity promotes axon formation

We provide several lines of evidence that the increase in cofilin phosphorylation we observed is, at least in part, responsible for the defects in axon formation in Cdc42 knockout neurons. First, cofilin phosphorylation is much lower (and cofilin activity respectively higher) in the axonal and presumptive future axonal growth cones of wild type hippocampal neurons. Second, in Cdc42 knockout neurons the phosphorylation of cofilin in the growth cones of the longest processes was highly increased. Third, overexpression of wild type or constitutively active (A3) cofilin enhanced axonal extension. Lastly, siRNA knockdown of endogenous cofilin resulted in polarity defects in wild type cells that were qualitatively and quantitatively very similar to the ones we observed in Cdc42 knockout neurons. Moreover, as with Cdc42 ablation, the defects following cofilin knockdown were specific for axonogenesis, because the length of the minor neurites was unaffected. Nevertheless, overexpression of wild type or non-phosphorylatable cofilin, as well as overexpression of the cofilin phosphatase SSH1 in Cdc42 mutant neurons was insufficient to rescue their axon forming capacity (data not shown). This may indicate that other effector pathways play additional roles downstream of Cdc42 to regulate the establishment of neuronal polarity. For example, we observed that

Figure 2.12 Characterization of Cofilin/ADF expression in mouse hippocampal neurons and quantification of adenovirus-mediated cofilin siRNA silencing

(A) Western blot of purified human cofilin and human ADF standards (left panel) and an extract of mouse hippocampal neurons (middle panel). The ratio of cofilin to ADF in extracts from three cultures averaged 12:1 when compared to the purified standards (bar chart, right panel). (B) Cofilin silencing measured by Western blots of cultured Swiss 3T3 cells at various times for uninfected (UI) cells and after infection of 100% of cells with adenoviruses expressing lacZ, human cofilin siRNA negative control (Ctrl) and mouse cofilin siRNA (Cof). The plot below the blots shows the amounts of remaining cofilin, normalized to GAPDH, which was used as a loading control. The error bars are standard deviations from triplicates of three independent experiments. The decline in the level of endogenous cofilin is about 50% per 24 hr period. No change in ADF levels was observed (not shown). (C) Western blots of mouse hippocampal neuronal extracts harvested at 96 hr after infection with adenovirus expressing human cofilin siRNA (control, Ctrl) or mouse cofilin siRNA (Cof). Tubulin was used as loading control (bottom panel). Cofilin was blotted with the monoclonal antibody MAb22 (top panel) and 1439 antibody (central panel), which also recognizes ADF (very faint lower band, indicated with an arrowhead). About 50% reduction in cofilin expression was calculated but only about 50-60% of the cells were infected based upon GFP fluorescence. The results shown are representative of two independent experiments. (D, E) Control siRNA expressing neurons and (F, G) mouse cofilin siRNA expressing neurons at 96 hr after infection. (D, F) Fluorescence images of GFP expression showing infected cells. (E, G) Fluorescence images of cofilin immunostaining showing a decline in cofilin expression in mouse neurons expressing cofilin siRNA. Scale bar: 20 μ m. (H) Quantification of relative cofilin levels 96 hr after infection with adenovirus expressing control siRNA (open bar) and mouse cofilin siRNA (black bar), measured over the cell soma. The error bars are standard deviations from three experiments ($n \geq 123$).

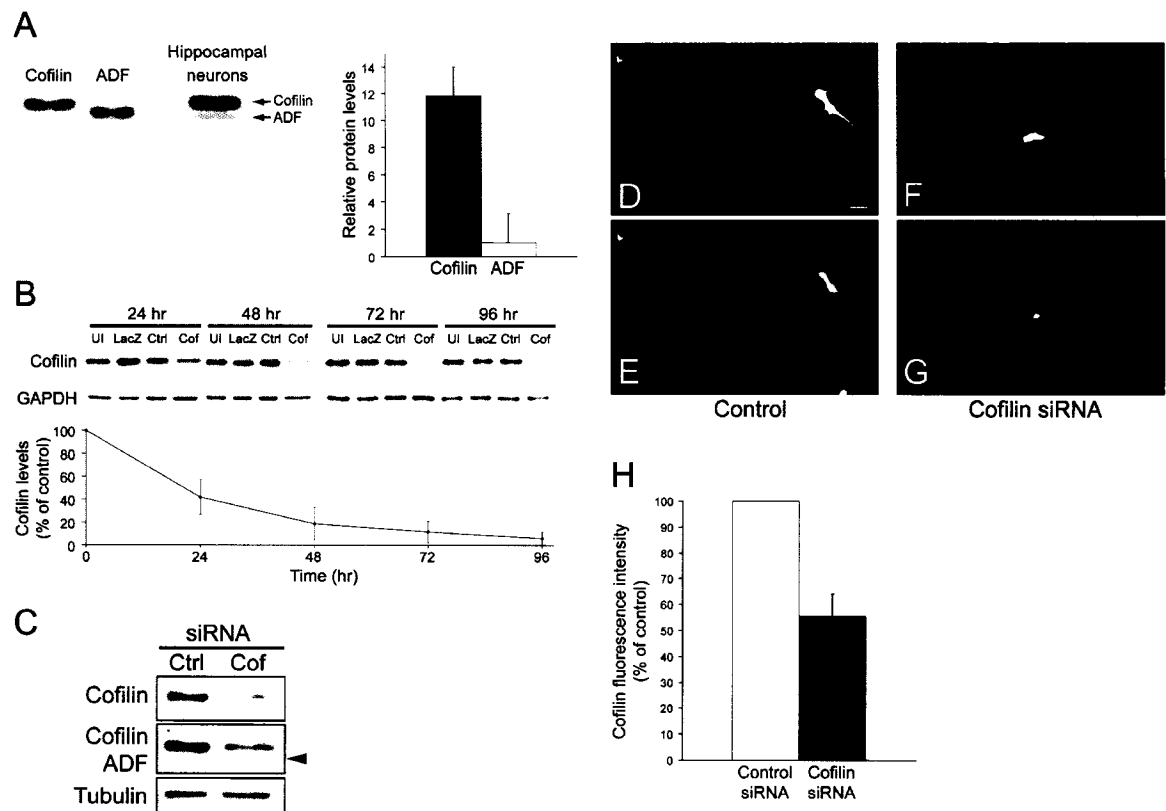
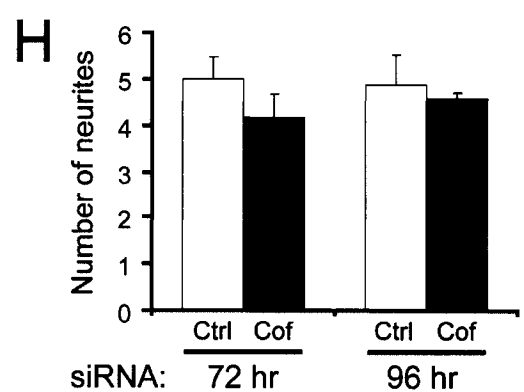
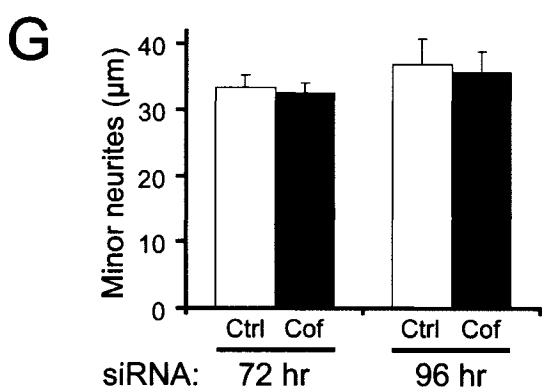
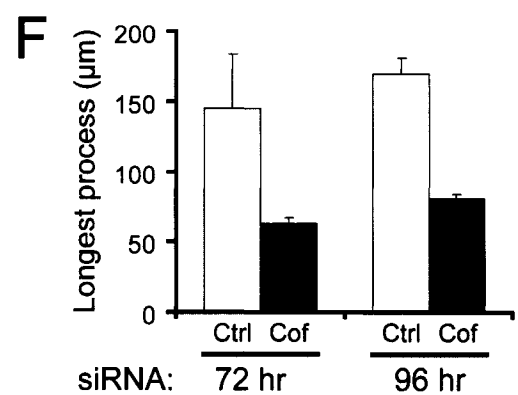
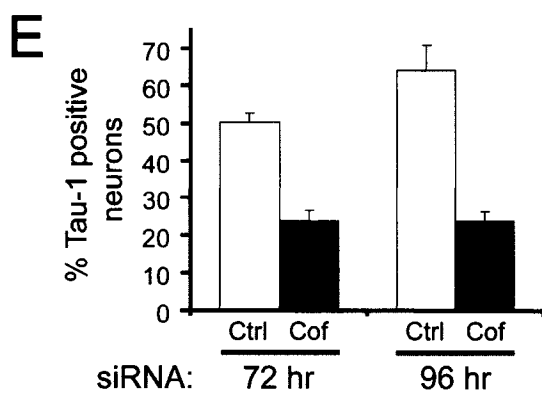
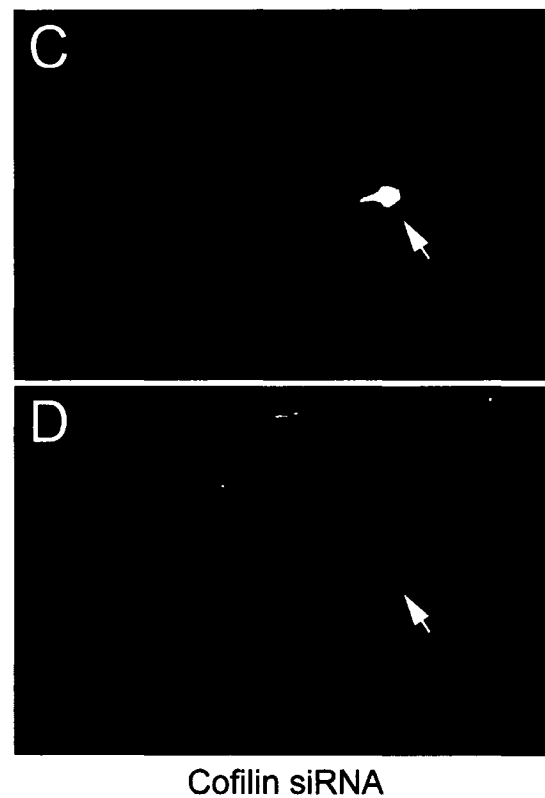
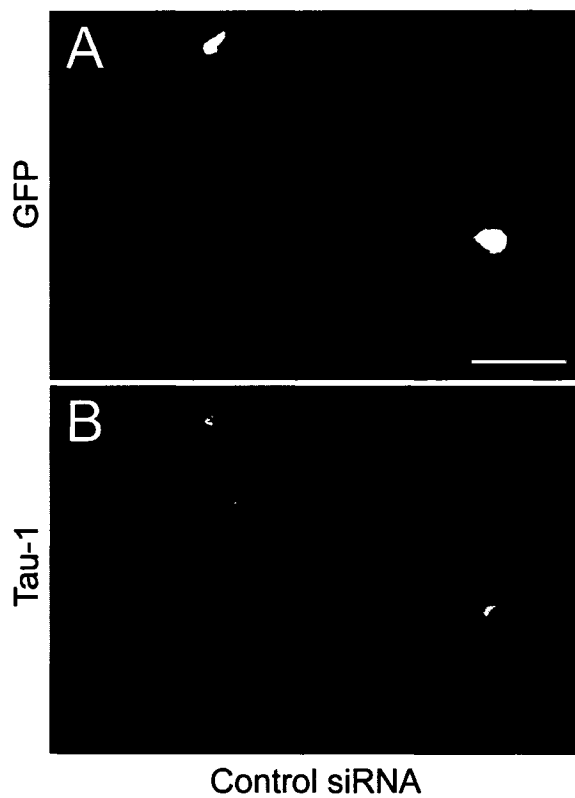


Figure 2.13. Cofilin is necessary for axon formation

(A-D) Mouse hippocampal neurons were infected with Adenoviruses expressing human cofilin siRNA (control) (A, B) or mouse cofilin siRNA (C, D). (A) and (C) show the GFP signal (GFP was co-expressed as a reporter for the presence of siRNA in the neurons); (B) and (D) show Tau-1 immunostaining of the infected neurons. The arrow in (C) and (D) indicates a neuron expressing cofilin siRNA. Scale bar: 50 μ m. (E) Quantification of the control infected neurons (open bars) and mouse cofilin siRNA infected neurons (black bars) with a single Tau-1 positive process (axon) measured at 72 hr and 96 hr post infection. The error bars are standard deviations from triplicate experiments at 72 hr ($n>60$; $p<0.01$) and from duplicate experiments at 96 hr ($n\geq 34$; $p<0.02$). (F-H) Quantification of the average length of the longest neurite (F), the length of the minor (non-longest) neurites (G) and the total number of neurites (H) in control infected neurons (open bars) and mouse cofilin siRNA infected neurons (black bars). The error bars are standard deviations from triplicate experiments at 72 hr ($n>60$) and from quadruplicate experiments at 96 hr ($n>89$). For the length of the longest neurite $p<0.001$ at both 72 and 96 hr; for the remaining measurements $p>0.05$.

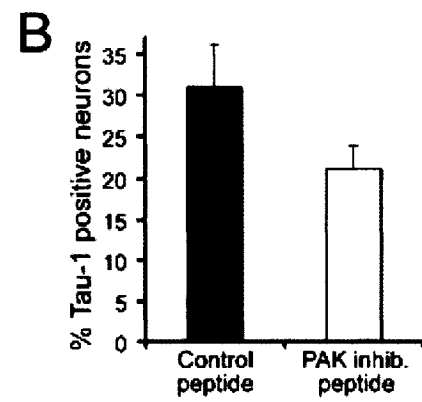
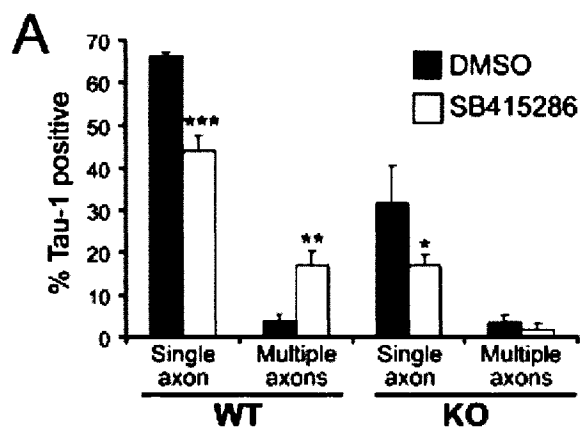


GSK-3 is hyperphosphorylated (inactivated) in the mutants, and inactivation of this protein has been linked to suppression of axonal growth (Kim et al., 2006). Consistently, inhibition of GSK-3 with pharmacological agents, could not restore the axon forming capacity of the Cdc42 null neurons, although it produced a multiaxonal phenotype in wild type neurons (Fig. 14A), as previously described (Jiang et al., 2005; Yoshimura et al., 2005). The activity of PAK was similarly decreased in the absence of Cdc42, and its inhibition could not rescue the polarity defects (Fig. 14B). Expression of wild type or active forms of PAK (Sells et al., 1997) was also unable to rescue the axon forming capacity of knockout neurons (data not shown); the latter finding is consistent with recent reports showing that PAK hyperactivation disrupts neuronal polarity (Jacobs et al., 2007). Our favoured interpretation of the above results is that a concentrated pool of active Cdc42 in the growth cone would be required to locally activate cofilin, as well as other effectors such as PAK or GSK-3, which can then promote axon growth. Thus, cofilin (or other downstream targets) alone, even if expressed in a constitutively active form, would not be able to initiate axon formation if Cdc42 isn't present to target their activation to a specific neurite. Consistent with this model, overexpression of wild type and unphosphorylatable cofilin had a pronounced effect on axon elongation, but led only to a modest increase in the number of axons per cell. In this context, a key challenge would be to develop adequate tools for monitoring localized Cdc42 activation in neurons.

Cofilin is responsible for actin filament severing and dynamics in the cell. Thus, the requirement of cofilin for axon formation is in agreement with previously proposed models for the establishment of polarity (Bradke and Dotti, 2000a), whereby enhanced actin instability or turnover in the future axon is a prerequisite for its growth. The increased cofilin activity in selected growth cones offers a molecular mechanism for the physiological, local regulation of actin dynamics, leading to the proper polarization of neurons.

Figure 2.14 Inhibition of GSK-3 and PAK further suppresses the axon forming capacity of Cdc42 null neurons

(A) Cdc42 knockout neurons in mixed cultures were treated with the GSK-3 inhibitor SB415286 (20 μ M). The percentage of neurons bearing a single axon or multiple axons (Tau-1 positive) was quantified. The error bars are standard deviations from 4 experiments ($n \geq 600$ per data point; * - $p < 0.05$; ** - $p < 0.01$; *** - $p < 0.001$). (B) Cdc42 knockout neurons were treated with a PAK inhibitory peptide and with control PAK peptide (Kiosses et al., 2002) at 100 μ g/mL. The percentage of neurons bearing Tau-1 positive axons was quantified. $n \geq 62$ per data point.



Garvalov, Flynn et al., Suppl. Fig. 6

Chapter 3

Evidence for the synergistic regulation of myosin inhibition and cofilin activation during the development of neuronal polarity

Preface and Acknowledgements

The work presented in this chapter will be a part of a continuing study in the laboratories of Frank Bradke and James Bamberg and will be prepared for publication after additional studies. The authors are Kevin C. Flynn, Boyan K. Garvalov, Robert Wysolmerski, Frank Bradke and James R. Bamberg. We would like to thank Chi Pak, Richard Davis, Barbara Bernstein, Alisa Shaw, O'Neil Wiggan, Shay Perea-Boettcher, and Laurie Minamide for helpful comments and suggestions. For help in preparation of mixed *cdc42*KO/GFP hippocampal culture, thanks are extended to Liane Meyn. We gratefully acknowledge support from the National Institutes of Health, grants NS40371 and DK69408 (J.R.B.), NS43115 (J.R.B. and K.C.F.), and NS48660 (K.C.F.).

Abstract: Neurons are morphologically complex cells, typically with multiple dendrites and one long axon. This structural specialization is crucial to the function of neurons where unidirectional electrical-chemical signals are received in somato-dendritic compartment and transmitted via the axon to postsynaptic targets. The development of the specialized compartments of a mature neuron initially occurs via the specification of the axon from one of multiple immature, “minor” processes. Recent work has identified various signaling proteins that are involved in the primary signaling events involved in axon specification including key regulators of the actin cytoskeleton, such as the Rho GTPase *cdc42*. However, these studies failed to show a direct functional link between these upstream signaling proteins and actin binding proteins which execute the necessary changes in the dynamics of the actin cytoskeleton to facilitate axon formation. In the current study we identify cofilin and myosin as two actin binding proteins that are crucial regulators of axonogenesis. Cofilin segregates preferentially to the developing axonal growth cone, and active myosin localizes

to the neurite shaft of all processes and to the proximal growth cone. The level of active cofilin is high in the initial stages of neuronal development, when neurite outgrowth is robust. Conversely, myosin activity increases at later stages of neuronal development when neurite growth is attenuated. Molecules known to induce axonogenesis, such as IGF-1 cause an increase in cofilin activity and decrease in myosin activity, whereas the knockout of *cdc42*, an axonogenic signaling protein, shows the opposite effect. Furthermore, the combination of myosin inhibition and cofilin over-expression induces supernumerary axons, whereas either treatment in isolation has less of an axonogenic effect. In hippocampal neurons lacking *cdc42*, which are deficient in axonogenesis, the combined inhibition of myosin and activation of cofilin partially rescues axon formation while each treatment individually does not. These data suggest that myosin inhibition and cofilin activation contribute synergistically to the regulation of the cytoskeleton during axon formation.

Introduction

The polarization of neurons is essential for the specification of axons and dendrites, which, consequently, leads to the proper function of mature neurons. Many molecular players have been identified *in vitro* using rodent hippocampal neurons as a model system. In culture, hippocampal neurons undergo a stereotypical developmental program which is morphologically classified into five stages (Dotti et al., 1988; Craig and Banker, 1994). At the stage 2-3 transition, an axon develops from one of several immature processes. This is the first phase of polarization. Later, the remaining processes acquire a dendritic phenotype (Stage 4) and the neurons become mature, forming functional synaptic contacts (Stage 5). Determining the mechanisms underlying the morphological changes as well as the development of the appropriate molecular compartmentalization of the axon, somata, and dendrites in neurons are important questions in neurobiology. Recent work has elucidated multiple mechanisms affecting intracellular trafficking as well as the modulation of the actin and microtubule cytoskeletons. The complex interrelationship of divergent and convergent signaling pathways ultimately promote a positive potential for microtubule assembly as well as increased actin dynamics during axonogenesis (reviewed in Bradke and Dotti, 2000;

Horton and Elhers, 2003; Yosimura et al., 2006; Arimura and Kaibuchi, 2007).

The initial development of polarity is thought to depend on the length of the axon relative to the other minor processes (Goslin and Banker, 1989). It is well appreciated that the restructuring of the actin and microtubule cytoskeletons, particularly at the growth cone, are required for neurite outgrowth. The organization of microtubules in neurons occurs via the transport of microtubule polymers (Wang and Brown, 2002) and assembly at their plus ends (Bamburg et al., 1986; Baas, 1997). Microtubule assembly has been shown to be the driving force behind neurite growth, since drugs that inhibit its incorporation at plus ends also attenuate outgrowth (Rochlin et al., 1996). Thus, it is not surprising that signaling pathways that affect microtubule assembly have been shown to play a role in axon specification. For example, neurons isolated from the Map1B knockout mouse are defective in their ability to form axons; an abnormality thought to stem from deficits in microtubule assembly (Gonzalez-Billaut et al., 2001). The plus-end microtubule binding protein (+TIP), EB1, which promotes microtubule assembly, can rescue polarity defects in Map1B deficient neurons (Jiménez-Mateos et al., 2005). The canonical polarity complex Par3/Par6/aPKC has also recently been shown to play a role in the development of neuronal polarity (Shi et al., 2003; Nishimura et al., 2004), which, through aPKC, can regulate microtubules via GSK3 β . Indeed GSK 3 β control of CRMP2 activity, which promotes microtubule assembly, has been shown to be crucial for axon specification (Yoshimura et al., 2005; Arimura et al., 2005).

Microtubule assembly and advance in the growth cone also is affected by changes in the actin cytoskeleton (Forscher and Smith, 1988). Treatment of growth cones with cytochalasin B causes an increase in microtubules penetrating into the peripheral growth cone and increases neurite outgrowth (Marsh and Letourneau, 1984). This result suggested that stable actin structures in the growth cone are obstructive for microtubule advance and neurite growth. Indeed, other studies have shown that actin instability (i.e. increased actin turnover) occurs in one growth cone prior to axon formation (Bradke and Dotti, 1999). Cofilin, an actin binding protein that increases actin turnover in growth cones (Meberg and Bamburg, 2000) has recently been shown to play a role in axon formation downstream of cdc42 (Garvalov et al., 2007).

The initial development of polarity not only involves localized increase in actin turnover in the growth cone, but also increased contractile forces generated by the growth cone which “pull” the axon forward (Heideman and Buxbaum, 1994, Lamoureux et al., 2002). The generation of contractile forces in growth cones has been attributed to actomyosin activity (Brown and Bridgman, 2003). Specifically, it seems that myosin II isoforms are important, since down regulation of myosin IIA and myosin IIB results in the attenuation of neurite growth in N2A cells (Wylie and Chantler, 2001). Furthermore, myosin II activity is responsible for neurite retraction (Gallo et al., 2002) and for guidance decisions at laminin borders (Turney and Bridgman, 2005). In fluorescence speckle microscopy studies in *Aplysia* bag cell growth cones, it was demonstrated that the retrograde movement of F-actin in growth cones depends equally on recycling of actin subunits (perhaps mediated by cofilin) and myosin II contractility (Medeiros et al., 2006).

Although recent studies have suggested a role for myosin activity in axonogenesis (Kim and Chang, 2004), there has been no detailed analysis of its upstream signaling proteins or the interaction of myosin activity with other actin binding proteins. The Rho GTPase, cdc42, is crucial for axon growth in *Drosophila* (Luo et al., 1994) and is involved in axon formation in neuronal cultures (Schwamborn and Pülschel, 2004) and *in vivo* (Garvalov et al., 2007). Cofilin was identified as an important effector downstream of cdc42; however, active versions of cofilin could not rescue polarity deficits in cdc42 KO neurons (Garvalov et al., 2007). Since manipulations of the actin cytoskeleton can rescue polarity deficits in cdc42 KO neurons, it is likely that multiple actin regulating proteins are necessary for axon formation downstream of cdc42. In addition to cofilin, another possible candidate is myosin II.

Here we characterize a role for myosin II in axon development in hippocampal neurons. Furthermore, we describe a potential synergistic interaction between myosin activity and cofilin activity downstream of cdc42 during axonogenesis. Interestingly, our results suggest that myosin II is active mostly in the neurite shafts and central domain of growth cones, with less activity in the peripheral growth cone, where cofilin activity is higher. We also see that myosin inhibition alone increases the presence of supernumerary

axons. In conjunction with cofilin over-expression, low levels of myosin inhibition, induces a greater increase in axonogenesis than either treatment alone. We show that myosin II inhibition and cofilin activation together can rescue axon formation in neurons lacking cdc42. These data provide evidence for multiple actin-regulating proteins downstream of cdc42 and other axon-promoting signals.

Materials and Methods

Neuronal Cultures: Primary hippocampal neurons from E16.5-17.5 mouse embryos were cultured essentially as described (Garvalov et al., 2007). For the mixed wild-type (GFP-positive)/Cdc42 knockout (GFP-negative) cultures, the hippocampi of embryos from a cdc42 KOs were dissected, trypsinized and dissociated individually for each embryo. In parallel, hippocampi from wild type, GFP positive embryos (expressing GFP under the ubiquitous “CAG” promoter)(Okabe et al., 1997; Ikawa et al., 1998) were dissected, trypsinized and dissociated. The cells were then washed in Hank’s balanced salt solution (HBSS), and $60\text{--}65 \times 10^3$ wild type cells were plated together with $80\text{--}90 \times 10^3$ Cdc42 knockout cells onto polylysine coated glass coverslips in 6 cm tissue culture dishes, containing minimal essential medium and 10% heat-inactivated horse serum. For transfection, $3\text{--}6 \times 10^5$ cells were electroporated following the manufacturer’s instructions (Amaxa). The cultures were grown in a humidified tissue culture incubator at 36.5°C , 5% CO_2 , and after 12-20 hr the coverslips were flipped in 6 cm dishes containing astrocytes in N2 medium. For wild-type neuronal cultures, E16.5 mouse hippocampal neurons used for the experiments cultured as described (Meberg and Miller, 2003).

Adenovirus expression: Adenovirus expression was performed as described (Garvalov et al., 2007). Neurons were plated in neurobasal medium + 5% FBS on clean, glass coverslips and infected at multiplicities of infection (MOIs) ranging from 150-300 focus forming units (ffu)/ml. Using this procedure neurons adhere lightly to the glass but do not extend processes. After 18-20 hours, the neurons were trypsinized and re-plated on polylysine coated coverslips with plating medium (HgdMEM/10% hyclone FBS). The media was

replaced with fresh neurobasal/B27/glutamine 2.5 hours later. This procedure results in transgene expression before axonogenesis, which typically occurs 24-48 hrs in culture.

Cell treatments: The Myosin II inhibitor, blebbistatin (Sigma Aldrich) was dissolved in DMSO at 100 mM and applied to neuronal cultures at final concentrations ranging from 50 nM - 25 μ M. Blebbistatin was added to growth media 16-18hrs after plating and left in until the termination of the experiment. The ROCK inhibitor Y-21372 (Sigma Aldrich) was dissolved in H₂O at a concentration of 5mM and applied to cells at a final concentration of 25-100 μ M 16-18 hrs post-plating. Insulin-like growth factor 1 (IGF-1, kind gift from Doug Ishii, Colorado State University) was dissolved in acetate buffer and used at final concentrations of 25 ng/ml and added to neuronal cultures 2 hrs after plating. NT-3 (Alomone labs, Jerusalem) was used at a final concentration of 100 ng/ml.

SDS-PAGE and Western Blotting: Whole brain lysates were prepared by resuspending dissected E17-E18 cortices in 20 μ l/mg wet tissue weight of the following buffer: 10 mM Tris pH7.5, 1% SDS, 0.5 mM DTT, 2 mM EGTA, 20 mM NaF, and 1 mM Na₃VO₄. After sonication for 3 sec the lysates were plunged in a boiling water bath for 10 min. In some cases samples were chloroform-methanol precipitated and subjected to a commassie dye-based protein assay (Minamede et al., 1990). Equal amounts of protein were separated by SDS PAGE (12.5% and 15% gels) and analyzed by Western blotting, using the following primary antibodies and dilutions: anti GAPDH mouse monoclonal antibody (Santa Cruz Biotech) at 1:3000, anti-phospho-cofilin (Ser³) rabbit polyclonal antibody (4321; Shaw et al., 2004) at 1:500, anti-cofilin mouse monoclonal antibody, Mab22 (Abe et al., 1989) at 1:200, anti-myosin goat heavy chain at 1:1000 (Robert Wysolmerski, University of West Virginia), and anti-phospho-myosin light chain (ser 19) at 1:1000. The secondary antibodies were goat anti-mouse or anti-rabbit IgG-HRP (Santa Cruz), and the blots were developed using Pierce Western Blotting Detection System. In some cases, fluorescent secondaries (goat anti rabbit IR 800 and goat anti mouse 680) were used and blots were developed using the Odyssey

Fluorescence imaging system according to manufactures guidelines.

Cortical neurons were plated at 2×10^6 cells/35mm dish and cultured for 4 days. Extracts from cultured neurons were prepared by rapidly rinsing the cultures 4-5 times in cold PBS, adding SDS lysis buffer (Morgan et al., 1993) or SDS sample preparation buffer (Laemmli, 1970) and heating to boiling for 5 min. Protein concentration was determined using a filter paper dye binding assay (Minamide and Bamburg, 1990). SDS-polyacrylamide gel electrophoresis was performed on 12.5% and 15% polyacrylamide gels and Western blotting was onto PVDF. Antibodies against cofilin (MAb22; Abe et al., 1989), phospho-ADF/cofilin (Meberg et al., 1998), and a common epitope encompassing amino acids 52-54 of mouse ADF and cofilin (rabbit 1439; Shaw et al., 2004) were used.

Immunofluorescence: The procedure for fixation and immunofluorescence was performed as previously described (Flynn and Bamburg, in preparation, Chapter 5). All cells were fixed in 4% paraformaldehyde in cytoskeletal preservation buffer (10 mM MES pH 6.1, 138 mM KCl, 3 mM $MgCl_2$, 10 mM EGTA, and 0.32 M sucrose MES) for 30 minutes at 37°C. Primary antibodies used in this study include the following monoclonal antibodies: Tau1 (1:1000, Chemicon), β tubulin (1:300, Sigma), and cofilin (MAb22; Abe et al., 1989). The following rabbit polyclonal antibodies were also used: phospho-ADF/cofilin (4321; Meberg et al., 1998), a total ADF/Cofilin (amino acids 52-54) (rabbit 1439; Shaw et al., 2004) A myosin heavy chain (1:350, sheep anti-goat; Robert Wysolmerski, University of West Virginia) and previously uncharacterized phospho-myosin light chain antibody (p-MLC^{ser19}) (1:750 dilution). Secondary IgG secondary antibodies (Molecular Probes, Eugene, Oregon) Fluorescein goat anti-mouse IgG, Texas Red goat anti-rabbit, and Alexa 350 goat anti-mouse. Texas Red or Alexa 488 conjugated Phalloidin was used to visualize actin filaments. Coverslips were mounted with Prolong Anti-fade (Molecular Probes).

Images were acquired with a Nikon Diaphot inverted microscope using a 40x oil immersion objective and a Coolsnap ES CCD camera (Roper Scientific, Tucson, AZ). Metamorph software (Universal Imaging, Westchester, PA) was used for image acquisition and analysis. For ratio imaging experiments, background fluorescence was subtracted from

the raw images, which were then overlaid as a stack. After alignment, the ratio of the total cofilin image over the phospho-cofilin image was obtained with the ratio images option in the Metamorph software (Molecular Devices).

Live-cell imaging: Live-cell imaging was performed using an Olympus IX81 microscope equipped with an Olympus CSU22 spinning disk confocal head with four diode lasers and an EM-CCD cascade II camera (Photometrics). This system also had a humidified, CO₂ regulated chamber which maintained a constant temperature of 37°C. The objectives used include the following: 20x U-Plan Fluorite (0.17 NA) air objectives, UAPO 40X/340W-DIC (1.35 NA), and Plan-APO 60x (1.42 NA) oil objectives. Image acquisition was controlled using Slidebook imaging software (3I, Denver, CO). In some live-cell experiments, 2.5μM blebbistatin (final concentration) was added to the culture dish while it was on the stage and imaging proceeded directly after application of the drug.

Image analysis: All image analysis was performed using Metamorph imaging software (Molecular Devices). Axons were defined from fixed cells as being $\geq 80\mu\text{m}$ in length and containing intermediate to high levels of Tau1 immunofluorescence. Neurites with an absence of Tau1 staining were not counted as axons regardless of length. Neurons were counted with multiple axons when they displayed two or more neurites $\geq 80\mu\text{m}$ in length and contained Tau1 immunofluorescence. For experiments using adenovirus infections, only cells with low to moderate fluorescent protein expression were included for analysis to avoid complications from virus and/or fluorescent protein toxicity. Neurons with less than three $\geq 20\mu\text{m}$ long neurites were not included in analysis. All figures were compiled and annotated using Adobe Photoshop (™) software.

Results

Myosin and Cofilin localization and expression in neurons

Within the growth cone, actin is organized into diverse higher order networks of filaments including the mesh-like networks of lamellipodia, the linear bundles in filopodia, and actin

arcs (Pak et al., 2008). Although distinct, these actin structures are overlapping and in combination comprise the peripheral domain of growth cones. We hypothesize that axon formation involves the regulation of the spatiotemporal dynamics these different actin structures. Although a plethora of actin binding proteins are likely involved, myosin II and ADF/cofilin are crucial regulators of growth cone actin structures (Sarmiere and Bamberg, 2003; Brown and Bridgman, 2003) and may define different populations of actin filaments in growth cones. Therefore, we examined the distribution and localization of myosin and cofilin in developing neurons.

Using cultured hippocampal and cortical neurons, we first sought to characterize how myosin II activity occurs during the development of a polarized neuronal morphology. In addition, we compared the localization of active myosin II to cofilin. We examined neurons at time points corresponding to the various stages laid out in previous studies (Dotti and Banker, 1988). pMLC levels are extremely low 16hrs after plating when the majority of cells are in stage 2, with no distinct axon (Figure 1C-D). Although pMLC levels increase over three fold after three days in culture, when the majority of neurons are in stage 3 with a rapidly growing axonal process (Figure 2), the levels are still low compared to later time points. By day five in culture (Stage 4) pMLC levels have increased over 20 fold and by seven days in culture pMLC levels have increased nearly 60 fold compared to the pMLC levels from the first day in culture (Figure 1C-D).

Although total cofilin levels rise over the developmental time course examined, the ratio of total cofilin to phospho-cofilin (Cof/pCof), representing cofilin activity, actually decreases (Figure 1B) as well as the absolute activity (data not shown). For neurons in culture up to three days in culture the Cof/pCof ratio is high compared to later time-points. By day 5 the Cof/pCof ratio has decreased by over 50% and by day 7 the ratio has decreased by over 60%. Together, these data show that as neurite growth attenuates there is an increase in myosin activity with a concomitant decrease in cofilin activity.

Active cofilin levels are predominately localized in the developing axonal growth cone of cultured hippocampal neurons (Garvalov et al., 2007). Total cofilin levels are also high in the large growth cone of stage 2 neurons (presumptive axon) as well as in the axonal

growth cones of stage 3 neurons (Figure 3). Interestingly, pMLC levels are concentrated in the neurite shafts of stage 2 neurons as well as in stage 3 neurons (Figure 3 and 4). In enlarged growth cones of stage 2+ neurons, active myosin MLC is distributed throughout the growth cone, but highest in the central domain whereas active cofilin is particularly enriched in the peripheral growth cone (Figure 5). In the stage 3 growth cones, myosin activity is still restricted to the neurite shaft and more proximal growth cone, and cofilin activity remains localized throughout the peripheral domain (Figure 4). These staining patterns are consistent with the hypothesis that myosin II may be involved with the consolidation phase of axon extension (Loundon et al., 2006).

Effects of myosin inhibition and cofilin activation on neuronal polarity

Rho activated kinase (ROCK) and myosin II have been implicated in axon formation in hippocampal neurons (Kim and Chang, 2004), may be related to their effects on the contractility in the proximal growth cone (Loundon et al., 2006) or in retrograde F-actin compression which can inhibit microtubule polymerization kinetics (Medeiros et al., 2007). Here we sought to determine the effects of inhibiting nonmuscle myosin II ATPase activity with the inhibitor blebbistatin on the development of neuronal polarity in hippocampal neurons. First, we performed a dose response curve examining the effects of increasing concentrations of blebbistatin on polarity phenotypes (Figure 6). There was a strong correlation with increasing axonogenesis with increasing blebbistatin concentrations. The percentage of neurons with multiple axon-like processes increases from 10% in control conditions to 80% in the presence of 25 μ M blebbistatin. Interestingly, the increase in blebbistatin concentrations also resulted in increased axonal branching, suggesting a role in myosin activity in restricting the formation of neurite arbors (Figure 7). There was also an apparent increase in wave-like structures along neurite shafts, which we have shown to be correlated to axon determination (see Chapter 4). Live-cell imaging experiments show that within three hours of blebbistatin treatment there are increased neurite growth rates as well as the formation of neurite branches (Figure 8).

We also sought to determine if axon-inducing effect of myosin inhibition worked in

Figure 3.1. Expression levels of active myosin and cofilin changes during neuronal development. Protein from neuronal cultures was examined at 16hrs, 3 days in vitro (div), 5 div, and 7 div. These time-points correspond to different stages of neuronal development, illustrated in the diagrams at the bottom of the figure. At 16 hrs the majority of the neurons are in stage 2; at 3 div the majority of the neurons are in stage 3; at 5 and 7 div the neurons are in stage 4.

(A) Western blot shows the levels of total cofilin levels and inactive phosphorylated cofilin (p-cofilin) as an indication of cofilin activity.

(B) Quantification shows ratio of cofilin/pcofilin relative to 16hr time-point (16hr = 1). At 3 div the cofilin/pcofilin ratio is 0.93; at 5 div the ratio is 0.5; at 7 div the ratio is 0.35. (C) Western blot shows the levels of phosphorylated myosin regulatory light chain (pMLC) and GAPDH (loading control).

(D) Quantification shows pMLC levels normalized to GAPDH relative to 16hr time-point (16hr = 1). At 3 div the levels of pMLC rises to 3.81; at 5 div the pMLC rises to 20.9; at 7 div the level of pMLC is 57.1 fold higher than the level at 16hr.

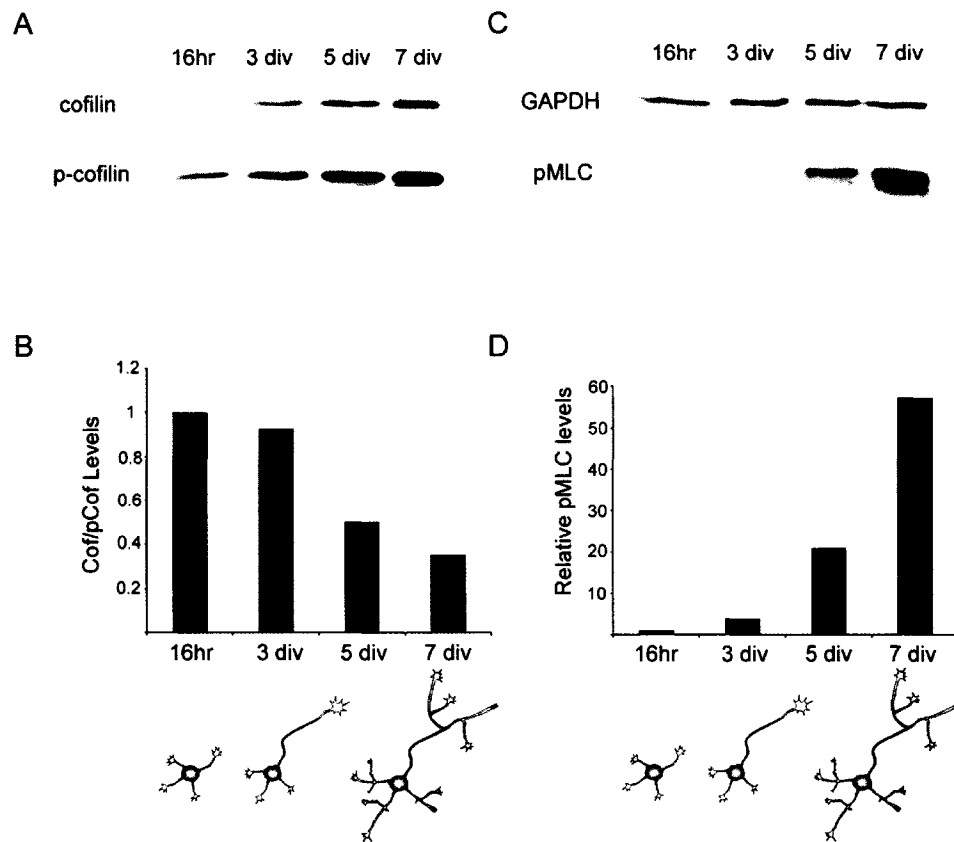
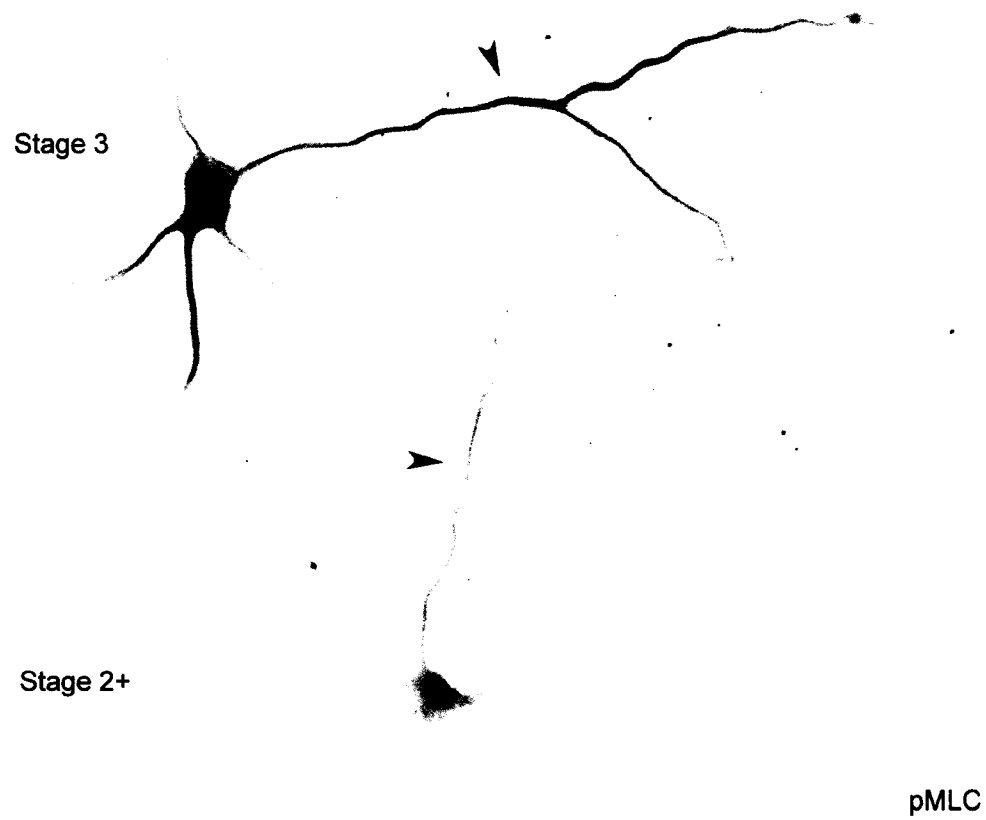


Figure 3.2. The levels of pMLC increase in more mature neurons in the same culture. An inverted fluorescence micrograph of pMLC intensity shows two neurons at different developmental stages. Note that the stage 3 neuron has a higher level of pMLC immunostaining than the stage 2+ neuron (arrows). This is particularly apparent in the neurite shaft (arrow).



coordination with cofilin. In a previous study, we demonstrated that exogenous expression of wild-type and active (S3A) cofilin only moderately increased the percentage of hippocampal neurons presenting multiple axons but greatly enhanced axon length (Garvalov et al., 2007). To determine if increasing cofilin expression levels and/or activity concurrently with myosin inhibition has a synergistic effect on axonogenesis we used a concentration of blebbistatin that induced an intermediate increase in the percentage of neurons with multiple axon-like processes (500nM) in conjunction with the over-expression of wildtype and S3A cofilin over-expression. In agreement with our earlier studies, we found that the expression of cofilin wt or A3 alone resulted in a slight increase in the percentage of neurons exhibiting multiple axons (Figure 9). Blebbistatin treatment of control neurons alone increased the prevalence of neurons with multiple axons, but had an even greater impact on axon phenotypes in conjunction with either cofilin wild-type or cofilin A3 expression (Figure 9). These data suggest that cofilin activation and myosin inactivation have synergistic effects on axon development.

IGF-1 decreases phosphorylated ADF/Cofilin and phosphorylated Myosin Light Chain

IGFs are known to enhance neurite growth in a variety of neurons including dorsal root ganglion neurons, sympathetic neurons, and neuronal cell lines (Martin *et al.*, 1991; Meghani *et al.*, 1993; Haselbacher *et al.*, 1985; Sumantran & Feldman, 1993). More recently, it was demonstrated that the IGF-1 receptor is essential for axon determination in hippocampal neurons (Sosa et al., 2005). Therefore, we sought to determine the effects of this potential axon growth-inducing cue on myosin II and cofilin activity. Treatment of neuronal cultures with 25 ng/ml of IGF 1 induced time-dependent changes in cofilin and myosin activity (Figure 10). Initially, both cofilin and myosin undergo increased phosphorylation within 2-5 minutes after IGF-1 stimulation. However, both myosin and cofilin undergo increased dephosphorylation 10-30 minutes following IGF-1 treatment. Thirty minutes after IGF-1 stimulation, MLC phosphorylation has decreased nearly 40% and cofilin phosphorylation has decreased over 30%. These data suggest that IGF-1 signaling triggers the concurrent activation of cofilin and deactivation of myosin.

ROCK is upstream of cofilin and myosin in neurons

The canonical Rho-ROCK-myosin pathway has been established as an important signaling pathway involved in neurite outgrowth (Brown and Bridgman, 2003). More recently, it has been demonstrated that ROCK also modulates cofilin activity in response to BDNF in retinal ganglion neurons (Gehler et al., 2004) and during neurite growth in PC12 cells (Birkenfeld et al., 2007). Treatment of hippocampal neurons with the ROCK inhibitors also induces multiple axon-like processes (Kim and Chang, 2004). Thus, we sought to determine if this intracellular signaling protein, whose activity attenuates axon formation signals to cofilin and myosin. The ROCK inhibitor Y27632 we observed a large decrease in cofilin phosphorylation and, albeit a less robust, reduction in MLC phosphorylation (Figure 11).

Myosin II and cofilin are mis-regulated in the Cdc42 knockout brain

There is a substantial increase in cofilin phosphorylation in the brains and in growth cones of isolated hippocampal neurons from mice lacking *cdc42* (Garvalov et al., 2007). Although cofilin plays a role in axon formation, cofilin activity alone is insufficient to account for the deficits in neuronal polarity observed. Since manipulations of actin structures can rescue the polarity deficits of *cdc42* null neurons, it is likely that other actin binding proteins are mis-regulated downstream of *cdc42*. We previously observed that profilin, an actin monomer binding protein implicated in neurite growth (DaSilva et al., 2003), did not exhibit changes in activity in the absence of *cdc42*. Here we sought to determine if myosin activity is mis-regulated in the absence of *cdc42*. Indeed, we observed a significant increase in myosin light chain phosphorylation in *cdc42* KO versus control brain (Figure 12). This data suggests that an increase in myosin activation could also contribute to the decreased ability of neurons to polarize in the absence of *cdc42*.

Myosin inhibition and cofilin activation rescues axonogenesis in *cdc42* nulls.

Cofilin and myosin may bind to different actin structures in growth cones, but may need to be coordinately regulated in order to achieve optimal actin remodeling to facilitate

Figure 3.3. Localization of active myosin and cofilin in during neuronal development.

Co-staining for cofilin (left column, red) and phosphorylated myosin light chain (pMLC) (middle column, green) shows that cofilin and pMLC are localized to different regions of developing neurons. In stage 2+ neurons (top row), cofilin is found throughout the cell, but with enrichment in the enlarged growth cone of the presumptive axon (arrow). pMLC is found mainly in the soma and neurite shafts, with particular enrichment in the shaft of the presumptive axon. The overlay of cofilin and pMLC stainings (right) shows pMLC is restricted to the proximal region of the growth cone, while cofilin is more heavily localized to the distal regions of the growth cone. In Stage 3 neurons (bottom row), cofilin remains enriched in the growth cones, with particularly high levels in the distal axon and the axonal growth cone. pMLC remains enriched in the neurite shafts of stage 3 neurons. The overlay of cofilin and pMLC stainings of stage 3 neurons (right) shows increased co-localization in the distal neurite shaft, but pMLC remains restricted to the proximal region of the growth cone, while cofilin remains more heavily localized to the distal regions of the growth cone.

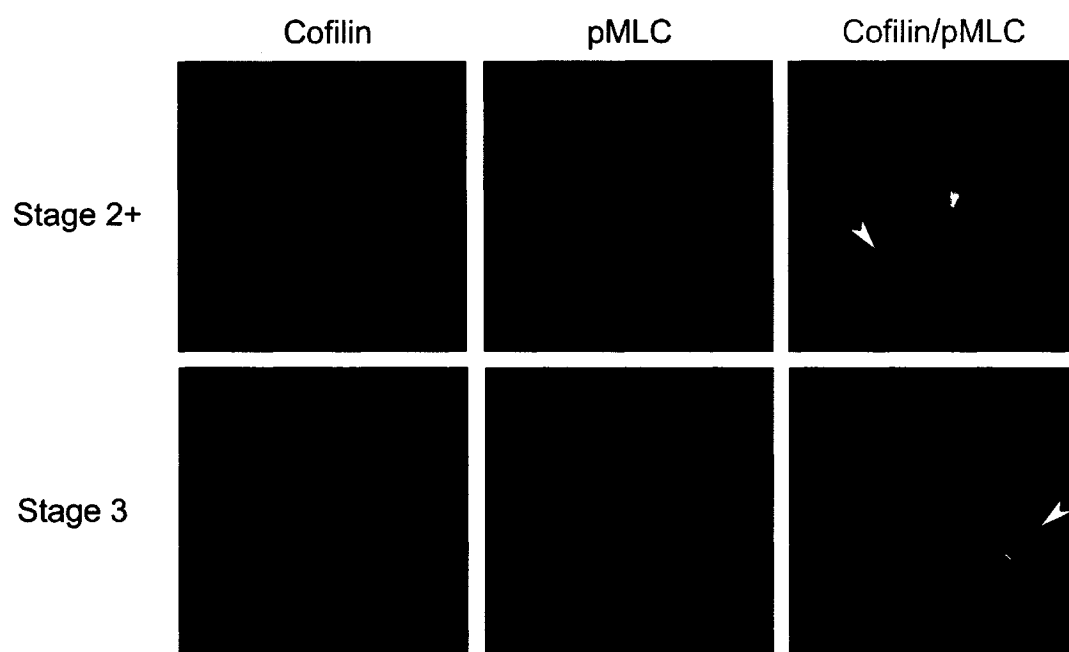


Figure 3.4. Active myosin and active cofilin have distinct localization in the presumptive axonal growth cone of stage 2+ neurons and in the axonal growth cone of stage 3 neurons. Hippocampal neurons at stage 2+ (first row; third row) and stage 3 (second row; bottom row) of development were fixed and stained with antibodies against total myosin heavy chain (top two rows; left column), phosphorylated myosin light chain (top two rows; middle column), total cofilin (bottom two rows, left column) and phosphorylated ADF/cofilin (pAC) (bottom two rows, middle column) . The ratio of the total myosin heavy chain to the pMLC reflects the relative levels and localization of active myosin using a pseudocolor intensity scale (top two rows; right column). Note that myosin activity is punctate throughout the growth cone but higher towards the central domain and in the neurite shafts (arrows). The ratio of the total cofilin to the pAC reflects the relative levels and localization of active cofilin using a pseudocolor intensity scale (top two rows; right column). Note that cofilin activity localized to the peripheral growth cone of both stage 2+ and stage 3 (arrows). Scale bar: 20 μ m.

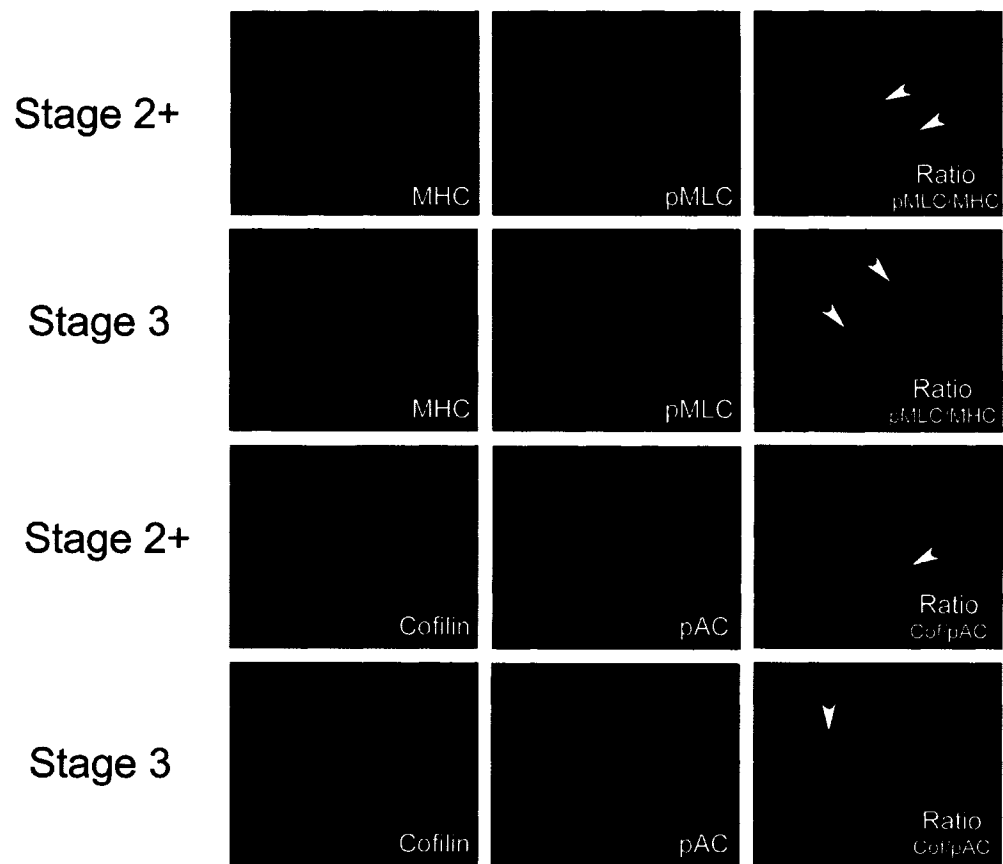
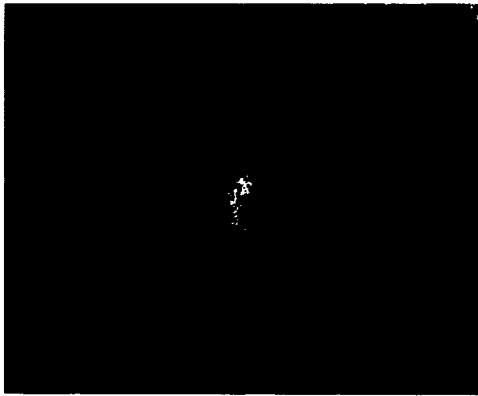


Figure 3.5. Active myosin and active cofilin have distinct localization in the presumptive axonal growth cone of stage 2+ neurons. Images of magnified views of growth cones of Hippocampal neurons at stage 2+. The active myosin image was generated by taking the ratio of staining of phosphorylated myosin light chain (pMLC) to actin staining with phalloidin. The ratio of pMLC to actin should convey the “hot spots” of myosin activity since myosin activity is defined by its association with actin (thus a higher level of pMLC relative to actin would indicate higher activity). A pseudocolor intensity scale reflects the relative levels and localization of active myosin (left). Note that myosin activity is highest in the proximal growth cone using this method. The ratio of the total cofilin to the pAC reflects the relative levels and localization of active cofilin using a pseudocolor intensity scale (right). Note that cofilin activity localized to the peripheral growth cone. Scale bar: 10 μ m.

Stage 2-3 Growth Cone



Active Myosin



Active Cofilin

Figure 3.6. Increasing inhibition of myosin II with blebbistatin is directly correlated to increasing axonogenesis. (A) Examples of neurons treated with DMSO (vehicle control), 100nM, 500nM, 2.5 μ M, and 25 μ M blebbistatin. Neurons were co-stained for actin with phalloidin (green) and the axonal marker Tau-1 (red). Note that control cells typically have one axon and that increases in blebbistatin concentrations have corresponding increases in neurite length and in the presence of supernumerary axons.

(B) Quantification of polarity phenotypes indicates effects of increasing concentrations of blebbistatin on polarity phenotypes (n>60 neurons from 2 experiments for each, except 50nM concentration, where n = 45 neurons, 1 experiment). The quantifications are as follows: DMSO: no axon = 16.4 \pm 6.6%, one axon = 73 \pm 4.1%, multiple axons = 10.53 \pm 5.5%; 50nM: no axon = 12.8%, one axon = 68.1%, multiple axons = 19%; 100nM no axon = 8.2 \pm 0.1%, one axon = 68.5 \pm 2.5%, multiple axons = 23.3 \pm 2.4%; 250nM: no axon = 6.35 \pm 2.3%, one axon = 62.25 \pm 2.5%, multiple axons = 31.4 \pm 4.8%; 500nM: no axon = 2.2 \pm 0.3%, one axon = 62.15 \pm 8.7%, multiple axons = 40.5 \pm 1.3%; 1 μ M no axon = 4.6 \pm 2.8%, one axon = 59.9 \pm 2.5%, multiple axons = 35.6 \pm 4.8%; 2.5 μ M no axon = 5.8 \pm 1.4%, one axon = 45.2 \pm 2%, multiple axons = 49 \pm 1.6%; 5 μ M no axon = 5.4 \pm 1.9%, one axon = 30.2 \pm 8.2%, multiple axons = 64.5 \pm 6.3%; 10 μ M no axon = 5.6 \pm 0.4%, one axon = 22.3 \pm 1.7%, multiple axons = 72.2 \pm 2.2%; 25 μ M no axon = 2.7 \pm 3.8%, one axon = 16.6 \pm 3.3%, multiple axons = 80.7 \pm 7.1%.

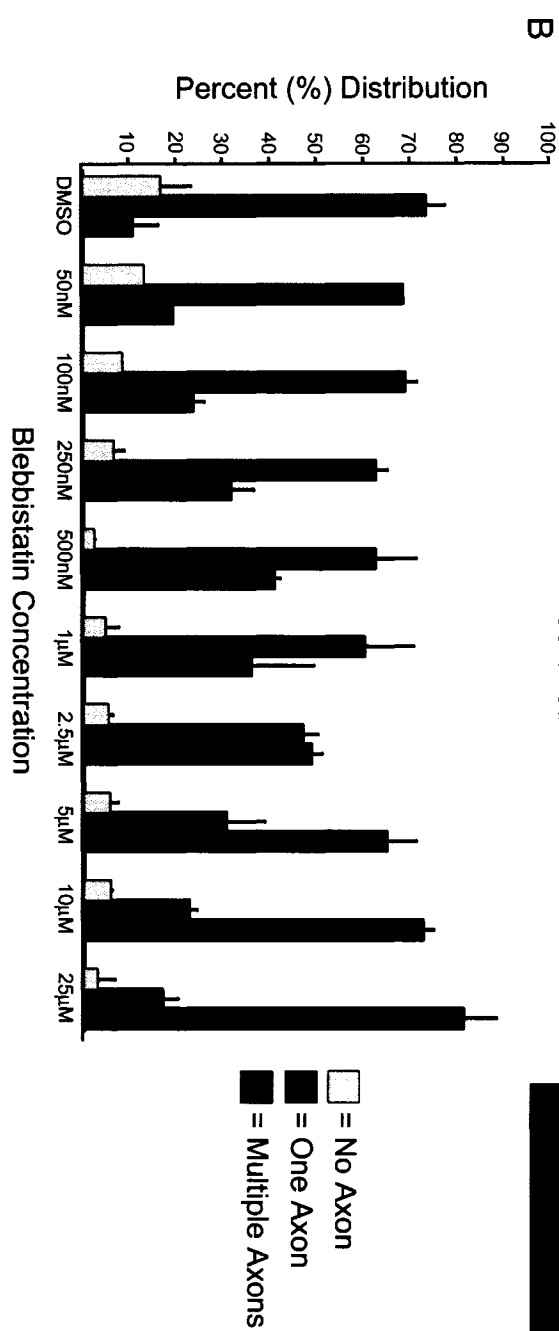
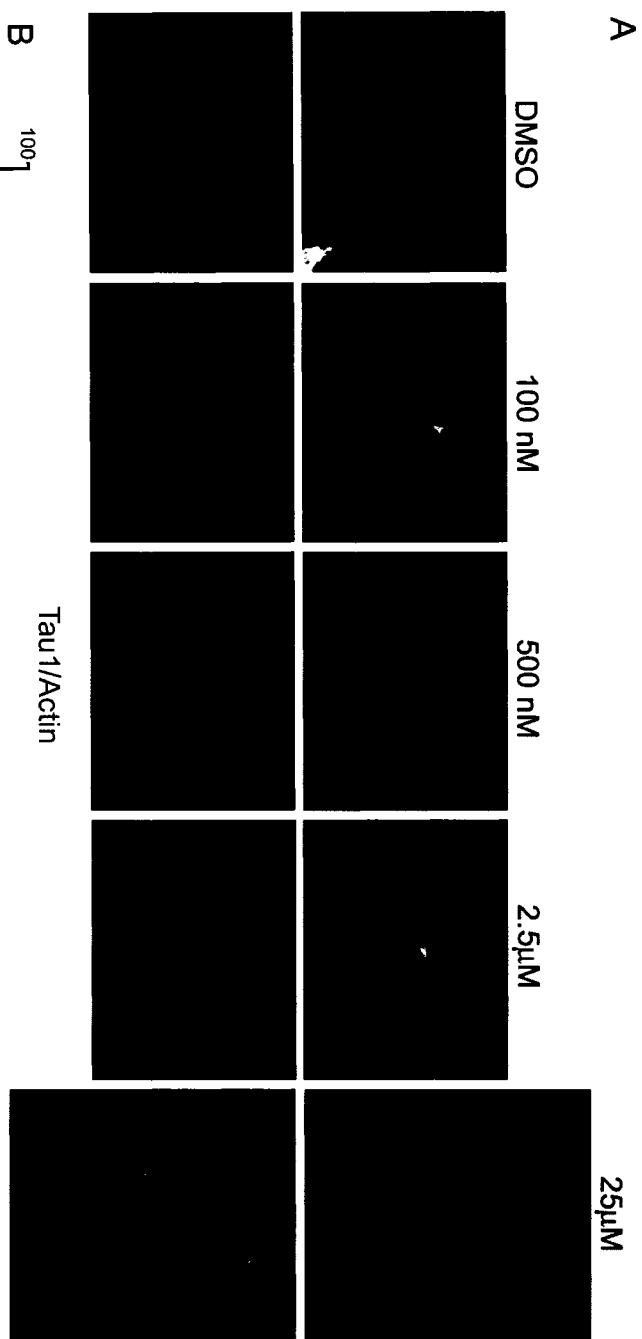
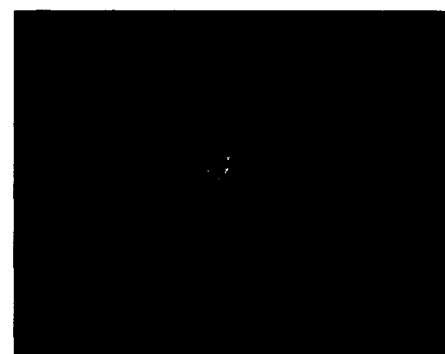
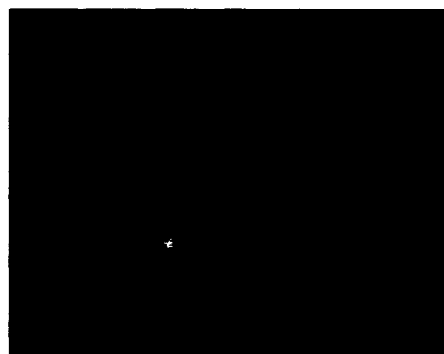
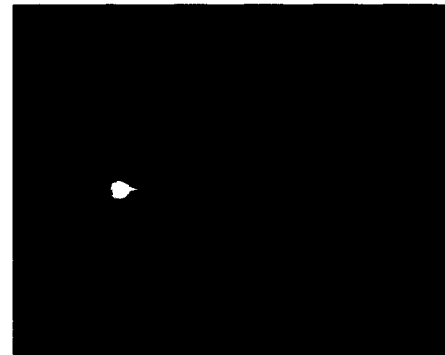
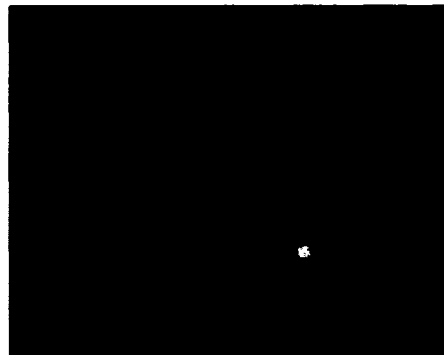
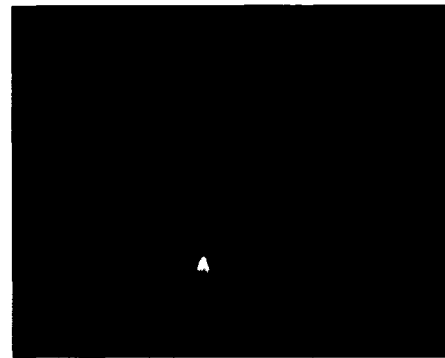


Figure 3.7. Myosin II inhibition results in increased neurite branching. Examples of control neurons treated with DMSO (left column) and neurons treated with 5-25 μ M blebbistatin (right column). Neurons were co-stained for actin with phalloidin (green) and the axonal marker Tau1 (red). Note that control cells typically have one axon and minimal branching. Neurons treated with blebbistatin have much more elaborate arbors, especially on Tau-1 positive axons.

Control

Blebbistatin



Tau1/Actin

Figure 3.8. Blebbistatin has rapid effects on neurite elongation and branching. 2.5 μ M blebbistatin was added to neuronal cultures and live-cell DIC images were acquired. Over a three hour period, control neurons only exhibit a small increase in the outgrowth of the longest process (top row, white arrow, $\sim 10\mu\text{m}/3\text{hrs}$). Neurons treated with blebbistatin have more robust outgrowth and increased branch growth (middle and bottom row). In some cases, only the longest process increases in outgrowth (middle row, white arrow, $\sim 30\mu\text{m}/3\text{hrs}$). Other neurons exhibit robust outgrowth of multiple neurites (bottom row, white arrows, in between $30\text{-}50\mu\text{m}/3\text{hrs}$). In blebbistatin treated neurons, growth of neurite branches is also evident (red arrows) (see Movie 3.1 and 3.2).

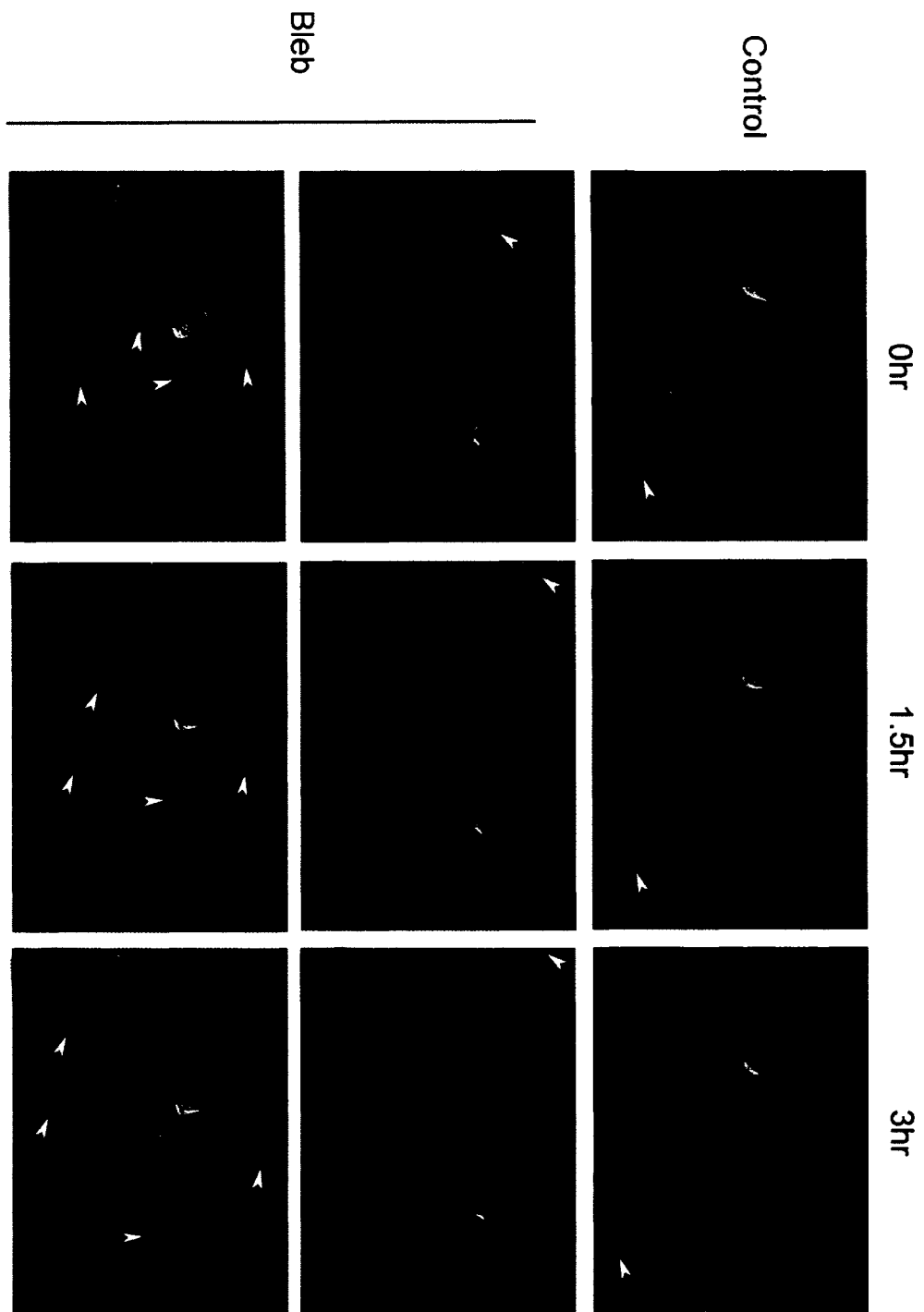
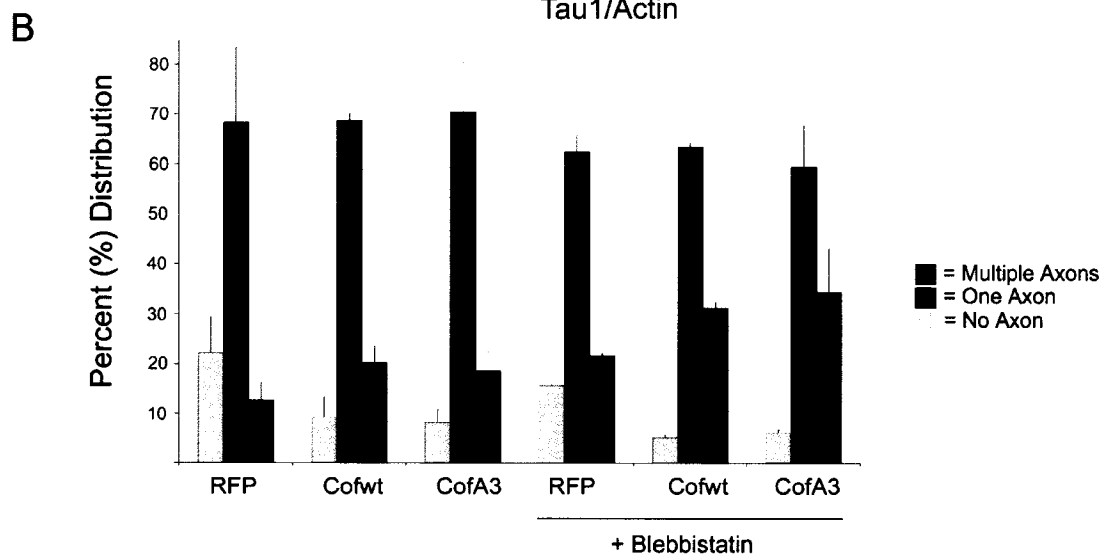
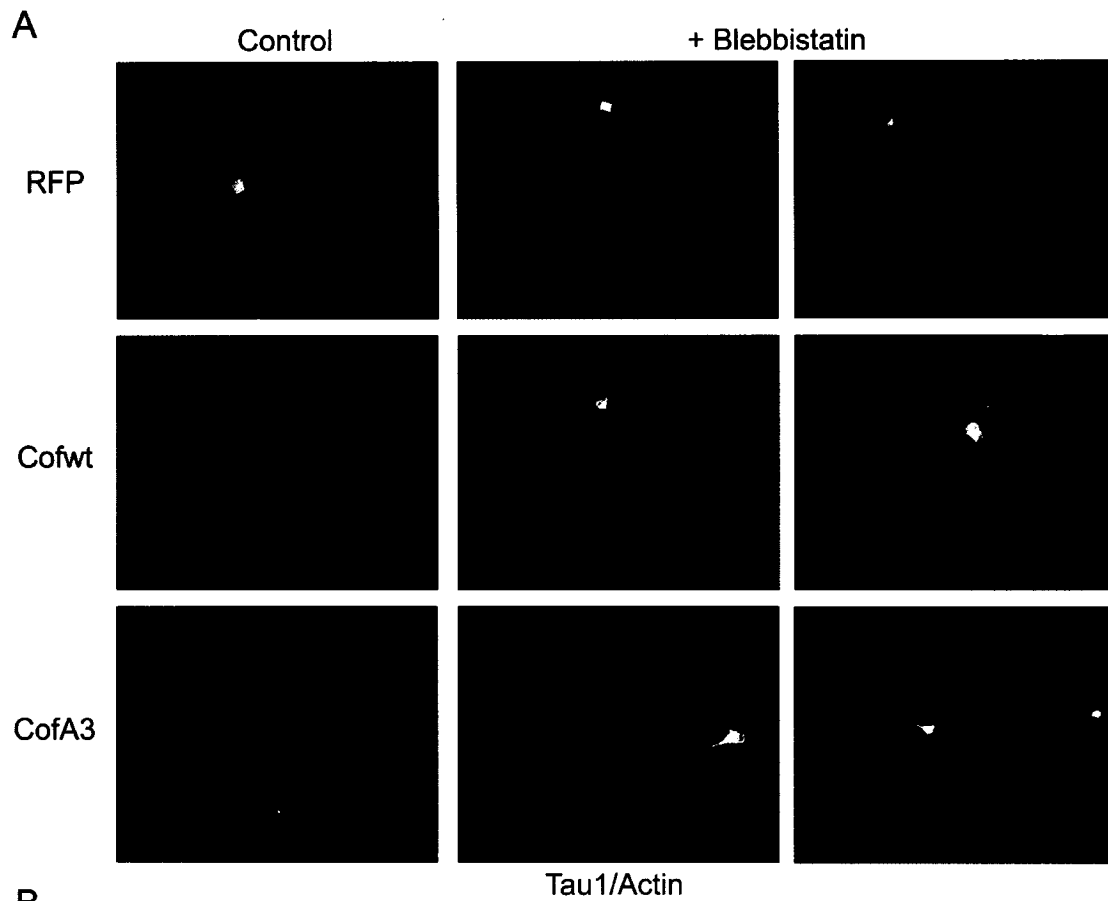


Figure 3.9. Cofilin over-expression and myosin inactivation have a synergistic effect on axonogenesis. (A) Examples of neurons expressing RFP (control, top row), wildtype cofilin (Cofwt, middle row) and active cofilin (CofA3, bottom row). Neurons were co-stained for actin with phalloidin (green) and the axonal marker Tau1 (red). Control neurons typically have one axon (left) and Blebbistatin treatment typically resulted in increased axon length (right). Neurons expressing cofwt and cofA3 typically have one long axon (left). Blebbistatin treatment enhances axon length (middle column) as well as increases the presence of supernumerary axons (right column). (B) Quantification of polarity phenotypes indicates effects of different treatments on neuronal development. RFP expressing neurons have 22.3±7.1% of neurons with no axon, 68.3±15.1% of neurons with one axon, and 12.7±3.4% with multiple axons. Cofwt and CofA3 expression alone marginally increases the presence of multiple axons (20.3±3.2% and 18.75%, respectively) and decreases the percentage of neurons with no axon (9.3±4% and 8.25±2.5%, respectively). In these experiments, blebbistatin treatment in RFP control neurons also has a marginal effect on axonogenesis (15.75±3.18% with no axon, 62.45±3.5% with one axon, and 21.8±0.3% with multiple axons). In conjunction with Blebbistatin, neurons expressing cofwt and cofA3 have an increased percentage of neurons with multiple axons (31.3±0.99% and 34.4±8.6%, respectively) and a decreased percentage of neurons with no axons (5.25±0.4% and 6.25±0.4%, respectively). For these experiments, n > 60 neurons from 2 experiments.



axonogenesis. Since myosin activity was increased and cofilin activity was dampened in neurons lacking *cdc42*, we sought to determine if the myosin inhibition in conjunction with cofilin activation would rescue polarity deficits in *cdc42* KO neurons. We used low levels of blebbistatin in conjunction with the expression of active cofilin (*cofA3*) to determine if polarity could be rescued in *cdc42* KO neurons (Figure 13). In these experiments, we observed that neither myosin inhibition nor *cofA3* expression increased the percent of neurons presenting a polarized phenotype. However, the combination of *cofA3* expression and myosin inhibition increased the percent of neurons with an axon from 35% in control *cdc42* KO neurons to 51%. Although not a complete rescue, the results are significant and suggested that myosin II and cofilin were two important players downstream of *cdc42* during the establishment of neuronal polarity. This implied that some coordinated regulation of these two actin binding proteins were necessary for optimal axon formation.

Discussion

At the leading edge of motile cells two distinct, though spatially overlapping, populations of actin filaments have been identified based on their different rates of movements in the actin retrograde flow (Ponti et al., 2004). Recent evidence has led to models whereby the binding of tropomyosins organize distinct actin structures in cells by antagonizing the binding of some actin-binding proteins while facilitating the binding of others (Delorme et al., 2007; Pak et al., 2008). For example, the binding of some isoforms of tropomyosin to actin competes with cofilin binding (Bernstein and Bamburg, 1982; Bryce et al., 2003), but sanctions the binding of myosin II (Bryce et al., 2003). Although not yet demonstrated in growth cones, the expression of different isoforms of tropomyosin regulate growth cone size and shape as well as the recruitment of myosin IIB (Schevzov et al., 2005). Thus, cofilin and myosin II may bind to and define distinct actin structures in growth cones. In support of this view, studies in *aplysia* growth cones have revealed two distinct regions of retrograde actin movements which could reflect two distinct actin structures in growth cones (Schaefer et al., 2002); perhaps one is bound by cofilin and the other bound by myosin II (and certain tropomyosins). The different actin structures bound by cofilin and myosin II are undergoing

different dynamic reorganizations: for cofilin-bound actin, filaments are undergoing severing, depolymerization and rapid turnover while myosin decorated filaments are undergoing contraction, compression and realignments. Conceivably, the balance between these the activity of myosin and cofilin may provide the controlled driving thrust underlying growth cone motility necessary for axon formation.

Myosin and cofilin expression and localization in developing neurons

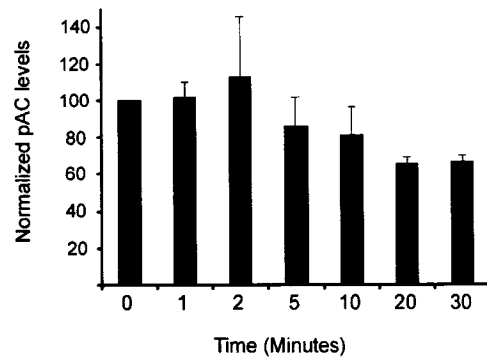
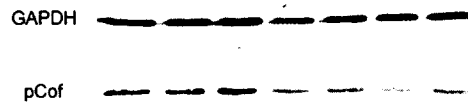
The major source of regulation for both myosin and cofilin is phosphorylation, although the results of this posttranslational modification on protein activity are opposite for these proteins. Unphosphorylated cofilin is active, binding to and severing actin filaments. Upon phosphorylation on Ser3, cofilin loses its ability to bind actin, thereby deactivating it (Bamburg, 1999). The converse is true of myosin, which is phosphorylated at Ser19 of the regulatory myosin light chain (MLC) (Schmidt et al., 2002). This phosphorylation activates the actin-binding activity of myosin and induces conformational changes permitting the formation of bipolar filaments (Suzuki et al., 1978). Thus, reference to the activity of these actin binding proteins also signifies the phosphorylation of their phosphorylation state.

In neurons undergoing axon formation, cofilin is localized throughout the peripheral domain of the axonal growth cone but is more active (looking at the ratio of total cofilin/ pcofilin) specifically near the leading edge (Figure 4). On the other hand, active myosin II is localized in neurite shaft of the neurites, and in the central domain of the growth cones. The intermittent staining of active myosin throughout the growth cone could represent sights of focal adhesion or regions of tropomyosin-bound actin structures. These data supports the notion that there are distinct actin networks in growth cones. Myosin II phosphorylation remains low in the axonal growth cone, but high in the axonal shaft in neurons until axonogenesis is nearly complete.

The level of phosphorylated myosin light chain increases dramatically after axonogenesis occurs. At time-points corresponding to early stages of neurite development (stage 2) and axonogenesis (stage 3), pMLC levels are low but at time-points corresponding to dendritic development and attenuations in axon growth (Stage 4), the level of pMLC

Figure 3.10. IGF-1 alters cofilin and myosin II activity. (A) IGF-1 (25ng/ml) treatment of cortical neurons has a time dependent effect of Cofilin phosphorylation. Representative western blot shows changes in phosphorylated Cofilin (pCof) and constant levels of GAPDH. Graph shows quantification of two experiments of p-Cofilin levels (relative to GAPDH) at time intervals normalized to time-point 0. The changes to pCofilin levels are: 1 minute = $101.55 \pm 8.6\%$; 2 minutes = $112.75 \pm 32.7\%$; 5 minutes = $85.79 \pm 15.8\%$; 10 minutes = $80.75 \pm 15.7\%$; 20 minutes = $65.045 \pm 4.16\%$; 30 minutes = $66.39 \pm 3.55\%$. (B) IGF-1 (25ng/ml) treatment of cortical neurons has a time dependent effect of myosin regulatory light chain phosphorylation (pMLC). Representative western blot shows changes in pMLC and constant levels of GAPDH, which was used as a loading control. Graph shows quantification of one experiments pMLC levels (relative to GAPDH) at time intervals normalized to time-point 0. The changes to pMLC are as follows: 1 minute = 86.5% ; 2 minutes = 114.1% ; 5 minutes = 137.7% ; 10 minutes = 90.5% ; 20 minutes = 75.9% ; 30 minutes = 65% .

A



B

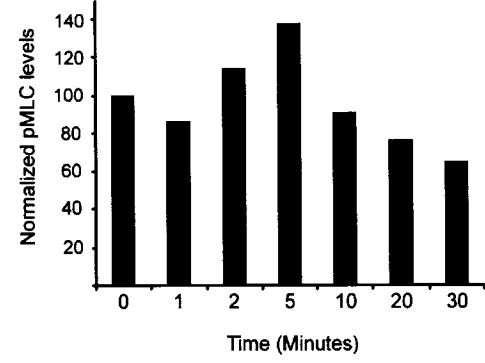
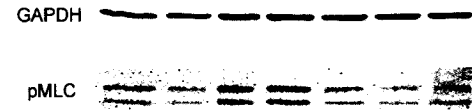


Figure 3.11. ROCK inhibition affects cofilin and myosin activity. Cortical neuron cultures (4 div) were treated with the ROCK inhibitor Y27632 (0.2 μ M) for 30 minutes and protein extracts were harvested. **(A)** Western blot shows the levels of cofilin and phosphorylated ADF and cofilin (pAC, top band is pcofilin and bottom is pADF) in extracts from neurons treated with vehicle (H₂O) and Y27632. Note the decrease in pAC levels in the Y27632 treated sample. **(B)** Quantification of the ratio of cofilin/pAC indicates that there is a 3.3 ± 0.7 fold increase in the levels of active cofilin in neurons treated with Y27632 compared to H₂O treated neurons (n=2). **(C)** Western blot shows the levels of GAPDH (loading control) and phosphorylated myosin light chain (pMLC) in extracts from neurons treated with vehicle (H₂O) and Y27632. Note the decrease in pMLC levels in the Y27632 treated sample. **(D)** Quantification of the ratio of pMLC normalized to GAPDH indicates that there is a 0.15 fold decrease in the levels of active myosin in neurons treated with Y27632 compared to H₂O treated neurons (n=1).

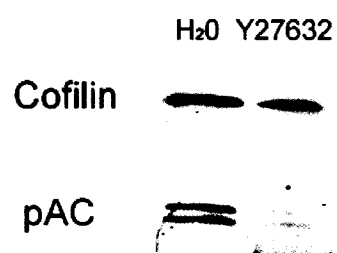
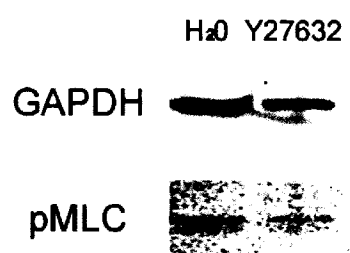
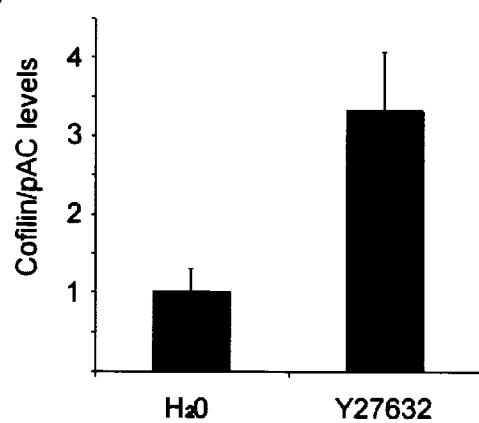
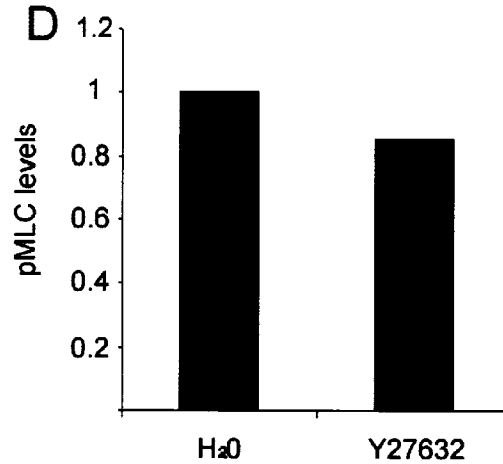
A**C****B****D**

Figure 3.12. Myosin II activity is increased in cdc42 KO brain. Brains from E17.5 wildtype and cdc42 KO brain was examined for the level of phosphorylated myosin light chain (pMLC). (A) Western blot shows the levels of GAPDH (loading control) and pMLC in wildtype and cdc42 KO brain. Note the increased level of pMLC in the cdc42 KO brain. (B) Quantification of pMLC levels normalized to GAPDH indicates that there is a 2.19 ± 0.13 increase in pMLC in cdc42 KO brain compared to wild-type brain (n=3).

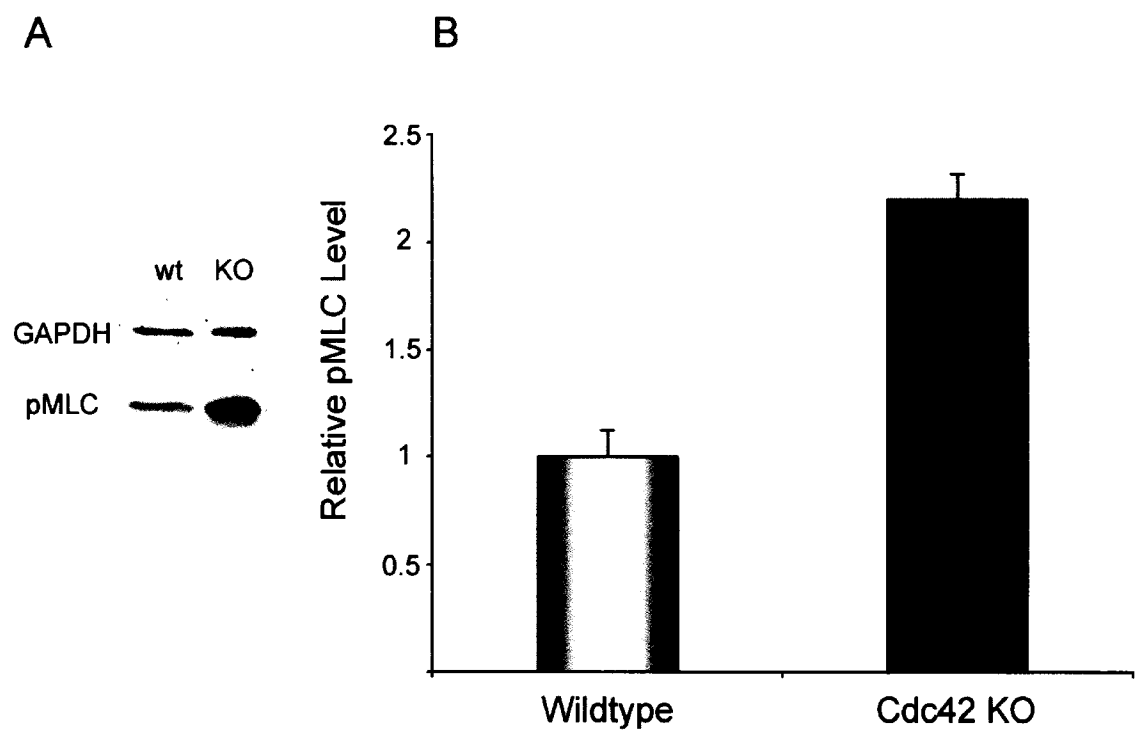
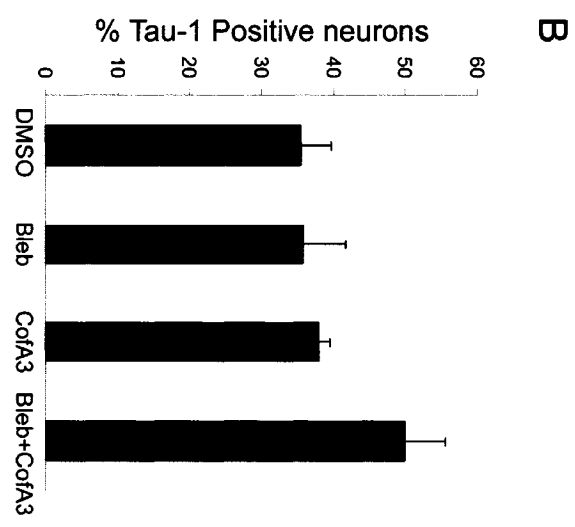
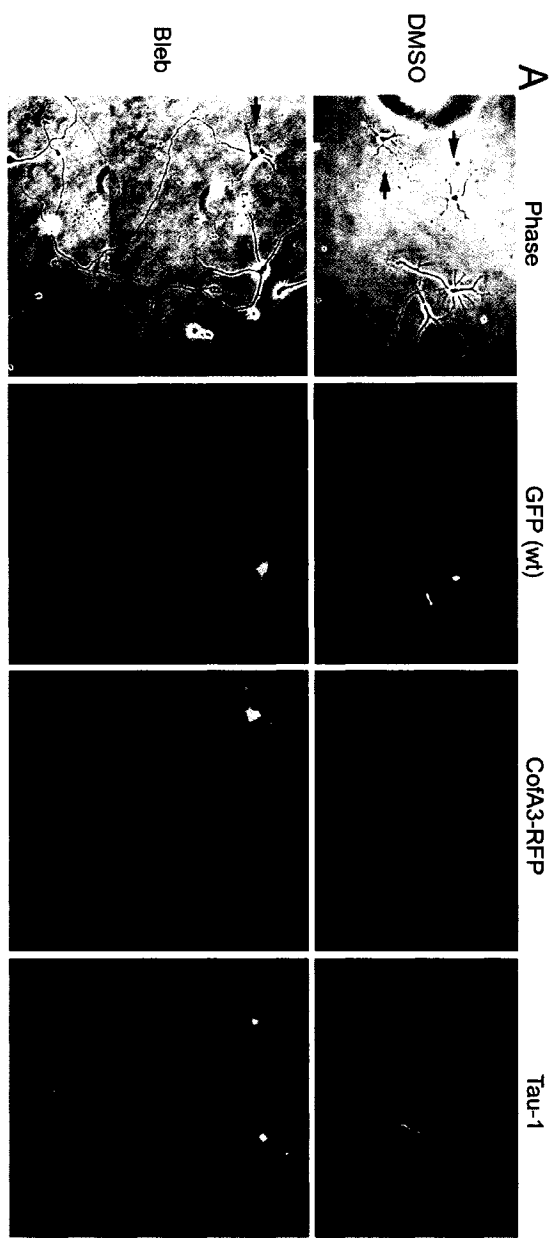


Figure 3.13. Myosin inactivation and cofilin activation rescue axon formation in *cdc42* KOs. (A) Hippocampal neurons from *Cdc42* knockout E16.5 embryos were plated with wild type hippocampal neurons from E16.5 embryos, ubiquitously expressing enhanced green fluorescent protein (GFP) (see Garvalov et al., 2007), resulting in mixed cultures of GFP-positive wild-type neurons and GFP-negative *Cdc42* knockout neurons. Phase images show that *cdc42* KO neurons typically project shorter processes in control conditions treated with DMSO (top row, left; arrow). Wild type neurons (GFP) in the same culture have Tau-1 positive axons (right panel). In the presence of low levels of blebbistatin (bottom row) in conjunction with active cofilin expression (CofA3-RFP) *cdc42* KO neurons (left panel, arrow) extend a Tau-1 positive axon (left). (B) Quantification of the percentage of *cdc42* neurons with Tau-1 positive neurons under different conditions. Control neurons (DMSO) have 35±4.9% with axons. Blebbistatin treatment and CofA3 expression do not increase the percentage of *cdc42* neurons with axons (35.5±6.1% and 37.8±2.1%, respectively). *Cdc42* KO neurons expressing CofA3 treated with Blebbistatin increases the percentage of neurons with axons to 51±4.6%. (n > 65 neurons for each conditions, 2 coverslips).



increases dramatically, about 60 fold the levels of pMLC expressed the first day in culture. Cofilin activity shows the opposite trend but does not change as robustly as the pMLC levels. At time-points in culture corresponding to stage 2 and stage 3, cofilin activity is high, and at stage 4, there was a 50-60% decrease in cofilin activity. The position active myosin II in neurons is also particularly interesting. The high levels of pMLC in the proximal growth cones and neurite shafts suggest a role for myosin activity in growth cone consolidation and maintaining the cylindrical structure via a contractile actin cortical network. The enhancement of branching by blebbistatin and the up-regulation of myosin II activity during stage 4, suggest a role for myosin II in this process.

We also have evidence that expression tropomyosin isoforms increase over the course of neuronal development, corresponding to the increases in active myosin II (data not shown). This could reflect the organizational role of tropomyosins in defining actin structures in neurons and facilitating the increased association of myosin II to actin (Schevzov et al., 2005). Increased myosin II activation may become particularly important later in neuronal development, when myosin may play an active role in maintaining neurite integrity and in restricting neurite arborization.

Effects of myosin inhibition and cofilin activation on neuronal polarity

Myosins have been implicated in various aspects of neuronal development dependent on changes in the actin cytoskeleton including neuronal migration, process outgrowth, and growth cone motility (reviewed in Brown and Bridgman, 2003a, b). Inhibition of myosin with the general myosin ATPase inhibitor, 2,3-butanedione-2-monoxime (BDM) (an inhibitor notorious for off-target effects) in *Aplysia* neurons resulted in a loss of retrograde actin flow (Lin et al., 1996). Neurons isolated from the myosin IIB knockout mouse, which is embryonic lethal, had decreased neurite outgrowth, altered growth cone motility, and the growth cones had abnormal actin bundles in more proximal regions, but not in peripheral filopodia (Bridgman et al., 2001). Interestingly, retrograde F-actin flow in growth cones lacking myosin IIB was increased, presumably do to the enhanced role of myosin IIA in retrograde F-actin flow (Brown and Bridgman, 2002). Thus, in neurons lacking myosin IIB,

there is a correlation with increased retrograde F-actin flow and decreased neurite outgrowth. This could be explained, at least partly, by the inhibitory effect of the actin network on rapid microtubule extension, the driving force underlying neurite growth.

The role of myosins in axon formation has been recently addressed in hippocampal neurons using the myosin ATPase inhibitor, BDM (Kim and Chang, 2004). Treatment of cells with BDM results in neurons exhibiting more axon-like processes. However, the nonspecific effects of BDM raise questions regarding these interpretations. Here we used the specific myosin II ATPase inhibitor, blebbistatin, to more clearly address the contribution of myosin II in axon formation. We found that with increasing concentrations of blebbistatin there is a corresponding increase in the percent of neurons exhibiting multiple axons as well as the number of axon-like processes per neuron. This suggests that altering the normal activation of one actin regulating protein could alter the “fate” of a neurite into becoming an axon rather than a dendrite. We observed increased microtubules in the growth cones of neurons treated with blebbistatin (data not shown), suggesting that the effects of myosin inhibition have indirect consequences on microtubule polymerization that could underlie increased axonogenesis. Interestingly, others have used blebbistatin and have observed that although neurite lengths increased, there was no increase in the percent of axonogenesis (Gallo, ASCB abstract). Rather, there was an increased differentiation and elongation of developing dendrites. This result could reflect subtle differences in technique or inherent differences in neuronal type investigated: chick forebrain neurons versus rodent hippocampal neurons.

The high levels of pMLC in the neurite proper suggests that myosin II may restrict neurite branching and/or regulate the cylindrical structure of the neurite shaft. With myosin inhibition we observe a substantial increase in neurite branching, particularly in the axon which is where we observe the most intense pMLC staining. Although we did not observe obvious changes in neurite shaft diameter or shape, in many neurons we did observe a considerable increase in shaft filopodial protrusions, which may bolster axonal branching. Thus, myosin II may also function in maintaining cortical actin structures in the shafts of neurites restricting neurite branch formation.

We observe that low levels of blebbistatin increased neurite length, but had a minimal increase in axonogenesis. Since increasing cofilin expression had similar effects on neurite length (Garvalov et al., 2007), we hypothesized that the combined effects of increasing cofilin activity (*via* over-expression) and myosin inactivity would have an additive effect on axon formation. Indeed, we observed that the combination significantly increased the percent of neurons with multiple axon-like processes (Figure 9). These data suggests that cofilin-mediated and myosin-mediated reorganizations of actin structures have opposing effects on axon differentiation. The regulation of both these proteins will facilitate optimal dynamics of the actin cytostructure for axon formation to commence.

Signals that promote axon formation modulate cofilin and myosin activity

There are various extracellular signals that promote axon differentiation and growth. One family of growth factors, the Insulin-like growth factors, promote neurite growth (Martin *et al.*, 1991; Meghani *et al.*, 1993; Haselbacher *et al.*, 1985; Sumantran & Feldman, 1993) and the IGF1-receptor is necessary for axon formation (Sosa et al., 2005). In this study we examined the effects of IGF-1 on cofilin and myosin II activity. With IGF-1 treatments, cofilin and MLC phosphorylation was altered. IGF-1 treatment induces a decrease in cofilin and MLC phosphorylation after 30 minutes, implying that cofilin activity is increased while myosin activity is decreased.

RhoA kinase (ROCK) has been implicated in signaling pathways downstream of various guidance cues that affect axon growth and guidance (Song and Poo, 2001; Gehler et al., 2005; Gallo, 2006). ROCK appears to control ADF/Cofilin activity downstream of BDNF and cdc42 treatment in retinal ganglion cells (Gehler et al., 2005; Chen et al., 2006). In hippocampal neurons, ROCK inhibition leads to the formation of multiple axon-like processes (Kim and Chang, 2004, our unpublished observations). Here we sought to determine if ROCK was upstream of cofilin and myosin in rodent CNS neurons. Treatment of neurons with the ROCK inhibitor Y27632 caused a reduction in both cofilin and MLC phosphorylation. Interestingly, in this study we see that cdc42 is also upstream of myosin II and cofilin activity, but in previous work ROCK activity did not appear altered downstream

of cdc42 (Garvalov et al., 2007), suggesting an independent signaling pathway. However, PAK activity was modulated downstream of cdc42 and could account for the differences in myosin and cofilin activity, since PAK has been shown to be upstream of both of these proteins (Edwards et al., 1999; Sanders et al., 1999; Govek et al., 2005). Importantly, these data suggest that alternative signaling pathways involved in axonogenesis may all converge on these two actin binding proteins.

Cdc42 signaling to cofilin and myosin II is important for axonogenesis

The Rho GTPase, cdc42 is a crucial mediator of the development of neuronal polarity (Schwamborn and Pulchel, 2004; Garvalov et al., 2007). In our previous studies, we observed that a signaling pathway leading to decreased cofilin activity is mis-regulated in the absence of cdc42 (Garvalov et al., 2007). However, active cofilin expression was unable to rescue polarity deficits in cdc42 KO neurons, suggesting that other cdc42 effectors may be crucial for axon determination. Here we observe that pMLC levels are increased (myosin II activity is increased) in the absence of cdc42 (Figure 12). In cdc42 KO brain, we did not find changes in the activity of other actin binding proteins, such as profilin (Garvalov et al., 2007). This suggested that cofilin and myosin II are fundamental cdc42 effectors during axon formation. In order to test this hypothesis, we performed experiments that would elevate cofilin activity and diminish myosin activation. Only 35% of cdc42 KO neurons develop axons compared to over 70% of wildtype neurons (Garvalov et al., 2007). Together, increasing cofilin activation and myosin inactivation resulted in a significant increase in the percent of neurons displaying axons (~50% with an axon), while neither treatment had any effect in isolation. This result implies not only that myosin II and cofilin are essential downstream effectors of cdc42, but also pointed to a synergistic effect of cofilin activation and myosin inactivation during axonogenesis. It is worthy to note that this concept of coordinated regulation of myosin and cofilin has support in other contexts. For example, semaphorin 3A (Sema3A) causes growth cone collapse and neurite retraction in dorsal root ganglion neurons; cofilin and myosin II appear to be crucial for these behaviors, respectively (Aizawa et al., 2001; Gallo, 2006). Rho and ROCK inhibition can reverse both Sema3A

mediated retraction and growth cone collapse (Gallo, 2006). Since cofilin and myosin II are downstream effectors it is likely that the coordinated regulation of these actin-binding proteins is crucial to the overall effects of Sema3A mediated guidance.

Chapter 4

Growth cone-like waves increase growth cone dynamics, transport actin and contribute to axon formation and branching

Preface and Acknowledgements

The work presented in this chapter is in preparation for submission to the journal *Developmental Neurobiology*. The authors are Kevin C. Flynn, Richard Davis, Alisa Shaw and James R. Bamberg. The authors would like to thank Barbara Bernstein, Chi Pak, O'Neil Wiggan, Shay Perea-Boettcher, Frank Bradke and Christian Gonzalez-Billaut for helpful comments and suggestions on the manuscript. Special thanks are extended to Laurie Minamide and Mike Maloney for help with the development of the hippocampal slice culture system. Furthermore, we thank Kristy McClellen, Gabe Knoll, and Stuart Tobet for maintaining colonies of and supplying the Thy1-YFP transgenic mice used in this study. We also thank Robert Wysolmerski for the phospho-myosin light chain antibody and Jennifer Lipponcott-Schwartz for the photoactivable GFP construct. Our deepest gratitude is reserved for Barbara Bernstein, who has patiently assisted with issues arising during live-cell microscopy experiments. We gratefully acknowledge support from the National Institutes of Health, grants NS40371 and DK69408 (J.R.B.), NS43115 (J.R.B. and K.C.F.), and NS48660 (K.C.F.).

Abstract

Axonogenesis requires a shift from the uniform delivery of materials to all neurites to preferentially delivery to the putative axon, supporting its more rapid extension. Waves, growth cone-like structures that propagate down the length of neurite, were shown previously to correlate with neurite growth in cultured hippocampal neurons and have been proposed as transporters of materials that support neurite outgrowth. Here we address the dynamics

of waves, their contribution to axon formation, and their relevance to outgrowth in a normal three dimensional matrix. Waves are similar to growth cones in their structure, composition and dynamics. In neurons undergoing axonogenesis, waves occur in all minor processes, but occur more frequently in the future axon. Molecules associated with axon development, including actin, localize to waves and are transported in wave structures, clearly demonstrating that waves represent a mechanism for actin transport. Wave frequency increases in neurons treated with stimuli that enhance axonogenesis. Wave transport actin and associated proteins and their arrival at the growth cone is coincident with increased dynamics. Waves occur along neurons in organotypic hippocampal slices where they have been observed propagating down growing mossy fiber axons. Taken together, our results indicate that waves contribute to axonogenesis via the transport of actin and by increasing growth cone dynamics.

Introduction

Neurons face unique challenges during development. After terminal differentiation they form neurites which then grow, arborize, and react to environmental cues to form complex synaptic connections. During their development, the extending neurites are initially similar, but then acquire different identities becoming either axons or dendrites. The acquisition of a polarized phenotype is necessary to the functional properties of a mature neuron and central to the operation of the nervous system at large. Hippocampal neurons in culture have served as a model for many aspects of development including neurite initiation, neurite growth, arborization, and the development of polarity (Craig and Banker, 1994; DaSilva and Dotti, 2002). Recently it has become clear that axon specification involves the modulation of actin filaments and microtubules, as well as the regulation of cellular transport (reviewed in Horton and Elhers, 2003, Arimura and Kaibuchi, 2007).

Intracellular transport changes during neuronal development. In stage 2 hippocampal neurons transport is apparently indiscriminate, with relatively uniform transport occurring in all the minor processes. Later, during the stage 2-3 transition during which axon

specification and growth occur, there is a specific increase in anterograde transport into the presumptive axon leading to the accumulation of organelles, ribosomes, cytosolic proteins and Golgi-derived vesicles, compared to the slower growing minor processes (Bradke and Dotti, 1997). This increase in transport is reflected by an engorgement of the growth cone of the emergent axon (Bradke and Dotti, 1997; Kunda et al., 2001), which also shows increased dynamics (Bradke and Dotti, 1999). Accumulating in the presumptive axon are proteins that impact the development of neuronal polarity and include Par3/Par6 (Shi et al., 2003) cdc42, Rap1B (Schwamborn and Pulchel, 2004), active CRMP 2 (Ignaki et al., 2001), and cofilin (Garvalov et al., 2007). A general increase in transport could contribute to the increase levels of these proteins in the axon, however, other mechanisms such as selective degradation of proteins in minor processes (Schwamborn et al., 2007) and selective association with axon-specific kinesin motors (Jacobson et al., 2006) are also at work. Many of the molecules that localize to the axon are actin-assembly regulatory proteins that contribute to the increased actin turnover, growth cone dynamics and neurite extension that occurs during axonogenesis.

In hippocampal neurons, the axon as well as the dendrites undergoes pulsatile growth, with periodic extensions and retractions. Ruthel and Banker initially identified and characterized another periodic phenomenon they called “waves” which could underlie, at least partially, the pulsatile outgrowth of hippocampal processes (1998, 1999). These studies demonstrated that waves appear similar to growth cones, originate at the soma, travel down the length of axons and dendrites, and are associated with spurts of outgrowth. It was proposed that waves may represent a means for actin transport since they travel at a speed consistent with slow component b (SCb) of axonal transport ($\sim 3 \mu\text{m}/\text{min}$), which has been proposed to be rate limiting for neurite growth (Wujek and Lasek, 1983; McQuarrie and Jacob, 1991). Thus waves may represent one mechanism to supply actin as well as other growth promoting proteins. However, this hypothesis was never directly tested in these studies, nor have the physiological relevance of waves been demonstrated *in vivo*. Furthermore, how the arrival of waves affects early axonogenesis, growth cone dynamics and neurite branching has not been examined.

Here we use time-lapse phase contrast and DIC imaging to characterize wave

behavior and effects on neuronal development. We confirm that waves are indeed similar to growth cones morphologically, but further show that their molecular composition, organization and dynamics are also similar. Waves contain various proteins associated with axon development. Coincident with wave arrival at the tips of neurites induces an increase in growth cone size and dynamics. Waves occur in all processes in stage 2 neurons but become more frequent in presumptive axons during the stage 2-3 transition and increase or decrease in frequency with treatments that, respectively, enhance or inhibit axonogenesis. Waves were observed along DiI or GFP-expressing neurons in organotypic hippocampal slices. In addition, the arrival of waves is often associated with engorgement of filopodia to create branch points. However, many neurons are found to polarize and grow without visible wave structures. The implications from these studies are that waves are not necessary for neuronal development, but when they occur they are physiologically relevant structures, contributing to neuronal development and axon growth by transporting actin and actin-regulating proteins, increasing growth cone dynamics and enhancing branching..

Materials and Methods

Neuronal Cell Culture: Rat and mouse hippocampal neurons were dissected and frozen from E18 and E16 brains respectively as previously described (Meberg and Miller, 2003). Cells were plated at densities ranging from 85-200 cells/mm² and cultured for 1-5 days, depending on the particular experiment. Cdc42 null hippocampal neurons were co-cultured with wild-type GFP expressing neurons as previously described (Garvalov et al., 2007). The neurons were cultured on poly-d-lysine (Sigma) coated glass coverslips in neurobasal (Gibco) supplemented with B-27 (Invitrogen, San Diego, CA) and glutamine (Minamide et al., 2000). In some experiments neurons were plated on polylysine/laminin (10mg/ml).

Adenoviral Infections: Replication deficient adenoviruses were produced (for details see Minamide et al., 2003) and used for transgene expression in neuronal cultures essentially as described (Garvalov et al., 2007). Briefly, neuronal culture medium was changed to Neurobasal/B27/glutamine + 5% hyclone FBS 2-4 h post-plating. The neurons were

infected with adenovirus at multiplicity of infections (MOI's) ranging from 150-400. Approximately half of the virus containing medium was removed 2 h later and fresh neurobasal/B27/glutamine was added. The viruses used in these studies include wild-type and nonphosphorylatable (active, S3A) human cofilin constructs fused to Red Fluorescent protein (RFP). An adenovirus containing the neuron-specific enolase promoter (NSE) driving cofilin expression was also used for live-cell imaging experiments. Beta-actin fused at its C-terminus to mRFP, GFP or a photo-activable GFP (kind gift of Jennifer Lippincott-Schwartz, National Institute of Health) were also used to visualize actin in live cells. For infections of slice preparations, adenoviral volumes for optimal infection were empirically determined (we estimate MOIs of 100-300). A volume of virus was added directly onto the slices grown on membrane inserts in 6-well plates, incubated for 2-3 h, and then removed and added to the underlying medium. Slices were prepared for time-lapse imaging 2-4 days post-infection (see below).

Immunocytochemistry: All neurons were fixed 30 min at 37°C in 4% paraformaldehyde in cytoskeletal preservation buffer (10 mM MES pH 6.1, 138 mM KCl, 3 mM MgCl₂, 10 mM EGTA, and 0.32 M sucrose). Cells were washed 3x in Phosphate Buffered Saline (PBS) and permeabilized in 0.5% Triton X-100 for 5 min. After blocking for 1 h in 1% Bovine Serum Albumin (BSA) and 2% goat serum in PBS, cells were immunostained with various antibodies. The following commercial primary antibodies were used: Tau1 (1:1000, Chemicon), β -tubulin (1:300, Sigma), Rap1 (1:250, BD Biosciences), and Gap43 (1:300, kind gift of M. Zuber), and cdc42 (1:250, Santa Cruz Biotech). Cells were incubated with primary antibodies for 1-2 h at room temperature or overnight at 4° C. For ratio imaging, staining was performed for total cofilin with 14.8 μ g/ml mouse monoclonal antibody (MAb22; Abe et al., 1989) and for phospho-cofilin with 1.1 μ g/ml affinity purified rabbit antibody (Meberg et al., 1998) in blocking buffer at 4 °C overnight. Cultures were then washed in PBS and incubated with secondary antibodies diluted 1:400 in 1% BSA-PBS for 1-2 h. IgG secondary antibodies (Molecular Probes, Eugene, Oregon) used were Fluorescein goat anti-mouse IgG, Texas Red goat anti-rabbit, Alexa 650 goat anti-mouse and Alexa 350 goat anti-mouse (all at 1:400).

Texas Red- or Alexa 488 conjugated phalloidin (1:200) was used to visualize actin filaments. Coverslips were mounted with Prolong Anti-fade (Molecular Probes). Images were acquired with a Nikon (Tokyo, Japan) Diaphot inverted microscope using 20X air (0.75 NA), 40x oil (1.3 NA) and 60X oil (1.4 NA) objectives and a Coolsnap ES CCD camera (Roper Scientific, Tucson, AZ). Metamorph software (Universal Imaging, Westchester, PA) was used for image acquisition and analysis.

Cell treatments: The myosin II inhibitor, blebbistatin (Sigma Aldrich) was dissolved in DMSO at 100 mM and applied to neuronal cultures at final concentrations ranging from 1-5 μ M. For long-term cultures, Blebbistatin was added to growth medium 16 h after plating through the termination of the experiment. The neurotrophin, NT-3 (Adamone Labs, Jerusalem, Israel) was used at a final concentration of 100 ng/ml and added to neuronal cultures 2 h after plating. In some experiments with neurotrophin treatment, neurons were plated on mixed poly-d-lysine-laminin substrate which facilitated increased axon growth compared to poly-d-lysine alone.

Organotypic hippocampal slice cultures: Slice culture of hippocampus was performed essentially as described (Davis et al., submitted). Briefly, postnatal day 0 to 5 Sprague-Dawley rat pups or Thy1-YFP mouse pups (line H, Feng et al., 2000, Jackson laboratory) were sacrificed by decapitation, the brains were isolated in ice-cold Guys Balanced Salt Solution (GBSS), the hind- and mid-brain were removed, and the forebrain was cut into 400 μ m sections using a McLlwain tissue chopper. The brain slices were cultured on 0.4 μ m polyester membranes in 6-well plates (Corning, New York) in 1.7 ml slice medium (2% glucose, MEM, B27, 100 mM glutamax, 10% horse serum). In some cases, DiI crystals (Molecular Probes) were carefully placed in the hilus region of the dentate gyrus essentially as described (Dailey et al, 1994), resulting in labeling of cells in the dentate gyrus as well as mossy fiber tracts (Figure 1). Slices were incubated for 3-48 h at 35° C prior to fixation or live-cell microscopy.

Live-cell microscopy: Live-cell microscopy was performed on an Olympus IX81 microscope equipped with a Yokagawa CSU22 spinning disk confocal head with four diode lasers, AOTF and an EM-CCD cascade II camera (Photometrics). This system also had a humidified, CO₂ regulated chamber which maintained a constant temperature of 37° C. The objectives used include the following: 10x U-Plan Fluorite (0.3 NA), 20x U-Plan Fluorite (0.17 NA) air objectives, UAPO 40X/340W-DIC (1.35 NA), and Plan-APO 60x (1.42 NA) oil objectives. The microscope also had a Lambda LS Xenon illumination source with a separate HQII camera. The system was integrated by Intelligent Imaging Innovations (Denver, CO) and computer controlled using Slidebook Software.

Long-term time-lapse imaging for analysis of wave effects on neuronal development was performed either in drilled out T-25 flasks to which German glass coverslips had been sealed or in 35mm dishes (Corning) to which glass coverslips had been sealed. E16 mouse hippocampal neurons were cultured in neurobasal medium, containing B27 supplement (Invitrogen, San Diego, CA) and 2 mM glutamine, which was pH equilibrated in 5% CO₂ incubator prior to imaging. The T-25 flask was sealed for the duration of the imaging and there was no noticeable change in the pH of the medium over a 72 h period. The 35 mm dishes were used in humidified, CO₂ regulated system at 37° C. Images were acquired every 2.5.-5 min using DIC optics with Slidebook imaging software (Olympus IX81 microscope). For some experiments a phase contrast objective on the heated stage of a Nikon Diaphot microscope equipped with a Metamorph controlled CCD camera was used. Short-term time-lapse experiments were performed under similar conditions as long-term imaging but used exclusively the DIC imaging on the Olympus IX81 with 40X or 60X objectives. Images were taken every 10 s for 5-60 min.

Live-cell fluorescent microscopy was performed on the spinning disc confocal microscope. Diode lasers with 473nm and 563nm peak wavelengths were used for GFP and RFP excitation, respectively. Image acquisition parameters varied depending on the particular experiment and were empirically determined to balance signal intensity and minimize cellular toxicity. Generally, exposure times were within the range of 50-300 ms at intervals of 10 s–2.5 min. In some cases neutral density filters were used to decrease excitation energy.

Adenoviral-mediated expression of photo-activatable-GFP fused to beta-actin required 3-4 d postinfection before photo-activation studies were performed. Activation used a computer-controlled Hg light source (405 nm) under control of the Mosaic Digital Diaphragm system (Photonics instruments). Waves were identified using bright field optics and a selected region encompassing the wave was photo-activated for 1-2 s. Confocal images at 473 nm excitation were then acquired at 30-60 s intervals.

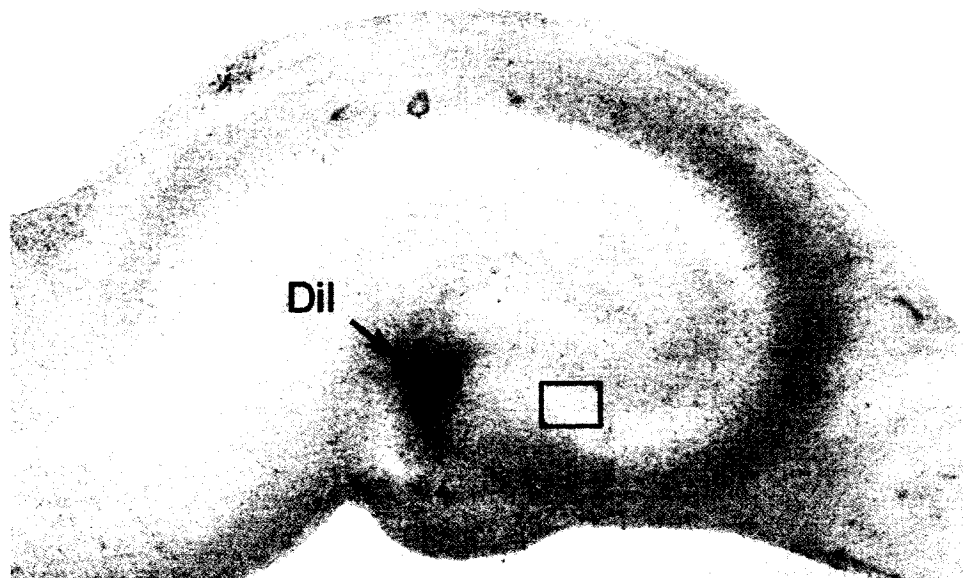
For live-cell imaging of hippocampal slices, an area of the membrane with 1-3 slices adhered was excised and placed slice-side down on a glass bottomed 35 mm dish. The slice was stabilized with a plasma clot made by mixing 20 μ l chick plasma with 6 μ l thrombin. After clot formation, 400-500 μ l of slice medium was added, completely submerging the slices. A 473 and 440 diode lasers were used for fluorescent imaging of DiI and Thy1-YFP labeled neurons, respectively. We were able to maintain for >24 h viable slices with growing neurites and dynamic growth cones. In some cases images were analyzed using Metamorph software.

Morphological analysis of growth cones and waves: Growth cone and wave dynamics were measured from time-lapse DIC images acquired with 40X and 60X oil objectives. We measured the change in area every ten seconds ($\Delta A/10s$) similar to other studies examining growth cone dynamics (Endo et al., 2003). A tiff series stack was compiled using Metamorph software. The growth cone or wave area was outlined at $T=0$ and this outline was then superimposed on the next image of the time sequence and the differential area was measured, providing the change in area for every 10 seconds. The average of a sequence of 10 images was used for each growth cone and wave. Growth cones were characterized as inactive or active depending on their dynamics; inactive growth cones are defined as those with $<12\% \Delta A/10s$ and active growth cones are defined as those with $\geq 12\% \Delta A/10s$.

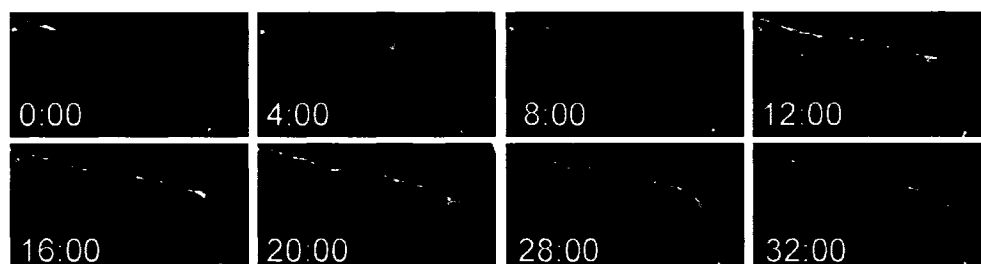
Axons were defined in fixed and immunostained cells as being $\geq 80\mu m$ in length and containing intermediate to high levels of Tau1 immunofluorescence (Schwamborn and Püschel, 2004; Jiang et al., 2005). Neurites with an absence of Tau1 staining were not counted as axons regardless of length. Neurons were counted with multiple axons when they

Figure 4.1. DiI labeling of neurons within an organotypic hippocampal slice. **A.** A low magnification image of a P4 hippocampal slice in culture for 12 h. A crystal of DiI has been placed in the hilus region of the dentate gyrus (arrow). Typically in these experiments imaging proceeds within 2-3 hours of DiI labeling and focuses on the mossy fiber tract (highlighted region) and locally labeled neurons in the dentate gyrus. Slices can be imaged up to 24h following DiI labeling with healthy neurons but in some cases the DiI fluorescence diffuses to surrounding regions. **B.** A time-lapse series of maximum intensity projections of DiI labeled mossy fiber axons (from boxed region in A). Note the axon is tipped with a motile growth cone which advances at $1.7\mu\text{m}/\text{min}$. We rarely observed waves on long axons in slice cultures.

A



B



displayed two or more neurites $\geq 80\mu\text{m}$ in length which contained Tau1 immunofluorescence. Waves were defined in fixed specimens as F-actin rich growth cone-like structures with filopodial and/or lamellipodial features. From our live-cell imaging experiments we observed that the majority ($>80\%$) of such structures were waves. Branches (branch tips) were defined as protrusions off of the primary neurite that were $\geq 20\mu\text{m}$.

In live-imaging studies, axon formation was defined as the moment when one neurite reached $\geq 80\mu\text{m}$ in length and was at least twice as long as the next longest neurite. Measurements of wave frequency were taken over three four hour intervals: stage 2, stage2-3 and stage 3. For the stage 2-3 transition the 4 h flanking (2 h before and 2 h after) axon formation was used for analysis. Neurite growth measurements after wave arrival were performed using Metamorph imaging software. Bursts of outgrowth were measured from the tips of growth cones immediately before to the tips of growth cones 10 minutes following wave arrival.

Results

Molecular composition and dynamics of waves.

Pioneering studies by Ruthel and Banker identified waves as growth cone-like structures containing actin, GAP-43, and cortactin (1998). Here we expand on these observations by characterizing wave motility in short-term time lapse imaging and by immunostaining for various components known to be in growth cones. Our observations from live-cell DIC imaging confirmed that waves travel at an average rate of $\sim 3\mu\text{m}/\text{min}$ as previously reported (Figure 2, Movie 4.1; Ruthel and Banker, 1998). Although the majority of waves observed in this study travel in the anterograde direction (i.e. towards the neurite tips), occasionally retrograde waves were also observed. Whereas anterograde waves are associated with bursts of outgrowth, retrograde waves are associated with a reduction in growth cone size and neurite retractions. Another interesting observation is that as waves approach the distal neurite a retraction precedes the arrival of the wave followed by a burst of outgrowth (Figure 2 and 3A; Ruthel and Banker, 1999). In some cases anterograde waves did not travel the full distance from the soma to the neurite tips, but consolidate into the neurite shaft. In these

situations, waves were not associated with enhanced neurite growth.

Growth cones are hand-like structures with a characteristic compartmentalization; typically they have an F-actin rich peripheral domain with lamellipodia and filopodia and a microtubule-rich central domain (Schaffer and Forscher, 2002; Letourneau 1996) that also can contain organelles such as mitochondria and endoplasmic reticulum. To confirm that waves are similar to growth cones in cytoskeletal organization, we examined them for the presence of actin, microtubules and other growth cone proteins. Waves had a similar composition to growth cones with distinct compartments. The peripheral regions of waves were F-actin rich with lamellipodia and filopodia. The core of the neurite contains bundled microtubules, which splay out into the peripheral regions (Figure 3B) much like microtubules extending from the central domain of growth cones (Figure 4). These data confirm earlier observations of waves showing actin and microtubules as structural components of waves (Ruthel and Banker, 1998). We also observed that ADF/Cofilin, Arp3, Gap43, and the RhoGTPases cdc42 and Rac1, which are typically enriched in axonal growth cones, are also enriched in waves (see below, data not shown). To further confirm the similarity between waves and growth cones, we compared their motility by live-cell DIC imaging. Waves and active growth cones were similar in their motility as determined by comparing the change in total area in ten second intervals over minute durations (Growth cones show $23.5 \pm 7.5\% \Delta A/10s$ and waves show $27.5 \pm 7.3\% \Delta A/10s$). These data together confirm waves are growth cone-like structures in their composition, organization and dynamics.

Waves and Branching

Another important aspect of the development of hippocampal neurons is neurite branching; for example, *in vivo*, CA3 pyramidal neurons have axons that branch into the Schaffer collateral pathway which innervates the CA1 region as well as collaterals towards the dentate gyrus (Gomez-Di Cesare, 1997). We observed that waves were often associated with enhanced neurite arborization. It was previously reported that waves encountering a branch would typically only traverse one branch, which would undergo increased growth, although in some cases waves would concomitantly down both branches (Ruthel and Banker, 1999).

We also observed the preferential translocation of a wave down one arbor at branch points and instances where waves would split at a branch point and concomitantly traverse both arbors and contribute to outgrowth along both branches (Figure 5A). Surprisingly, we also observed waves initiating nascent neurite branches. In these cases, waves arrive at a region of the neurite shaft where a filopodium protrudes and cause elongation and engorgement of this filopodium, giving rise to a new branch point (Figure 5B, Movie 4.2). The propagation of multiple waves in tandem also can influence neurite branch formation and growth (Figure 6). It was observed previously that growth cones can give rise to neurite branches by engorgement of a stabilized filopodia (Dent and Kalil, 2001) and that such a mechanism contributes to growth cone pathfinding at guidepost cells in grasshopper embryos (O'Conner et al., 1990).

Waves are correlated with axonogenesis

Although waves occur in both minor processes and axons of hippocampal neurons with a morphologically distinct axon (stage 3; Ruthel and Banker, 1999), waves have not been studied in relation to axonogenesis during the stage 2 to 3 transition. By following the same neuron over long time periods the process that develops into the axon can be identified and time-lapse movies studied at the earlier stages to see how waves impacted axon development. In neurons preceding axon formation (stage 2), waves occurred in all processes, but they occurred 1.8 fold more frequently in the process that later developed into the axon (Figure 7). At this developmental stage the impact of waves on transient neurite elongation was essentially the same for all minor processes (the impact of waves in the neurite destined to become the axon is 1.1 fold the other processes). As the axon formed (see definition in materials and methods) the wave frequency in the developing axon increased 2.8 fold over the minor neurites (Figure 7B, Movie 4.3). Furthermore, the waves that amalgamated with the growth cones increased outgrowth by 1.5 fold that of the minor neurites. The frequency of waves remained 2.0 fold higher in axons of young stage 3 neurons compared to the minor processes, and the impact of waves on neurite growth remained higher in the axon compared to the minor neurites (1.7 fold). These data show that waves correlate with axon

differentiation and the initial enhancement of neurite outgrowth.

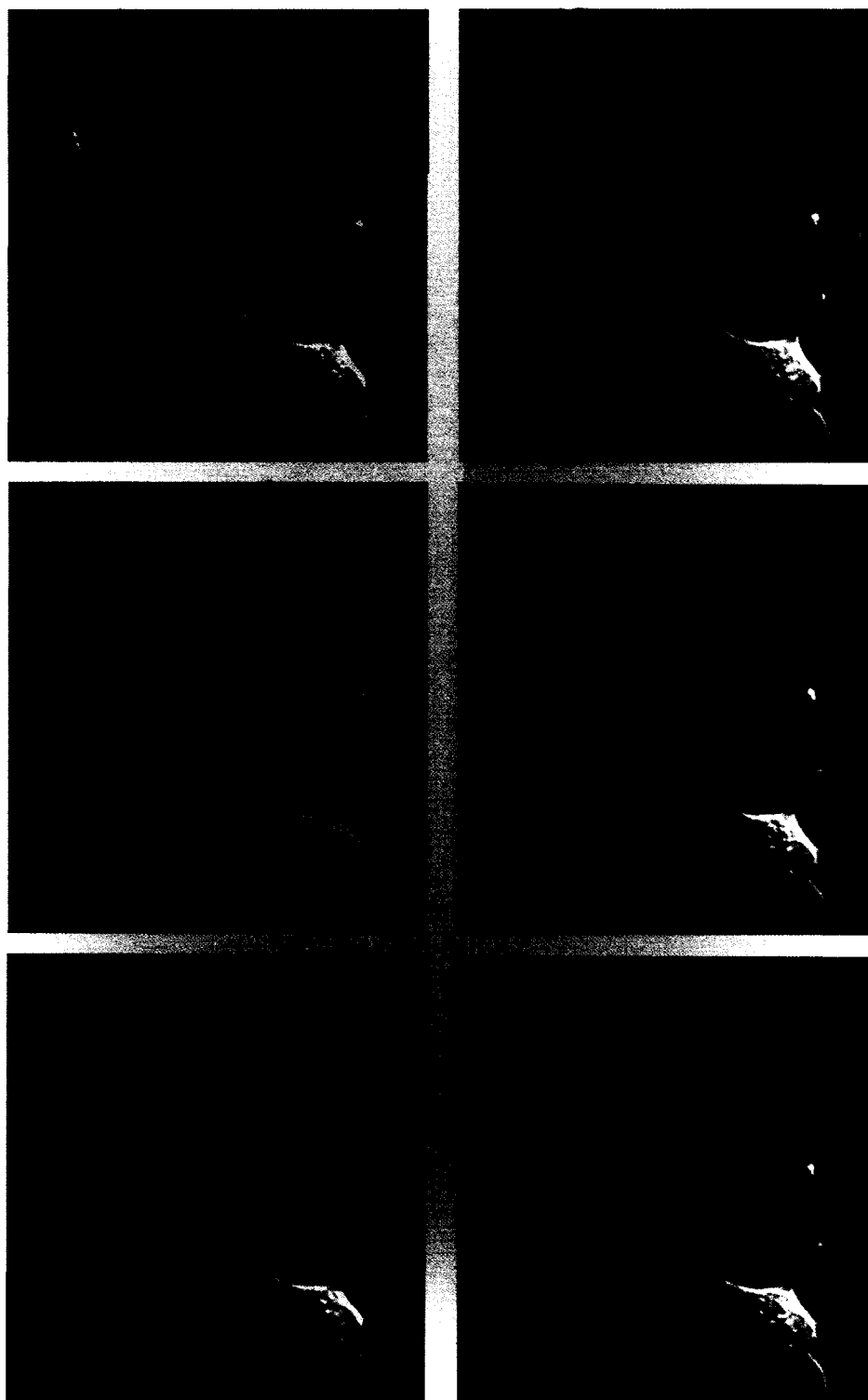
To further the role of waves in axon formation we next determined if axonal proteins known to play a role in axonogenesis were enriched in waves. Indeed, proteins such as the RhoGTPases Rap1B, cdc42, Rac1 (Kunda et al., 2001, Schwamborn and Pulcel, 2004), as well as actin regulating proteins such as ADF/Cofilin (Garvolov et al., 2007) Lim Kinase (Rosso et al., 2004) Slingshot phosphatase (Endo et al, 2002), and Arp3 (Strasser et al., 2004) are enriched in waves (Figure 8, data not shown).

NT3 and laminin affects axon formation, branching and waves

To determine if exogenous signaling/adhesion molecules that increase axonogenesis also induce waves we used the neurotrophin, NT3, which increases axon growth and branching in hippocampal neurons (Labelle and Leclerc, 2000; Yosimura et al., 2005). Interestingly, we found that when neurons are plated on poly-d-lysine alone, NT3 treatment actually attenuates axon formation (Figure 9). This is contrary to the report of Labelle and Leclerc (2000), which showed a potent increase in axon elongation and branching. However, Yosimura et al. (2005) demonstrated the NT3 effects for neurons grown on a laminin substrate. When we emulated those culture conditions, we observed similar results. Since laminin, perhaps through integrin signaling pathways, is known to modulate the responses of other guidance cues (Suh et al., 2004), the effect of NT3 inducing axon growth on laminin but attenuating growth on polylysine is not surprising. Actually, this finding was serendipitous, in that we could use the same NT3 signal to cause opposite effects on axon growth; decreasing axonogenesis on poly-d-lysine alone and increasing axonogenesis on poly-d-lysine/laminin.

When hippocampal neurons on poly-d-lysine alone were treated with NT3, there was a significant increase in the percent of neurons not extending axons (51.5% vs 35% for control) as well as a decrease in neurite branching (Figure 9). There was also a similar decrease in the percent of neurons exhibiting wave-like structures (0.75 fold of control). Opposite results were found when neurons were plated on a mixture of poly-d-lysine and laminin, where NT3 treatment resulted in an increase in the percent of neurons projecting one or more axons and a decrease in the percent of neurons with no axon compared to

Figure 4.2. Wave traveling in the anterograde direction. Time-lapse DIC series of a hippocampal neuron in culture exhibiting a wave (arrow) that propagates down the axon shaft until it merges with the growth cone. This wave travels 45 μ m in 12 minutes (3.75 μ m/minute). We observe waves traveling at velocities ranging from 1.5-5.6 μ m/minute in culture. Images shown are at 3 minute intervals with time indicated relative to first image in lower right corner. Scale bar = 15 μ m.



controls (Figure 9). Neurons on laminin treated with NT3 also had greatly increased neurite branching density. There was also an increase in the percent of neurons exhibiting wave-like structures versus control neurons (1.43 fold increase).

Live-cell DIC imaging experiments confirmed and extended these findings. There was a 30% decrease in the frequency of waves in neurons treated with NT3 plated on polylysine (Figure 9). On a laminin substrate, neurons treated with NT3 displayed a 26% increase in wave frequency compared to control neurons plated on polylysine.

Actin regulating proteins affect waves

We next examined the effects of manipulating intracellular proteins known to play a role in axonogenesis. Myosin activity has been shown to be antagonistic to neurite growth from numerous studies (Ahmed et al., 2000; Gallo et al., 2002) and it has been suggested that the inhibition of myosin induces axon formation in hippocampal neurons (Kim and Chang, 2004). Therefore, we examined the effects of the myosin inhibitor blebbistatin on wave formation. We found that the addition of 2.5 μ M blebbistatin, which has a drastic axonogenic effect (unpublished observations), increased wave frequency by 22% compared to controls (Figure 10B). Furthermore the impact of waves on neurite growth is modulated with myosin inhibition. Preceding wave arrival at the distal neurite, the neurite retracts several microns (Figure 10C). After blebbistatin treatment, there is a 2-fold reduction in the distance of retraction compared to control neurites. The average magnitude of outgrowth following blebbistatin treatment also increased relative to control neurons (1.6 fold increase, Figure 10D, Movie 4.4 and 4.5). We also examined the presence of active myosin II (phosphorylated myosin light chain MLC) in neurons (Figure 11). Interestingly, pMLC was found in high levels just distal and proximal to the wave but reduced within the wave itself.

Cofilin has recently been shown to be a positive factor in axon formation (Garvalov et al, 2007). In this study, we observe that active cofilin is enriched in the growth cone of the developing axon. We also found a high ratio of active cofilin in waves, similar to levels observed in the growth cones of developing axons (Figure 12A)

Furthermore, neurons over-expressing either wild-type and active cofilin have increased

percentage of neurons with wave like structures compared to control neurons (Figure 12B). We have previously shown that the over-expression of the wild type and active cofilin facilitates axon formation (Garvalov et al., 2007).

Waves increase growth cone size and dynamics

Preceding the rapid growth of the axon, there is an increase in the size and dynamics of the growth cone of the presumptive axon (Bradke and Dotti, 1997, 1999; Kunda et al., 2001). Therefore, we sought to determine if wave arrival at the distal neurite increased growth cone size and dynamics. Short interval DIC time-lapse imaging revealed that wave arrival at the neurite tip increased growth cone size by 2.6 fold (Figure 13, Movie 4.6 and 4.7) and growth cone dynamics by 2 fold compared to the growth cone before wave arrival. Furthermore, we often observed collapsed, non-dynamic growth cones transform into large and extremely dynamic growth cones upon wave arrival (Figure 14). Growth cones that were dynamic prior to wave arrival also underwent a moderate, albeit significant, increase in dynamics. These data suggest that waves increase growth cone size and dynamics, two features correlated with axon specification.

Waves transport actin

Although it was previously suggested that actin, and perhaps other proteins, may be transported in waves, evidence supporting this hypothesis was based only on protein localization in static pictures of waves. To visualize actin in live-cell experiments, we utilized Red Fluorescent Protein fused to actin (RFP-actin). When expressed in hippocampal neurons RFP-actin incorporates into the growth cones exhibiting robust filopodial and lamellipodial dynamics. In neurons with waves, RFP-actin was dynamic and incorporated into actin structures within growth cones resulting in a net increase in their fluorescence intensity (Figure 15A and 16, Movie 4.8 and 4.9). Because the waves induce a rearrangement of cortical actin in the neurite shaft, it is possible that actin in waves does not translocate along with the wave. To address this possibility, we utilized a photoactivatable GFP fused to β actin (PA-GFP-actin). Using DIC we identified probable wave structures,

Figure 4.3. Waves are growth cone-like structures that propagate along the lengths of neurites. **A.** DIC images of a wave advancing down a neurite shaft. Note that the wave appears like a motile growth cone. Relative times in minutes are indicated in lower right corner. **B.** Fluorescent images of F-actin (phalloidin), tubulin, and cofilin in a hippocampal neuron with two waves (arrows). Note the high levels of F-actin and cofilin and the splaying of microtubules in the waves. A merged image of actin/tubulin is shown in the right panel. **C.** DIC time-lapse images (10 second intervals) of growth cone (top panel) and wave (bottom panel), which both contain dynamic filopodial and lamellipodial protrusions. Relative times are shown in seconds in the lower right of the images. **D.** Quantification of change in growth cone and wave area over ten second intervals ($\Delta A/10s$) indicates that growth cones and waves have similar dynamics. Growth cones show $23.5 \pm 7.5\% \Delta A/10s$ and waves show $27.5 \pm 7.3\% \Delta A/10s$ (N.S.).

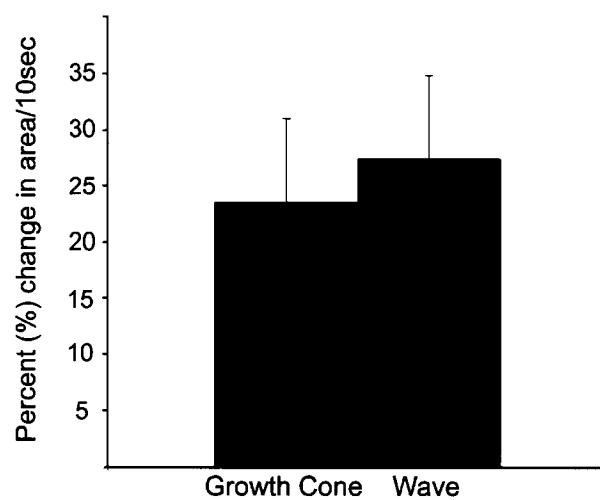
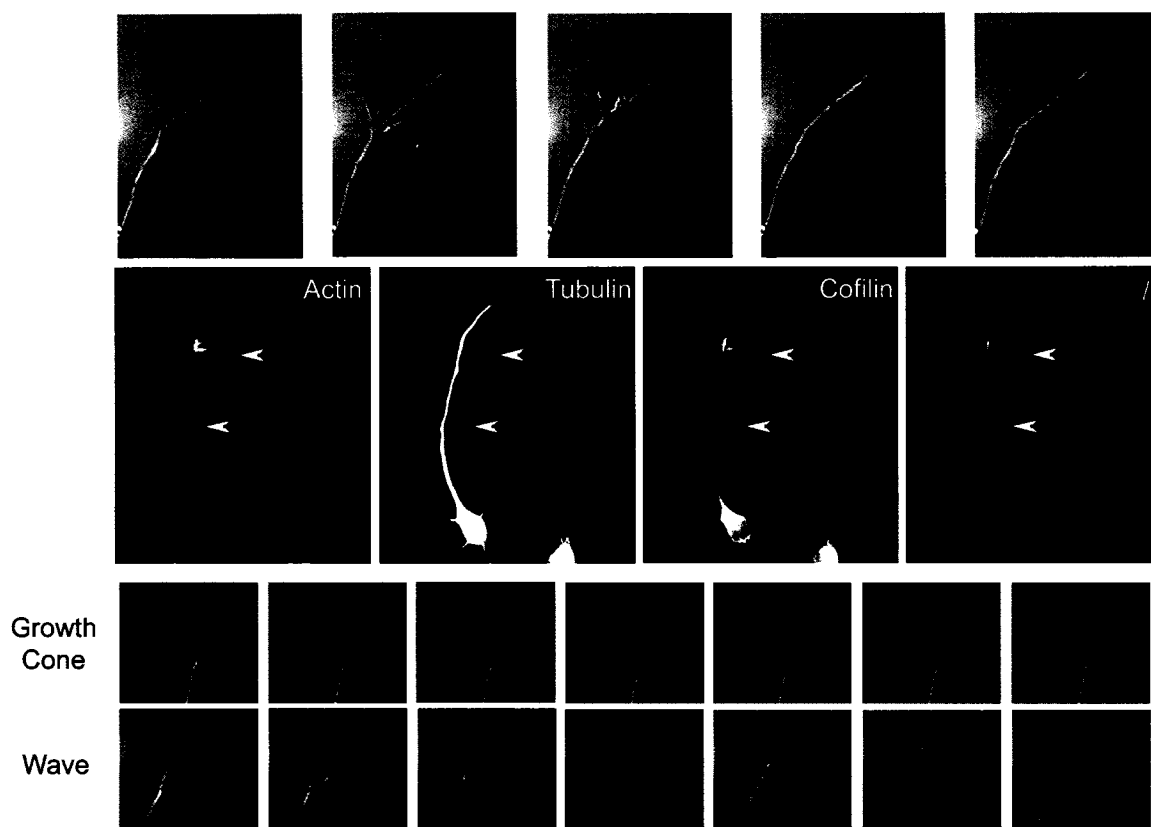


Figure 4.4. Waves have a similar composition as growth cones.

Fluorescent images are shown of a growth cone (top row) and a wave (bottom row) labeled for F-actin (green, phalloidin) and tubulin (red, indirect immunofluorescence). The actin staining (left) reveals that both the growth cone and the wave exhibit actin-based filopodia (red arrows) and lamellipodia (white arrows). Tubulin staining shows that in the proximal regions of both the growth cone and the wave, there are tightly packed microtubule bundles while in the peripheral region there are the penetration of the occasional splaying microtubules (arrows). The overlay of actin and tubulin staining (right) indicates that waves can be subdivided into distinct domains similar to growth cones with a microtubule-rich central domain (outlined in white points) and an actin-rich peripheral domain.

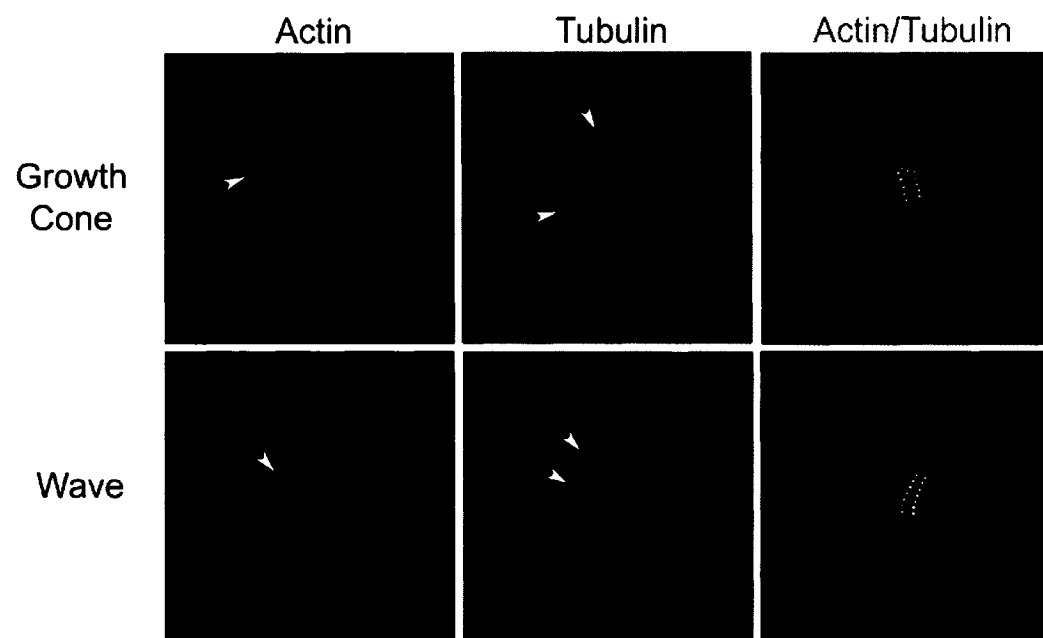
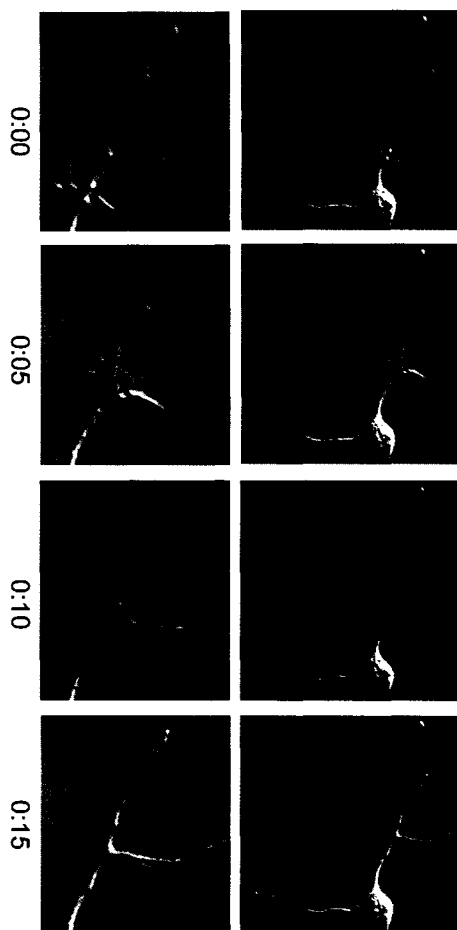


Figure 4.5. Waves are involved in the formation and growth of neurite branches.

A. Time-lapse DIC series is shown of a hippocampal neuron undergoing neurite branch growth. The bottom row of images shows magnified views of the branch point in the images above. Time is indicated below the images (minutes). A wave (arrow) travels along the neurite to the branch-point and bifurcates along each branch (0:05) contributing to the extension of both branches. **B.** Time-lapse DIC series of a hippocampal neuron undergoing neurite branch formation. The bottom row of images shows magnified views of the branch point in the images above. Time is indicated below the images (minutes). Notice the small filopodia protruding from the shaft before wave arrival (arrow, bottom row). A wave propagates along the axon (arrow) and engorges the filopodium (0:05) inducing the subsequent elongation of a new branch (see Movie 4.2).

A



B

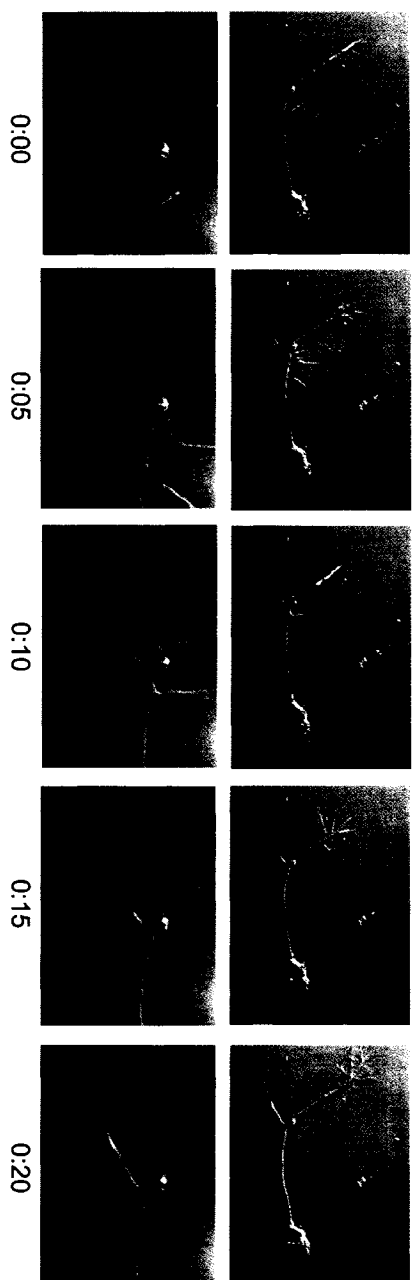


Figure 4.6. Waves support the formation and growth of new neurite arbors. A time-lapse series is shown of a stage 3 hippocampal neuron undergoing neurite branch development. Time is indicated in lower right of every image (hour:minute). Initially there is only the primary neurite. A wave propagates along the axon (arrow) and induces a protrusion from the neurite shaft (0:10). This protrusion remains at 0:50 (white arrowhead) as another wave advances down the axon. As the wave approaches the branch point, it engorges the initial protrusion (1:05) and induces its subsequent elongation.

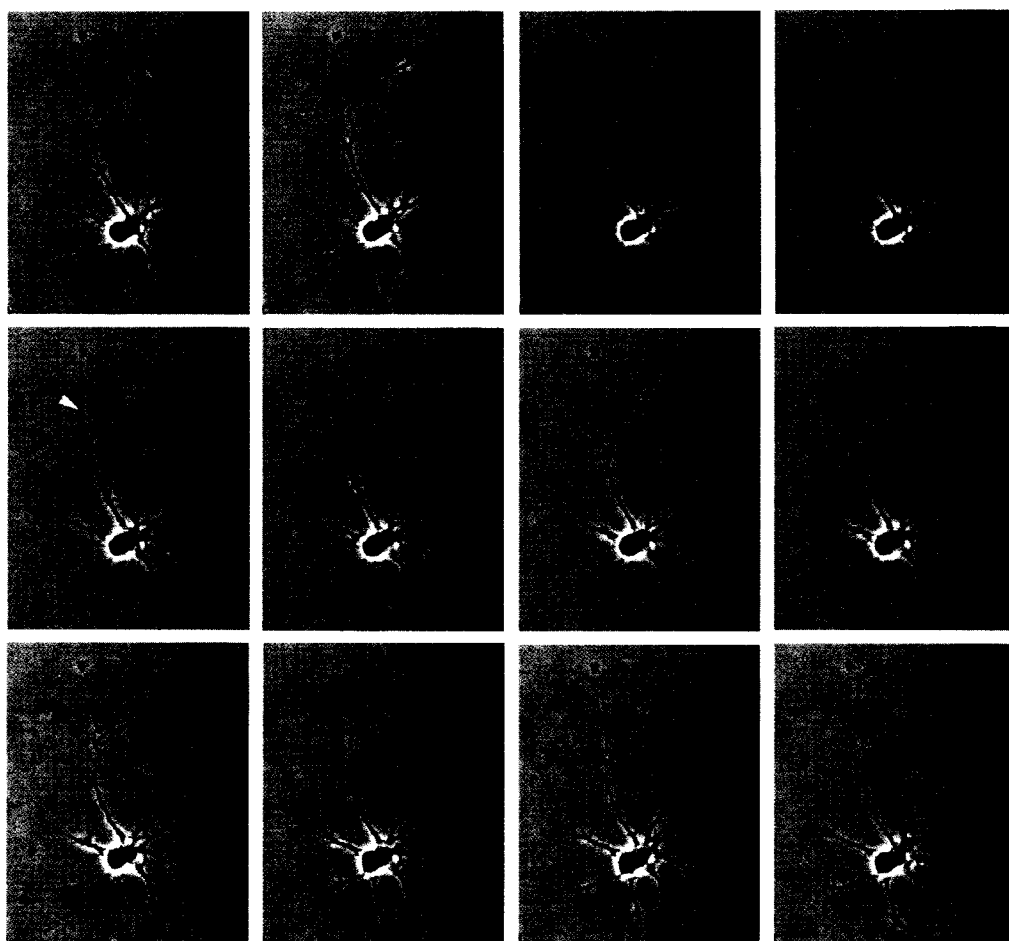


photo-activated the GFP-actin in the wave and followed the GFP-actin in time-lapse imaging. At least a portion of the activated PA-GFP-actin traveled in waves to the neurite tip (Figure 15B). However, some fluorescent actin appeared to remain in the neurite shaft and some appeared to diffuse back to other regions of the cell.

From our immunofluorescence studies, we also hypothesize that other proteins involved in axon growth (and neurite growth in general) are also transported in waves. For example, the ADF/cofilin proteins are known to influence neurite growth, growth cone dynamics and pathfinding and axon formation (Meberg and Bamberg, 2000; Kuhn et al., 2001; Wen et al., 2007; Garvalov et al., 2007). Fluorescently labeled cofilin behaved similarly to RFP-actin and also appeared to be transported to growth cones in waves (Figure 17). We observed in other cases a gradual increase in cofilin-GFP in growth cones (data not shown).

Evidence that waves occur *in vivo*

Although waves are a prevalent phenomena in our cultured neurons and others have reported wave-like structures (Ruthel and Banker, 1998, 1999; Heideman et al., 2003, Rosso et al., 2004; Toriyama et al., 2006; Turnsun et al., 2007), it is possible they are an artifact of culturing neurons on a 2D substrate. To determine if waves are physiologically relevant *in vivo*, we examined fixed and live hippocampal slices in which neurons were fluorescently labeled either with the lipophilic dye, DiI, or via the expression of Thy1-YFP, both of which label cellular membranes (Feng et al., 2000). In our studies we focused on neurons in the dentate gyrus and the mossy fiber tract because previous work showed neurogenesis, neurite formation and outgrowth occur robustly there early in postnatal development (Dailey et al., 1994; Knoll et al., 2005). We also observed other regions of the hippocampus including CA3 and CA1 as well as entorhinal cortex and cerebral cortex. We observed wave-like structures in neurons from all of these regions, but they were especially robust in the dentate gyrus from the Thy1-YFP transgenic mice (Figure 18).

To confirm that these structures were waves we performed 3-dimensional time-lapse confocal microscopy of individual neurons in organotypic hippocampal slices. We

observed growth cone advance in DiI and Thy1-YFP labeled mossy fiber axons occurring at rates between 0.9 $\mu\text{m}/\text{min}$ and 2.5 $\mu\text{m}/\text{min}$ (Figure 1). In these slice preparations we also observed waves in neurons in the dentate gyrus and CA3 regions of the hippocampus. In DiI labeled neurons, we often observed waves beginning at the cell body traveling down the entire length of processes (Figure 19, Movie 4.10). We also observed waves in Thy1-YFP neurons (Figure 20). Wave velocity in slices was similar to that observed in culture, ranging between 0.8 μm and 5.6 $\mu\text{m}/\text{min}$ with an average of 2.28 $\mu\text{m}/\text{min}$. This velocity is similar to that of rapid growth cone advance and within the range of slow axonal transport. In addition, neurons in slices expressing GFP-actin contained dynamic actin in waves that appeared similar to growth cones (Figure 21). Waves were also observed to induce neurite branching in hippocampal slices via the engorgement and extension of shaft filopodia (Figure 21, Movie 5.3).

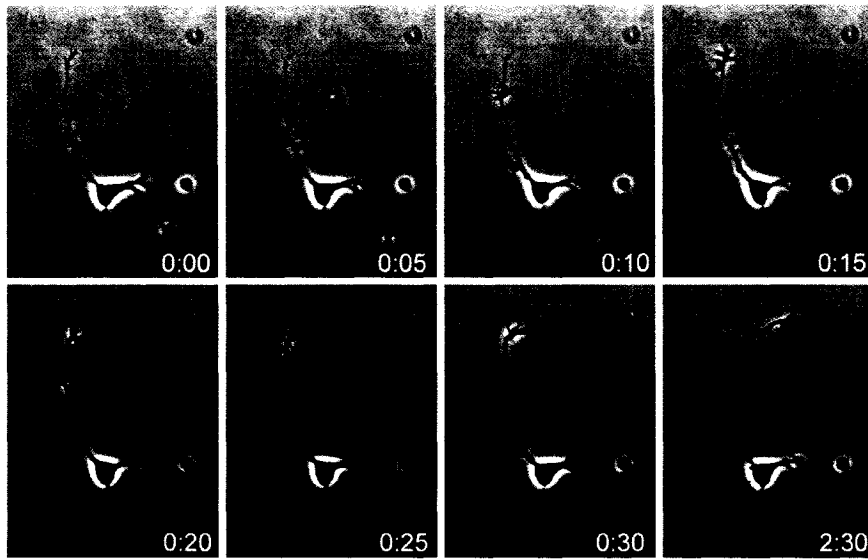
We rarely observed waves in long axons of the mossy fiber tract, suggesting that waves may occur preferentially earlier in neuronal development. This finding is in agreement with our observations in culture where wave frequency is high in the first few days (0.25-3 div) of culture as neurites are rapidly extending, but are not prominent later in culture (4-5 days), when neurite growth has attenuated (data not shown; also shown in Ruthel and Banker, 1999)

Discussion

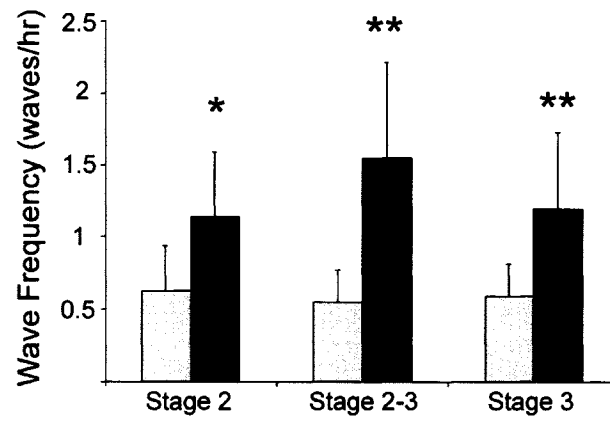
Waves represent an under-characterized phenomenon in neuronal development. Initial work identified them as growth cone-like structures that typically form at the soma, undergo anterograde transport at an average rate of 3 $\mu\text{m}/\text{min}$ merging with the distal neurite causing bursts of outgrowth (Ruthel and Banker, 1998, 1999). Because waves travel at a rate consistent with slow component b of axonal transport and contain high levels of actin and other proteins, Ruthel and Banker hypothesized that waves may represent a form of axonal transport. Since this initial work, a handful of studies observed waves in other cultured neurons and speculated that they could be important for axonal transport and neurite

Figure 4.7. Wave frequency and impact on neurite growth are associated with axonogenesis. **A.** DIC images of waves in stage 2-3 neurons. Notice that multiple waves occur in the developing axon (arrows). Time is indicated in lower right corners of images (in hours:minutes). **B.** Quantification of the frequency of anterograde waves in neurites of stage 2, stage 2-3 and stage 3 neurons (see definition in methods). The same neurons were followed for 24-72 hours as they underwent the development of neuronal polarity. Notice that at all stages, the developing axon has a higher frequency of waves compared to the minor processes. At the stage 2-3 transition, there is a notable increase in wave frequency in the developing axon. During stage 2, the neurite destined to become the axon averages 1.14 ± 0.45 waves/hour and minor neurites average 0.63 ± 0.31 waves/hour. During the stage 2-3 transition, the developing axon averages 1.55 ± 0.67 waves/hour while the minor neurites average 0.55 ± 0.22 waves/hour. During stage 3, the newly formed axon averages 1.2 ± 0.53 waves/hour while the minor neurites average 0.59 ± 0.22 waves/hour. Significance is indicated: * $p < 0.01$; ** $p < 0.005$. Error bars = standard deviation. **B.** The contribution of waves to bursts of neurite outgrowth is different for developing axons and minor processes and varies at different stages. In stage 2 neurons, the relative contribution of waves (relative to the minor processes) to growth is nearly the same for minor processes and for presumptive axon (1.1 ± 0.2 fold higher than minor processes). However, during the stage 2-3 transition the impact of waves on neurite growth is greater in the developing axon compared to the minor processes (1.5 ± 0.2 fold greater). During stage 3 the relative contribution of waves to neurite growth remains high in the axon compared to the minor processes (1.7 ± 0.3 fold greater).

A



B



C

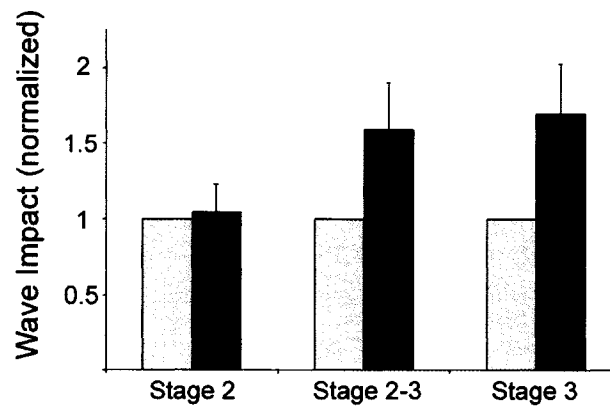


Figure 4.8. Proteins associated with axon growth localize to waves. Immunofluorescence experiments indicate a localization of positive regulators of axon growth to waves in cultured hippocampal neurons. Waves are indicated by a white arrowhead and distal neurite tips are indicated by a red arrowhead. The ADF/cofilin regulating proteins slingshot phosphatase (SSH) and Lim kinase (LIMK) co-localize with cofilin in wave-like structures (top row). Growth-Associated Protein 43 (GAP 43, red) also co-localizes with cofilin (green) in waves (second row). The Rho GTPase, Rap1, which is necessary for axon formation, localizes to waves (third row). Another Rho GTPase essential for normal axon formation, cdc42, co-localizes with cofilin, a downstream effector, in waves (bottom row).

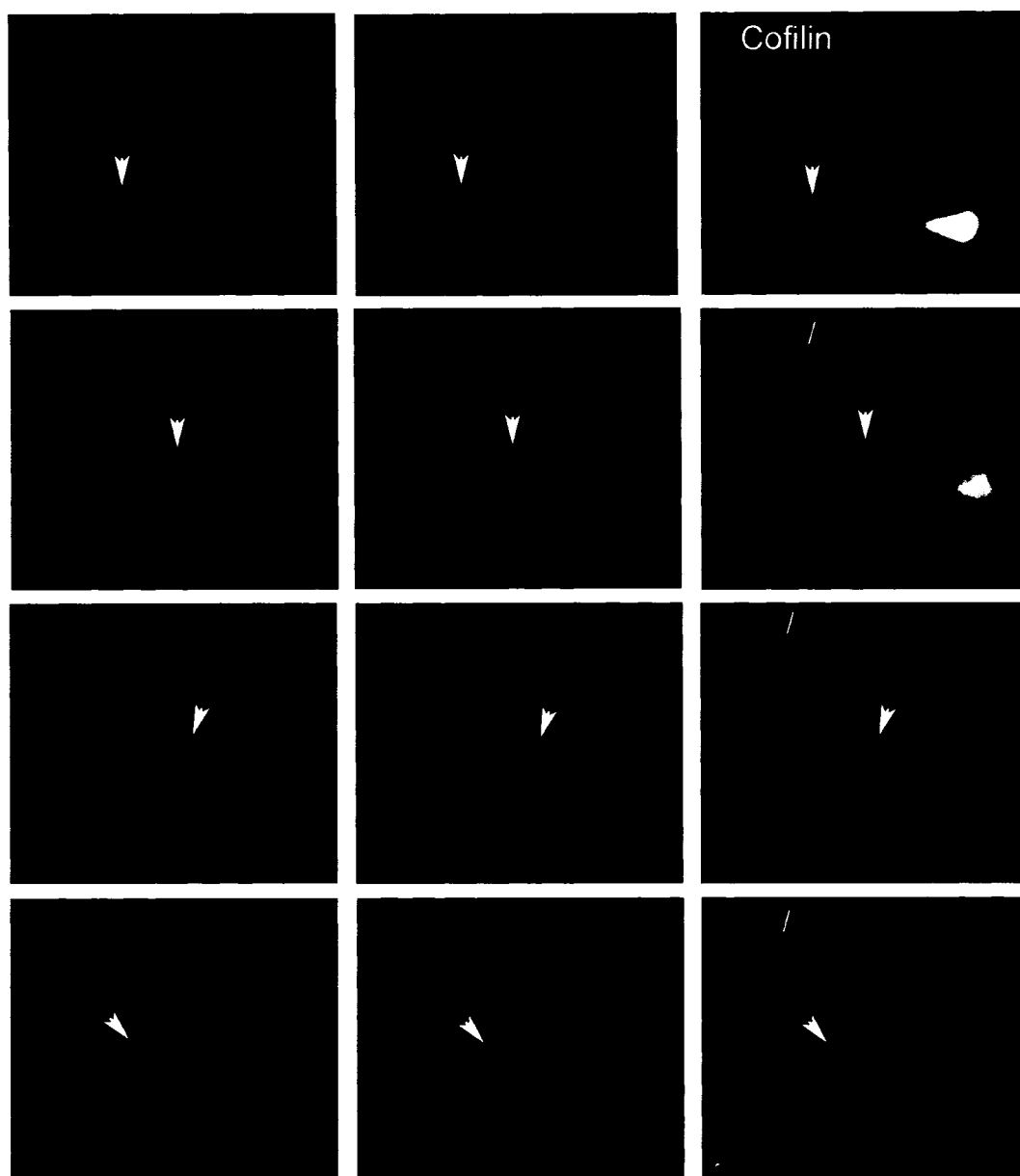


Figure 4.9. NT-3 has substrate-dependent effects on axonogenesis, neurite branching and wave frequency. **A.** Representative images of hippocampal neurons cultured under different conditions and immunostained for the axonal marker Tau1 and actin with Texas Red phalloidin. Note that on polylysine (A, third image down), NT-3 (100ng/ml) treated cells have shorter processes with no distinguishable axon. Conversely, NT-3 treated neurons cultured on laminin (A, bottom panel) have longer axons and more extensive neuritic arbors. The large arrows indicate axons. Wave-like structures are highlighted by small arrowheads. **B.** Quantification of neuronal polarity phenotypes under different culture conditions. In these experiments, neurons cultured on polylysine have 35.4±1.7% with no axon, 55.9±6.6% with one axon, and 7.5±3.2% with multiple axons. Neurons plated on polylysine and treated with NT3 have 51.5±8.4% with no axon, 42.4±8.7% with one axon and 6.2±0.3% with multiple axons. Neurons plated on laminin and treated with NT3 have 16.55±1.3% with no axon, 68.2±0.9% with one axon and 15.3±0.4% with multiple axons. **C.** Quantification of branching of neurons cultured under different conditions. On polylysine, neurons have an average of 1.6%±0.3 branches/neuron. Neurons on polylysine treated with NT3 have reduced branching averaging 0.99±0.3 branches/neuron. On laminin, NT3 treated neurons have an average of 2.5±0.13 branches/neuron. **D.** Quantification of relative number of neurons exhibiting wave-like structures under different conditions. NT3 treated neurons on polylysine have 0.76±0.1 waves/neuron; on laminin, NT3 treated neurons have 1.43±0.1 waves/neuron. **E.** Quantification of wave frequency of neurons cultured under different conditions (from time-lapse imaging; error bars are SEM). On polylysine neurons exhibit 1.9±0.3 waves/hr. NT3 treated neurons on polylysine have 1.34±0.2 waves/hr. On laminin, NT3 treated neurons have 2.4±0.4 waves/hr.

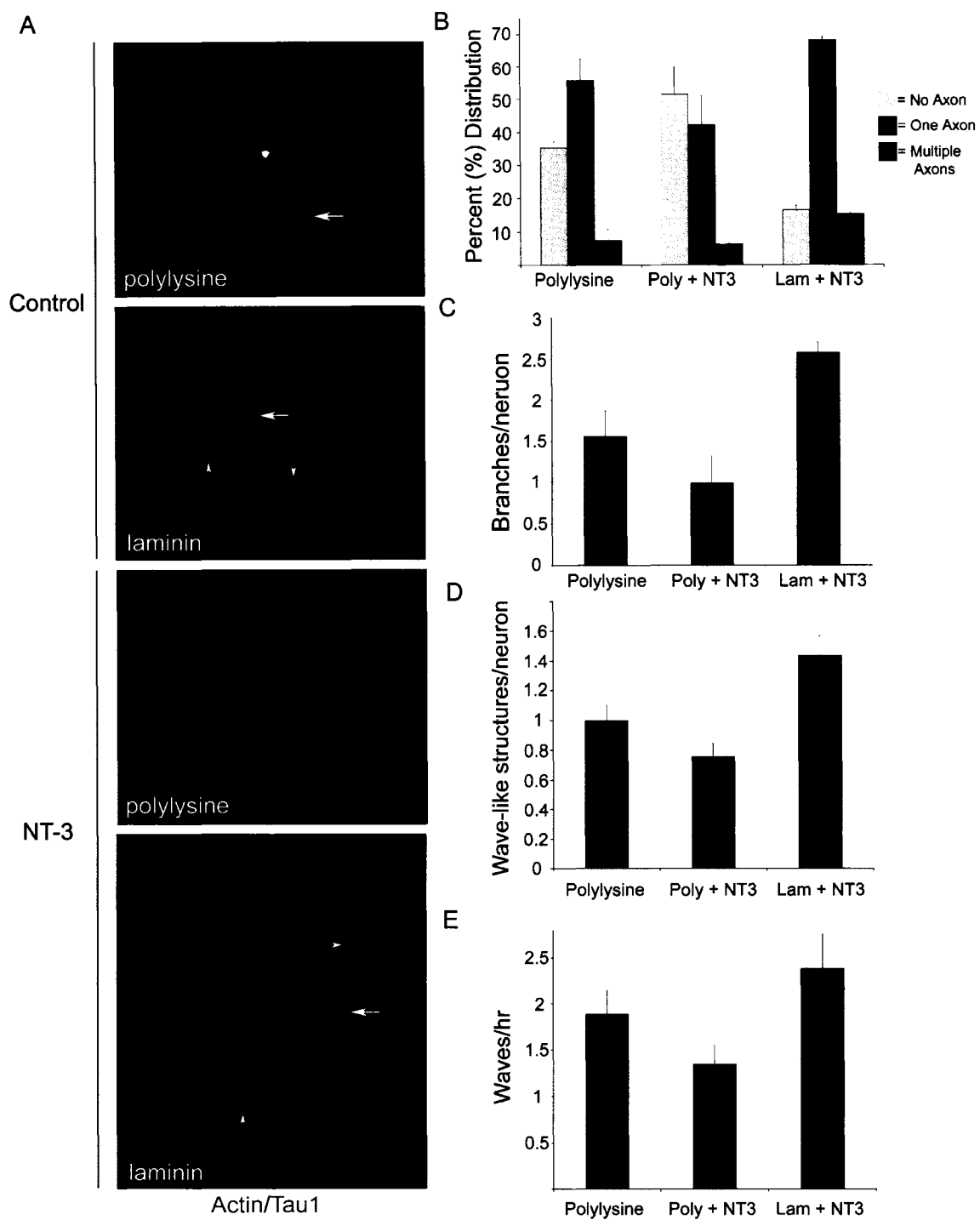


Figure 4.10. Inhibition of myosin II influences wave dynamics. **A.** Time-lapse images of the same neuron before and after treatment with blebbistatin (bleb), a specific myosin II inhibitor. Under normal conditions, as waves (white arrow) approach the growth cone there is slight retraction of the neurite, followed by a small outburst of growth (right column). After bleb treatment, a wave propagating down the same neurite does not cause retraction preceding outgrowth and the subsequent burst in neurite outgrowth is more robust and sustained for longer time periods. **B.** Analysis of time-lapse images shows that myosin inhibition marginally increases wave frequency $22.2 \pm 0.09\%$ (error bars= SEM). **C.** Myosin II inhibition decreases the average retraction distance induced by waves. In control neurons before bleb treatment neurites retract an average of $5.6 \pm 0.7 \mu\text{m}$ before wave arrival (error bars = SEM). After bleb treatment neurites retract an average of $2.3 \pm 0.5 \mu\text{m}$ before wave arrival. **D.** Myosin II inhibition also causes waves to have an increased impact on subsequent neurite growth. In these experiments neurites on control neurons extend an average of $9.9 \pm 0.2 \mu\text{m}$ following wave arrival (error bars = SEM). After bleb treatment neurites extend an average of $15.9 \pm 1.6 \mu\text{m}$ following wave arrival (see Movie 4.4 and 4.5).

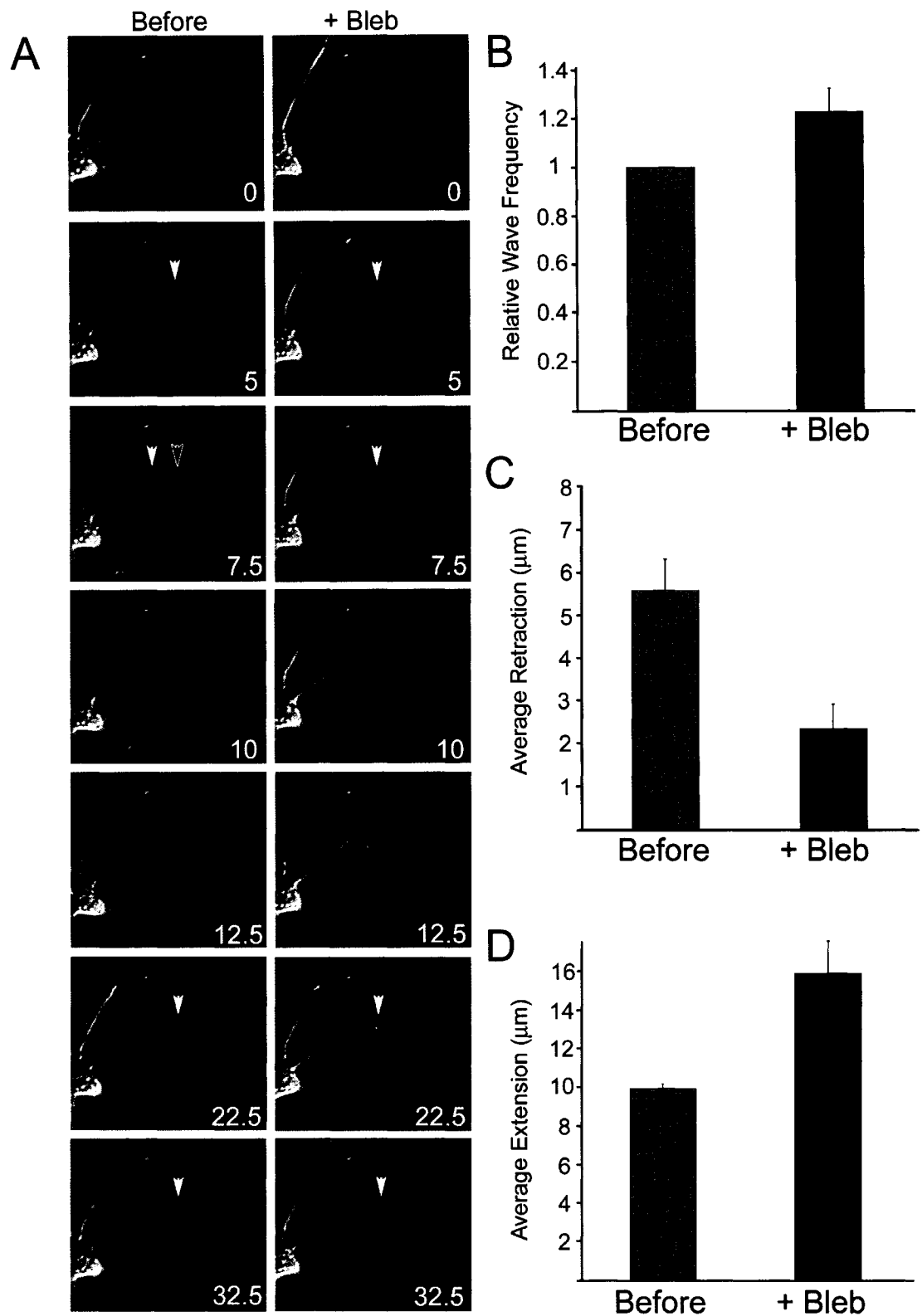


Figure 4.11. Active myosin II is enriched in advance of and in the wake of waves.

Fluorescent images of F-actin (green, phalloidin) and active, phosphorylated myosin light chain (red, pMLC) in a hippocampal neuron with a wave (white arrowhead). An overlay of actin and pMLC is depicted in the right panel. Note that there is an enrichment of pMLC in regions distal to the wave and proximal to the wave (red arrowheads) while deficient in the wave itself.

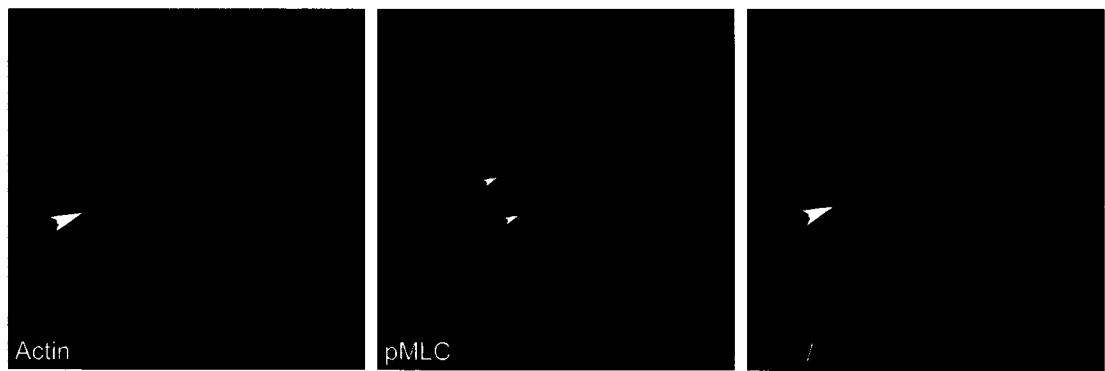
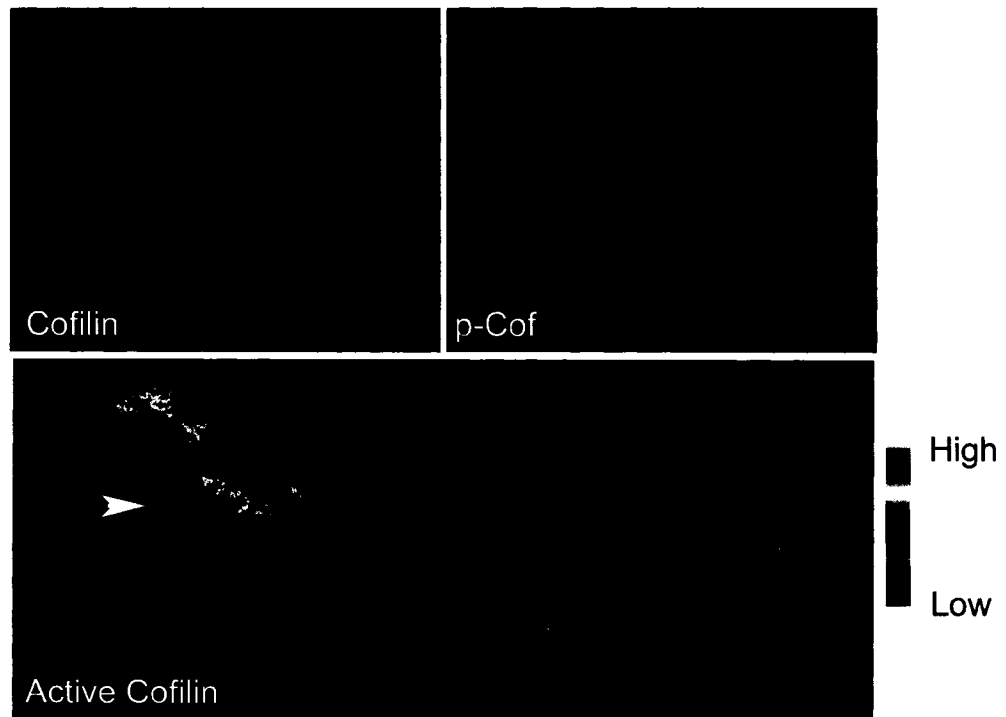


Figure 4.12. Cofilin activity may be involved in wave propagation. **A.** Fluorescent images of neurons stained from total cofilin (top left) and inactive phosphorylated cofilin (pCof, top right) in a young stage 3 neuron. The ratio of total cofilin/pCof, presented as a pseudocolor intensity profile image, provides information about the relative distribution of dephosphorylated (putatively active) cofilin. A wave in the axonal neurite shaft (arrow) has a particularly high level of dephosphorylated cofilin, especially in the peripheral regions of the wave. **B.** The over-expression of inactive (E3), wild-type (wt), and active (A3) cofilin has different effects on the presence of wave-like structures in neurons. Control neurons expressing RFP have $34.4 \pm 3.5\%$ of neurons exhibiting waves. The expression of cofilin-E3 is similar to controls with $34.7 \pm 4.9\%$ of neurons exhibiting waves. The expression of either wild-type or active cofilin-A3 increases the percent of neurons with waves ($48.1 \pm 7.4\%$ and $48.8 \pm 10.8\%$, respectively).

A



B

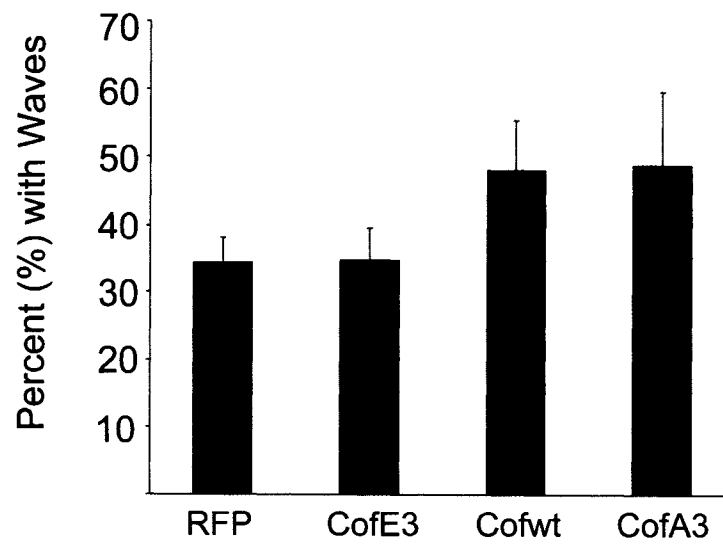
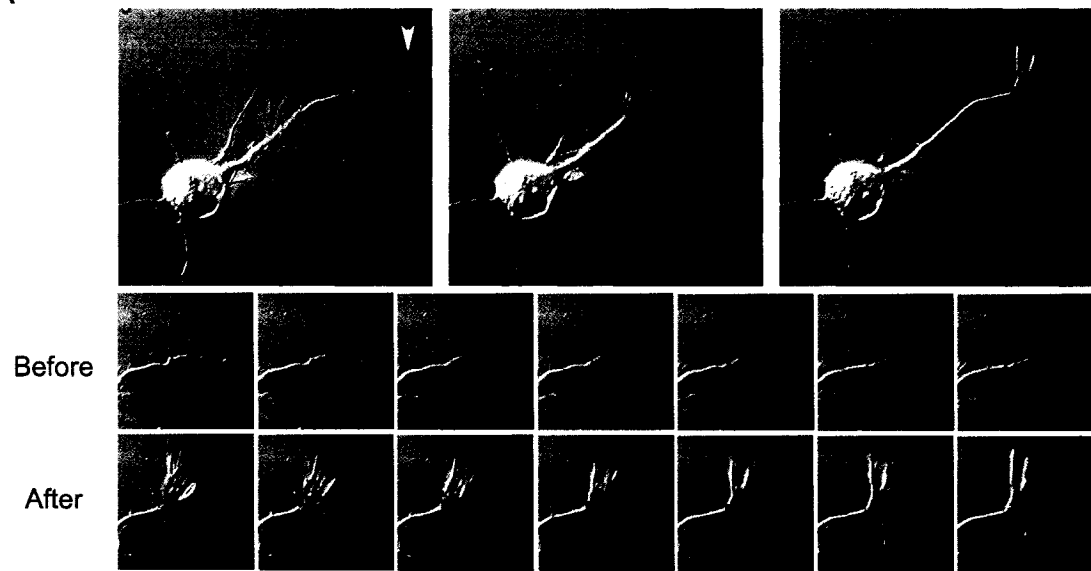
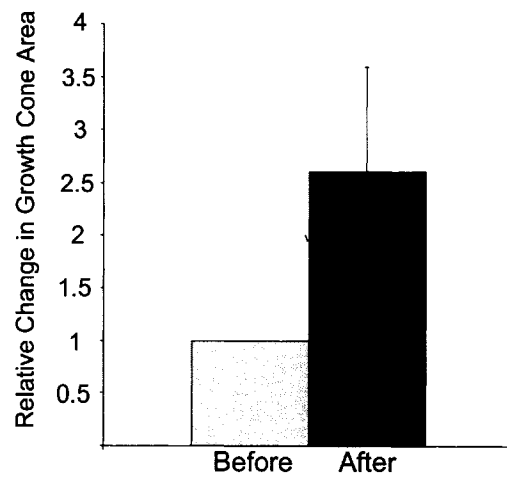


Figure 4.13. Waves increase growth cone size and dynamics. **A.** Time-lapse DIC images of neuron with propagating wave (top row, arrow). **B.** Magnified view of time-lapse images of growth cone from neuron before (top row) and after (bottom row) wave arrival. Time is denoted in seconds in lower right corner of panels. The growth cone enlarges and becomes more dynamic following wave arrival (see Movie 4.6 and 4.7). **C.** Quantification of relative growth cone size before and after anterograde wave arrival (n=18). Growth cone size increases 2.6 ± 0.7 fold following wave arrival. **D.** Quantification is shown of all growth cones examined for relative change in area every ten seconds ($\Delta A/10s$) (n = 15). Before wave arrival growth cones average $16.1 \pm 6.6\% \Delta A/10s$. After wave arrival, growth cones average $22.5 \pm 6.2\% \Delta A/10s$ ($p < 0.001$).

A



B



C

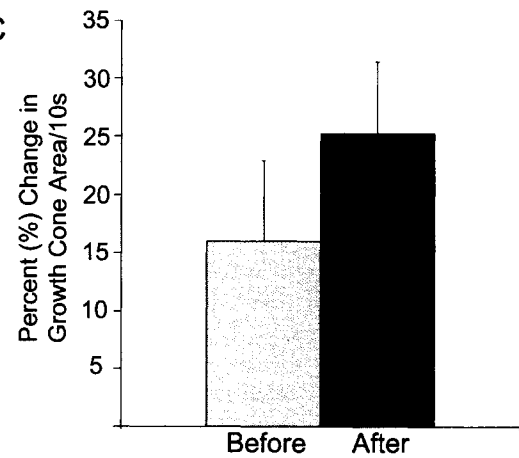


Figure 4.14. Wave-mediated changes in growth cone dynamics depends on the existing dynamics of the growth cone when waves arrive. Growth cones were characterized as dynamic or non-dynamic before wave arrival depending on the relative change in area every ten seconds ($\Delta A/10s$). Dynamic growth cones are those with $\Delta A/10s > 12\%$; non-dynamic growth cones are those with $\Delta A/10s \leq 12\%$. **A.** Summary quantification is shown of all growth cones examined ($n = 15$). Before wave arrival growth cones average $16.1 \pm 6.6\%$ $\Delta A/10s$. After wave arrival, growth cones average $25.3 \pm 6.2\%$ $\Delta A/10s$ ($p < 0.001$). **B.** Quantification is shown of non-dynamic growth cones examined ($n = 8$). Before wave arrival growth cones average $11.1 \pm 1.7\%$ $\Delta A/10s$. After wave arrival, growth cones average $25.3 \pm 3.3\%$ $\Delta A/10s$ ($p < 0.001$). **C.** Quantification is shown of dynamic growth cones examined ($n = 7$). Before wave arrival growth cones average $23.5 \pm 4.2\%$ $\Delta A/10s$. After wave arrival, growth cones average $29.4 \pm 7.6\%$ $\Delta A/10s$ ($p < 0.01$).

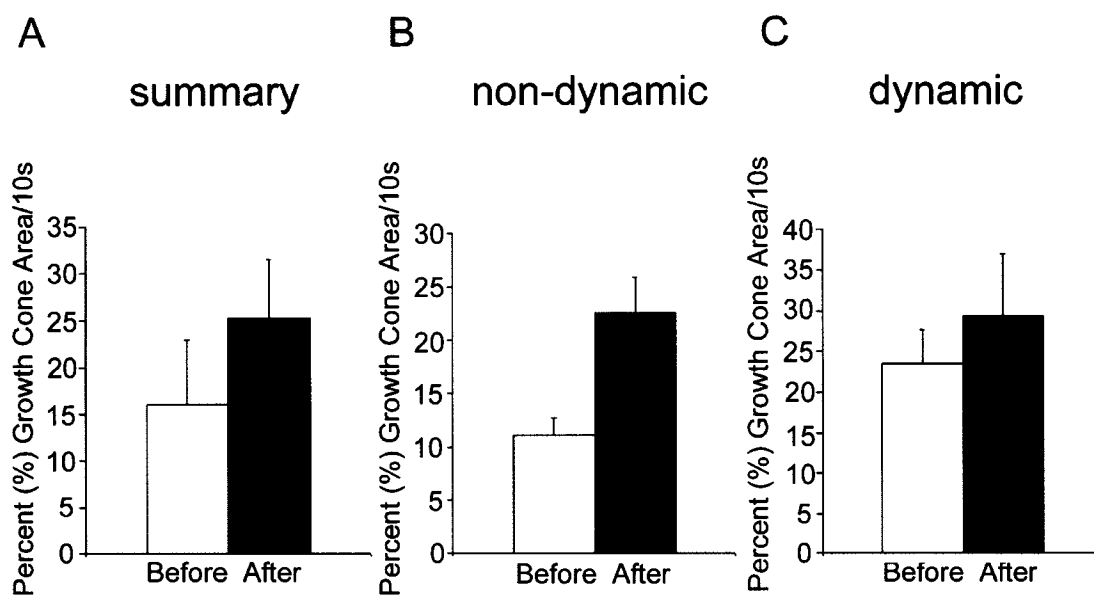
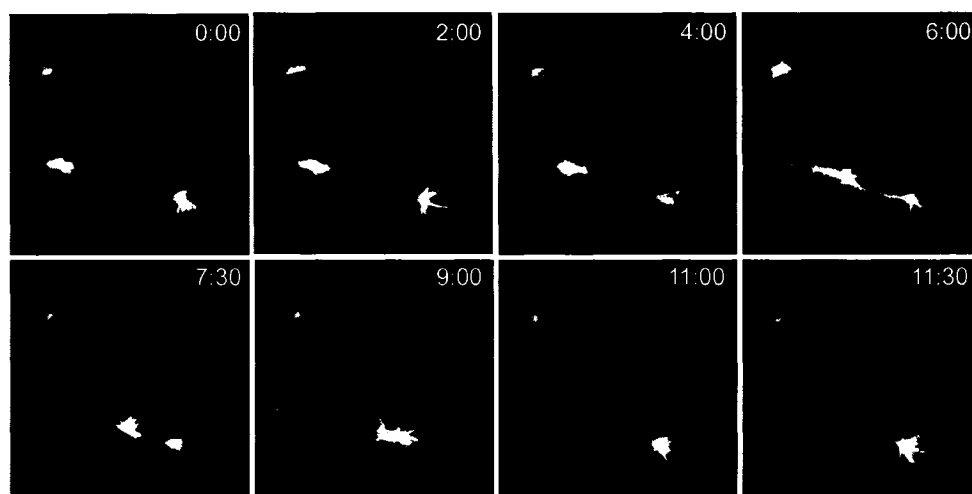


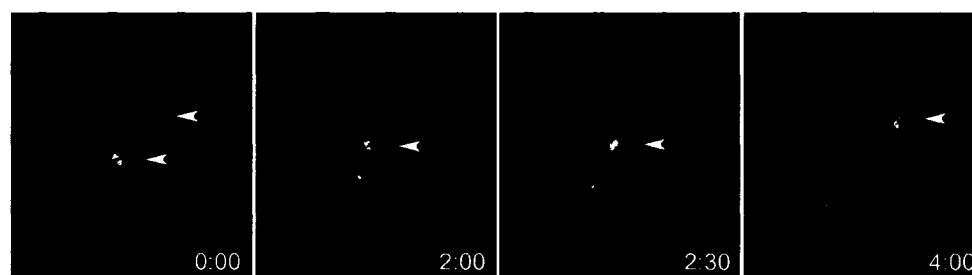
Figure 4.15. Waves transport actin. **A.** Time-lapse images of a hippocampal neuron expressing RFP-actin. The wave is dynamic, extending and retracting actin-based filopodia and lamellipodia (see Movie 4.8 and 4.9). **B.** Time-lapse images of a hippocampal neuron expressing photoactivatable-GFP actin (PA-GFP) with the actin photoactivated only within the wave. The distal neurite tip is indicated by the white arrowhead. Notice that the PA-GFP actin travels with the wave down the process to the growth cone (green arrowhead). Although some GFP signal remains in the neurite shaft, some of the PA-GFP-actin arrives at the growth cone after traveling with a wave over 20 μ m.

A



RFP-Actin

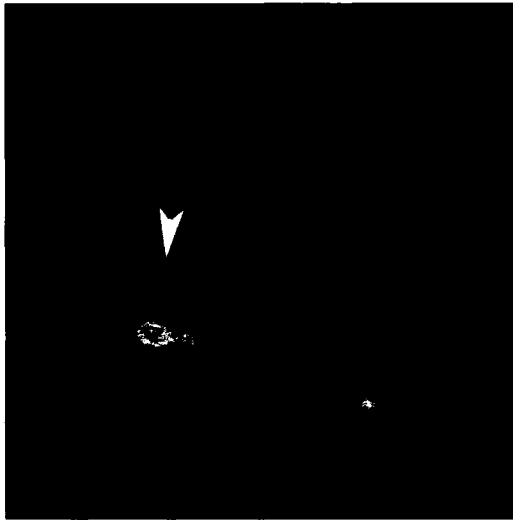
B



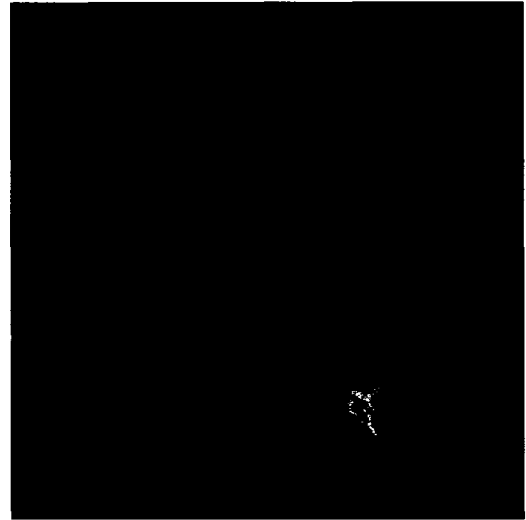
Photoactivatable-GFP-Actin

Figure 4.16. Waves increase actin levels in the growth cone. Two pseudocolor images are shown of a neuron expressing RFP-actin before and after wave amalgamation with the growth cone. Notice that the RFP-actin intensity increases in the growth cone after wave arrival, suggesting that the wave increased the level of actin in the growth cone.

Before



After



Actin intensity

Figure 4.17. Cofilin travels in waves. Time-lapse images are shown of a hippocampal neuron expressing cofilin-GFP. Time is denoted in lower left corner of the images (minutes). Note the high levels of cofilin in growth cones except the neurite with a collapsed ending (arrowhead, time 0:00). A wave enriched in cofilin travels down a short neurite (arrowhead, 0:04) causing an increase in cofilin-GFP intensity and the size of the growth cone.

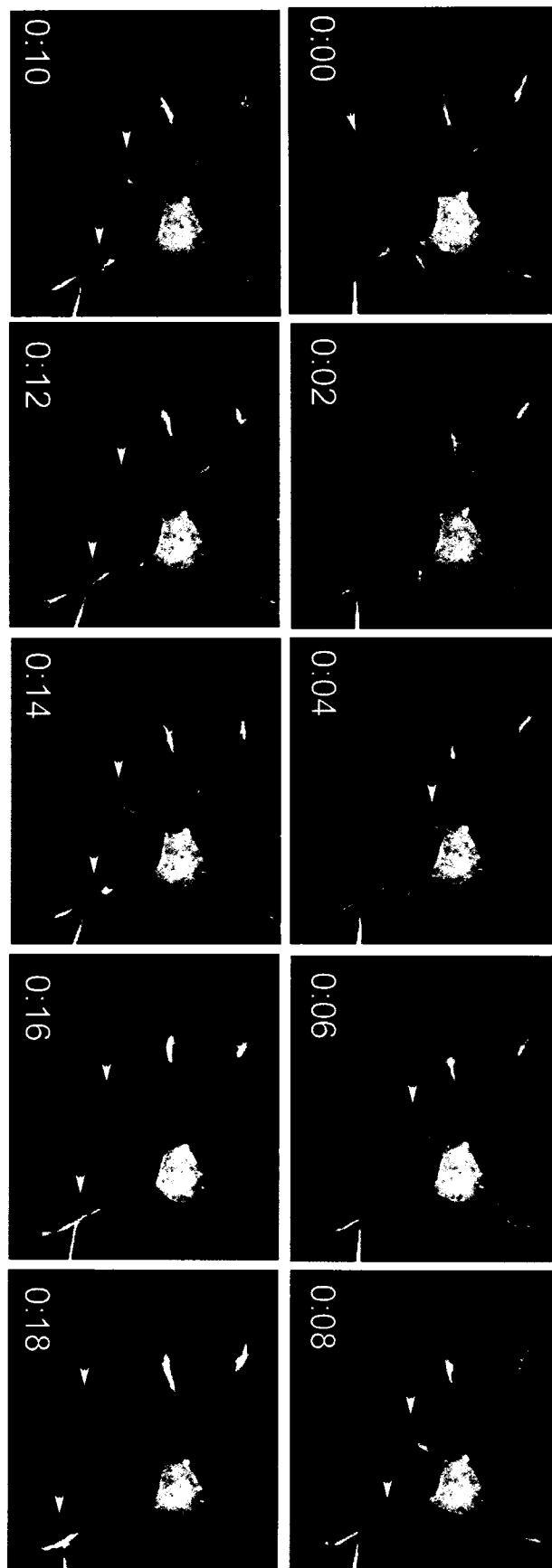


Figure 4.18. Wave-like structures occur *in vivo*. **A.** A hippocampal slice from a perfusion-fixed P0 transgenic Thy-1-YFP mouse has numerous neurons expressing YFP (immunostained for GFP to intensify signal). **B.** High magnification maximum intensity projection image is shown of region highlighted in panel A. This is a neuron adjacent to the dentate gyrus and CA1 which is undergoing robust neurogenesis at this stage of development. Note the shorter process extending from the soma has a wave-like structure (arrow) and a small growth cone (arrow).



Figure 4.19. Waves can be visualized in neurons within hippocampal slices by DiI labeling their membrane. **A.** A maximum intensity projection image of a DiI labeled neuron in the dentate gyrus of a P2 hippocampal slice. The image is a projection of a 22, 1 μm steps of a Z-series. The arrowhead indicates a wave traveling along a neurite that extends over 15 μm in the Z direction in the 3-dimensional slice environment. **B.** Time-lapse images following the propagation of a wave along the neurite indicated in A. In order to visualize the wave over time each of these images are maximum projections of 5 μm stacks moving up the Z series. Time is indicated in the lower right corner of the images in minutes. The wave travels in the anterograde direction along the neurite (arrowhead) over 20 min. (see Movie 4.10).

A



B

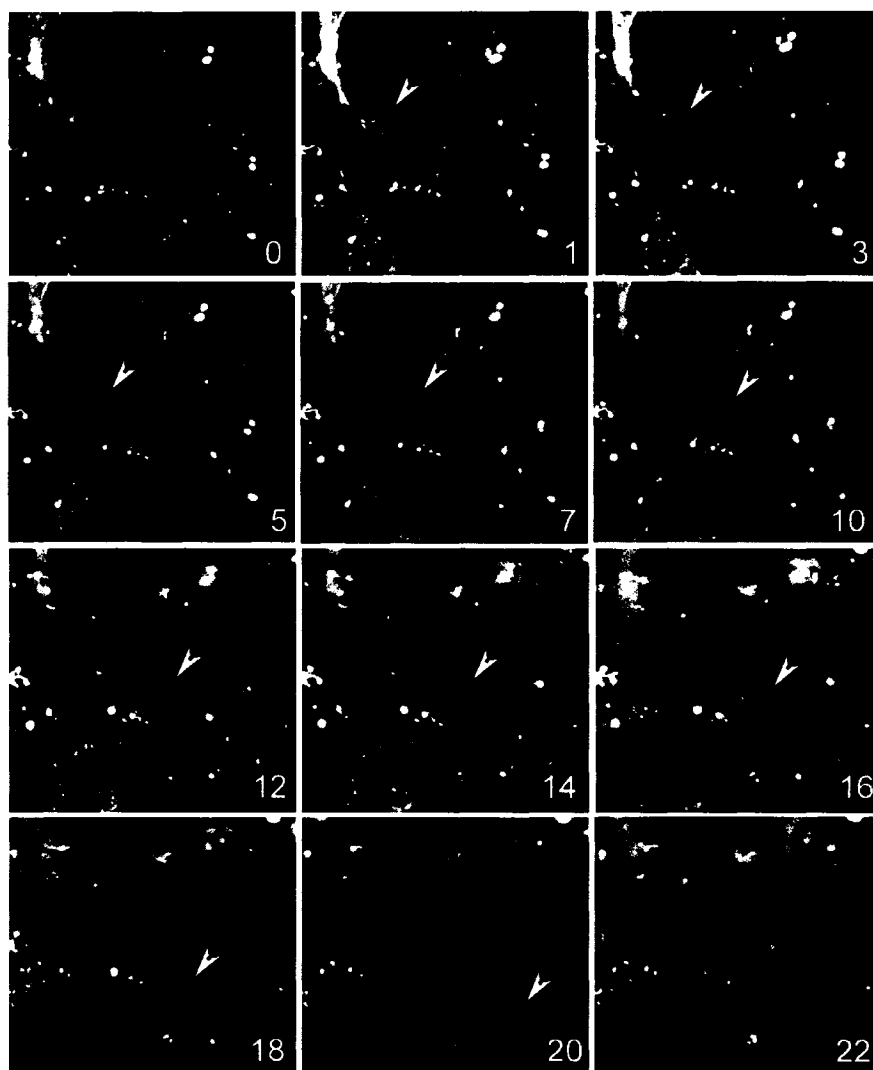
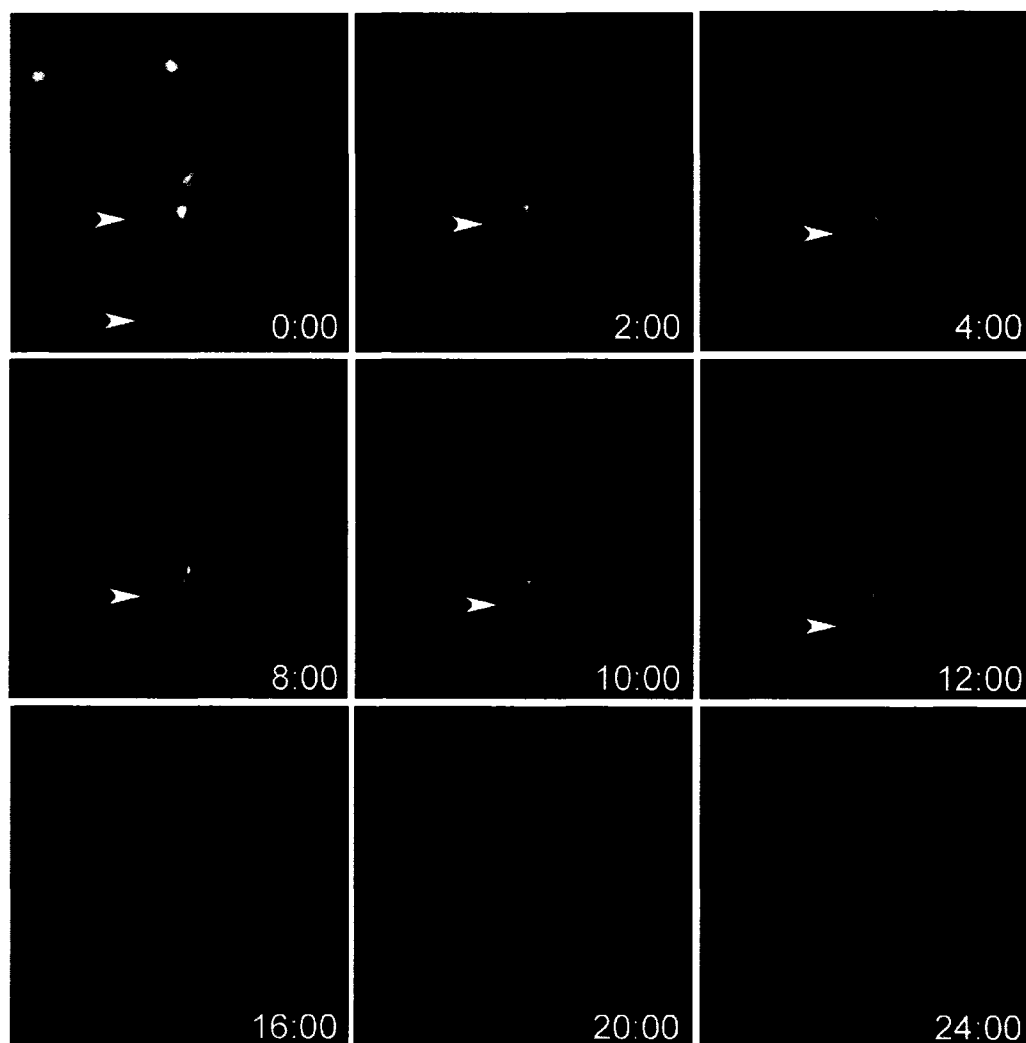


Figure 4.20. Waves occur in Thy1-YFP labeled neurons in hippocampal slices. A time-lapse series is shown of a Thy1-YFP expressing neuron near the CA3 region of a P1 hippocampal slice. The images are maximum projections of 6, 1 μm steps of a Z series. The soma of this neuron is not within the field of view. The white arrowhead indicates a wave traveling towards the distal tip of the neurite (red arrowhead). This wave travels $\sim 30 \mu\text{m}$ in 20 min (average speed of $1.5 \mu\text{m}/\text{min}$).



Thy1-YFP

Figure 4.21. Waves occur in neurons expressing GFP-actin in hippocampal slices: waves contribute to branch growth in hippocampal slice cultures. A time-lapse series is shown of a GFP-actin expressing neuron in the dentate gyrus of a P2 hippocampal slice 3 days post-infection. The images are single planes in a Z-series. Time in minutes is indicated in lower right corner of the images. The soma of this neuron is above the field of view. The white arrowhead indicates a wave traveling anterograde along the neurite. Notice the prominent shaft filopodia on this neurite (green arrowhead). This wave travels at an average speed of $\sim 2.4\mu\text{m}/\text{min}$ until reaching the shaft protrusion (0:16). The wave then engorges the filopodia (0:20) and subsequently extends a new branch (see Movie 4.11).

20:00	0:00
24:00	4:00
28:00	8:00
32:00	12:00
38:00	16:00

outgrowth (Heideman et al., 2003; Rosso et al., 2004; Toriyama et al., 2006; Turnsun et al., 2007). Our study presents the first evidence that waves occur in the more physiologically relevant brain slice in which neurons maintain many of their normal cell contacts and continue to grow in a 3D matrix. Waves contribute to axon differentiation, perhaps via the transport of actin and other growth-promoting molecules and by elevating growth cone dynamics.

What are waves?

Our observations from time-lapse imaging confirm earlier work suggesting that waves have a growth cone-like structure, and contain actin filaments and microtubules (Ruthel and Banker, 1998). Waves have a similar hand-like morphology to growth cones and contain a core of microtubules which splay into the actin-rich peripheral lamellipodial and filopodial domains (see Figure 3 and 4). Since actively propagating waves undergo arrest and collapse in the presence of cytochalasin and nocodazole, but not in the presence of Brefeldin A, it appears both microtubules and actin, but not Golgi-derived vesicles, are necessary for their propagation (Ruthel and Banker, 1998), similar to the behavior of growth cones (Bradke and Dotti, 2000; Ruthel and Hollenbeck, 2001). Our results show that various positive regulators of growth cone motility are enriched in waves, including cofilin, Lim kinase, Slingshot, Arp3, Rap1, Rac1 and cdc42. Wave dynamics are virtually identical to highly motile growth cones, but not to more quiescent growth cones. This implies that waves contain a repertoire of molecules that facilitate their dynamics, including cytoskeleton-regulating proteins. Conceivably, the loss or inactivation of some key component(s) underlies decreases in wave motility, eventually leading to their collapse into the neurite shaft, which we observed in a small number of instances. This may be similar to growth cone collapse, which can be induced by changes in actin regulating proteins (Gallo and Letourneau, 2004). We also observed that waves travel at a rates ranging from 1-6 μ m/min, a rate similar to the advance rates of rapidly extending axonal growth cones.

How waves are initiated remains unclear from our studies. Reminiscent of growth cone initiation (Delmelt and Halpain, 2003; Dent et al., 2007), we often observed

lamellipodial ruffling and filopodial extensions occurring at the soma prior to wave matriculation. However, in other instances waves materialize at the base of neurites with no obvious previous increase membrane dynamics. We favor a model in which high level of biosynthesis occurring in the soma, leads to the local accumulation of molecular repertoires for wave production in discrete regions of the soma. When a certain threshold or minimal requirement is reached, there is local activation of actin assembly leading to membrane protrusion along a pre-existing neurite, which serves as the path of least resistance. The locations of wave formation may initially be random, but later as axon development proceeds sites of wave initiation may become defined to discrete locations.

Waves and axon development

To investigate the function of waves in neuronal development we performed long-term live-cell imaging experiments on hippocampal neurons in culture. In young, stage 2 neurons, waves occur indiscriminately in all of the minor processes. However, in a neuron undergoing a stage 2-3 transition, there is over a 2 fold increase in wave propagation in the developing axon compared to the other minor processes. Furthermore, waves have a greater impact on transitory growth spurts in the developing axon compared to the other neurites. Thus, not only is wave frequency increased in the developing axon, but also the impact of waves is greater in the axon versus the minor processes. This suggests that individual waves may have fundamental differences (all waves are not equal) or that the growth cones of different neurites have pre-existing differences producing varied responses upon wave arrival (all growth cones are not equal). Although we observed that waves were diverse in their size and advance rates, our studies cannot rule out that inherent diversity of growth cones biases differential responses to wave arrival, especially considering that wave-induced changes in growth cone dynamics depended on the preexisting dynamic state of the growth cone. We also observed that abrupt, short-term increases in wave frequency provided greater impetus for neurite extension than waves arriving in isolation. In one case we observed a train of 5 waves occur in tandem immediately preceding a rapid burst of growth and the subsequent development of the axon.

The observation that waves occur more frequently and have greater impact on growth in the developing axon suggests that waves provide some impetus for axon differentiation. To further study the involvement of waves in axon development we looked at the influence of molecular signals that are axonogenic, i.e. cues that promote axon development and/or axon length. Neurotrophin 3 (NT3), a potent axonogenic cue, greatly increases axon length and branching of hippocampal neurons (LaBelle et al., 2000; Yoshimura et al., 2005). However, NT3 treatment reduced axon differentiation, growth and neurite branching on poly-lysine, but increased axon growth and branching in neurons cultured on poly-lysine-laminin substrates. This finding is interesting and leads to further questions for future studies regarding the signaling pathways that lead to these contrasting phenotypes. In parallel with the changes in axon development were corresponding changes in wave frequency. These data further support our hypothesis that waves promote axon specification since molecules that induce axon formation also increase the propagation of waves.

Waves and neurite branching

During development *in vivo* and in culture, most neurons form extensively branched neurite networks. In cortical neurons, axonal branching requires interactions between dynamic microtubules and actin filaments. Axonal branching can be inhibited by treatment of developing neurons with drugs that disrupt the dynamics of either microtubule or actin but at concentrations below those affecting axon outgrowth (Dent and Kalil, 2001). Interestingly, treatment of neurons with actin destabilizing drugs also impedes wave propagation (Ruthel and Banker, 1999) suggesting a possible link between waves and branching. Axon branches can form as a bifurcation from large paused growth cones, when an accumulation of F-actin forms a filopodium, which becomes stabilized and invaded by polymerizing microtubules (Dent and Kalil, 2001). Occasionally, when a wave reaches the growth cone, a new branch is formed, perhaps by modulating the interactions of dynamic microtubules and actin.

After a single axon has multiple branches, it has been reported that there is an intrinsic competition for growth among the branches such that when one branch elongates, there is concomitant retraction of other branches (Ruthel and Hollenbeck, 2001). We have observed that waves reaching a branch point may “choose” one branch or the other and

thereby can contribute to the differential growth of axonal branches as previously reported (Ruthel and Banker, 1999). However, we have also observed situations where a wave bifurcates at a branch point, traversing both branches which undergo a burst of outgrowth.

In addition to the formation of branches at the growth cone, collateral branches can also form along the neurite shafts, although a detailed time-lapse experiment characterizing this collateral sprouting is lacking. We have observed waves inducing collateral branching in the neurite shaft. In these situations, it appears that the wave reaches a stable shaft filopodium and induces its engorgement, elongation, and the formation of a branch. Thus, it appears that waves not only lead to differential branch growth, but also can induce new axon collateral branches.

Further circumstantial evidence for the involvement of waves in branch formation comes from our NT3 studies. NT3 treatment of neurons on a laminin substrate increased axon branching by >2-fold compared to untreated neurons. The increase in wave frequency under these conditions suggests that waves may be involved in NT3-induced axon branching. Another possibility is that the observed increase in filopodia structures in the presence of NT3 presented more opportunities for neurite branching to occur, since stable filopodia appear to be features conducive for branch growth.

Waves increase growth cone motility

Previous studies on axon formation have shown that the growth cone of one of multiple minor processes enlarges and displays increased dynamics (Bradke and Dotti, 1997, 1999; Ruthel and Hollenbeck, 2001; Kunda et al., 2001). This neurite undergoes rapid elongation forming the axon. Other studies have shown a correlation between rapidly extending neurites and dynamic growth cones (Gallo and Letourneau, 2004). Thus, we sought to determine how wave arrival at the distal tips of neurites affects growth cone motility. In these experiments we observed over a 2.5 fold increase in growth cone size and over a 1.6 fold increase in growth cone dynamics. However, the influence of waves on growth cone dynamics depended on the prior activity of the growth cone. Although wave arrival caused increased dynamics in growth cones that were previously active, waves

merging with inactive growth cones had a much greater effect on growth cone activity. Thus, waves influence axon development by increasing growth cone dynamics, which is a prerequisite for axon specification. One reason that may underlie the observed increase in growth cone dynamics as well as the burst of outgrowth is that waves transport a bolus of materials that promote growth cone activity and neurite extension. Theoretically, if size is the only thing that matters, wave arrival can provide enough material for the extension of 20 μm of neurite shaft if growth cone area expands from 50 μm^2 to 150 μm^2 . This is based on our measurement where 10 μm of shaft < 50 μm^2 and we commonly observed an increase in the size of a growth cone following wave arrival of > 100 μm^2 .

Waves represent a transport mechanism

Over 30 years ago, actin was identified to travel in slow component b (SCb) of axonal transport in mature neurons (Black and Lasek, 1979; Lasek, 1982). Yet three decades later, exactly how actin is transported remains elusive. It has been suggested that actin is transported in a filamentous form along microtubules, as are tubulin and neurofilament proteins (Baas and Buster, 2004) or via the less dogmatic mechanism of propagating growth-cone like waves that carry actin to the distal neurite (Ruthel and Banker, 1999). More recent evidence has shown that beta actin mRNA is transported down axons to the growth cone where local translation synthesizes at least some nascent actin protein (Piper and Holt, 2004). However, it seems unlikely that mRNA transport and local protein synthesis alone could support the rapid elongation of growing neurites. Furthermore, the observation that actin synthesized in the soma is later incorporated in actin structures in the distal neurite, suggests that the delivery of actin is important to neuronal development and function. Although it has been suggested that actin is transported via waves, there has been no empirical evidence supporting this hypothesis.

Here we directly observed the anterograde movement of fluorescently labeled actin in waves. Because we could not rule out the possibility that as waves move forward they cause a rearrangement of the cortical actin in the neurite shaft and result in no net translocation of actin, we used photo-activatable GFP-actin, which was only activated within the wave,

to ascertain if actin was traveling with the wave. We observed that a portion of this actin reached the growth cone after traveling a 25 μm distance. However, it did not appear that all of the actin arrived at the neurite tip. This suggests that as the wave travels forward, actin subunits turnover in the wave and some of these exchange with the existing actin subunit pool in the neurite shaft while the majority is recycled through actin filaments in the wave as it advances forward. This is reminiscent of the situation within growth cones. When paGFP-actin in growth cones is photo-activated, the actin initially remains associated with dynamic filaments and most subunits released from treadmilling filaments get reincorporated but some subunits exchange with unlabeled ones and the fluorescence eventually dissipates. The tendency for actin to remain associated with the growth cone is related to its advance rate, which is related to the continuous reutilization of subunits in treadmilling filaments (Marsh and Letourneau, 1984; Letourneau et al., 1987). If paGFP-actin is activated in growth cones where advance does not occur, fluorescence is found to dissipate more rapidly and appear back in the soma within 5-10 min. Analogously, waves that contribute to greater neurite outgrowth may also deliver more actin and/or other important growth promoting factors.

One other axon growth promoting molecule we observe traveling in waves is cofilin, which was previously reported to be transported with actin in SCb (Mills et al., 1996). Proteins of the ADF/cofilin family are actin dynamizing proteins, important for neurite outgrowth, axon development, growth cone motility and pathfinding (Meberg and Bamburg, 2000; Endo et al., 2001; Garvalov et al., 2007; Wen et al., 2007). Not only is cofilin transported with waves, but it appears to be the dephosphorylated (active) form that is most prevalent, suggesting its role in wave motility is similar to its role in growth cones. Another axon-promoting molecule, Shootin, was also recently shown to be transported in waves (Toriyama et al., 2006). Thus, waves may represent a mechanism for transporting large amounts of growth promoting molecules to growth cones, thereby promoting axonogenesis. Although an attractive hypothesis, this is certainly not the only means for transport of these molecules. We have observed a small percentage (<10%) of neurons do not exhibit waves over a time-course of hours in culture, yet still have active neurite outgrowth and periodic fluctuations in growth cone size and motility. In addition, we have observed gradual

accumulations of cofilin in growth cones without any obvious wave transport. Thus waves appear to represent an alternative or supplemental transport mechanism to the quintessential microtubule motor-based transport. Waves are unique in that they can supply large amounts of materials and can be employed during early neuronal development when there are rapid phases of neurite outgrowth and neurite lengths are much shorter.

Waves occur *in vivo*

Among his many contributions to neuroscience, the legendary Santiago Ramón y Cajal described the anatomy and development of the hippocampus (Ramón y Cajal, 1911). In one particularly famous drawing from this work, Ramón y Cajal diagramed the circuitry of an embryonic cat hippocampus from his silver chromate staining of fixed specimens. This schematic illustrates the tips of neurites, which, Ramón y Cajal designated in an earlier publication as the “growth cone” and, with amazing intuition, described as a structure “... endowed with amoeboid movements” (Ramón y Cajal, 1894). Unfortunately, he did not elaborate on the other growth cone-like structures that were present along the shaft of the neurite in the mossy fiber tract as well as those illustrated in sections of developing chick spinal cord (Ramón y Cajal, 1894). In examining these century old illustrations we asked ourselves, did Ramón y Cajal depict waves in these illustrations? Did Ramón y Cajal discover waves? Regrettably, we were unable to find any descriptions by Ramón y Cajal that the structure illustrated in the developing neurons were waves. Nor could we find any other *in vivo* references to waves.

Because waves have only been described in cultured neurons, their relevance to *in vivo* neuronal development is rightfully questioned. Thus we sought to determine if waves are pertinent to neuronal development in neurons maintained within a more *in vivo* environment, the organotypic hippocampal slice culture. We used three approaches to determine if waves could be visualized within slices: the use of transgenic mice expressing Thy1-GFP which labels membrane, labeling of neuronal membranes with DiI, and adenoviral-mediated transgene expression of fluorescent proteins. From all of these methods to label neuronal membranes, we observed waves traveling down neurites in developing neurons.

Interestingly, we never observed long axons with active growth cones that also exhibited waves. This may suggest that waves are only important during the initial, rapid phase of neurite growth, but it might also reflect the limited number of long axons we examined.

Waves of the Future

A decade has passed since waves were first described, yet only a handful of papers in recent years have recognized the possibility that waves may have important functions in neuronal development. Here we have pursued an extensive investigation of the role of waves in during axon development and neurite branching. Future work will hopefully further elucidate the molecular underpinnings of waves and their role in other processes such as axon guidance and regeneration.

Chapter 5

General Discussion and Future Directions

General Discussion

Neurons comprise a very heterogeneous cell type, differing in their locality, their size, shape and the chemical messages they use for communication. They can be glutamatergic, GABAergic, or dopaminergic (etc...). They can be sensory, motor, autonomic or fall into many other categories as well. They can be multipolar, bipolar, or unipolar. In spite of their differences, all neurons share the one common attribute of being polarized. All neurons need to be able to receive and transmit signals (typically in a unidirectional fashion). To achieve this end, neurons have evolved distinct structural and molecular compartmentalization providing unique properties to different regions of the cell. This is at the epicenter of nervous system function. Therefore it is imperative to understand how neurons become polarized during development. Furthermore, this knowledge may hold the key for treating developmental disorders, disease and trauma-related nervous system damage that may compromise neuronal polarity.

The work embodied here contributes to the growing progress that is being made towards understanding neuronal polarization. There are complex diverging and converging signaling pathways involving a multitude of molecular players affecting the cellular cytoskeleton (Yoshimura et al., 2007). Here we define a role for the GTPase, cdc42 as well as two actin binding proteins, cofilin and myosin II, during neuronal polarization. These proteins appear to be part of a common polarization pathway. However, none of these proteins acts in isolation or without the input of a repertoire of other molecules. Furthermore, some neurons completely lacking cdc42 can still polarize. Neurons with greatly reduced cofilin levels can still polarize in some cases. Neurons without myosin activity run amuck with supernumerary axons, but some of these still form one axon. Nevertheless, it is obvious that without the 'normal' function of each of these proteins neuronal polarization is compromised to some degree.

The regulation of intracellular trafficking is also important for the development of neuronal polarity. Of particular importance is the transport of actin in the axon, which may be rate-limiting for neurite extension. Despite years of effort to elucidate a mechanism, how actin is transported in neurons has remained elusive. Ruthel and Banker (1998, 1999) presented the hypothesis that growth cone-like waves may be a mechanism for actin transport in neurons. Here we provide evidence supporting this hypothesis and show that waves deliver actin to the distal neurite. We also characterize waves in greater detail as traveling in a manner consistent with growth cone motility, correlating with axonogenesis, increasing growth cone dynamics and occurring in an *in vivo*-like environment. Waves may also have an important role in the formation of neurite arbors; another essential feature of neuronal polarization and neural circuitry.

A unified model for cdc42, myosin II, cofilin, and waves during neuronal polarization.

The evidence from our work suggests interplay between intracellular pathways involving cdc42, cofilin, myosin II and wave propagation during the establishment of neuronal polarity. At first the link appears tenuous, but upon more careful assessment of the evidence we shall see that there is the foundation for a unified model. This evidence comes not only from our work, but also from diverse studies in neurons as well as non-neuronal systems. We will briefly consider extracellular signals that impinge upon all these proteins and waves, the common features of growth cones and waves, how the effects these proteins may have parallel effects on growth cones and waves, and the distinction of different actin structures in motile cells which may apply to distinct actin filament sub-populations in growth cones and waves.

First of all, extracellular signals known to affect axon development and growth can affect the activity of cdc42, cofilin, and myosin II. Furthermore, these signals may affect the generation and/or dynamics of wave propagation. Let us first consider the neurotrophin, NT3. Its role in enhancing axon growth and branching in hippocampal neurons is well documented (Labelle and Leclerc, 2000; Yoshimura et al., 2005; Flynn and Bamberg, 2008). NT3 can lead to increased activation of cdc42 (Yamauchi et al., 2005) and cofilin (Flynn unpublished observations). Although evidence for its modulation of myosin II activity is lacking, NT3

does change ROCK activity (Chan et al., 2008), a known upstream regulator of myosin II activity (Totsukawa et al., 2000). Furthermore, we see in our work that wave propagation is augmented with NT3 treatment. Another extracellular signal, IGF-1, whose receptor is essential for neuronal polarization, also signals to cdc42 (Sosa et al., 2005), cofilin and myosin II (Flynn et al., 2008). It remains unknown if IGF-1 affects waves.

In growth cones, the morphological consequences of cdc42 activation, cofilin activity, and myosin II inhibition have some similarities, yet important distinctions. Cdc42 activation and increasing cofilin activity can result in growth cones with increased size (Brown et al., 2000; Meberg and Bamberg, 2000; Gehler et al., 2005). All three of these modifications result in altered filopodial protrusions (Brown et al., 2000; Gehler et al., 2005; Bridgeman et al., 2001). Cdc42 has a drastic impact on the organization of F-actin in growth cones. The increased activation of cdc42 results in decreased F-actin in the central domain, but increased F-actin bundles in the peripheral domain (Kuhn et al., 2000). This could facilitate microtubule protrusions into the peripheral domain of growth cones, which is known to occur along parallel F-actin bundles. Interestingly, the ablation of cdc42 expression results in larger growth cones as well, with decreased F-actin in the central domain but decreased filopodia and no increase in F-actin bundles in the peripheral domain. The microtubules did penetrate deeper and splayed out into the growth cone, but often looped around as if inhibited from the most distal regions (Garvalov et al., 2007). Increased cofilin expression permits the penetration of microtubules deeper into the growth cone (Meberg and Bamberg, 2000) as does the inhibition of myosin II (Ketschek et al., 2007).

The increased microtubule penetration is significant for growth cones and waves. First of all, microtubule penetration into the peripheral domain of the growth cone is thought to signify increased neurite outgrowth, and this may be due, at least in part, to microtubule-mediated modifications of actin dynamics. For example, microtubules penetrating into the growth cone induce localized sites of actin polymerization called intrapodia (Rochlin et al., 1999). Microtubules may deliver molecules that regulate actin dynamics or may affect actin via cross-linking proteins. Thus, in growth cones there is a cyclical feedback of actin and microtubule interactions to provide for optimal growth cone advance. Since microtubules

penetrate into the peripheral actin-rich regions in waves, this actin-microtubule crosstalk is likely important for wave propagation as well. Indeed, microtubule destabilizing drugs prohibit wave advance, causing the dissipation of the wave (Ruthel and Banker, 1998). Microtubule advance into growth cones also underlies the formation of neurite branches via microtubule engorgement of stable filopodia (Dent and Kalil, 2001). This appears to be true of waves as well, which can engorge shaft filopodia and induce collateral formation from the neurite shaft.

Cofilin and myosin II may contribute to actin dynamics in the growth cone by modulating different populations of actin filaments (or actin superstructures) (Pak et al., 2008). We see that there is the highest level of cofilin activation in the peripheral domain of the developing axonal growth cone. Conversely, myosin II activity is punctate throughout the peripheral domain, but more heavily concentrated towards the central domain of growth cones. Myosin II activity regulates the compression and dissolution of actin arcs in a ROCK-dependent manner in the transitional domain but also regulates actin retrograde flow in the peripheral domain of growth cones in a ROCK-independent manner (Zhang et al., 2003). Retrograde flow still occurs due to actin turnover (Medeiros et al., 2006) which may be mediated by ADF/cofilin. Indeed we have observed decreased dynamics and F-actin retrograde flow in neurons with reduced levels of cofilin (see future directions, Figure 4). These data support the notion that there may be distinct populations of actin filaments in growth cones, one dominated by myosin II and the other dominated by cofilin. In the peripheral domain, these actin structures may spatially overlap and, in combination, are responsible for actin turnover, underlying filopodia and lamellipodial dynamics in the growth cone. Although distinct, these actin networks are in a constant state of flux; they may be interconverted via the binding of different ensembles of actin binding proteins. For example the competition between tropomyosin and cofilin binding can be shifted by cofilin activation, resulting in a displacement of tropomyosin and loss of myosin II contractile activity, which seems to be associated with tropomyosin-decorated filaments.

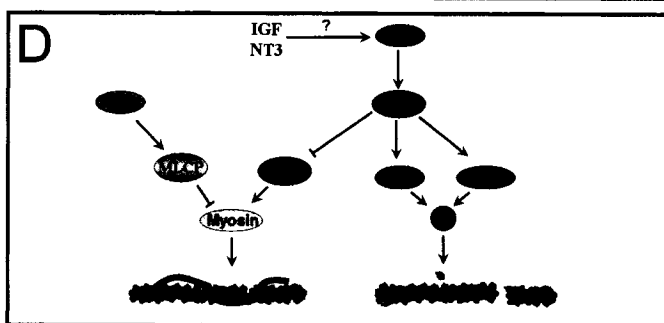
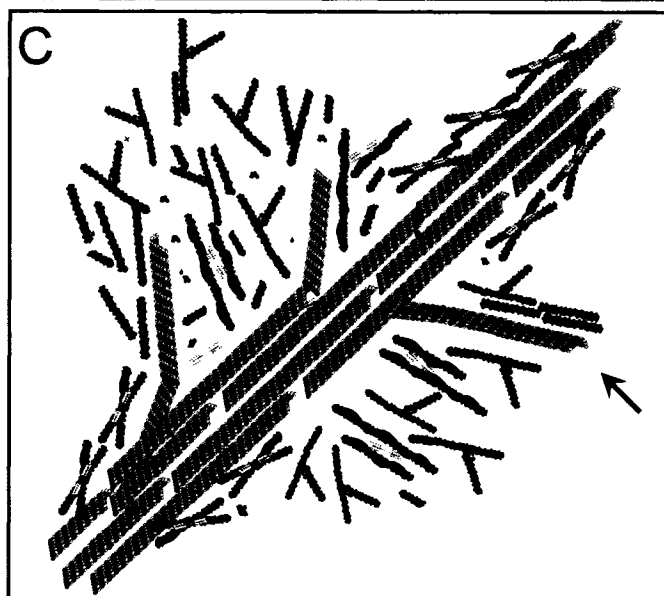
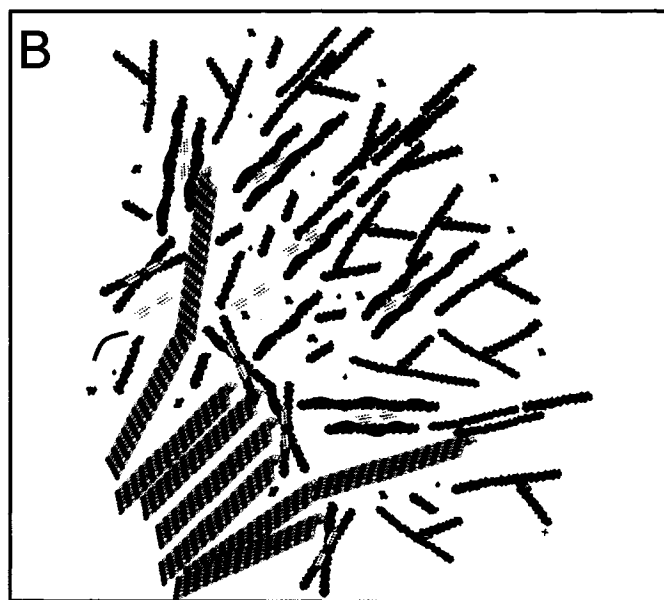
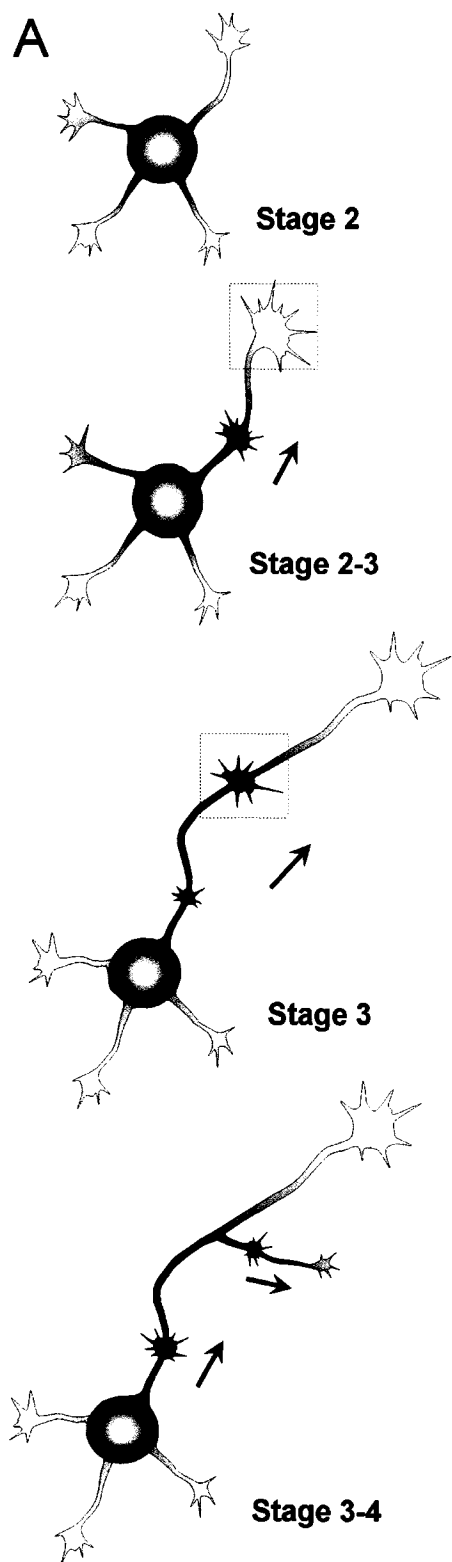
Although other actin binding proteins are certainly involved, cdc42 modulation of both myosin II and cofilin is required for optimal axon formation. Thus the modulation of various

populations actin structures, including those binding tropomyosin/myosin II or cofilin, are downstream of cdc42 (Figure 1).

In waves, there may be a similar segregation of distinct, overlapping actin networks. Like growth cones, waves have the distinct actin structures of filopodia and lamellipodia in the periphery as well as splaying microtubules. Cofilin and myosin II may also be two proteins that are involved in partitioning different actin populations in waves. As in growth cones, cofilin activity is localized to the peripheral domain of waves (see chapter 4). Although not examined in detail, myosin II activity seems limited within the wave itself to the central region, perhaps even below the amounts found in growth cones. However, increased myosin activity is seen in advance of and behind waves, suggesting a role for actomyosin contraction in regulating the extent and/or propagation of waves by modifying surrounding actin structures. Increasing cofilin activity via over-expression and inhibiting myosin II with blebbistatin both result in the increased presence of waves. Furthermore, we see a greater impact of wave arrival on neurite growth when myosin II is inhibited, suggesting that myosin activity acts to restrict waves from influencing neurite growth. The role of cdc42 in regulating waves has not been directly examined in these studies, but it would not be surprising if cdc42 regulates actin dynamics in waves.

A model is presented in Figure 1 of the discussion. During the stage 2-3 transition, growth cone dynamics increases in one neurite. This change is mediated by increased cofilin activity, decreased myosin activity, and the arrival of waves (Figure 1A). The combined effects of these measures increase actin based motility of the growth cone, including increasing actin turnover and filopodia protrusions. The increased actin dynamics, mediated by decreased actomyosin contractility (of HMW tropomyosin decorated filaments) and increased cofilin-mediated actin turnover, in turn, also influences microtubule dynamics, which penetrate into more distal regions of the growth cone (Figure 1B). Waves mediate axon development by delivery of actin and other molecules that increase actin dynamics and create a positive potential for microtubule extension. In the waves, cofilin and myosin regulate different actin networks, modulating the dynamics and rate of wave propagation (Figure 1C). The actin in waves is being recycled and interchanged with the cortical actin in the neurite as the wave

Figure 5.1. A comprehensive model for the role of cdc42, cofilin, myosin II and waves during neuronal polarization. **A.** A schematic diagram of the morphological changes that occur during axonogenesis. A stage 2 neuron has multiple minor neurites with the similar levels of cdc42, cofilin and myosin II activity. This results in similar growth cones actin dynamics. Intracellular transport, including waves delivering actin are occurring occur relatively uniformly in all processes. At the stage 2-3 transition there is a stochastic shift (in the absence of extracellular cues) in one of the growth cones with increased size and dynamics. There is also an increase in the frequency of waves to that growth cone which contributes to the increases in growth cone size and dynamics. As a result the axon elongates forming a stage 3 neuron which maintains increased growth cone dynamics and increased wave frequency. In stage 3-4 neurons axonal branching occurs and this is facilitated by waves. **B.** A simplified view of the intracellular cytoskeleton of a Stage 2-3 growth cone. There is increased cofilin activity (purple molecule), binding to a subpopulation of actin filaments (red filaments) and inducing increased actin turnover. Interspersed with cofilin bound filaments are another subpopulation of filaments decorated with HMW tropomyosin (brown lines), which competes with cofilin binding. These filaments (green filaments) can recruit myosin II (yellow) which can increase actin retrograde flow and the compression and severing of filaments in actin arcs towards the central domain of the growth cone. In the stage 2-3 growth cones reduced acto-myosin contractility and increased cofilin activity release inhibitory interactions allowing microtubule advance into the peripheral growth cone, creating a favorable environment for axon growth. **C.** In waves there are similar features of the actin cytoskeleton with increased cofilin activity (red filaments) and decreased myosin activity (green filaments). Microtubules also penetrate into the peripheral wave, which can facilitate wave advance. There are regions of myosin II activation in advance of and trailing the wave. This could modulate the extent and propagation of waves and limit filopodial protrusions. Occasionally waves, in the void of myosin activation, will allow a stable penetration of microtubules along F-actin creating protrusions that can serve as new branch points (arrow). Subsequent waves, delivering supportive materials, may be involved in the maturation of new branches. **D.** Signaling pathways involving cdc42 regulation of myosin II and Cofilin (AC) are involved in these cytoskeletal changes facilitating axon formation. Signaling to multiple types of actin structures facilitate optimal actin dynamics during axonogenesis.



propagates. However, a portion of actin travels with the wave, delivering increased actin to the axonal growth cone. This increase of actin in growth cones is also necessary for growth cone consolidation, during which is assembled the cylindrical actin network of the extending neurite shaft.

Furthermore, waves induce and support new branch formation. This entails the engorgement of a stabilized filopodium, which act as the foundation for new branch growth. Subsequent wave arrivals can then deliver actin and support the extension of the newly formed branch (arrow in Figure 1C). There is evidence that cdc42, cofilin and myosin II are all involved in branching. Of these, a particularly prominent force is myosin II activity, which is normally high in the cortical actin of the neurite shaft. A flux in myosin II activity can release some inhibitory constraint on branch formation, perhaps a simple loss of an actin barrier to microtubule advance into a filopodia, which initiates the beginning of a new branch. Cofilin can also participate in this by increasing actin turnover and the generation of shaft filopodia (Meberg and Bamburg, 2000). Waves can provide this localized increase in cofilin activity and actin dynamics as well as a void in myosin II activity. The materials carried in the wave then can be effectively delivered at the branch-point.

Cdc42 has not been directly examined for a function in wave formation. However, given its regulation of cofilin and myosin II in growth cones and in axon formation as well as the fact cdc42 is enriched in waves, it seems likely that cdc42 signaling facilitates wave propagation. Furthermore, cdc42 knockout neurons have reduced shaft filopodia and branching (Boyan Garvalov, personal communication). This suggests a role of cdc42 in wave propagation and neurite branching, perhaps mediated via cofilin and myosin.

Future Directions

A commonplace in science is that the more we know, the more questions we have. This statement holds true with this dissertation. There are gaps in our knowledge, interesting observations begging further study, and temporal-related questions; what happens next or what happened before?

Gaps in our knowledge

Despite the progress, there are gaps in our understanding of neuronal polarization. Some are obvious, some more obscure. Ideally we strive for a continuum in the experimental results leading to a nice linear story. Unfortunately, there are breaches in that continuum. This is not for the lack of trying, but the lack of tools (and time) necessary for their proper pursuit. Here we will consider some of the obvious gaps that arise from this study.

Although it is apparent that *cdc42* regulates cofilin and myosin II during neuronal polarization, there are mysterious breaches in the signaling pathways confusing a clear understanding of *cdc42*-mediated signal transduction during axonogenesis. For example, PAK1 activity is decreased while LimK activity is increased in the *cdc42* knockout brain. This is perplexing because the canonical signaling pathways that have been worked out in most other systems show that PAK1 phosphorylates and activates LimK on thr 508 of LIMK1 or 505 of LIMK2. Thus, in *cdc42* KO brain, there should be a decrease in Lim Kinase activity and an increase in dephosphorylated cofilin, but the converse is observed. Interestingly, a *cdc42*-dependent activation of ADF/cofilin has been observed in the growth cones of retinal ganglion neurons, which appears to function through a decrease in Rho GTPase/ROCK/LIMK1 pathway for cofilin phosphorylation, suggesting that in *cdc42* null neurons the ROCK/LIMK1 pathway might be enhanced. However, the ROCK pathway does not appear to be a significant player in axiogenesis (Garvalov et al., 2007). An alternative possibility is that slingshot phosphatase, which in addition to activating cofilin, can dephosphorylate and inactivate LimK (Soosairajah et al., 2005), declines in *cdc42* knockout brain. Although we did observe a decrease in the cofilin phosphatase activity, we do not know if this activity is from slingshot or chronophin, and if it is slingshot, whether or not slingshot's activity toward LimK is altered. It would be interesting to determine if slingshot acts as a diverging signaling protein in this context, activating cofilin directly while indirectly blocking its phosphorylation through LimK.

Because Rho activity does not seem to change in the *cdc42* knockout mice, the Rho-ROCK-MLCK signaling pathway is probably not involved in the activation of myosin II activity in the *cdc42* knockout brain. However, decreased activity of PAK1 may possibly

lead to changes in myosin activity either via the decreased phosphorylation and increased activation of MLCK (Sanders et al., 1999), leading to increased Myosin II activity. A more direct experimental approach would clarify how myosin activity is perturbed in the *cdc42* knockout.

There are a multitude of other actin binding proteins present in growth cones, many of which also may be of importance in axon formation (Dent and Gertler, 2003). Furthermore, many of these proteins may act downstream of *cdc42*. One such protein, or complex of proteins is the Arp2/3 complex, which can act downstream of *cdc42* via nWasp (Millard et al., 2004). The Arp2/3 complex is an actin nucleator, involved in the generation of branched actin networks in motile cells (Pollard et al., 2001) and axon extension and guidance in hippocampal neurons (Strasser et al., 2004). In preliminary studies, we determined that Arp2/3 localizes to the developing axonal growth cone (Figure 2). In unpublished work, we used siRNA to knockdown endogenous Arp3, which effectively inhibits the activity of Arp2/3 complex and leads to a reduction in axon formation in a cell-to-cell contact dependent manner, suggesting that engagement of integrin (or another cell-cell extracellular mediated) signaling pathways may compensate for the loss of Arp3 during axon formation (Figure 3). Growth cones from neurons with reduced Arp3 levels also displayed abnormal morphology with decreased F-actin staining and decreased size. These data suggest that Arp3 plays a role in axon formation, but it remains unknown if Arp3 acts downstream of *cdc42*.

Interesting Observations.

Neurons with reduced cofilin levels are deficient in their ability to develop an axon. There are numerous possible mechanistic explanations for this deficiency, but one particularly attractive explanation is that cofilin knockdown results in perturbations in growth cone dynamics. In order to explore this possibility we observed the growth cones of neurons expressing RFP-actin and either control siRNA or cofilin siRNA. We observed an overall reduction in growth cone dynamics in neurons expressing cofilin siRNA (Figure 4). In particular we notice that growth cones with reduced cofilin levels had delayed filopodial retraction. This could reflect decreased actin turnover in the growth cone, which is difficult to assess from these

Figure 5.2. Arp3 is distributed to the developing axonal growth cone. Hippocampal neurons from the transgenic mouse expressing GFP under the control of the constitutive CAG promoter were fixed and immunostained for Arp3. GFP serves as a volumetric marker (right). The ratio of Arp3/GFP, presented as a pseudocolor intensity image (right) indicates localization of Arp2/3 complex in developing neurons. In the stage 2 neuron, Arp3 is enriched in the neurite with the largest growth cone of the presumptive axon (top row). Arp3 is enriched in the growth cone of the axon in stage 3 neurons (bottom row).

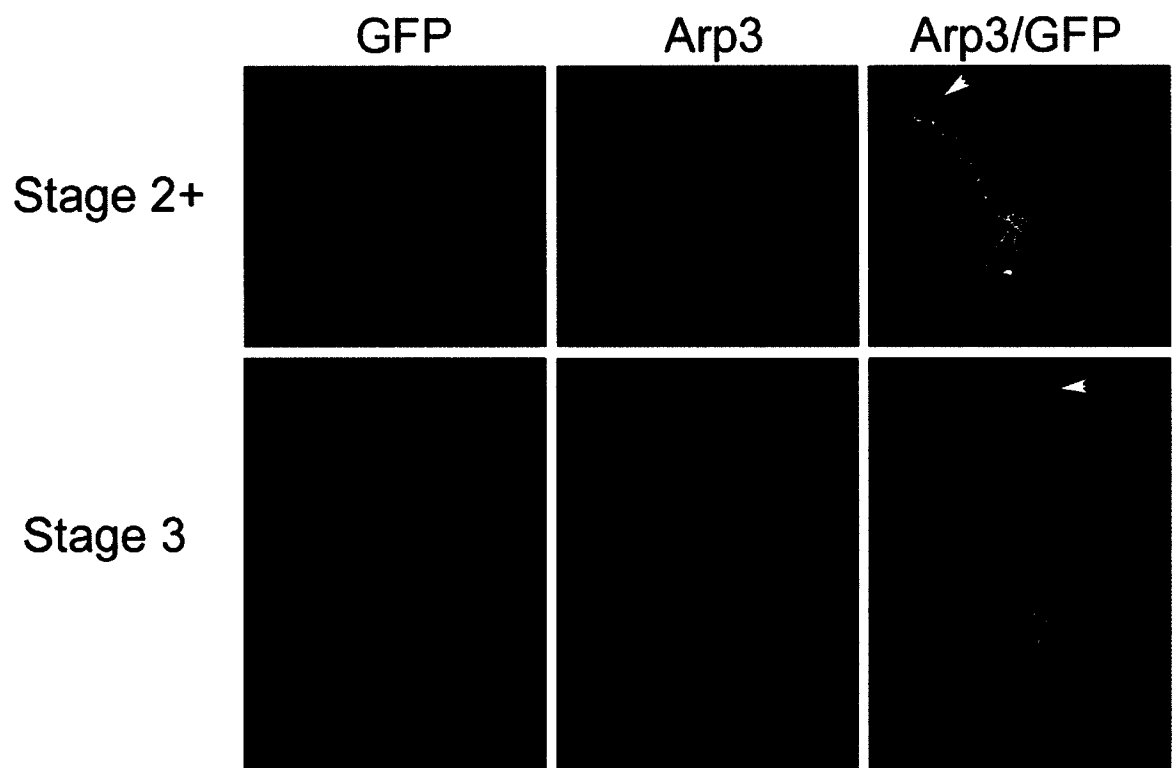
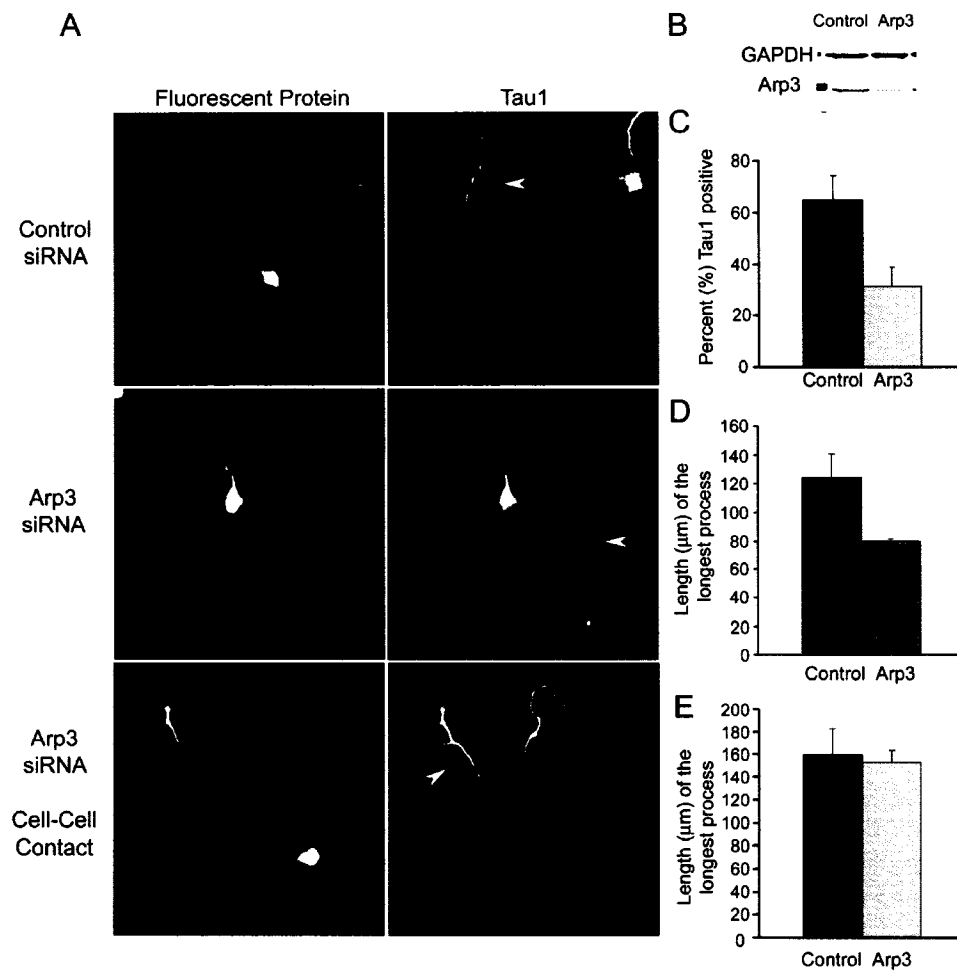


Figure 5.3 siRNA-mediated silencing of Arp3 depresses axon formation in a cell-cell contact dependent manner. **A.** Hippocampal neurons expressing siRNA target to Arp3 via adenovirus mediated delivery were fixed and stained for the axonal marker Tau-1 at 4 div (right). Fluorescent protein was co-expressed with the siRNA from a separate promoter on the in the same DNA (left). Neurons expressing control siRNA (targets GFP) typically had one long Tau1 positive process (top row). Isolated neurons, (those not making contacts with other cells) expressing Arp3 siRNA had treduced Tau1 positive axons (middle row). However, when neurons expressing Arp3 siRNA are in contact with other cells, they form Tau1 positive axons (Bottom row). **B.** Adenoviral-mediated delivery of siRNA was effective in knocking down expression of Arp3 by 75 percent in Swiss 3T3 fibroblasts as confirmed by Western Blot, normalized to the GAPDH loading control. **C.** The percentage of Tau-1 positive neurites was calculated from control neurons infected with a GFP siRNA and in Arp3 siRNA expressing neurons that were not in contact with other cells. In control neurons, 64.7% of the neurons had Tau-1 processes, while only 31.3% of Arp3 siRNA expressing cells had Tau-1 positive processes. **D.** The length of longest neurite was decreased in neurons expressing Arp3 siRNA when they are not in contact with other cells. The average length of the longest neurites of isolated cells expressing Arp3 siRNA was 79.7 μ m, while the average length of the longest process in control neurons was 124.7 μ m. **E.** When neurons are in contact with other cells, the length of the longest process in Arp3 silenced neurons was not different from controls. The average length of the longest neurite of neurons expressing Arp 3 siRNA was 152.7 μ m and neurons expressing control siRNA was 159.6 μ m.



experiments. We could utilize photoactivatable-GFP-actin in order to address this issue. We have been able to successfully photoactivate a thin, 2-5 μm line perpendicular to the axis of the neurite proper and observe F-actin retrograde flow (Figure 5). It will be interesting in future studies to determine if retrograde F-actin flow is in fact altered by cofilin knockdown (or by its over-expression). Further studies on actin dynamics are also necessary to determine the mechanism underlying myosin II-regulation of axon formation. Does myosin II play a similar role in F-actin retrograde flow in hippocampal growth cones as reported in the large immobile growth cones of *Aplysia* Bag cell neurons (Medeiros et al., 2006)?

Without stable, yet polymerization-competent microtubules, axon formation does not occur. Does the modulation of actin dynamics by cofilin and myosin II alter microtubule advance into growth cones? This issue can be pursued via the use of GFP tagged-EB1, which is a live-cell marker for the polymerizing + ends of microtubules. In growth cones we have observed EB-1 decorated microtubules which can be followed over time and observed exploring peripheral regions of the growth cone (Figure 6).

These above mentioned experiments are also applicable for studies of wave dynamics. Do cofilin and myosin II have similar effects in waves? For example, with myosin inhibition we observed qualitatively that waves had longer and apparently more dynamic filopodia. This observation could reflect fundamental differences in the retrograde actin flow in waves.

With myosin inhibition we observed more extensive neurite branching, but the underlying mechanism is unclear. This mechanism could be related to waves. We observed a region of myosin activation preceding and trailing waves. This bracketing of wave boundaries could help limit the ability of waves to initiate new branches. In support of this idea, we do observe in some cases when myosin II is inhibited that waves seemed to give rise to more neurite branches than in control neurons. This observation could explain the increased neurite arborization observed in neurons treated with blebbistatin.

What happened before?

Before there is an axon there are neurites. From our studies, *cdc42* does not seem to affect neuritogenesis: after 16hrs in culture *cdc42* KO neurons are indistinguishable from control

Figure 5.4. Growth cone motility is decreased in neurons with depleted cofilin levels.

Shown are time-lapse images of neurons expressing RFP-actin and either control siRNA (left) of cofilin siRNA (right). Time is indicated in lower right corner of images (in minutes:seconds). Hippocampal neurons expressing control siRNA (left) have dynamic growth cones, extending and retracting filopodia and lamellipodia protrusions. Growth cones of neurons expressing cofilin siRNA have depressed growth cone motility (right). Notice that over the time-course presented, the overall shape of the growth cone expressing siRNA does not change significantly. The three filopodial protrusions observed at 0:00 are still present at time 0:50. Future studies can be pursued quantifying the growth cone dynamics of neurons with depleted cofilin levels and of neurons with decreased myosin activity.

Control siRNA

Cofilin siRNA

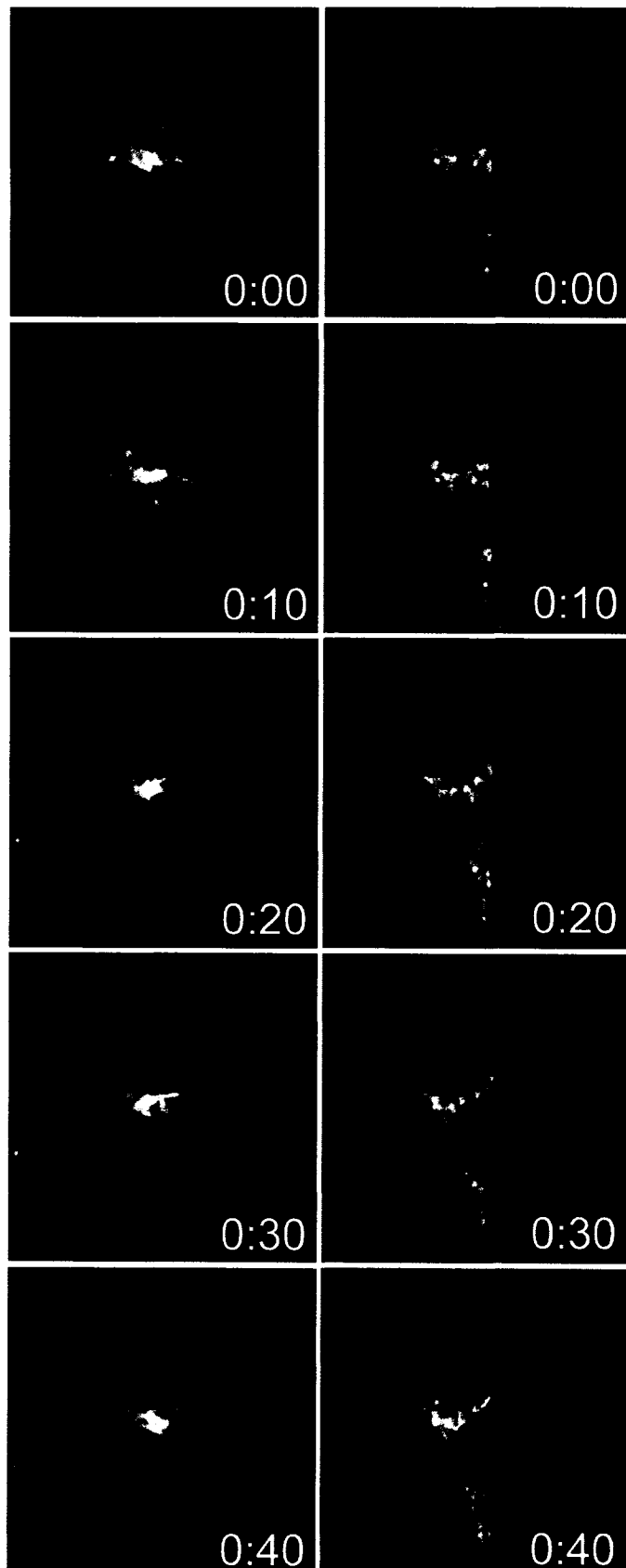
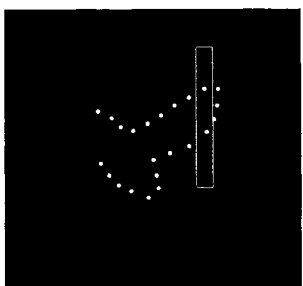


Figure 5.5. Photoactivation of PA-GFP-actin can be used to follow retrograde actin flow in growth cones. Time-lapse images of a neuronal growth cone expressing photoactivatable-GFP-actin are shown. The time following photoactivation (1.5 second 405nm light pulse) is shown in lower right corner (seconds). Before photoactivation there is an extremely dim GFP signal in this hippocampal growth cone (outline with white points). Time is indicated in lower right corner of images (in minutes:seconds). The region photoactivated was a 2.5 μ m wide line indicated in the top panel. The retrograde flow of actin is apparent in the subsequent images. 18 seconds following photactivation the displacement of actin was 2.1 μ m (arrow). For this growth cone, the actin retrograde flow was $\sim 7\mu\text{m}/\text{min}$.



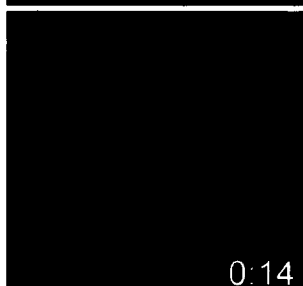
0:02



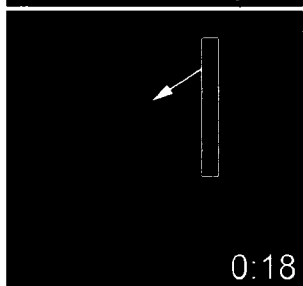
0:06



0:10



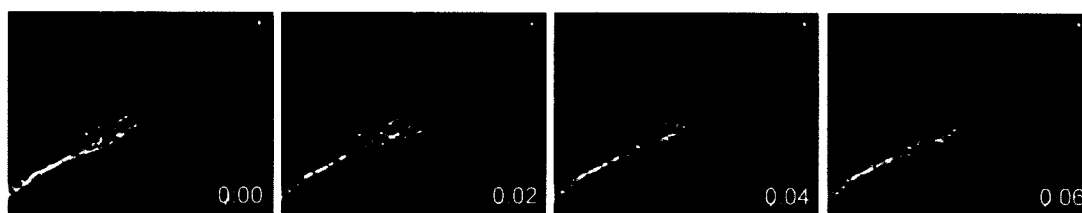
0:14



0:18

Figure 5.6. EB-1-GFP dynamics in growth cones allows tracking of microtubule tips.

Shown is a time-series of a growth cone from a hippocampal neuron expressing EB-1 fused to GFP. EB1 associates only to the growing tips of microtubule + ends. Time is indicated in the lower right corner of images. Notice that the fluorescent signal is highest in the central domain of the growth cone, but many dynamic microtubules extend into the peripheral growth cone. When microtubules stop polymerization and undergo a catastrophe, EB-1 falls off the microtubule. In this growth cone, EB1-GFP tips can be observed advancing and then disappear (arrow at 0:00), presumably indicating a catastrophe. EB-1-GFP expression in growth cones can be used in experiments studying the effects of myosin II inhibition and cofilin activity on microtubule dynamics.



neurons and form neurites normally. This observation is unremarkable in and of itself, but in light of new work, suggesting that filopodia are absolutely essential for neurite formation (Dent et al., 2007) the ability for *cdc42* neurons to extend processes is perplexing. It is perplexing because *cdc42* KO neurons are extremely deficient in their ability to form filopodia (Garvalov et al., 2007). Without filopodia, how do *cdc42* KO neurons generate neurites? A simple time-lapse imaging experiment of freshly seeded *cdc42* KO neurons would answer this question and if neurites do form, it would strongly support the alternative model of Dehmelt et al. (2007) in which microtubule bundling within the extended lamellipodium leads to the formation of the neurite shaft without a filopodial requirement.

We often observe extensive lamellipodial and filopodial dynamics around the somata of neurons preceding wave propagation. In short neurites, waves are difficult to detect and appear as ruffling membranes. Recent work has shown that Hem1/Scar/WAVE complex-mediated F-actin waves organize leading edge advance in non-neuronal cells (Weiner et al., 2007). Do waves organize the leading edge protrusions of nascent neurites? Is Hem1/Scar/WAVE complex involved in actin waves in neurons? Although the Hem1 waves were clearly discernable via TIRF, they could also be detected via confocal microscopy. It would be interesting to see if wave-like structures (lamellipodia) organize the protrusion of neurites.

What happens next?

There is a drastic decrease in wave activity in older hippocampal neurons in culture (Ruthel and Banker, 1999) and in slices (Chapter 4). Is there a further decrease in wave activity in even older neurons (Stage 5)? After neurite growth has stopped completely, how is actin transported in mature neurons? Although actin travels in slow component b of axonal transport, it is still unclear how actin is transported in mature neurons.

After an axon forms, it must navigate to a target for synaptogenesis. Although cofilin has been clearly shown act as a binary switch mediating both attractive and repulsive growth cone turning events in *Xenopus* spinal neurons (Wen et al., 2007), it is unknown if cofilin is crucial for the guidance of hippocampal axons. Semaphorins are plausible candidates for restricting axon growth along discrete routes in the hippocampus (Chédotal et al., 1998)

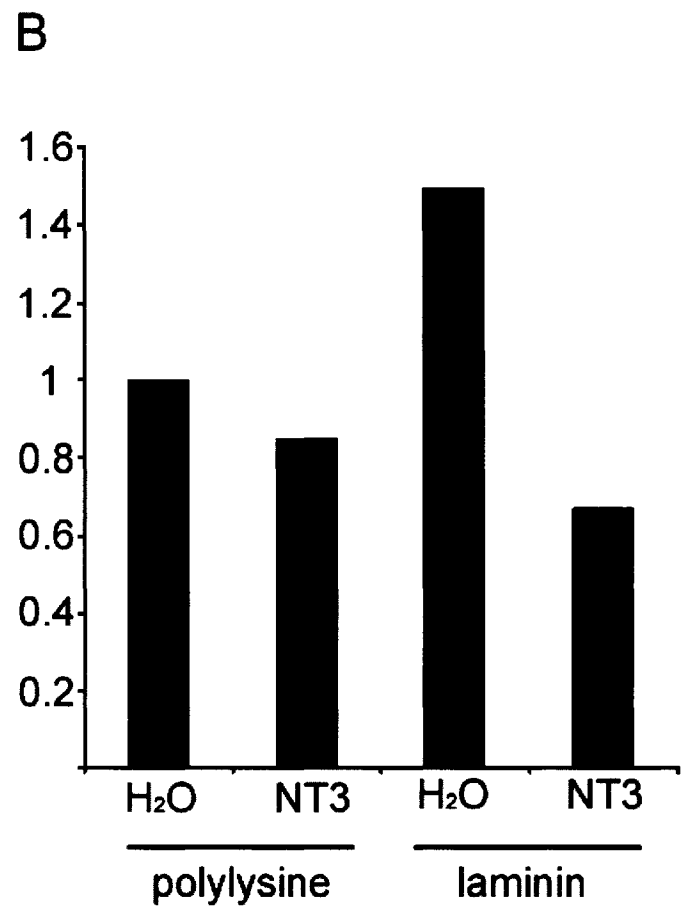
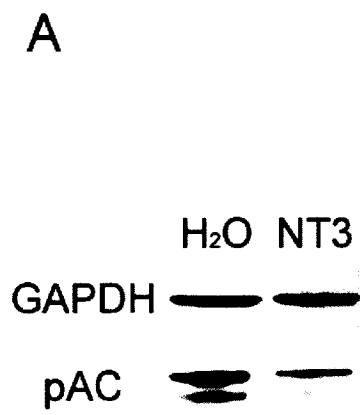
and cofilin activity is necessary for sema3A-mediated growth cone collapse in dorsal root ganglion neurons (Aiwi et al., 2001). Are hippocampal neuronal growth cones also regulated by semaphorin-mediated guidance? Another potential positive cue is NT3, which increases axon growth and branching in culture and is expressed in developing hippocampus (Friedman et al., 1991). NT3 treatment increases cofilin activity (Figure 7). It will be interesting to see if NT3 is an important guidance cue for the formation of neural circuits in the hippocampus and if cdc42, myosin II and cofilin are its downstream effectors.

In mature neurons cdc42, cofilin and myosin II may also be part of a common signaling pathway in the morphogenesis of dendritic spines. It would be interesting to determine if cdc42 KO neurons can form dendritic spines and if cofilin and myosin contribute downstream of cdc42 to regulate spine formation. This hypothesis seems probable since filopodia are precursors to spine morphogenesis and cdc42, cofilin and myosin II all contribute to filopodial protrusions in younger neurons (Garvalov et al., 2007; Chen et al., 2006; Bridgman et al., 2001). However, the experiments may not be very feasible since long term survival of cdc42 null neurons is difficult to achieve, even when using apoptotic inhibitors in the culture medium.

Lastly, a major goal of research in axon growth and guidance is understanding the developmental mechanisms with the prospect of applying that knowledge in promoting neural regeneration following trauma or disease. During such damage the axon is often compromised, while the somato-dendritic compartment remains intact. In the mammalian adult CNS, axon regeneration is inhibited by a multitude of inhibitory factors that appear at the site of injury, including myelin associated inhibitors (Nogo, MAG, etc...), chondroitin proteoglycan sulfates and reactive glial cells (Yiu and He, 2006). One possible approach to overcoming regenerative failure is to harness signaling molecules involved in axon extension and growth cone motility. The Rho GTPases, including cdc42, and their downstream effectors have thus been considered possible targets for intervention. Signaling pathways affecting myosin II and cofilin activity are engaged by myelin associated inhibitors and axon growth can be restored via the manipulation of signals upstream in neuronal cultures (Hsieh et al., 2006; Alabed et al., 2006). It remains to be seen the effects of modulating cofilin and

Figure 5.7. Neurotrophin 3 affects ADF/cofilin phosphorylation in neurons. A.

Neuronal extracts were collected from cortical neurons (4div) treated with vehicle (PBS) or NT3 (100ng/ml) for 30 minutes. Western blot shows phosphorylated ADF/cofilin (pAC) (lower band) and GAPDH (upper band). Note the decrease in pAC levels in neurons treated with NT3. These extracts are from neurons plated on laminin, which could modulate NT3-mediated signaling pathways. **B.** Quantification of densitometry (total lab) of western blots shows that the effect of NT3 on the level of pAC varies depending on substrate. On polylysine, NT3 treatment resulted in a small decrease in pAC. On laminin, which has a higher level of constitutive pAC levels, NT3 treatment causes over a 2-fold reduction in pAC levels. Future experiments can explore the signal cascades involved in NT3-mediated enhancement of axon formation.



myosin II activity during *in vivo* axonal regeneration. It will also be of interest to determine if waves are reinitiated during axonal regeneration in culture and *in vivo*.

Significant progress has been made in deciphering the roles of cdc42, cofilin, and myosin II regulation of actin structures in growth cones and waves during neuronal development. As evidenced here, there are many unanswered questions. New avenues of research involving new tools from various fields of science (for example, proteomics and nanotechnology) will continue to provide insight into how actin structures are organized and regulated in cells.

After all, the goal is nothing less than a comprehensive understanding of the role of actin-regulating proteins (especially cofilin) in every aspect of neuronal development and disease.

References

- Abe, H., T. Obinata, L.S. Minamide, and J.R. Bamburg. 1996. Xenopus laevis actin-depolymerizing factor/cofilin: a phosphorylation-regulated protein essential for development. *Journal of Cell Biology*. 132:871-85.
- Abe, H., S. Ohshima, and T. Obinata. 1989. A cofilin-like protein is involved in the regulation of actin assembly in developing skeletal muscle. *J Biochem*. 106:696-702.
- Abe, T., M. Kato, H. Miki, T. Takenawa, and T. Endo. 2003. Small GTPase Tc10 and its homologue RhoT induce N-WASP-mediated long process formation and neurite outgrowth. *J Cell Sci*. 116:155-68.
- Adams, M.E., L.S. Minamide, G. Duester, and J.R. Bamburg. 1990. Nucleotide sequence and expression of a cDNA encoding chick brain actin depolymerizing factor. *Biochemistry*. 29:7414-20.
- Agnew, B.J., L.S. Minamide, and J.R. Bamburg. 1995. Reactivation of phosphorylated actin depolymerizing factor and identification of the regulatory site. *Journal of Biological Chemistry*. 270:17582-7.
- Aguda, A.H., L.D. Burtnick, and R.C. Robinson. 2005. The state of the filament. *EMBO Rep*. 6:220-6.
- Ahmad, F.J., W. Yu, F.J. McNally, and P.W. Baas. 1999. An essential role for katanin in severing microtubules in the neuron. *J Cell Biol*. 145:305-15.
- Aitken, A., D.B. Collinge, B.P. van Heusden, T. Isobe, P.H. Roseboom, G. Rosenfeld, and J. Soll. 1992. 14-3-3 proteins: a highly conserved, widespread family of eukaryotic proteins. *Trends in Biochemical Sciences*. 17:498-501.
- Aizawa, H., S. Wakatsuki, A. Ishii, K. Moriyama, Y. Sasaki, K. Ohashi, Y. Sekine-Aizawa, A. Sehara-Fujisawa, K. Mizuno, Y. Goshima, and I. Yahara. 2001a. Phosphorylation of cofilin by LIM-kinase is necessary for semaphorin 3A-induced growth cone collapse. *Nat Neurosci*. 4:367-73.
- Aizawa, H., S. Wakatsuki, A. Ishii, K. Moriyama, Y. Sasaki, K. Ohashi, Y. Sekine-Aizawa, A. Sehara-Fujisawa, K. Mizuno, Y. Goshima, and I. Yahara. 2001b. Phosphorylation of cofilin by LIM-kinase is necessary for semaphorin 3A-induced growth cone collapse. *Nature Neuroscience*. 4:367-73.
- Alabed, Y.Z., E. Grados-Munro, G.B. Ferraro, S.H. Hsieh, and A.E. Fournier. 2006. Neuronal responses to myelin are mediated by rho kinase. *J Neurochem*. 96:1616-25.
- Alberts, P., R. Rudge, T. Irinopoulou, L. Danglot, C. Gauthier-Rouviere, and T. Galli. 2006. Cdc42 and actin control polarized expression of TI-VAMP vesicles to neuronal growth cones and their fusion with the plasma membrane. *Mol.Biol.Cell*. 17:1194-1203.
- Amano, M., K. Chihara, N. Nakamura, Y. Fukata, T. Yano, M. Shibata, M. Ikebe, and K. Kaibuchi. 1998. Myosin II activation promotes neurite retraction during the action of Rho and Rho-kinase. *Genes Cells*. 3:177-88.
- Anderson, SS, Bi GQ. 2000. Axon formation: a molecular model for the generation of neuronal polarity. *BioEssays* 22:172-179
- Andrianantoandro, E., L. Blanchoin, D. Sept, J.A. McCammon, and T.D. Pollard. 2001. Kinetic mechanism of end-to-end annealing of actin filaments. *J Mol Biol*. 312:721-30.
- Andrianantoandro, E., and T.D. Pollard. 2006. Mechanism of actin filament turnover by

- severing and nucleation at different concentrations of ADF/cofilin. *Mol Cell*. 24:13-23.
- Aoki, K., T. Nakamura, and M. Matsuda. 2004. Spatio-temporal regulation of Rac1 and Cdc42 activity during nerve growth factor-induced neurite outgrowth in PC12 cells. *J Biol Chem*. 279:713-9.
- Arakawa, Y., H. Bito, T. Furuyashiki, T. Tsuji, S. Takemoto-Kimura, K. Kimura, K. Nozaki, N. Hashimoto, and S. Narumiya. 2003. Control of axon elongation via an SDF-1alpha/Rho/mDia pathway in cultured cerebellar granule neurons. *J Cell Biol*. 161:381-91.
- Arber, S., F.A. Barbayannis, H. Hanser, C. Schneider, C.A. Stanyon, O. Bernard, and P. Caroni. 1998. Regulation of actin dynamics through phosphorylation of cofilin by LIM-kinase.[see comment]. *Nature*. 393:805-9.
- Arimura, N., and K. Kaibuchi. 2005. Key regulators in neuronal polarity. *Neuron*. 48:881-884.
- Arimura, N., and K. Kaibuchi. 2007. Neuronal polarity: from extracellular signals to intracellular mechanisms. *Nat Rev Neurosci*. 8:194-205.
- Ashworth, S.L., E.L. Southgate, R.M. Sandoval, P.J. Meberg, J.R. Bamburg, and B.A. Molitoris. 2003. ADF/cofilin mediates actin cytoskeletal alterations in LLC-PK cells during ATP depletion. *Am J Physiol Renal Physiol*. 284:F852-62.
- Baas, P.W. 1996. The neuronal centrosome as a generator of microtubules for the axon. *Curr Top Dev Biol*. 33:281-98.
- Baas, P.W. 1997. Microtubules and axonal growth. *Curr Opin Cell Biol*. 9:29-36.
- Baas, P.W., and A. Brown. 1997. Slow axonal transport: the polymer transport model. *Trends Cell Biol*. 7:380-4.
- Baas, P.W., and D.W. Buster. 2004. Slow axonal transport and the genesis of neuronal morphology. *J Neurobiol*. 58:3-17.
- Balcer, H.I., A.L. Goodman, A.A. Rodal, E. Smith, J. Kugler, J.E. Heuser, and B.L. Goode. 2003. Coordinated regulation of actin filament turnover by a high-molecular-weight Srv2/CAP complex, cofilin, profilin, and Aip1. *Curr Biol*. 13:2159-69.
- Bamburg, J., L. Minamide, T. Morgan, S. Hayden, K. Giuliano, and A. Koffer. 1991. Purification and characterization of Low-molecular weight actin-depolymerizing proteins from brain and cultured cells. *Methods Enzymol*. 196:125-140.
- Bamburg, J.R. 1999a. Proteins of the ADF/cofilin family: essential regulators of actin dynamics. *Developmental Biology*. 15:185-230.
- Bamburg, J.R. 1999b. Proteins of the ADF/cofilin family: essential regulators of actin dynamics. *Annu Rev Cell Dev Biol*. 15:185-230.
- Bamburg, J.R., and B.W. Bernstein. 2008. ADF/Cofilin. *Curr Biol*. 18:R273-5.
- Bamburg, J.R., and D. Bray. 1987. Distribution and cellular localization of actin depolymerizing factor. *Journal of Cell Biology*. 105:2817-2825.
- Bamburg, J.R., D. Bray, and K. Chapman. 1986a. Assembly of microtubules at the tip of growing axons. *Nature*. 321:788-90.
- Bamburg, J.R., D. Bray, and K. Chapman. 1986b. Microtubule assembly in the axon. *Nature*. 323:400.
- Bamburg, J.R., H.E. Harris, and A.G. Weeds. 1980a. Partial purification and characterization of an actin depolymerizing factor from brain. *FEBS Letters*. 121:178-82.
- Bamburg, J.R., H.E. Harris, and A.G. Weeds. 1980b. Partial purification and characterization of an actin depolymerizing factor from brain. *FEBS Lett*. 121:178-82.

- Bamburg, J.R., A. McGough, and S. Ono. 1999. Putting a new twist on actin: ADF/cofilins modulate actin dynamics. *Trends Cell Biol.* 9:364-70.
- Bamburg, J.R., and O.P. Wiggan. 2002. ADF/cofilin and actin dynamics in disease. *Trends Cell Biol.* 12:598-605.
- Barzik, M., T.I. Kotova, H.N. Higgs, L. Hazelwood, D. Hanein, F.B. Gertler, and D.A. Schafer. 2005. Ena/VASP proteins enhance actin polymerization in the presence of barbed end capping proteins. *J Biol Chem.* 280:28653-62.
- Bassell, G.J., H. Zhang, A.L. Byrd, A.M. Femino, R.H. Singer, K.L. Taneja, L.M. Lifshitz, I.M. Herman, and K.S. Kosik. 1998. Sorting of beta-actin mRNA and protein to neurites and growth cones in culture. *J Neurosci.* 18:251-65.
- Bear, J.E., T.M. Svitkina, M. Krause, D.A. Schafer, J.J. Loureiro, G.A. Strasser, I.V. Maly, O.Y. Chaga, J.A. Cooper, G.G. Borisy, and F.B. Gertler. 2002. Antagonism between Ena/VASP proteins and actin filament capping regulates fibroblast motility. *Cell.* 109:509-21.
- Bellenchi, G.C., C.B. Gurniak, E. Perlas, S. Middei, M. Ammassari-Teule, and W. Witke. 2007. N-cofilin is associated with neuronal migration disorders and cell cycle control in the cerebral cortex. *Genes Dev.* 21:2347-2357.
- Bernstein, B.W., and J.R. Bamburg. 1982. Tropomyosin binding to F-actin protects the F-actin from disassembly by brain actin-depolymerizing factor (ADF). *Cell Motility.* 2:1-8.
- Bernstein, B.W., and J.R. Bamburg. 2003. Actin-ATP hydrolysis is a major energy drain for neurons. *Journal of Neuroscience.* 23:1-6.
- Bernstein, B.W., H. Chen, J.A. Boyle, and J.R. Bamburg. 2006. Formation of actin-ADF/cofilin rods transiently retards decline of mitochondrial potential and ATP in stressed neurons. *Am J Physiol Cell Physiol.* 291:C828-39.
- Bernstein, B.W., W.B. Painter, H. Chen, L.S. Minamide, H. Abe, and J.R. Bamburg. 2000a. Intracellular pH modulation of ADF/cofilin proteins. *Cell Motility & the Cytoskeleton.* 47:319-36.
- Bernstein, B.W., W.B. Painter, H. Chen, L.S. Minamide, H. Abe, and J.R. Bamburg. 2000b. Intracellular pH modulation of ADF/cofilin proteins. *Cell Motil Cytoskeleton.* 47:319-36.
- Birkenfeld, J., H. Betz, and D. Roth. 2003. Identification of cofilin and LIM-domain-containing protein kinase 1 as novel interaction partners of 14-3-3 zeta. *Biochemical Journal.* 369:45-54.
- Bishop, A.L., and A. Hall. 2000. Rho GTPases and their effector proteins. *Biochem J.* 348 Pt 2:241-55.
- Black, M.M., and R.J. Lasek. 1979. Axonal transport of actin: slow component b is the principal source of actin for the axon. *Brain Res.* 171:401-13.
- Blanchoin, L., K.J. Amann, H.N. Higgs, J.B. Marchand, D.A. Kaiser, and T.D. Pollard. 2000a. Direct observation of dendritic actin filament networks nucleated by Arp2/3 complex and WASP/Scar proteins. *Nature.* 404:1007-11.
- Blanchoin, L., T.D. Pollard, and R.D. Mullins. 2000b. Interactions of ADF/cofilin, Arp2/3 complex, capping protein and profilin in remodeling of branched actin filament networks. *Curr Biol.* 10:1273-82.
- Blanchoin, L., R.C. Robinson, S. Choe, and T.D. Pollard. 2000c. Phosphorylation of Acanthamoeba actophorin (ADF/cofilin) blocks interaction with actin without a change in atomic structure. *J Mol Biol.* 295:203-11.

- Boillee, S., C. Vande Velde, and D.W. Cleveland. 2006. ALS: a disease of motor neurons and their nonneuronal neighbors. *Neuron*. 52:39-59.
- Bonifacino, J.S., and L.M. Traub. 2003. Signals for sorting of transmembrane proteins to endosomes and lysosomes. *Annu Rev Biochem*. 72:395-447.
- Bradke, F., and C.G. Dotti. 1997. Neuronal polarity: vectorial cytoplasmic flow precedes axon formation. *Neuron*. 19:1175-1186.
- Bradke, F., and C.G. Dotti. 1999. The role of local actin instability in axon formation. *Science*. 283:1931-4.
- Bradke, F., and C.G. Dotti. 2000a. Differentiated neurons retain the capacity to generate axons from dendrites. *Curr.Biol*. 10:1467-1470.
- Bradke, F., and C.G. Dotti. 2000b. Establishment of neuronal polarity: lessons from cultured hippocampal neurons. *Curr.Opin.Neurobiol*. 10:574-581.
- Bray, D., and K. Chapman. 1985. Analysis of microspike movements on the neuronal growth cone. *J Neurosci*. 5:3204-13.
- Bray, D., N.P. Money, F.M. Harold, and J.R. Bamberg. 1991. Responses of growth cones to changes in osmolality of the surrounding medium. *Journal of Cell Science*. 98:507-15.
- Bray, J.J., P. Fernyhough, J.R. Bamberg, and D. Bray. 1992. Actin depolymerizing factor is a component of slow axonal transport. *J Neurochem*. 58:2081-7.
- Bridgman, P.C., S. Dave, C.F. Asnes, A.N. Tullio, and R.S. Adelstein. 2001. Myosin IIB is required for growth cone motility. *J Neurosci*. 21:6159-69.
- Brown, J., and P.C. Bridgman. 2003a. Role of myosin II in axon outgrowth. *J Histochem Cytochem*. 51:421-8.
- Brown, M.D., B.J. Cornejo, T.B. Kuhn, and J.R. Bamberg. 2000. Cdc42 stimulates neurite outgrowth and formation of growth cone filopodia and lamellipodia. *Journal of Neurobiology*. 43:352-64.
- Brown, M.E., and P.C. Bridgman. 2003b. Retrograde flow rate is increased in growth cones from myosin IIB knockout mice. *J Cell Sci*. 116:1087-94.
- Brown, M.E., and P.C. Bridgman. 2004a. Myosin function in nervous and sensory systems. *J Neurobiol*. 58:118-30.
- Brummelkamp, T.R., R. Bernards, and R. Agami. 2002. A system for stable expression of short interfering RNAs in mammalian cells. *Science*. 296:550-3.
- Bryce, N.S., G. Schevzov, V. Ferguson, J.M. Percival, J.J. Lin, F. Matsumura, J.R. Bamberg, P.L. Jeffrey, E.C. Hardeman, P. Gunning, and R.P. Weinberger. 2003. Specification of actin filament function and molecular composition by tropomyosin isoforms. *Mol Biol Cell*. 14:1002-16.
- Burack, M.A., M.A. Silverman, and G. Banker. 2000. The role of selective transport in neuronal protein sorting. *Neuron*. 26:465-72.
- Burnette, D.T., A.W. Schaefer, L. Ji, G. Danuser, and P. Forscher. 2007. Filopodial actin bundles are not necessary for microtubule advance into the peripheral domain of Aplysia neuronal growth cones. *Nat.Cell Biol*. 9:1360-1369.
- Cai, L., A.M. Makhov, and J.E. Bear. 2007. F-actin binding is essential for coronin 1B function in vivo. *J Cell Sci*. 120:1779-90.
- Carlier, M.F. 1990. Actin polymerization and ATP hydrolysis. *Adv Biophys*. 26:51-73.
- Carlier, M.F., V. Laurent, J. Santolini, R. Melki, D. Didry, G.X. Xia, Y. Hong, N.H. Chua, and D. Pantaloni. 1997. Actin depolymerizing factor (ADF/cofilin) enhances the rate of filament turnover: implication in actin-based motility. *J Cell Biol*. 136:1307-22.

- Chedotal, A., J.A. Del Rio, M. Ruiz, Z. He, V. Borrell, F. de Castro, F. Ezan, C.S. Goodman, M. Tessier-Lavigne, C. Sotelo, and E. Soriano. 1998. Semaphorins III and IV repel hippocampal axons via two distinct receptors. *Development*. 125:4313-23.
- Chen, H. 2001. In vitro analysis of the functional differences between proteins in the ADF/cofilin family. Colorado State University, Fort Collins, CO.
- Chen, H., B.W. Bernstein, and J.R. Bamburg. 2000. Regulating actin-filament dynamics in vivo. *Trends in Biochemical Sciences*. 25:19-23.
- Chen, H., B.W. Bernstein, J.M. Sneider, J.A. Boyle, L.S. Minamide, and J.R. Bamburg. 2004. In vitro activity differences between proteins of the ADF/cofilin family define two distinct subgroups. *Biochemistry*. 43:7127-42.
- Chen, T.J., S. Gehler, A.E. Shaw, J.R. Bamburg, and P.C. Letourneau. 2006. Cdc42 participates in the regulation of ADF/cofilin and retinal growth cone filopodia by brain derived neurotrophic factor. *J Neurobiol*. 66:103-14.
- Chen, X., and I.G. Macara. 2006. Par-3 mediates the inhibition of LIM kinase 2 to regulate cofilin phosphorylation and tight junction assembly. *J Cell Biol*. 172:671-8.
- Chuang, J.Z., T.Y. Yeh, F. Bollati, C. Conde, F. Canavosio, A. Caceres, and C.H. Sung. 2005. The dynein light chain Tctex-1 has a dynein-independent role in actin remodeling during neurite outgrowth. *Dev Cell*. 9:75-86.
- Clark, M.G., and D.C. Amberg. 2007. Biochemical and genetic analyses provide insight into the structural and mechanistic properties of actin filament disassembly by the Aip1p cofilin complex in *Saccharomyces cerevisiae*. *Genetics*. 176:1527-39.
- Cohan, C.S., E.A. Welnhofer, L. Zhao, F. Matsumura, and S. Yamashiro. 2001. Role of the actin bundling protein fascin in growth cone morphogenesis: localization in filopodia and lamellipodia. *Cell Motil Cytoskeleton*. 48:109-20.
- Cohen, P., and S. Frame. 2001. The renaissance of GSK3. *Nat Rev Mol Cell Biol*. 2:769-76.
- Condeelis, J. 2001. How is actin polymerization nucleated in vivo? *Trends in Cell Biology*. 11:288-93.
- Cowan, C.M., and L.A. Raymond. 2006. Selective neuronal degeneration in Huntington's disease. *Curr Top Dev Biol*. 75:25-71.
- Craig, A.M., and G. Banker. 1994. Neuronal polarity. *Annu Rev Neurosci*. 17:267-310.
- Craig, A.M., C.D. Blackstone, R.L. Huganir, and G. Banker. 1993. The distribution of glutamate receptors in cultured rat hippocampal neurons: postsynaptic clustering of AMPA-selective subunits. *Neuron*. 10:1055-68.
- Czuchra A., Wu X, Meyer H, van Hengel J, Schroeder T, Geffers R, Rottner K, Brakebusch C. 2005. Cdc42 is not essential for filopodium formation directed migration, cell polarization, and mitosis in fibroblastoid cells. *Mol Biol Cell*. 16: 4473-4484
- Da Silva, J.S., and C.G. Dotti. 2002. Breaking the neuronal sphere: regulation of the actin cytoskeleton in neuritogenesis. *Nat Rev Neurosci*. 3:694-704.
- Da Silva, J.S., M. Medina, C. Zuliani, A. Di Nardo, W. Witke, and C.G. Dotti. 2003. RhoA/ROCK regulation of neuritogenesis via profilin IIa-mediated control of actin stability. *J Cell Biol*. 162:1267-79.
- Dai, S., P.D. Sarmiere, O. Wiggan, J.R. Bamburg, and D. Zhou. 2004. Efficient *Salmonella* entry requires activity cycles of host ADF and cofilin. *Cell Microbiol*. 6:459-71.
- Dailey, M.E., and P.C. Bridgman. 1991. Structure and organization of membrane organelles along distal microtubule segments in growth cones. *J Neurosci Res*. 30:242-58.
- Dailey, M.E., J. Buchanan, D.E. Bergles, and S.J. Smith. 1994a. Mossy fiber growth and synaptogenesis in rat hippocampal slices in vitro. *J Neurosci*. 14:1060-78.

- Dang, D., J.R. Bamburg, and D.M. Ramos. 2006. Alpha β 3 integrin and cofilin modulate K1735 melanoma cell invasion. *Exp Cell Res.* 312:468-77.
- Dawe, H.R., L.S. Minamide, J.R. Bamburg, and L.P. Cramer. 2003a. ADF/cofilin controls cell polarity during fibroblast migration. *Curr Biol.* 13:252-7.
- Dawid, I.B. 1998. LIM protein interactions: Drosophila enters the stage. *Trends Genet.* 14:480-2.
- Dawid, I.B., J.J. Breen, and R. Toyama. 1998. LIM domains: multiple roles as adapters and functional modifiers in protein interactions. *Trends Genet.* 14:156-62.
- de Anda, F.C., G. Pollarolo, J.S. Da Silva, P.G. Camoletto, F. Feiguin, and C.G. Dotti. 2005. Centrosome localization determines neuronal polarity. *Nature.* 436:704-8.
- de Hoop, M.J., Meyn, L., and Dotti, C. G. 1998. Culturing Hippocampal Neurons and Astrocytes from Fetal Rodent Brain. Academic Press, San Diego. 154-163 pp.
- Dehmelt, L., and S. Halpain. 2004. Actin and microtubules in neurite initiation: are MAPs the missing link? *Journal of Neurobiology.* 58:18-33.
- Dehmelt, L., F.M. Smart, R.S. Ozer, and S. Halpain. 2003. The role of microtubule-associated protein 2c in the reorganization of microtubules and lamellipodia during neurite initiation. *J Neurosci.* 23:9479-90.
- Delorme, V., M. Machacek, C. DerMardirossian, K.L. Anderson, T. Wittmann, D. Hanein, C. Waterman-Storer, G. Danuser, and G.M. Bokoch. 2007. Cofilin activity downstream of pak1 regulates cell protrusion efficiency by organizing lamellipodium and lamella actin networks. *Dev.Cell.* 13:646-662.
- Dent, E.W., and F.B. Gertler. 2003. Cytoskeletal dynamics and transport in growth cone motility and axon guidance. *Neuron.* 40:209-227.
- Dent, E.W., and K. Kalil. 2001. Axon branching requires interactions between dynamic microtubules and actin filaments. *J.Neurosci.* 21:9757-9769.
- Dent, E.W., A.V. Kwiatkowski, L.M. Mebane, U. Philippar, M. Barzik, D.A. Robinson, S. Gupton, J.E. Van Veen, C. Furman, J. Zhang, A.S. Alberts, S. Mori, and F.B. Gertler. 2007. Filopodia are required for cortical neurite initiation. *Nat. Cell Biol.* 9:1347-1359.
- Desai, A., and T.J. Mitchison. 1997. Microtubule polymerization dynamics. *Annu Rev Cell Dev Biol.* 13:83-117.
- DesMarais, V., I. Ichetovkin, J. Condeelis, and S.E. Hitchcock-DeGregori. 2002. Spatial regulation of actin dynamics: a tropomyosin-free, actin-rich compartment at the leading edge. *J Cell Sci.* 115:4649-60.
- DesMarais, V., F. Macaluso, J. Condeelis, and M. Bailly. 2004. Synergistic interaction between the Arp2/3 complex and cofilin drives stimulated lamellipod extension. *J Cell Sci.* 117:3499-510.
- Devineni, N., L.S. Minamide, M. Niu, D. Safer, R. Verma, J.R. Bamburg, and V.T. Nachmias. 1999. A quantitative analysis of G-actin binding proteins and the G-actin pool in developing chick brain. *Brain Res.* 823:129-40.
- Dos Remedios, C.G., D. Chhabra, M. Kekic, I.V. Dedova, M. Tsubakihara, D.A. Berry, and N.J. Nosworthy. 2003. Actin binding proteins: regulation of cytoskeletal microfilaments. *Physiol Rev.* 83:433-73.
- Dotti, C.G., and G. Banker. 1991. Intracellular organization of hippocampal neurons during the development of neuronal polarity. *J Cell Sci Suppl.* 15:75-84.
- Dotti, C.G., and G.A. Banker. 1987. Experimentally induced alteration in the polarity of developing neurons. *Nature.* 330:254-6.

- Dotti, C.G., G.A. Banker, and L.I. Binder. 1987. The expression and distribution of the microtubule-associated proteins tau and microtubule-associated protein 2 in hippocampal neurons in the rat in situ and in cell culture. *Neuroscience*. 23:121-30.
- Dotti, C.G., C.A. Sullivan, and G.A. Banker. 1988. The establishment of polarity by hippocampal neurons in culture. *J Neurosci*. 8:1454-68.
- Edson, K., B. Weisshaar, and A. Matus. 1993. Actin depolymerisation induces process formation on MAP2-transfected non-neuronal cells. *Development*. 117:689-700.
- Edwards, D.C., L.C. Sanders, G.M. Bokoch, and G.N. Gill. 1999a. Activation of LIM-kinase by Pak1 couples Rac/Cdc42 GTPase signalling to actin cytoskeletal dynamics. *Nat Cell Biol*. 1:253-9.
- Elbashir, S.M. 2001. Duplexes of 21-nucleotide RNAs mediate RNA interference in cultured mammalian cells.[see comment]. *Nature*. 411:494-498.
- Endo, M., K. Ohashi, Y. Sasaki, Y. Goshima, R. Niwa, T. Uemura, and K. Mizuno. 2003. Control of growth cone motility and morphology by LIM kinase and Slingshot via phosphorylation and dephosphorylation of cofilin. *Journal of Neurosci*. 23:2527-37.
- Eng, H., K. Lund, and R.B. Campenot. 1999. Synthesis of beta-tubulin, actin, and other proteins in axons of sympathetic neurons in compartmented cultures. *J Neurosci*. 19:1-9.
- Esch, T., V. Lemmon, and G. Banker. 1999. Local presentation of substrate molecules directs axon specification by cultured hippocampal neurons. *Journal of Neuroscience*. 19:6417-26.
- Estornes, Y., F. Gay, J.C. Gevrey, S. Navoizat, M. Nejari, J.Y. Scoazec, J.A. Chayvialle, J.C. Saurin, and J. Abello. 2007. Differential involvement of destrin and cofilin-1 in the control of invasive properties of Isreco1 human colon cancer cells. *Int J Cancer*. 121:2162-71.
- Etienne-Manneville, S., and A. Hall. 2002. Rho GTPases in cell biology. *Nature*. 420:629-35.
- Etienne-Manneville, S., and A. Hall. 2003. Cdc42 regulates GSK-3beta and adenomatous polyposis coli to control cell polarity. *Nature*. 421:753-6.
- Etienne-Manneville, S. 2004. Cdc42-the centre of polarity. *J Cell Sci* 117: 1291-1300
- Faix, J., and R. Grosse. 2006. Staying in shape with formins. *Dev Cell*. 10:693-706.
- Falk, J., A. Bechara, R. Fiore, H. Nawabi, H. Zhou, C. Hoyo-Becerra, M. Bozon, G. Rougon, M. Grumet, A.W. Puschel, J.R. Sanes, and V. Castellani. 2005. Dual functional activity of semaphorin 3B is required for positioning the anterior commissure. *Neuron*. 48:63-75.
- Fass, J., S. Gehler, P. Sarmiere, P. Letourneau, and J.R. Bamberg. 2004. Regulating filopodial dynamics through actin-depolymerizing factor/cofilin. *Anat Sci Int*. 79:173-83.
- Feng, G., R.H. Mellor, M. Bernstein, C. Keller-Peck, Q.T. Nguyen, M. Wallace, J.M. Nerbonne, J.W. Lichtman, and J.R. Sanes. 2000. Imaging neuronal subsets in transgenic mice expressing multiple spectral variants of GFP. *Neuron*. 28:41-51.
- Fletcher, T.L., P. Cameron, P. De Camilli, and G. Banker. 1991. The distribution of synapsin I and synaptophysin in hippocampal neurons developing in culture. *J Neurosci*. 11:1617-26.
- Flynn, K.C., Pak, C., Bamberg, J. R. 2006. Regulation of growth cone initiation and actin dynamics by ADF/Cofilin. *In Intracellular Mechanisms of Neuritogenesis*. Vol. 1. I. de Curtis, editor. Springer, Heidelberg. 25-56.
- Foletta, V.C., N. Moussi, P.D. Sarmiere, J.R. Bamberg, and O. Bernard. 2004a. LIM kinase 1, a key regulator of actin dynamics, is widely expressed in embryonic and adult tissues. *Exp Cell Res*. 294:392-405.

- Forscher, P., and S.J. Smith. 1988. Actions of cytochalasins on the organization of actin filaments and microtubules in a neuronal growth cone. *J. Cell Biol.* 107:1505-1516.
- Fox, J.W., E.D. Lamperti, Y.Z. Eksioglu, S.E. Hong, Y. Feng, D.A. Graham, I.E. Scheffer, W.B. Dobyns, B.A. Hirsch, R.A. Radtke, S.F. Berkovic, P.R. Huttenlocher, and C.A. Walsh. 1998. Mutations in filamin 1 prevent migration of cerebral cortical neurons in human periventricular heterotopia. *Neuron.* 21:1315-25.
- Friedman, W.J., P. Ernfors, and H. Persson. 1991. Transient and persistent expression of NT-3/HDNF mRNA in the rat brain during postnatal development. *J Neurosci.* 11:1577-84.
- Fukata, Y., T.J. Itoh, T. Kimura, C. Menager, T. Nishimura, T. Shiromizu, H. Watanabe, N. Inagaki, A. Iwamatsu, H. Hotani, and K. Kaibuchi. 2002. CRMP-2 binds to tubulin heterodimers to promote microtubule assembly. *Nat Cell Biol.* 4:583-91.
- Galkin, V.E., A. Orlova, N. Lukyanova, W. Wriggers, and E.H. Egelman. 2001. Actin depolymerizing factor stabilizes an existing state of F-actin and can change the tilt of F-actin subunits. *J Cell Biol.* 153:75-86.
- Galkin, V.E., A. Orlova, M.S. VanLoock, I.N. Rybakova, J.M. Ervasti, and E.H. Egelman. 2002a. The utrophin actin-binding domain binds F-actin in two different modes: implications for the spectrin superfamily of proteins. *Journal of Cell Biology.* 157:243-51.
- Galkin, V.E., M.S. VanLoock, A. Orlova, and E.H. Egelman. 2002b. A new internal mode in F-actin helps explain the remarkable evolutionary conservation of actin's sequence and structure. *Current Biology.* 12:570-5.
- Gallo, G. 2003. Making proteins into drugs: assisted delivery of proteins and peptides into living neurons. *Methods in Cell Biology.* 71:325-38.
- Gallo, G. 2006. RhoA-kinase coordinates F-actin organization and myosin II activity during semaphorin-3A-induced axon retraction. *J Cell Sci.* 119:3413-23.
- Gallo, G., and P.C. Letourneau. 2004. Regulation of growth cone actin filaments by guidance cues. *J Neurobiol.* 58:92-102.
- Gallo, G., H.F. Yee, Jr., and P.C. Letourneau. 2002. Actin turnover is required to prevent axon retraction driven by endogenous actomyosin contractility. *J. Cell Biol.* 158:1219-1228.
- Gan WB, Grutzendler J, Wong WT, Wong RO, Lichtman JW. 2000. Multicolor DiOlistic labeling of the nervous system using lipophilic dye combinations. *Neuron* 27: 219-225
- Garvalov, B.K., K.C. Flynn, D. Neukirchen, L. Meyn, N. Teusch, X. Wu, C. Brakebusch, J.R. Bamberg, and F. Bradke. 2007. Cdc42 regulates cofilin during the establishment of neuronal polarity. *J Neurosci.* 27:13117-29.
- Gehler, S., A.E. Shaw, P.D. Sarmiere, J.R. Bamberg, and P.C. Letourneau. 2004. Brain-derived neurotrophic factor regulation of retinal growth cone filopodial dynamics is mediated through actin depolymerizing factor/cofilin. *J Neurosci.* 24:10741-9.
- Ghosh, M., X. Song, G. Mouneimne, M. Sidani, D.S. Lawrence, and J.S. Condeelis. 2004. Cofilin promotes actin polymerization and defines the direction of cell motility. *Science.* 304:743-6.
- Giuliano, K.A., F.A. Khatib, S.M. Hayden, E.W. Daoud, M.E. Adams, D.A. Amorese, B.W. Bernstein, and J.R. Bamberg. 1988. Properties of purified actin depolymerizing factor from chick brain. *Biochemistry.* 27:8931-8.
- Goebbels, S., I. Bormuth, U. Bode, O. Hermanson, M.H. Schwab, and K.A. Nave. 2006. Genetic targeting of principal neurons in neocortex and hippocampus of NEX-Cre mice. *Genesis.* 44:611-21.

- Gohla, A., J. Birkenfeld, and G.M. Bokoch. 2005. Chronophin, a novel HAD-type serine protein phosphatase, regulates cofilin-dependent actin dynamics. *Nat Cell Biol.* 7:21-9.
- Gohla, A., and G.M. Bokoch. 2002. 14-3-3 regulates actin dynamics by stabilizing phosphorylated cofilin. *Current Biology.* 12:1704-10.
- Goldberg, D.J., and D.W. Burmeister. 1989. Looking into growth cones. *Trends Neurosci.* 12:503-6.
- Goldberg, D.J., M.S. Foley, D. Tang, and P.W. Grabham. 2000. Recruitment of the Arp2/3 complex and mena for the stimulation of actin polymerization in growth cones by nerve growth factor. *J Neurosci Res.* 60:458-67.
- Gomez-Di Cesare, C.M., K.L. Smith, F.L. Rice, and J.W. Swann. 1997. Axonal remodeling during postnatal maturation of CA3 hippocampal pyramidal neurons. *J Comp Neurol.* 384:165-80.
- Gonzalez-Billault, C., J. Avila, and A. Caceres. 2001. Evidence for the role of MAP1B in axon formation. *Molecular Biology of the Cell.* 12:2087-98.
- Goold, R.G., and P.R. Gordon-Weeks. 2004. Glycogen synthase kinase 3beta and the regulation of axon growth. *Biochem Soc Trans.* 32:809-11.
- Goold, R.G., and P.R. Gordon-Weeks. 2005. The MAP kinase pathway is upstream of the activation of GSK3beta that enables it to phosphorylate MAP1B and contributes to the stimulation of axon growth. *Mol Cell Neurosci.* 28:524-34.
- Gopalakrishnan, S.M., N. Teusch, C. Imhof, M.H. Bakker, M. Schurdak, D.J. Burns, and U. Warrior. 2008. Role of Rho kinase pathway in chondroitin sulfate proteoglycan-mediated inhibition of neurite outgrowth in PC12 cells. *J Neurosci Res.*
- Gordon-Weeks, P.R., N. Giffin, C.S. Weekes, and C. Barben. 1989. Transient expression of laminin immunoreactivity in the developing rat hippocampus. *J Neurocytol.* 18:451-63.
- Goshima, Y., F. Nakamura, P. Strittmatter, and S.M. Strittmatter. 1995. Collapsin-induced growth cone collapse mediated by an intracellular protein related to UNC-33. *Nature.* 376:509-14.
- Goslin, K., and G. Banker. 1989. Experimental observations on the development of polarity by hippocampal neurons in culture. *J Cell Biol.* 108:1507-16.
- Goslin, K., and G. Banker. 1990. Rapid changes in the distribution of GAP-43 correlate with the expression of neuronal polarity during normal development and under experimental conditions. *J Cell Biol.* 110:1319-31.
- Goslin, K., E. Birgbauer, G. Banker, and F. Solomon. 1989. The role of cytoskeleton in organizing growth cones: a microfilament-associated growth cone component depends upon microtubules for its localization. *J Cell Biol.* 109:1621-31.
- Goslin, K., D.J. Schreyer, J.H. Skene, and G. Banker. 1988. Development of neuronal polarity: GAP-43 distinguishes axonal from dendritic growth cones. *Nature.* 336:672-4.
- Goslin, K., D.J. Schreyer, J.H. Skene, and G. Banker. 1990. Changes in the distribution of GAP-43 during the development of neuronal polarity. *J Neurosci.* 10:588-602.
- Govek, E.E., S.E. Newey, and L. Van Aelst. 2005a. The role of the Rho GTPases in neuronal development. *Genes Dev.* 19:1-49.
- Graus-Porta, D., S. Blaess, M. Senften, A. Littlewood-Evans, C. Damsky, Z. Huang, P. Orban, R. Klein, J.C. Schittny, and U. Muller. 2001. Beta1-class integrins regulate the development of laminae and folia in the cerebral and cerebellar cortex. *Neuron.* 31:367-79.

- Greka, A., B. Navarro, E. Oancea, A. Duggan, and D.E. Clapham. 2003. TRPC5 is a regulator of hippocampal neurite length and growth cone morphology. *Nat Neurosci.* 6:837-45.
- Grenningloh, G., S. Soehrman, P. Bondallaz, E. Ruchti, and H. Cadas. 2004. Role of the microtubule destabilizing proteins SCG10 and stathmin in neuronal growth. *J Neurobiol.* 58:60-9.
- Gualdoni, S., C. Albertinazzi, S. Corbetta, F. Valtorta, and I. de Curtis. 2007. Normal levels of Rac1 are important for dendritic but not axonal development in hippocampal neurons. *Biol Cell.* 99:455-64.
- Gungabissoon, R.A., and J.R. Bamburg. 2003. Regulation of growth cone actin dynamics by ADF/cofilin. *J Histochem Cytochem.* 51:411-20.
- Gunning, P., E. Hardeman, P. Jeffrey, and R. Weinberger. 1998. Creating intracellular structural domains: spatial segregation of actin and tropomyosin isoforms in neurons. *Bioessays.* 20:892-900.
- Gunning, P.W., G. Schevzov, A.J. Kee, and E.C. Hardeman. 2005. Tropomyosin isoforms: divining rods for actin cytoskeleton function. *Trends Cell Biol.* 15:333-41.
- Gunsalus, K.C., S. Bonaccorsi, E. Williams, F. Verni, M. Gatti, and M.L. Goldberg. 1995. Mutations in twinstar, a Drosophila gene encoding a cofilin/ADF homologue, result in defects in centrosome migration and cytokinesis. *Journal of Cell Biology.* 131:1243-59.
- Gupton, S.L., K.L. Anderson, T.P. Kole, R.S. Fischer, A. Ponti, S.E. Hitchcock-DeGregori, G. Danuser, V.M. Fowler, D. Wirtz, D. Hanein, and C.M. Waterman-Storer. 2005. Cell migration without a lamellipodium: translation of actin dynamics into cell movement mediated by tropomyosin. *J Cell Biol.* 168:619-31.
- Gurniak, C.B., E. Perlas, and W. Witke. 2005. The actin depolymerizing factor n-cofilin is essential for neural tube morphogenesis and neural crest cell migration. *Dev Biol.* 278:231-41.
- Hall, A. 2005. Rho GTPases and the control of cell behaviour. *Biochem Soc Trans.* 33:891-5.
- Hannigan, G., A.A. Troussard, and S. Dedhar. 2005. Integrin-linked kinase: a cancer therapeutic target unique among its ILK. *Nat Rev Cancer.* 5:51-63.
- Hannigan, M.O., C.K. Huang, and D.Q. Wu. 2004. Roles of PI3K in neutrophil function. *Curr Top Microbiol Immunol.* 282:165-75.
- Harris, B.Z., and W.A. Lim. 2001. Mechanism and role of PDZ domains in signaling complex assembly. *J Cell Sci.* 114:3219-31.
- Haselbacher, G.K., M.E. Schwab, A. Pasi, and R.E. Humbel. 1985. Insulin-like growth factor II (IGF II) in human brain: regional distribution of IGF II and of higher molecular mass forms. *Proc Natl Acad Sci USA.* 82:2153-7.
- Hayden, S.M., P.S. Miller, A. Brauweiler, and J.R. Bamburg. 1993. Analysis of the interactions of actin depolymerizing factor with G- and F-actin. *Biochemistry.* 32:9994-10004.
- He, T.C., S. Zhou, L.T. da Costa, J. Yu, K.W. Kinzler, and B. Vogelstein. 1998. A simplified system for generating recombinant adenoviruses. *Proc Natl Acad Sci USA* 95:2509-14.
- Heidemann, S.R., and R.E. Buxbaum. 1994. Mechanical tension as a regulator of axonal development. *Neurotoxicology.* 15:95-107.
- Heidemann, S.R., M. Reynolds, K. Ngo, and P. Lamoureux. 2003. The culture of chick forebrain neurons. *Methods Cell Biol.* 71:51-65.

- Henley, J.R., K.H. Huang, D. Wang, and M.M. Poo. 2004. Calcium mediates bidirectional growth cone turning induced by myelin-associated glycoprotein. *Neuron*. 44:909-16.
- Hiraoka, J., I. Okano, O. Higuchi, N. Yang, and K. Mizuno. 1996. Self-association of LIM-kinase 1 mediated by the interaction between an N-terminal LIM domain and a C-terminal kinase domain. *FEBS Lett.* 399:117-21.
- Hirokawa, N. 1998. Kinesin and dynein superfamily proteins and the mechanism of organelle transport. *Science*. 279:519-26.
- Hollenbeck, P.J., and J.R. Bamberg. 2003. Comparing the properties of neuronal culture systems: a shopping guide for the cell biologist. *Methods in Cell Biology*. 71:1-16.
- Horton, A.C., and M.D. Ehlers. 2003. Neuronal polarity and trafficking. *Neuron*. 40:277-295.
- Horton, A.C., B. Racz, E.E. Monson, A.L. Lin, R.J. Weinberg, and M.D. Ehlers. 2005. Polarized secretory trafficking directs cargo for asymmetric dendrite growth and morphogenesis. *Neuron*. 48:757-71.
- Hotulainen, P., E. Paunola, M.K. Vartiainen, and P. Lappalainen. 2005. Actin-depolymerizing factor and cofilin-1 play overlapping roles in promoting rapid F-actin depolymerization in mammalian nonmuscle cells. *Mol Biol Cell*. 16:649-64.
- Hsieh, S.H., G.B. Ferraro, and A.E. Fournier. 2006. Myelin-associated inhibitors regulate cofilin phosphorylation and neuronal inhibition through LIM kinase and Slingshot phosphatase. *J Neurosci*. 26:1006-15.
- Iida, K., K. Moriyama, S. Matsumoto, H. Kawasaki, E. Nishida, and I. Yahara. 1993. Isolation of a yeast essential gene, COF1, that encodes a homologue of mammalian cofilin, a low-M(r) actin-binding and depolymerizing protein. *Gene*. 124:115-20.
- Iijima, M., Y.E. Huang, and P. Devreotes. 2002. Temporal and spatial regulation of chemotaxis. *Dev Cell*. 3:469-78.
- Ikawa, M., S. Yamada, T. Nakanishi, and M. Okabe. 1998. 'Green mice' and their potential usage in biological research. *FEBS Lett.* 430:83-7.
- Ikeda, S., L.A. Cunningham, D. Boggess, C.D. Hobson, J.P. Sundberg, J.K. Naggert, R.S. Smith, and P.M. Nishina. 2003. Aberrant actin cytoskeleton leads to accelerated proliferation of corneal epithelial cells in mice deficient for destrin (actin depolymerizing factor).[erratum appears in Hum Mol Genet. 2003 Jun 1;12(11):1359]. *Human Molecular Genetics*. 12:1029-37.
- Inagaki, N., K. Chihara, N. Arimura, C. Menager, Y. Kawano, N. Matsuo, T. Nishimura, M. Amano, and K. Kaibuchi. 2001a. CRMP-2 induces axons in cultured hippocampal neurons. *Nat Neurosci*. 4:781-2.
- Inagaki, N., K. Chihara, N. Arimura, C. Menager, Y. Kawano, N. Matsuo, T. Nishimura, M. Amano, and K. Kaibuchi. 2001b. CRMP-2 induces axons in cultured hippocampal neurons. *Nature Neuroscience*. 4:781-2.
- Ishikawa, R., S. Yamashiro, and F. Matsumura. 1989a. Annealing of gelsolin-severed actin fragments by tropomyosin in the presence of Ca²⁺. Potentiation of the annealing process by caldesmon. *J Biol Chem*. 264:16764-70.
- Ishikawa, R., S. Yamashiro, and F. Matsumura. 1989b. Differential modulation of actin-severing activity of gelsolin by multiple isoforms of cultured rat cell tropomyosin. Potentiation of protective ability of tropomyosins by 83-kDa nonmuscle caldesmon. *J Biol Chem*. 264:7490-7.
- Jacob, R., and H.Y. Naim. 2001. Apical membrane proteins are transported in distinct vesicular carriers. *Curr Biol*. 11:1444-50.
- Jacobs, T., F. Causeret, Y.V. Nishimura, M. Terao, A. Norman, M. Hoshino, and M. Nikolic.

2007. Localized activation of p21-activated kinase controls neuronal polarity and morphology. *J. Neurosci.* 27:8604-8615.
- Jacobson, C., B. Schnapp, and G.A. Banker. 2006. A change in the selective translocation of the Kinesin-1 motor domain marks the initial specification of the axon. *Neuron.* 49:797-804.
- Jaffe, A.B., and A. Hall. 2005. Rho GTPases: biochemistry and biology. *Annu Rev Cell Dev Biol.* 21:247-69.
- Janetopoulos, C., and P. Devreotes. 2006. Phosphoinositide signaling plays a key role in cytokinesis. *J Cell Biol.* 174:485-90.
- Jareb, M., and G. Banker. 1997. Inhibition of axonal growth by brefeldin A in hippocampal neurons in culture. *J Neurosci.* 17:8955-63.
- Jiang, H., W. Guo, X. Liang, and Y. Rao. 2005. Both the establishment and the maintenance of neuronal polarity require active mechanisms: critical roles of GSK-3 β and its upstream regulators. *Cell.* 120:123-135.
- Jimbo, T., Y. Kawasaki, R. Koyama, R. Sato, S. Takada, K. Haraguchi, and T. Akiyama. 2002. Identification of a link between the tumour suppressor APC and the kinesin superfamily. *Nat Cell Biol.* 4:323-7.
- Jimenez-Mateos, E.M., G. Paglini, C. Gonzalez-Billault, A. Caceres, and J. Avila. 2005. End binding protein-1 (EB1) complements microtubule-associated protein-1B during axonogenesis. *J Neurosci Res.* 80:350-9.
- Jin, Z., and S.M. Strittmatter. 1997. Rac1 mediates collapsin-1-induced growth cone collapse. *J Neurosci.* 17:6256-63.
- Kanamori, T., M. Suzuki, and K. Titani. 1998. Complete amino acid sequences and phosphorylation sites, determined by Edman degradation and mass spectrometry, of rat parotid destrin- and cofilin-like proteins. *Archives of Oral Biology.* 43:955-67.
- Karabay, A., W. Yu, J.M. Solowska, D.H. Baird, and P.W. Baas. 2004. Axonal growth is sensitive to the levels of katanin, a protein that severs microtubules. *J Neurosci.* 24:5778-88.
- Kashina, A.S. 2006. Differential arginylation of actin isoforms: the mystery of the actin N-terminus. *Trends Cell Biol.* 16:610-5.
- Kawano, Y., T. Yoshimura, D. Tsuboi, S. Kawabata, T. Kaneko-Kawano, H. Shirataki, T. Takenawa, and K. Kaibuchi. 2005. CRMP-2 is involved in kinesin-1-dependent transport of the Sra-1/WAVE1 complex and axon formation. *Mol Cell Biol.* 25:9920-35.
- Kerckhoff, E. 2006. Cellular functions of the Spir actin-nucleation factors. *Trends Cell Biol.* 16:477-83.
- Ketschek, A.R., S.L. Jones, and G. Gallo. 2007. Axon extension in the fast and slow lanes: substratum-dependent engagement of myosin II functions. *Dev Neurobiol.* 67:1305-20.
- Kim, W.Y., F.Q. Zhou, J. Zhou, Y. Yokota, Y.M. Wang, T. Yoshimura, K. Kaibuchi, J.R. Woodgett, E.S. Anton, and W.D. Snider. 2006. Essential roles for GSK-3 α and GSK-3 β in neurotrophin-induced and hippocampal axon growth. *Neuron.* 52:981-96.
- Kim, Y., and S. Chang. 2004a. Modulation of actomyosin contractility by myosin light chain phosphorylation/dephosphorylation through Rho GTPases signaling specifies axon formation in neurons. *Biochem. Biophys. Res. Commun.* 318:579-587.
- Kim, Y., and S. Chang. 2004b. Modulation of actomyosin contractility by myosin light chain phosphorylation/dephosphorylation through Rho GTPases signaling specifies axon

- formation in neurons. *Biochem Biophys Res Commun.* 318:579-87.
- Kiosses, W.B., J. Hood, S. Yang, M.E. Gerritsen, D.A. Cheres, N. Alderson, and M.A. Schwartz. 2002. A dominant-negative p65 PAK peptide inhibits angiogenesis. *Circ Res.* 90:697-702.
- Kishi, M., Y.A. Pan, J.G. Crump, and J.R. Sanes. 2005. Mammalian SAD kinases are required for neuronal polarization. *Science.* 307:929-32.
- Kobayashi, T., B. Storrie, K. Simons, and C.G. Dotti. 1992. A functional barrier to movement of lipids in polarized neurons. *Nature.* 359:647-50.
- Kokuzawa, J., S. Yoshimura, H. Kitajima, J. Shinoda, Y. Kaku, T. Iwama, R. Morishita, T. Shimazaki, H. Okano, T. Kunisada, and N. Sakai. 2003. Hepatocyte growth factor promotes proliferation and neuronal differentiation of neural stem cells from mouse embryos. *Molecular & Cellular Neurosciences.* 24:190-7.
- Kole, H.K., K. Brown, M. Naramura, S. Fukuhara, R.J. Hu, I.K. Jang, J.S. Gutkind, E. Shevach, H. Gu, and T. Esch. 2000. Local presentation of substrate molecules directs axon specification by cultured hippocampal neurons. *Nature.* 403:216-20.
- Korets-Smith, E., L. Lindemann, K.L. Tucker, C. Jiang, N. Kabacs, G. Belteki, J. Haigh, M. Gertsenstein, and A. Nagy. 2004. Cre recombinase specificity defined by the tau locus. *Genesis.* 40:131-8.
- Kovar, D.R., and T.D. Pollard. 2004. Progressing actin: Formin as a processive elongation machine. *Nat Cell Biol.* 6:1158-9.
- Kozma, R., S. Sarner, S. Ahmed, and L. Lim. 1997. Rho family GTPases and neuronal growth cone remodelling: relationship between increased complexity induced by Cdc42Hs, Rac1, and acetylcholine and collapse induced by RhoA and lysophosphatidic acid. *Mol Cell Biol.* 17:1201-11.
- Kranenburg, O., M. Poland, F.P. van Horek, D. Drechsel, A. Hall, and W.H. Moolenaar. 1999. Activation of RhoA by lysophosphatidic acid and Galpha12/13 subunits in neuronal cells: induction of neurite retraction. *Mol Biol Cell.* 10:1851-7.
- Kuhn, T.B., M.D. Brown, and J.R. Bamberg. 1998a. Rac1-dependent actin filament organization in growth cones is necessary for beta1-integrin-mediated advance but not for growth on poly-D-lysine. *J Neurobiol.* 37:524-40.
- Kuhn, T.B., P.J. Meberg, M.D. Brown, B.W. Bernstein, L.S. Minamide, J.R. Jensen, K. Okada, E.A. Soda, and J.R. Bamberg. 2000a. Regulating actin dynamics in neuronal growth cones by ADF/cofilin and rho family GTPases. *J Neurobiol.* 44:126-44.
- Kuhn, T.B., P.J. Meberg, M.D. Brown, B.W. Bernstein, L.S. Minamide, J.R. Jensen, K. Okada, E.A. Soda, and J.R. Bamberg. 2000b. Regulating actin dynamics in neuronal growth cones by ADF/cofilin and rho family GTPases. *Journal of Neurobiology.* 44:126-44.
- Kuhn, T.B., C.V. Williams, P. Dou, and S.B. Kater. 1998b. Laminin directs growth cone navigation via two temporally and functionally distinct calcium signals. *J Neurosci.* 18:184-94.
- Kunda, P., G. Paglini, S. Quiroga, K. Kosik, and A. Caceres. 2001. Evidence for the involvement of Tiam1 in axon formation. *J Neurosci.* 21:2361-72.
- Kwiatkowski, A.V., D.A. Robinson, E.W. Dent, J. Edward van Veen, J.D. Leslie, J. Zhang, L.M. Mebane, U. Philippar, E.M. Pinheiro, A.A. Burds, R.T. Bronson, S. Mori, R. Fassler, and F.B. Gertler. 2007. Ena/VASP Is Required for neuritogenesis in the developing cortex. *Neuron.* 56:441-55.
- Labelle, C., and N. Leclerc. 2000. Exogenous BDNF, NT-3 and NT-4 differentially regulate neurite outgrowth in cultured hippocampal neurons. *Brain Res.Dev.Brain Res.* 123:1-11.

- Laemmli, U. K. 1970. Cleavage of structural proteins during the assembly of the head of bacteriophage T4. *Nature* 227: 680-685.
- Lamoureux, P., G. Ruthel, R.E. Buxbaum, and S.R. Heidemann. 2002. Mechanical tension can specify axonal fate in hippocampal neurons. *J. Cell Biol.* 159:499-508.
- Lappalainen, P., M.M. Kessels, M.J. Cope, and D.G. Drubin. 1998. The ADF homology (ADF-H) domain: a highly exploited actin-binding module. *Molecular Biology of the Cell.* 9:1951-9.
- Larson, L., S. Arnaudeau, B. Gibson, W. Li, R. Krause, B. Hao, J.R. Bamburg, D.P. Lew, N. Demareux, and F. Southwick. 2005. Gelsolin mediates calcium-dependent disassembly of Listeria actin tails. *Proc Natl Acad Sci U S A.* 102:1921-6.
- Lasek, R.J. 1982. Translocation of the neuronal cytoskeleton and axonal locomotion. *Philos Trans R Soc Lond B Biol Sci.* 299:313-27.
- Lebrand, C., E.W. Dent, G.A. Strasser, L.M. Lanier, M. Krause, T.M. Svitkina, G.G. Borisy, and F.B. Gertler. 2004. Critical role of Ena/VASP proteins for filopodia formation in neurons and in function downstream of netrin-1. *Neuron.* 42:37-49.
- Lena, J.Y., J.R. Bamburg, A. Rabie, and C. Faivre-Sarrailh. 1991. Actin-depolymerizing factor (ADF) in the cerebellum of the developing rat: a quantitative and immunocytochemical study. *Journal of Neuroscience Research.* 30:18-27.
- Letourneau, P.C. 1983. Differences in the organization of actin in the growth cones compared with the neurites of cultured neurons from chick embryos. *J Cell Biol.* 97:963-73.
- Leung, T., E. Manser, L. Tan, and L. Lim. 1995. A novel serine/threonine kinase binding the Ras-related RhoA GTPase which translocates the kinase to peripheral membranes. *J Biol Chem.* 270:29051-4.
- Lewis, A.K., and P.C. Bridgman. 1992. Nerve growth cone lamellipodia contain two populations of actin filaments that differ in organization and polarity. *J Cell Biol.* 119:1219-43.
- Li, S., B.P. Liu, S. Budel, M. Li, B. Ji, L. Walus, W. Li, A. Jirik, S. Rabacchi, E. Choi, D. Worley, D.W. Sah, B. Pepinsky, D. Lee, J. Relton, and S.M. Strittmatter. 2004. Blockade of Nogo-66, myelin-associated glycoprotein, and oligodendrocyte myelin glycoprotein by soluble Nogo-66 receptor promotes axonal sprouting and recovery after spinal injury. *J Neurosci.* 24:10511-20.
- Lin, C.H., and P. Forscher. 1993. Cytoskeletal remodeling during growth cone-target interactions. *Journal of Cell Biology.* 121:1369-83.
- Lin, C.H., and P. Forscher. 1995. Growth cone advance is inversely proportional to retrograde F-actin flow. *Neuron.* 14:763-71.
- Loudon, R.P., L.D. Silver, H.F. Yee, Jr., and G. Gallo. 2006. RhoA-kinase and myosin II are required for the maintenance of growth cone polarity and guidance by nerve growth factor. *J. Neurobiol.* 66:847-867.
- Lu, M., W. Witke, D.J. Kwiatkowski, and K.S. Kosik. 1997a. Delayed retraction of filopodia in gelsolin null mice. *J. Cell Biol.* 138:1279-1287.
- Luo, L., T.K. Hensch, L. Ackerman, S. Barbel, L.Y. Jan, and Y.N. Jan. 1996. Differential effects of the Rac GTPase on Purkinje cell axons and dendritic trunks and spines. *Nature.* 379:837-40.
- Luo, L., Y.J. Liao, L.Y. Jan, and Y.N. Jan. 1994. Distinct morphogenetic functions of similar small GTPases: Drosophila Drac1 is involved in axonal outgrowth and myoblast fusion. *Genes & Development.* 8:1787-802.
- Lykissas, M.G., A.K. Batistatou, K.A. Charalabopoulos, and A.E. Beris. 2007. The role of neurotrophins in axonal growth, guidance, and regeneration. *Curr Neurovasc Res.*

4:143-51.

- Maccioni, R.B., and V. Cambiazo. 1995. Role of microtubule-associated proteins in the control of microtubule assembly. *Physiol Rev.* 75:835-64.
- Maciver, S.K. 1998. How ADF/cofilin depolymerizes actin filaments. *Curr Opin Cell Biol.* 10:140-4.
- Maciver, S.K., B.J. Pope, S. Whytock, and A.G. Weeds. 1998. The effect of two actin depolymerizing factors (ADF/cofilins) on actin filament turnover: pH sensitivity of F-actin binding by human ADF, but not of *Acanthamoeba* actophorin. *Eur J Biochem.* 256:388-97.
- Maciver, S.K., and A.G. Weeds. 1994. Actophorin preferentially binds monomeric ADP-actin over ATP-bound actin: consequences for cell locomotion. *FEBS Lett.* 347:251-6.
- Maekawa, M., T. Ishizaki, S. Boku, N. Watanabe, A. Fujita, A. Iwamatsu, T. Obinata, K. Ohashi, K. Mizuno, and S. Narumiya. 1999. Signaling from Rho to the actin cytoskeleton through protein kinases ROCK and LIM-kinase. *Science.* 285:895-8.
- Maloney, M.T., and J.R. Bamburg. 2007. Cofilin-mediated neurodegeneration in Alzheimer's disease and other amyloidopathies. *Mol Neurobiol.* 35:21-44.
- Maloney, M.T., L.S. Minamide, A.W. Kinley, J.A. Boyle, and J.R. Bamburg. 2005. Beta-secretase-cleaved amyloid precursor protein accumulates at actin inclusions induced in neurons by stress or amyloid beta: a feedforward mechanism for Alzheimer's disease. *J Neurosci.* 25:11313-21.
- Mandelkow, E.M., E. Mandelkow, and R.A. Milligan. 1991. Microtubule dynamics and microtubule caps: a time-resolved cryo-electron microscopy study. *J Cell Biol.* 114:977-91.
- Manser, E., T. Leung, H. Salihuddin, Z.S. Zhao, and L. Lim. 1994. A brain serine/threonine protein kinase activated by Cdc42 and Rac1. *Nature.* 367:40-6.
- Marsh, L., and P.C. Letourneau. 1984. Growth of neurites without filopodial or lamellipodial activity in the presence of cytochalasin B. *J Cell Biol.* 99:2041-7.
- Martin, A.A., F.M. Tomas, P.C. Owens, S.E. Knowles, F.J. Ballard, and L.C. Read. 1991. IGF-I and its variant, des-(1-3)IGF-I, enhance growth in rats with reduced renal mass. *Am J Physiol.* 261:F626-33.
- Matsuo, N., M. Terao, Y. Nabeshima, and M. Hoshino. 2003. Roles of STEF/Tiam1, guanine nucleotide exchange factors for Rac1, in regulation of growth cone morphology. *Molecular & Cellular Neurosciences.* 24:69-81.
- McGee, A.W., and D.S. Bredt. 1999. Identification of an intramolecular interaction between the SH3 and guanylate kinase domains of PSD-95. *J Biol Chem.* 274:17431-6.
- McGough, A. 1998. F-actin-binding proteins. *Current Opinion in Structural Biology.* 8:166-76.
- McGough, A., and W. Chiu. 1999. ADF/cofilin weakens lateral contacts in the actin filament. *Journal of Molecular Biology.* 291:513-9.
- McGough, A., B. Pope, W. Chiu, and A. Weeds. 1997. Cofilin changes the twist of F-actin: implications for actin filament dynamics and cellular function. *Journal of Cell Biology.* 138:771-81.
- McGough, A., B. Pope, and A. Weeds. 2001. The ADF/cofilin family: accelerators of actin reorganization. *Results & Problems in Cell Differentiation.* 32:135-54.
- McKerracher, L., M. Chamoux, and C.O. Arregui. 1996. Role of laminin and integrin interactions in growth cone guidance. *Molecular Neurobiology.* 12:95-116.
- McKim, K.S., C. Matheson, M.A. Marra, M.F. Wakarchuk, and D.L. Baillie. 1994. The

- Caenorhabditis elegans unc-60 gene encodes proteins homologous to a family of actin-binding proteins. *Molecular & General Genetics*. 242:346-57.
- McQuarrie, I.G., and J.M. Jacob. 1991. Conditioning nerve crush accelerates cytoskeletal protein transport in sprouts that form after a subsequent crush. *J Comp Neurol*. 305:139-47.
- Meberg, P.J., and J.R. Bamberg. 2000. Increase in neurite outgrowth mediated by overexpression of actin depolymerizing factor. *J Neurosci*. 20:2459-69.
- Meberg, P.J., and M.W. Miller. 2003. Culturing hippocampal and cortical neurons. *Methods in Cell Biology*. 71:111-27.
- Meberg, P.J., S. Ono, L.S. Minamide, M. Takahashi, and J.R. Bamberg. 1998. Actin depolymerizing factor and cofilin phosphorylation dynamics: response to signals that regulate neurite extension. *Cell Motil Cytoskeleton*. 39:172-90.
- Medeiros, N.A., D.T. Burnette, and P. Forscher. 2006. Myosin II functions in actin-bundle turnover in neuronal growth cones. *Nat Cell Biol*. 8:215-26.
- Meghani, M.A., D.M. Martin, J.R. Singleton, and E.L. Feldman. 1993. Effects of serum and insulin-like growth factors on human neuroblastoma cell growth. *Regul Pept*. 48:217-24.
- Menager, C., N. Arimura, Y. Fukata, and K. Kaibuchi. 2004. PIP is involved in neuronal polarization and axon formation. *J Neurochem*. 89:109-118.
- Meng, Y., Y. Zhang, V. Tregoubov, C. Janus, L. Cruz, M. Jackson, W.Y. Lu, J.F. MacDonald, J.Y. Wang, D.L. Falls, and Z. Jia. 2002. Abnormal spine morphology and enhanced LTP in LIMK-1 knockout mice.[see comment]. *Neuron*. 35:121-33.
- Millard, T.H., S.J. Sharp, and L.M. Machesky. 2004. Signalling to actin assembly via the WASP (Wiskott-Aldrich syndrome protein)-family proteins and the Arp2/3 complex. *Biochem J*. 380:1-17.
- Mills, R.G., L.S. Minamide, A. Yuan, J.R. Bamberg, and J.J. Bray. 1996. Slow axonal transport of soluble actin with actin depolymerizing factor, cofilin, and profilin suggests actin moves in an unassembled form. *J Neurochem*. 67:1225-34.
- Minamide, L.S., and J.R. Bamberg. 1990. A filter paper dye-binding assay for quantitative determination of protein without interference from reducing agents or detergents. *Anal Biochem*. 190:66-70.
- Minamide, L.S., W.B. Painter, G. Schevzov, P. Gunning, and J.R. Bamberg. 1997. Differential regulation of actin depolymerizing factor and cofilin in response to alterations in the actin monomer pool. *J Biol Chem*. 272:8303-9.
- Minamide, L.S., A.E. Shaw, P.D. Sarmiere, O. Wiggan, M.T. Maloney, B.W. Bernstein, J.M. Sneider, J.A. Gonzalez, and J.R. Bamberg. 2003. Production and use of replication-deficient adenovirus for transgene expression in neurons. *Meth Cell Biol*. 71:387-416.
- Minamide, L.S., A.M. Striegl, J.A. Boyle, P.J. Meberg, and J.R. Bamberg. 2000. Neurodegenerative stimuli induce persistent ADF/cofilin-actin rods that disrupt distal neurite function. *Nat Cell Biol*. 2:628-36.
- Miyagishi, M., and K. Taira. 2002. U6 promoter-driven siRNAs with four uridine 3' overhangs efficiently suppress targeted gene expression in mammalian cells. *Nature Biotech*. 20:497-500.
- Mizuno, K., I. Okano, K. Ohashi, K. Nunoue, K. Kuma, T. Miyata, and T. Nakamura. 1994. Identification of a human cDNA encoding a novel protein kinase with two repeats of the LIM/double zinc finger motif. *Oncogene*. 9:1605-12.
- Mongiu, A.K., E.L. Weitzke, O.Y. Chaga, and G.G. Borisy. 2007. Kinetic-structural analysis of neuronal growth cone veil motility. *J Cell Sci*. 120:1113-25.

- Moon, A.L., P.A. Janmey, K.A. Louie, and D.G. Drubin. 1993. Cofilin is an essential component of the yeast cortical cytoskeleton. *Journal of Cell Biology*. 120:421-35.
- Morgan, T.E., R.O. Lockerbie, L.S. Minamide, M.D. Browning, and J.R. Bamburg. 1993. Isolation and characterization of a regulated form of actin depolymerizing factor. *Journal of Cell Biology*. 122:623-33.
- Morii, H., Y. Shiraishi-Yamaguchi, and N. Mori. 2006. SCG10, a microtubule destabilizing factor, stimulates the neurite outgrowth by modulating microtubule dynamics in rat hippocampal primary cultured neurons. *J Neurobiol*. 66:1101-14.
- Moriyama, K., K. Iida, and I. Yahara. 1996. Phosphorylation of Ser-3 of cofilin regulates its essential function on actin. *Genes Cells*. 1:73-86.
- Moriyama, K., and I. Yahara. 2002a. The actin-severing activity of cofilin is exerted by the interplay of three distinct sites on cofilin and essential for cell viability. *Biochemical Journal*. 365:147-55.
- Moriyama, K., and I. Yahara. 2002b. The actin-severing activity of cofilin is exerted by the interplay of three distinct sites on cofilin and essential for cell viability. *Biochem J*. 365:147-55.
- Morrison, D. 1994. 14-3-3: modulators of signaling proteins? *Science*. 266:56-57.
- Morrison, E.E. 2007. Action and interactions at microtubule ends. *Cell Mol Life Sci*. 64:307-17.
- Moseley, J.B., F. Bartolini, K. Okada, Y. Wen, G.G. Gundersen, and B.L. Goode. 2007. Regulated binding of adenomatous polyposis coli protein to actin. *J Biol Chem*. 282:12661-8.
- Mseka, T., J.R. Bamburg, and L.P. Cramer. 2007. ADF/cofilin family proteins control formation of oriented actin-filament bundles in the cell body to trigger fibroblast polarization. *J Cell Sci*. 120:4332-44.
- Mullins, R.D., J.A. Heuser, and T.D. Pollard. 1998. The interaction of Arp2/3 complex with actin: nucleation, high affinity pointed end capping, and formation of branching networks of filaments. *Proc Natl Acad Sci U S A*. 95:6181-6.
- Munemitsu, S., B. Souza, O. Muller, I. Albert, B. Rubinfeld, and P. Polakis. 1994. The APC gene product associates with microtubules in vivo and promotes their assembly in vitro. *Cancer Res*. 54:3676-81.
- Myers, K.A., and P.W. Baas. 2007. Kinesin-5 regulates the growth of the axon by acting as a brake on its microtubule array. *J Cell Biol*. 178:1081-91.
- Nachmias, V.T., and H.E. Huxley. 1970. Electron microscope observations on actomyosin and actin preparations from *Physarum polycephalum*, and on their interaction with heavy meromyosin subfragment I from muscle myosin. *Journal of Molecular Biology*. 50:83-90.
- Nagano, T., S. Morikubo, and M. Sato. 2004. Filamin A and FILIP (Filamin A-Interacting Protein) regulate cell polarity and motility in neocortical subventricular and intermediate zones during radial migration. *J Neurosci*. 24:9648-57.
- Nagaoka, R., H. Abe, and T. Obinata. 1996. Site-directed mutagenesis of the phosphorylation site of cofilin: its role in cofilin-actin interaction and cytoplasmic localization. *Cell Motil Cytoskeleton*. 35:200-9.
- Nagata-Ohashi, K., Y. Ohta, K. Goto, S. Chiba, R. Mori, M. Nishita, K. Ohashi, K. Kousaka, A. Iwamatsu, R. Niwa, T. Uemura, and K. Mizuno. 2004. A pathway of neuregulin-induced activation of cofilin-phosphatase Slingshot and cofilin in lamellipodia. *J Cell Biol*. 165:465-71.

- Nakada, C., K. Ritchie, Y. Oba, M. Nakamura, Y. Hotta, R. Iino, R.S. Kasai, K. Yamaguchi, T. Fujiwara, and A. Kusumi. 2003. Accumulation of anchored proteins forms membrane diffusion barriers during neuronal polarization. *Nat Cell Biol.* 5:626-32.
- Ng, J., and L. Luo. 2004. Rho GTPases regulate axon growth through convergent and divergent signaling pathways. *Neuron.* 44:779-93.
- Nishida, E. 1985. Opposite effects of cofilin and profilin from porcine brain on rate of exchange of actin-bound adenosine 5'-triphosphate. *Biochemistry.* 24:1160-4.
- Nishida, E., S. Maekawa, and H. Sakai. 1984. Cofilin, a protein in porcine brain that binds to actin filaments and inhibits their interactions with myosin and tropomyosin. *Biochemistry.* 23:5307-13.
- Nishimura, T., K. Kato, T. Yamaguchi, Y. Fukata, S. Ohno, and K. Kaibuchi. 2004. Role of the PAR-3-KIF3 complex in the establishment of neuronal polarity. *Nat Cell Biol.* 6:328-34.
- Nishimura, T., T. Yamaguchi, K. Kato, M. Yoshizawa, Y. Nabeshima, S. Ohno, M. Hoshino, and K. Kaibuchi. 2005. PAR-6-PAR-3 mediates Cdc42-induced Rac activation through the Rac GEFs STEF/Tiam1. *Nat Cell Biol.* 7:270-7.
- Nishita, M., Y. Wang, C. Tomizawa, A. Suzuki, R. Niwa, T. Uemura, and K. Mizuno. 2004. Phosphoinositide-3-Kinase-mediated Activation of Cofilin Phosphatase Slingshot and Its role for Insulin-induced Membrane Protrusion. *J. Biol. Chem.* 279:7193-7198.
- Niwa, R., K. Nagata-Ohashi, M. Takeichi, K. Mizuno, and T. Uemura. 2002. Control of actin reorganization by Slingshot, a family of phosphatases that dephosphorylate ADF/cofilin. *Cell.* 108:233-46.
- Nyasae, L.K., A.L. Hubbard, and P.L. Tuma. 2003. Transcytotic efflux from early endosomes is dependent on cholesterol and glycosphingolipids in polarized hepatic cells. *Mol Biol Cell.* 14:2689-705.
- O'Connor, T.P., J.S. Duerr, and D. Bentley. 1990. Pioneer growth cone steering decisions mediated by single filopodial contacts in situ. *J Neurosci.* 10:3935-46.
- Okabe, M., M. Ikawa, K. Kominami, T. Nakanishi, and Y. Nishimune. 1997. 'Green mice' as a source of ubiquitous green cells. *FEBS Lett.* 407:313-9.
- Okada, K., L. Blanchoin, H. Abe, H. Chen, T.D. Pollard, and J.R. Bamburg. 2002a. Xenopus actin-interacting protein 1 (XAip1) enhances cofilin fragmentation of filaments by capping filament ends. *Journal of Biological Chemistry.* 277:43011-6.
- Okada, K., L. Blanchoin, H. Abe, H. Chen, T.D. Pollard, and J.R. Bamburg. 2002b. Xenopus actin-interacting protein 1 (XAip1) enhances cofilin fragmentation of filaments by capping filament ends. *J Biol Chem.* 277:43011-6.
- Ono, S., and G.M. Benian. 1998. Two *Caenorhabditis elegans* actin depolymerizing factor/cofilin proteins, encoded by the *unc-60* gene, differentially regulate actin filament dynamics. *J Biol Chem.* 273:3778-83.
- Ono, S., K. Mohri, and K. Ono. 2004. Microscopic evidence that actin-interacting protein 1 actively disassembles actin-depolymerizing factor/Cofilin-bound actin filaments. *J Biol Chem.* 279:14207-12.
- Ono, S., and K. Ono. 2002. Tropomyosin inhibits ADF/cofilin-dependent actin filament dynamics.[erratum appears in J Cell Biol 2002 May 13;157(4):727]. *Journal of Cell Biology.* 156:1065-76.
- Otey, C.A., M.H. Kalnoski, J.L. Lessard, and J.C. Bulinski. 1986. Immunolocalization of the gamma isoform of nonmuscle actin in cultured cells. *J Cell Biol.* 102:1726-37.
- Pak, C.W., K.C. Flynn, and J.R. Bamburg. 2008. Actin-binding proteins take the reins in growth cones. *Nat Rev Neurosci.* 9:136-47.

- Pandey, D., P. Goyal, J.R. Bamburg, and W. Siess. 2006. Regulation of LIM-kinase 1 and cofilin in thrombin-stimulated platelets. *Blood*. 107:575-83.
- Paul, C.P., P.D. Good, I. Winer, and D.R. Engelke. 2002. Effective expression of small interfering RNA in human cells.[see comment]. *Nature Biotechnology*. 20:505-8.
- Piper, M., and C. Holt. 2004. RNA translation in axons. *Annu Rev Cell Dev Biol*. 20:505-23.
- Pollard, T.D., L. Blanchoin, and R.D. Mullins. 2001. Actin dynamics. *J Cell Sci*. 114:3-4.
- Pollard, T.D., and G.G. Borisy. 2003. Cellular motility driven by assembly and disassembly of actin filaments.[erratum appears in Cell. 2003 May 16;113(4):549]. *Cell*. 112:453-65.
- Pollard, T.D., I. Goldberg, and W.H. Schwarz. 1992. Nucleotide exchange, structure, and mechanical properties of filaments assembled from ATP-actin and ADP-actin. *J Biol Chem*. 267:20339-45.
- Ponnio, T., and O.M. Conneely. 2004. nor-1 regulates hippocampal axon guidance, pyramidal cell survival, and seizure susceptibility. *Mol Cell Biol*. 24:9070-8.
- Ponti, A., A. Matov, M. Adams, S. Gupton, C.M. Waterman-Storer, and G. Danuser. 2005. Periodic patterns of actin turnover in lamellipodia and lamellae of migrating epithelial cells analyzed by quantitative Fluorescent Speckle Microscopy. *Biophys J*. 89:3456-69.
- Ponti, A., P. Vallotton, W.C. Salmon, C.M. Waterman-Storer, and G. Danuser. 2003. Computational analysis of F-actin turnover in cortical actin meshworks using fluorescent speckle microscopy. *Biophys J*. 84:3336-52.
- Pope, B.J., S.M. Gonsior, S. Yeoh, A. McGough, and A.G. Weeds. 2000. Uncoupling actin filament fragmentation by cofilin from increased subunit turnover. *Journal of Molecular Biology*. 298:649-61.
- Prekeris, R., D.L. Foletti, and R.H. Scheller. 1999. Dynamics of tubulovesicular recycling endosomes in hippocampal neurons. *J Neurosci*. 19:10324-37.
- Pruyne, D., M. Evangelista, C. Yang, E. Bi, S. Zigmond, A. Bretscher, and C. Boone. 2002. Role of formins in actin assembly: nucleation and barbed-end association. *Science*. 297:612-5.
- Qiang, L., W. Yu, A. Andreadis, M. Luo, and P.W. Baas. 2006. Tau protects microtubules in the axon from severing by katanin. *J Neurosci*. 26:3120-9.
- Quinlan, M.E., J.E. Heuser, E. Kerkhoff, and R.D. Mullins. 2005. Drosophila Spire is an actin nucleation factor. *Nature*. 433:382-8.
- Ramón y Cajal, S. 1898. *Texture del Sistema Nervioso del Hombre y de los Vertebrados*. Moya, Madrid.
- Ramón y Cajal, S. 1911. *Histologie du systeme nerveux de l'homme et des vertebres*. Paris: Maloine.
- Ressad, F., D. Didry, C. Egile, D. Pantaloni, and M.F. Carlier. 1999. Control of actin filament length and turnover by actin depolymerizing factor (ADF/cofilin) in the presence of capping proteins and ARP2/3 complex. *Journal of Biological Chemistry*. 274:20970-6.
- Rivas, R.J., D.W. Burmeister, and D.J. Goldberg. 1992. Rapid effects of laminin on the growth cone. *Neuron*. 8:107-15.
- Rochlin, M.W., M.E. Dailey, and P.C. Bridgman. 1999. Polymerizing microtubules activate site-directed F-actin assembly in nerve growth cones. *Mol Biol Cell*. 10:2309-27.
- Rochlin, M.W., K.M. Wickline, and P.C. Bridgman. 1996a. Microtubule stability decreases axon elongation but not axoplasm production. *J Neurosci*. 16:3236-46.

- Rochlin, M.W., K.M. Wickline, and P.C. Bridgman. 1996b. Microtubule stability decreases axon elongation but not axoplasm production. *Journal of Neuroscience*. 16:3236-46.
- Romero, S., C. Le Clainche, D. Didry, C. Egile, D. Pantaloni, and M.F. Carlier. 2004. Formin is a processive motor that requires profilin to accelerate actin assembly and associated ATP hydrolysis. *Cell*. 119:419-29.
- Rosenblatt, J., B.J. Agnew, H. Abe, J.R. Bamburg, and T.J. Mitchison. 1997a. Xenopus actin depolymerizing factor/cofilin (XAC) is responsible for the turnover of actin filaments in *Listeria monocytogenes* tails. *J Cell Biol*. 136:1323-32.
- Rosenblatt, J., P. Peluso, and T.J. Mitchison. 1995. The bulk of unpolymerized actin in Xenopus egg extracts is ATP-bound. *Mol Biol Cell*. 6:227-36.
- Rosso, S., F. Bollati, M. Bisbal, D. Peretti, T. Sumi, T. Nakamura, S. Quiroga, A. Ferreira, and A. Caceres. 2004. LIMK1 regulates Golgi dynamics, traffic of Golgi-derived vesicles, and process extension in primary cultured neurons. *Mol Biol Cell*. 15:3433-49.
- Roth, D., and R.D. Burgoyne. 1995. Stimulation of catecholamine secretion from adrenal chromaffin cells by 14-3-3 proteins is due to reorganisation of the cortical actin network. *FEBS Letters*. 374:77-81.
- Ruchhoeft, M.L., S. Ohnuma, L. McNeill, C.E. Holt, and W.A. Harris. 1999. The neuronal architecture of Xenopus retinal ganglion cells is sculpted by rho-family GTPases in vivo. *J Neurosci*. 19:8454-63.
- Ruthel, G., and G. Banker. 1998. Actin-dependent anterograde movement of growth-cone-like structures along growing hippocampal axons: a novel form of axonal transport? *Cell Motil.Cytoskeleton*. 40:160-173.
- Ruthel, G., and G. Banker. 1999. Role of moving growth cone-like "wave" structures in the outgrowth of cultured hippocampal axons and dendrites. *J.Neurobiol*. 39:97-106.
- Ruthel, G., and P.J. Hollenbeck. 2000. Growth cones are not required for initial establishment of polarity or differential axon branch growth in cultured hippocampal neurons. *J Neurosci*. 20:2266-74.
- Sabry, J.H., T.P. O'Connor, L. Evans, A. Toroian-Raymond, M. Kirschner, and D. Bentley. 1991. Microtubule behavior during guidance of pioneer neuron growth cones in situ. *Journal of Cell Biology*. 115:381-95.
- Sammak, P.J., and G.G. Borisy. 1988. Direct observation of microtubule dynamics in living cells. *Nature*. 332:724-6.
- Sampo, B., S. Kaeck, S. Kunz, and G. Banker. 2003. Two distinct mechanisms target membrane proteins to the axonal surface. *Neuron*. 37:611-24.
- Samstag, Y., and G. Nebl. 2003. Interaction of cofilin with the serine phosphatases PP1 and PP2A in normal and neoplastic human T lymphocytes. *Adv Enzyme Regul*. 43:197-211.
- Sander, E.E., J.P. ten Klooster, S. van Delft, R.A. van der Kammen, and J.G. Collard. 1999. Rac downregulates Rho activity: reciprocal balance between both GTPases determines cellular morphology and migratory behavior. *J Cell Biol*. 147:1009-22.
- Sander, E.E., S. van Delft, J.P. ten Klooster, T. Reid, R.A. van der Kammen, F. Michiels, and J.G. Collard. 1998. Matrix-dependent Tiam1/Rac signaling in epithelial cells promotes either cell-cell adhesion or cell migration and is regulated by phosphatidylinositol 3-kinase. *J Cell Biol*. 143:1385-98.
- Sanders, L.C., F. Matsumura, G.M. Bokoch, and P. de Lanerolle. 1999. Inhibition of myosin light chain kinase by p21-activated kinase. *Science*. 283:2083-5.

- Sarmiere, P.D., and J.R. Bamberg. 2004. Regulation of the neuronal actin cytoskeleton by ADF/cofilin. *J Neurobiol.* 58:103-17.
- Sarner, S., R. Kozma, S. Ahmed, and L. Lim. 2000. Phosphatidylinositol 3-kinase, Cdc42, and Rac1 act downstream of Ras in integrin-dependent neurite outgrowth in N1E-115 neuroblastoma cells. *Mol Cell Biol.* 20:158-72.
- Satoh, S., and T. Tominaga. 2001. mDia-interacting protein acts downstream of Rho-mDia and modifies Src activation and stress fiber formation. *J Biol Chem.* 276:39290-4.
- Schaefer, A.W., N. Kabir, and P. Forscher. 2002. Filopodia and actin arcs guide the assembly and transport of two populations of microtubules with unique dynamic parameters in neuronal growth cones. *J. Cell Biol.* 158:139-152.
- Schevzov, G., N.S. Bryce, R. Almonte-Baldonado, J. Joya, J.J. Lin, E. Hardeman, R. Weinberger, and P. Gunning. 2005a. Specific features of neuronal size and shape are regulated by tropomyosin isoforms. *Mol. Biol. Cell.* 16:3425-3437.
- Schevzov, G., N.S. Bryce, R. Almonte-Baldonado, J. Joya, J.J. Lin, E. Hardeman, R. Weinberger, and P. Gunning. 2005b. Specific features of neuronal size and shape are regulated by tropomyosin isoforms. *Mol Biol Cell.* 16:3425-37.
- Schevzov, G., P. Gunning, P.L. Jeffrey, C. Temm-Grove, D.M. Helfman, J.J. Lin, and R.P. Weinberger. 1997. Tropomyosin localization reveals distinct populations of microfilaments in neurites and growth cones. *Mol Cell Neurosci.* 8:439-54.
- Schmidt, J.T., P. Morgan, N. Dowell, and B. Leu. 2002. Myosin light chain phosphorylation and growth cone motility. *J Neurobiol.* 52:175-88.
- Schumacher, N., J.M. Borawski, C.B. Leberfinger, M. Gessler, and E. Kerkhoff. 2004. Overlapping expression pattern of the actin organizers Spir-1 and formin-2 in the developing mouse nervous system and the adult brain. *Gene Expr Patterns.* 4:249-55.
- Schwamborn, J.C., M. Muller, A.H. Becker, and A.W. Puschel. 2007. Ubiquitination of the GTPase Rap1B by the ubiquitin ligase Smurf2 is required for the establishment of neuronal polarity. *EMBO J.* 26:1410-1422.
- Schwamborn, J.C., and A.W. Puschel. 2004. The sequential activity of the GTPases Rap1B and Cdc42 determines neuronal polarity. *Nat Neurosci.* 7:923-9.
- Schwamborn, J.C., and A.W. Puschel. 2004. The sequential activity of the GTPases Rap1B and Cdc42 determines neuronal polarity. *Nat. Neurosci.* 7:923-929.
- Sells, M.A., U.G. Knaus, S. Bagrodia, D.M. Ambrose, G.M. Bokoch, and J. Chernoff. 1997. Human p21-activated kinase (Pak1) regulates actin organization in mammalian cells. *Curr Biol.* 7:202-10.
- Setola, V., M. Terao, D. Locatelli, S. Bassanini, E. Garattini, and G. Battaglia. 2007. Axonal-SMN (a-SMN), a protein isoform of the survival motor neuron gene, is specifically involved in axonogenesis. *Proc Natl Acad Sci U S A.* 104:1959-64.
- Shamah, S.M., M.Z. Lin, J.L. Goldberg, S. Estrach, M. Sahin, L. Hu, M. Bazalakova, R.L. Neve, G. Corfas, A. Debant, and M.E. Greenberg. 2001. EphA receptors regulate growth cone dynamics through the novel guanine nucleotide exchange factor ephexin. *Cell.* 105:233-44.
- Shaw, A.E., L.S. Minamide, C.L. Bill, J.D. Funk, S. Maiti, and J.R. Bamberg. 2004b. Cross-reactivity of antibodies to actin-depolymerizing factor/cofilin family proteins and identification of the major epitope recognized by a mammalian actin-depolymerizing factor/cofilin antibody. *Electrophoresis.* 25:2611-20.
- Sheen, V.L., M. Topcu, S. Berkovic, D. Yalnizoglu, I. Blatt, A. Bodell, R.S. Hill, V.S. Ganesh, T.J. Cherry, Y.Y. Shugart, and C.A. Walsh. 2003. Autosomal recessive form of periventricular heterotopia. *Neurology.* 60:1108-12.

- Shi, S.H., T. Cheng, L.Y. Jan, and Y.N. Jan. 2004. APC and GSK-3 β are involved in mPar3 targeting to the nascent axon and establishment of neuronal polarity. *Curr Biol.* 14:2025-32.
- Shi, S.H., L.Y. Jan, and Y.N. Jan. 2003. Hippocampal neuronal polarity specified by spatially localized mPar3/mPar6 and PI 3-kinase activity. *Cell.* 112:63-75.
- Shibata, A., M.V. Wright, S. David, L. McKerracher, P.E. Braun, and S.B. Kater. 1998. Unique responses of differentiating neuronal growth cones to inhibitory cues presented by oligodendrocytes. *J Cell Biol.* 142:191-202.
- Shim, S., E.L. Goh, S. Ge, K. Sailor, J.P. Yuan, H.L. Roderick, M.D. Bootman, P.F. Worley, H. Song, and G.L. Ming. 2005. XTRPC1-dependent chemotropic guidance of neuronal growth cones. *Nat Neurosci.* 8:730-5.
- Song, X., X. Chen, H. Yamaguchi, G. Mouneimne, J.S. Condeelis, and R.J. Eddy. 2006. Initiation of cofilin activity in response to EGF is uncoupled from cofilin phosphorylation and dephosphorylation in carcinoma cells. *J Cell Sci.* 119:2871-81.
- Soosairajah, J., S. Maiti, O. Wiggan, P. Sarniere, N. Moussi, B. Sarcevic, R. Sampath, J.R. Bamburg, and O. Bernard. 2005. Interplay between components of a novel LIM kinase-slingshot phosphatase complex regulates cofilin. *Embo J.* 24:473-86.
- Sosa, L., S. Dupraz, L. Laurino, F. Bollati, M. Bisbal, A. Caceres, K.H. Pfenninger, and S. Quiroga. 2006. IGF-1 receptor is essential for the establishment of hippocampal neuronal polarity. *Nat Neurosci.* 9:993-5.
- Steward, O., L. Davis, C. Dotti, L.L. Phillips, A. Rao, and G. Banker. 1988. Protein synthesis and processing in cytoplasmic microdomains beneath postsynaptic sites on CNS neurons. A mechanism for establishing and maintaining a mosaic postsynaptic receptive surface. *Mol Neurobiol.* 2:227-61.
- Strasser, G.A., N.A. Rahim, K.E. VanderWaal, F.B. Gertler, and L.M. Lanier. 2004. Arp2/3 is a negative regulator of growth cone translocation. *Neuron.* 43:81-94.
- Strathdee, C.A., M.R. McLeod, and J.R. Hall. 1999. Efficient control of tetracycline-responsive gene expression from an autoregulated bi-directional expression vector. *Gene.* 229:21-9.
- Suh, L.H., S.F. Oster, S.S. Sohrman, G. Grenningloh, and D.W. Sretavan. 2004. L1/Laminin modulation of growth cone response to EphB triggers growth pauses and regulates the microtubule destabilizing protein SCG10. *J Neurosci.* 24:1976-86.
- Sui, G., C. Soohoo, B. Affar el, F. Gay, Y. Shi, and W.C. Forrester. 2002. A DNA vector-based RNAi technology to suppress gene expression in mammalian cells. *Proceedings of the National Academy of Sciences of the United States of America.* 99:5515-20.
- Sumantran, V.N., and E.L. Feldman. 1993. Insulin-like growth factor I regulates c-myc and GAP-43 messenger ribonucleic acid expression in SH-SY5Y human neuroblastoma cells. *Endocrinology.* 132:2017-23.
- Sumi, T., K. Matsumoto, Y. Takai, and T. Nakamura. 1999. Cofilin phosphorylation and actin cytoskeletal dynamics regulated by rho- and Cdc42-activated LIM-kinase 2. *Journal of Cell Biology.* 147:1519-32.
- Sun, H.Q., K. Kwiatkowska, and H.L. Yin. 1996. Actin monomer binding proteins. *Curr Opin Cell Biol.* 7:102-110.
- Suter, D.M., and P. Forscher. 2000. Substrate-cytoskeletal coupling as a mechanism for the regulation of growth cone motility and guidance. *J Neurobiol.* 44:97-113.
- Suurna, M.V., S.L. Ashworth, M. Hosford, R.M. Sandoval, S.E. Wean, B.M. Shah, J.R. Bamburg, and B.A. Molitoris. 2006. Cofilin mediates ATP depletion-induced endothelial cell actin alterations. *Am J Physiol Renal Physiol.* 290:F1398-407.

- Svitkina, T.M., E.A. Bulanova, O.Y. Chaga, D.M. Vignjevic, S. Kojima, J.M. Vasiliev, and G.G. Borisy. 2003. Mechanism of filopodia initiation by reorganization of a dendritic network. *J Cell Biol.* 160:409-21.
- Svitkina, T.M., A.B. Verkhovsky, K.M. McQuade, and G.G. Borisy. 1997. Analysis of the actin-myosin II system in fish epidermal keratocytes: mechanism of cell body translocation. *J Cell Biol.* 139:397-415.
- Tanabe, K., T. Tachibana, T. Yamashita, Y.H. Che, Y. Yoneda, T. Ochi, M. Tohyama, H. Yoshikawa, and H. Kiyama. 2000. The small GTP-binding protein TC10 promotes nerve elongation in neuronal cells, and its expression is induced during nerve regeneration in rats. *J Neurosci.* 20:4138-44.
- Tanaka, E.M., and M.W. Kirschner. 1991. Microtubule behavior in the growth cones of living neurons during axon elongation. *J Cell Biol.* 115:345-63.
- Tanner, G.A., R.M. Sandoval, B.A. Molitoris, J.R. Bamburg, and S.L. Ashworth. 2005. Micropuncture gene delivery and intravital two-photon visualization of protein expression in rat kidney. *Am J Physiol Renal Physiol.* 289:F638-43.
- ten Donkelaar, H.J., M. Lammens, P. Wesseling, A. Hori, A. Keyser, and J. Rotteveel. 2004. Development and malformations of the human pyramidal tract. *J Neurol.* 251:1429-42.
- Teuling, E., S. Ahmed, E. Haasdijk, J. Demmers, M.O. Steinmetz, A. Akhmanova, D. Jaarsma, and C.C. Hoogenraad. 2007. Motor neuron disease-associated mutant vesicle-associated membrane protein-associated protein (VAP) B recruits wild-type VAPs into endoplasmic reticulum-derived tubular aggregates. *J Neurosci.* 27:9801-15.
- Thirion, C., R. Stucka, B. Mendel, A. Gruhler, M. Jaksch, K.J. Nowak, N. Binz, N.G. Laing, and H. Lochmuller. 2001. Characterization of human muscle type cofilin (CFL2) in normal and regenerating muscle. *Eur J Biochem.* 268:3473-82.
- Threadgill, R., K. Bobb, and A. Ghosh. 1997. Regulation of dendritic growth and remodeling by Rho, Rac, and Cdc42. *Neuron.* 19:625-34.
- Toriyama, M., T. Shimada, K.B. Kim, M. Mitsuba, E. Nomura, K. Katsuta, Y. Sakumura, P. Roepstorff, and N. Inagaki. 2006. Shootin1: A protein involved in the organization of an asymmetric signal for neuronal polarization. *J Cell Biol.* 175:147-157.
- Toshima, J., T. Watanabe, and K. Mizuno. 2001a. Cell-type-specific expression of a TESK1 promoter-linked lacZ gene in transgenic mice. *Journal of Biological Chemistry.* 276:43471-81.
- Toshima, J.Y., M. Suzuki, T. Noda, K. Mizuno, and J. Toshima. 2001b. Cofilin phosphorylation and actin reorganization activities of testicular protein kinase 2 and its predominant expression in testicular Sertoli cells. *Biochemical & Biophysical Research Communications.* 286:566-73.
- Toshimasu, M., D.L. Xu, T. Shinjo, Y. Goto, and J. Toshima. 2001. Cofilin phosphorylation and actin reorganization activities of testicular protein kinase 2 and its predominant expression in testicular Sertoli cells. *Journal of Veterinary Medical Science.* 63:827-9.
- Totsukawa, G., Y. Yamakita, S. Yamashiro, D.J. Hartshorne, Y. Sasaki, and F. Matsumura. 2000. Distinct roles of ROCK (Rho-kinase) and MLCK in spatial regulation of MLC phosphorylation for assembly of stress fibers and focal adhesions in 3T3 fibroblasts. *J Cell Biol.* 150:797-806.
- Tseng, Y., K.M. An, O. Esue, and D. Wirtz. 2004. The bimodal role of filamin in controlling the architecture and mechanics of F-actin networks. *J Biol Chem.* 279:1819-26.
- Tseng, Y., K.M. An, and D. Wirtz. 2002. Microheterogeneity controls the rate of gelation of

- actin filament networks. *J Biol Chem.* 277:18143-50.
- Tsui, H.C., H. Ris, and W.L. Klein. 1983. Ultrastructural networks in growth cones and neurites of cultured central nervous system neurons. *Proc Natl Acad Sci U S A.* 80:5779-83.
- Tuma, P.L., and A.L. Hubbard. 2003. Transcytosis: crossing cellular barriers. *Physiol Rev.* 83:871-932.
- Tuma, P.L., L.K. Nyasae, and A.L. Hubbard. 2002. Nonpolarized cells selectively sort apical proteins from cell surface to a novel compartment, but lack apical retention mechanisms. *Mol Biol Cell.* 13:3400-15.
- Turney, S.G., and P.C. Bridgman. 2005. Laminin stimulates and guides axonal outgrowth via growth cone myosin II activity. *Nat Neurosci.* 8:717-9.
- Tursun, B., A. Schluter, M.A. Peters, B. Viehweger, H.P. Ostendorff, J. Soosairajah, A. Drung, M. Bossenz, S.A. Johnsen, M. Schweizer, O. Bernard, and I. Bach. 2005a. The ubiquitin ligase Rnf6 regulates local LIM kinase 1 levels in axonal growth cones. *Genes Dev.* 19:2307-19.
- Vartiainen, M.K., T. Mustonen, P.K. Mattila, P.J. Ojala, I. Thesleff, J. Partanen, and P. Lappalainen. 2002a. The three mouse actin-depolymerizing factor/cofilins evolved to fulfill cell-type-specific requirements for actin dynamics. *Mol Biol Cell.* 13:183-94.
- Verhey, K.J., and J. Gaertig. 2007. The tubulin code. *Cell Cycle.* 6:2152-60.
- Vignal, E., M. De Toledo, F. Comunale, A. Ladopoulou, C. Gauthier-Rouviere, A. Blangy, and P. Fort. 2000. Characterization of TCL, a new GTPase of the rho family related to TC10 and Ccdc42. *J Biol Chem.* 275:36457-64.
- Vignjevic, D., D. Yarar, M.D. Welch, J. Peloquin, T. Svitkina, and G.G. Borisy. 2003. Formation of filopodia-like bundles in vitro from a dendritic network. *J Cell Biol.* 160:951-62.
- Walker, R.A., N.K. Pryer, and E.D. Salmon. 1991. Dilution of individual microtubules observed in real time in vitro: evidence that cap size is small and independent of elongation rate. *J Cell Biol.* 114:73-81.
- Wang, G.X., and M.M. Poo. 2005. Requirement of TRPC channels in netrin-1-induced chemotropic turning of nerve growth cones. *Nature.* 434:898-904.
- Wang, L., and A. Brown. 2002. Rapid movement of microtubules in axons. *Curr Biol.* 12:1496-1501.
- Wang, L.H., and S.M. Strittmatter. 1996. A family of rat CRMP genes is differentially expressed in the nervous system. *J Neurosci.* 16:6197-207.
- Wang, W., R. Eddy, and J. Condeelis. 2007. The cofilin pathway in breast cancer invasion and metastasis. *Nat.Rev.Cancer.* 7:429-440.
- Watabe-Uchida, M., E.E. Govek, and L. Van Aelst. 2006a. Regulators of Rho GTPases in neuronal development. *J Neurosci.* 26:10633-5.
- Watabe-Uchida, M., K.A. John, J.A. Janas, S.E. Newey, and L. Van Aelst. 2006b. The Rac activator DOCK7 regulates neuronal polarity through local phosphorylation of stathmin/Op18. *Neuron.* 51:727-39.
- Weed, S.A., A.V. Karginov, D.A. Schafer, A.M. Weaver, A.W. Kinley, J.A. Cooper, and J.T. Parsons. 2000. Cortactin localization to sites of actin assembly in lamellipodia requires interactions with F-actin and the Arp2/3 complex. *J Cell Biol.* 151:29-40.
- Wegner, A. 1982. Treadmilling of actin at physiological salt concentrations. An analysis of the critical concentrations of actin filaments. *Journal of Molecular Biology.* 161:607-15.

- Weiner, O.D., W.A. Marganski, L.F. Wu, S.J. Altschuler, and M.W. Kirschner. 2007. An actin-based wave generator organizes cell motility. *PLoS Biol.* 5:e221.
- Wen, Z., L. Han, J.R. Bamburg, S. Shim, G.L. Ming, and J.Q. Zheng. 2007. BMP gradients steer nerve growth cones by a balancing act of LIM kinase and Slingshot phosphatase on ADF/cofilin. *J. Cell Biol.* 178:107-119.
- Wiggan, O., B.W. Bernstein, and J.R. Bamburg. 2005. A phosphatase for cofilin to be HAD. *Nat Cell Biol.* 7:8-9.
- Wiggan, O.P., and J.R. Bamburg. 2002. ADF/cofilin and actin dynamics in disease. *Trends in Cell Biology.* 12:598-605.
- Wills, Z., L. Marr, K. Zinn, C.S. Goodman, and D. Van Vactor. 1999. Profilin and the Abl tyrosine kinase are required for motor axon outgrowth in the *Drosophila* embryo. *Neuron.* 22:291-9.
- Winckler, B., P. Forscher, and I. Mellman. 1999. A diffusion barrier maintains distribution of membrane proteins in polarized neurons. *Nature.* 397:698-701.
- Winckler, B., and I. Mellman. 1999. Neuronal polarity: controlling the sorting and diffusion of membrane components. *Neuron.* 23:637-40.
- Witke, W., A.V. Podtelejnikov, A. Di Nardo, J.D. Sutherland, C.B. Gurniak, C. Dotti, and M. Mann. 1998. In mouse brain profilin I and profilin II associate with regulators of the endocytic pathway and actin assembly. *Embo J.* 17:967-76.
- Witke, W., A.H. Sharpe, J.H. Hartwig, T. Azuma, T.P. Stossel, and D.J. Kwiatkowski. 1995. Hemostatic, inflammatory, and fibroblast responses are blunted in mice lacking gelsolin. *Cell.* 81:41-51.
- Witte, H., D. Neukirchen, and F. Bradke. 2008. Microtubule stabilization specifies initial neuronal polarization. *J Cell Biol.* 180:619-32.
- Wittmann, T., G.M. Bokoch, and C.M. Waterman-Storer. 2004. Regulation of microtubule destabilizing activity of Op18/stathmin downstream of Rac1. *J Biol Chem.* 279:6196-203.
- Wodarz, A. 2002. Establishing cell polarity in development. *Nat Cell Biol.* 4:E39-44.
- Worthylake, R.A., and K. Burridge. 2003. RhoA and ROCK promote migration by limiting membrane protrusions; RhoA is required for monocyte tail retraction during transendothelial migration. *Journal of Biological Chemistry.* 278:13578-84.
- Wu, X., Quondamatteo, F., Lefever, T., Czuchra, A., Meyer, H., Chrostek, A., Paus, R., Langbein, L., and Brakebusch, C. 2006. Cdc42 controls progenitor cell differentiation and beta-catenin turnover in skin. *Genes Dev* 20: 571-585.
- Wujek, J.R., and R.J. Lasek. 1983. Correlation of axonal regeneration and slow component B in two branches of a single axon. *J Neurosci.* 3:243-51.
- Wylie, S.R., and P.D. Chantler. 2001. Separate but linked functions of conventional myosins modulate adhesion and neurite outgrowth. *Nat Cell Biol.* 3:88-92.
- Yamashiro, S., K. Mohri, and S. Ono. 2005. The two *Caenorhabditis elegans* actin-depolymerizing factor/cofilin proteins differently enhance actin filament severing and depolymerization. *Biochemistry.* 44:14238-47.
- Yamauchi, J., J.R. Chan, Y. Miyamoto, G. Tsujimoto, and E.M. Shooter. 2005. The neurotrophin-3 receptor TrkC directly phosphorylates and activates the nucleotide exchange factor Dbs to enhance Schwann cell migration. *Proc Natl Acad Sci U S A.* 102:5198-203.
- Yang, N., O. Higuchi, K. Ohashi, K. Nagata, A. Wada, K. Kangawa, E. Nishida, and K. Mizuno. 1998. Cofilin phosphorylation by LIM-kinase 1 and its role in Rac-mediated

- actin reorganization. *Nature*. 393:809-12.
- Yeoh, S., B. Pope, H.G. Mannherz, and A. Weeds. 2002. Determining the differences in actin binding by human ADF and cofilin. *Journal of Molecular Biology*. 315:911-25.
- Yiu, G., and Z. He. 2006. Glial inhibition of CNS axon regeneration. *Nat Rev Neurosci*. 7:617-27.
- Yonezawa, N., Y. Homma, I. Yahara, H. Sakai, and E. Nishida. 1991. A short sequence responsible for both phosphoinositide binding and actin binding activities of cofilin. *Journal of Biological Chemistry*. 266:17218-21.
- Yoshimura, T., N. Arimura, and K. Kaibuchi. 2006a. Molecular mechanisms of axon specification and neuronal disorders. *Ann N Y Acad Sci*. 1086:116-25.
- Yoshimura, T., N. Arimura, and K. Kaibuchi. 2006b. Signaling networks in neuronal polarization. *J Neurosci*. 26:10626-30.
- Yoshimura, T., N. Arimura, Y. Kawano, S. Kawabata, S. Wang, and K. Kaibuchi. 2006c. Ras regulates neuronal polarity via the PI3-kinase/Akt/GSK-3 β /CRMP-2 pathway. *Biochem Biophys Res Commun*. 340:62-8.
- Yoshimura, T., Y. Kawano, N. Arimura, S. Kawabata, A. Kikuchi, and K. Kaibuchi. 2005. GSK-3 β regulates phosphorylation of CRMP-2 and neuronal polarity. *Cell*. 120:137-149.
- Yuan, A., R.G. Mills, J.R. Bamburg, and J.J. Bray. 1997. Axonal transport and distribution of cyclophilin A in chicken neurones. *Brain Res*. 771:203-12.
- Zebda, N., O. Bernard, M. Bailly, S. Welti, D.S. Lawrence, and J.S. Condeelis. 2000. Phosphorylation of ADF/cofilin abolishes EGF-induced actin nucleation at the leading edge and subsequent lamellipod extension. *Journal of Cell Biology*. 151:1119-28.
- Zhan, Q., J.R. Bamburg, and J.A. Badwey. 2003. Products of phosphoinositide specific phospholipase C can trigger dephosphorylation of cofilin in chemoattractant stimulated neutrophils. *Cell Motil Cytoskeleton*. 54:1-15.
- Zhang, X.F., A.W. Schaefer, D.T. Burnette, V.T. Schoonderwoert, and P. Forscher. 2003. Rho-dependent contractile responses in the neuronal growth cone are independent of classical peripheral retrograde actin flow. *Neuron*. 40:931-44.
- Zhang, Z., A.K. Ottens, S.F. Larner, F.H. Kobeissy, M.L. Williams, R.L. Hayes, and K.K. Wang. 2006. Direct Rho-associated kinase inhibition induces cofilin dephosphorylation and neurite outgrowth in PC-12 cells. *Cell Mol Biol Lett*. 11:12-29.
- Zhou, F.Q., and W.D. Snider. 2005. Cell biology. GSK-3 β and microtubule assembly in axons. *Science*. 308:211-4.
- Zhou, F.Q., C.M. Waterman-Storer, and C.S. Cohan. 2002. Focal loss of actin bundles causes microtubule redistribution and growth cone turning. *J Cell Biol*. 157:839-49.
- Zigmond, S.H. 1993. Recent quantitative studies of actin filament turnover during cell locomotion. *Cell Motility & the Cytoskeleton*. 25:309-16.